University of Reading

A phylogenomic study of *Saxifraga* L. (Saxifragaceae)

A thesis submitted by

Michelangelo Sergio Moerland

for the degree of Doctor of Philosophy

School of Biological Sciences

University of Reading

April 2023

Declaration

I confirm that this is my own work and the use of all material from other sources has been properly and fully acknowledged.

Michelangelo Sergio Moerland

Utrecht, April 2023

Abstract

Saxifraga L. (Saxifragaceae) is a species-rich genus (> 440 spp.), which occurs mainly in mountainous and arctic regions of the Northern Hemisphere. The species-richness of *Saxifraga*, and its strong ecological and morphological differentiation make it an ideal model system for studying alpine lineage evolution. However, those efforts require a robust phylogenetic framework. This thesis explores the evolutionary relationships within *Saxifraga* by designing hybrid-capture targets that are compatible with existing high-throughput sequencing data, to produce the most densely sampled phylogeny for the genus based on sequence information of 329 nuclear loci. High sequence coverage is obtained for target loci, although not all loci are retrieved for all sections of the genus, and certain taxa have a high incidence of paralogous copies due to the wide occurrence of polyploids in *Saxifraga*. DNA samples are predominantly sourced from museum material and the effect of locus retrieval and paralog detection is tested against sample age, where a slow decline in retrieved target length is observed and, importantly, a decline in paralog detection occurs with sample age that could mask high persistence of paralogous copies in phylogenomic datasets. The species tree based on newly generated and publicly available data confirms many recent taxonomic revisions and finds overall higher support for the topological placement of monophyletic sections. However, slight revisions are suggested for sect. *Ciliatae* and placement of *Saxifraga cuneifolia* L. in sect. *Gymnopera* is tenuous due to a complex evolutionary history likely involving intersectional introgression. A new set of divergence time estimations is performed with additional outgroups and calibration points. Relatively recent nodes were found to be older than had been previously estimated based on phylogenies of few concatenated loci. Likely, all sections of *Saxifraga* existed within the Miocene during strong climate cooling and mountain uplift in its geographic range. Finally, the adaptation of *Saxifraga* to high solar radiation conditions, that are typical for the alpine biome, is explored within a phylogenetic framework. Leaf temperature data and associated environmental data is presented from a common garden experiment. The leaf temperature increase over air temperature from heating through solar irradiance differs among taxa, while leaf functional traits that are known to impact temperature regulation ability had no effect on the ratio of leaf heating. However, closely related taxa are shown to have a similar leaf heating response to radiation and some clades are more abundant in taxa that are more likely to overheat with high radiation than others. Unlike the clades that can efficiently manage leaf temperatures towards an optimum, these clades are prone to reach unfavourable conditions upon exposure and are suggested to be more prone to future climate change.

Acknowledgments

This thesis would not have been possible without the continued support, mentorship, motivation, and patience of my supervisors Wolf Eiserhardt (PI) and Jurriaan de Vos. I would like to thank them for giving me this opportunity and for sharing their expertise. I am also very much indebted to my supervisors Bill Baker and Julie Hawkins for their advice and help to stay focused on the end goal of the project. I am also deeply grateful to the David and Claudia Harding Alpine Plant Conservation and Research Programme, that provided the funding for the project. Without this source of funding the project would not have been possible.

To Tom Carruthers I would like to extend my thanks for his help with divergence time estimation, and for his help with organising our remote workspace when the 2020 pandemic hit. To Matthew Jeffery I want to extend my thanks for his commitment to his MSc project on *Saxifraga* trait evolution and his company during the expedition to the Slovenian Alps, through which he contributed greatly to the project. A special thanks to the other postgraduates that I often discussed my project with, namely Ben Kuhnhaeuser, Livio Bätscher, Seraina Rodewald, Patricia dos Santos and Rafael Pülfer. I also want to thank the Kew PhD student community, all past office mates, and members of the Integrated Monography team, as well as extended colleagues that welcomed me part of their group at University of Basel and Aarhus University.

I would like to thank my family and friends, both at home and in the UK, for their support throughout my studies and pursuit of my interests, especially my mother Margreet Letter. To Tessa Driessen I want to extend my sincere thanks for her support during the highs and lows of the project.

Chapter 2 and 3

A big thanks goes out to László Csiba, for help with protocols for DNA extractions from herbarium material, and lab management in general. The training and help I received for DNA library preparation, hybridization and sequencing by Robyn Cowan was vital to the success of the labwork and I am grateful for her help. I have been supported by many others during lab work and bait design that were keen to provide advice and discussion in any way, among whom are Juan Viruel, Bruce Murphy, Sidonie Bellot, Grace Brewer, Alex Papadopoulos, Penny Malakasi, Rowan Schley and Dion Devey. I thank Ryan Folk, Doug Soltis and Rebecca Stubbs for providing sequence data from their projects on hybrid-capture methods for Saxifragales and *Micranthes* ahead of publication for us to use in bait design. Their willingness to work together and share data towards a better understanding of Saxifraga phylogenetics has been a boon. I thank the many herbarium and botanic garden staff that hosted me at their institute or prepared and sent samples by mail. High species coverage would not have been possible without all the helpful interactions I had with them. In addition, I want to thank all those who hosted me or helped collect samples or facilitated field excursions in the European Alps and in the Hengduan mountains.

Chapter 4

I am indebted to Günther Hoch for his investment in this project and advise on study design and data analysis. The data collected in this chapter was also made entirely possible thanks to the amazingly diverse and well-tended living collections at the Royal Botanic Gardens, Kew and the Botanic Gardens of Cambridge. I thank here specifically garden managers Thomas Freeth (RBGK) and Simon Wallis and Paul Aston (BGC) for hosting me and allowing me to obtain samples from, and somewhat mistreat, the plant collection they are responsible for.

Table of contents

List of tables

List of figures

Fig. 3.2: ASTRAL species tree generated from 329 exon nDNA gene trees. Branch labels show ASTRAL local posterior probability (LPP) value, which are not reported when LPP = 1. Branch lengths are based on coalescent units and terminal branches are dimensionless. Connections between figure panels A, B,C,D are shown within figures. Occurrence of key traits is shown on branches: red: filiform stolons, green: lime-secreting hydathodes on leaf margins, blue: zygomorphic flowers, black: foliar calcium oxalate crystals, orange: bulbils (either replacing flowers or partially underground near base of stalk, secondary loss within subsect. *Saxifraga*).

Fig. 3.4: BEAST chronogram of Saxifragales to the right of the tree. Numbers to the right of nodes represent median node age and the blue bars represent the 95% highest posterior density (HPD) of node ages. The six nodes with minimum age priors are indicated with an asterisk. Specific stem and crown node median age and HPD are given in Table 3.2**.**

Fig. 4.1: The (A) leaf temperature (T_{LEAF}) set out against air temperature (T_{AIR}), and (B) T_{AIR} plotted over the time of day. Data points are coloured by vapour pressure deficit (VPD), which shows higher values with increased T_{AIR}, with highest outlier values close to midday, due to temporary high T_{AIR} and low relative humidity.

Fig. 4.2: The temperature difference between T_{AIR} and leaf temperature (ΔT) (where the latter is measured using thermocouples (T_{LEAF}) (A); or infrared thermometer (Tir) (B) as a function of solar irradiance (SI) across all species. Data points are coloured by species ID; see Appendix 11 for analogous plots for individual species, which all have a significant positive slope. For this figure, values obtained during periods of extreme VPD (>5 kPa) were excluded.

Fig. 4.3: Phylomorphospace plots of the slope of ΔT~SI as a function of plant morphological variables. Variables shown here on the x-axis are (A) leaf width (mm) and (B) leaf perimeter (mm), for which clear differentiation in section *Porphyrion* is visible (red barrier). The species identities are indicated by four letter abbreviations (large dots), and the ancestral states are reconstructed for each internal node (small dots). None of the slopes are significant.

Fig. 4.4: (A) PCoA ordination plot showing distances among 25 *Saxifraga* species and *Micranthes nivalis* outgroup for which all trait values are present. The data points are coloured as per the value of the slope of ΔT~SI, for which a legend is embedded. Principal component 1 is mostly affected by traits relating to leaf size, and component 2 is mostly affected by whole plant dimensions and leaf density. Phylomorphospace plot (B) of the same taxa and axes is also given. As no significant correlations were found between ΔT~SI slopes and individual traits, so again do no patterns emerge from the PCA matrix. Individual PCoA values are presented in APPENDIX 4.4.

Fig. 4.5: Phylogenetic tree of *Saxifraga* with slope of ΔT~SI estimated on branches. The species identities are indicated by four letter abbreviations. Closely related species have more similar values (λ = 0.744296).

APPENDIX 2.2: Gene and site concordance factor calculated for branches in IQ-tree for datasets a) COMPLETE and b) PARALOGTRIM. Data points are coloured by ASTRAL local posterior probability value.

APPENDIX 3.1: ASTRAL species tree generated from 329 supercontig nDNA gene trees. Branch labels show ASTRAL local posterior probability (LPP) value. Branch lengths are based on coalescent units and terminal branches are dimensionless. Connections between figure panels A,B,C,D are shown within figures.

APPENDIX 4.1: Slope of T_{LEAF} (°C) measured by T_{AIR} (°C). Black point and line colours depict entire dataset for a taxon, while other colours depict individual plants. Inset numbers show slope values (b). Includes species removed due to being marked as unfit due to leaf deterioration.

APPENDIX 4.2: Slope of ΔT (°C) measured by SI (W m^{-2}). Black point and line colours depict entire dataset for a taxon, while other colours depict individual plants. Inset numbers show slope values (b). Includes species removed due to being marked as unfit due to leaf deterioration.

APPENDIX 4.3: Phylomorphospace plots of the slope of the temperature offset (ΔT ~ SI) as a function of plant morphological variables. The species identities are indicated by four letter abbreviations (large dots), and the ancestral states are reconstructed for each internal node (small dots). None of the slopes are significant.

APPENDIX 4.6: Phylogenetic trees with continuous traits mapped to branches. For the traits included in the figure the related species have more similar values under a lambda (ʎ) model of evolution (see APPENDIX 4.5 for ʎ values).

Chapter 1: General introduction

1.1 Ecology of the alpine biome and plant adaptation

Plants have adapted numerous times to the demanding ecological conditions of the vegetation zone above the natural treeline, also defined as the alpine biome (Jaccard, 1912; Körner, 2003; Körner, 2011). A restricted number of plant families now dominates high mountain habitats (Aeschimann and Lauber, 2004). The currently dominant patterns of alpine plant diversity have been shaped by movement and diversification of arctic and alpine plants since the Late Pliocene and Pleistocene (Billings, 1974), facilitated by geologic events and climate change (Comes and Kadereit, 2003; Hughes and Atchison, 2015; Wallis et al., 2016). Climatic conditions in higher elevation are strongly linked to lower atmospheric partial pressure, lower air temperature, higher solar radiation under clear weather conditions, and higher proportion of UV-B radiation within the spectrum of radiation (Körner, 2007; Körner, 2011). Notable are the high and more constant solar radiation towards the equator (Rundel et al., 1994), and that temperature change is three to ten times greater over the course of a day than over seasons in tropical montane biota while seasonal variation is most pronounced in temperate mountains (Rundel et al., 1994). In combination with strongly varying alpine biome characteristics that are less driven by elevation, such as moisture availability, wind exposure, and hours of sunshine per day, a wide variety of microclimates can occur above the treeline.

Plant lineages that have migrated and diversified into alpine habitats show strong convergent evolution, resulting in relatively low diversity in shape and size. Typical traits include small habit and perenniality (Billings, 1974; Hughes and Atchison, 2015), with few exceptions, such as the tall caulescent *Espeletia* spp. (Billings, 1974), and some annual species (Landolt and Urbanska, 2003). Angiosperms dominate most of the alpine regions of the world and are represented as graminoids, rosettes, cushions, forbs and prostrate herbs (Billings, 1974). Adaptive radiations in alpine plant linages are frequently recognized after occurrence of major genetic events or the emergence of unique alpine specialist characters linked to increased speciation rates (Hughes and Atchinson, 2015; Ebersbach et al., 2017b; Joly et al., 2019; Su et al., 2022). In addition, leaf functional traits change with elevation, among which specific leaf area (SLA) generally decreases with higher elevation across species, representing the slow end of the leaf economic spectrum in the alpine biome (Woodward, 1983). In spite of the many studies conducted on alpine climate and its stringent demands on alpine plant adaptations (e.g., Reisigl and Keller, 1987; Körner, 2003; Lütz,

2010), how plant growth forms and leaf morphology in the alpine biome predict temperature regulation capacity under varying air temperature and radiation is not widely studied (Michaletz et al., 2015). However, plenty of studies are available on temperature regulation capacity and thermal optima and tolerance of crops (e.g., Bote et al., 2018; Emmel et al., 2020) and tree canopies (e.g., Slot and Winter, 2017; Drake et al., 2018; Slot et al., 2021), where high radiation effects on growth and are well-studied topics.

Far-reaching changes have been predicted for mountain areas across all latitudes due to human induced climate change (Nogués-Bravo et al., 2007; Buytaert et al., 2010), as well as a changing frequency and intensity of extreme climatic events (Pachauri et al., 2007). Specifically, a disproportionate degree of habitat displacement is expected to occur in mountain regions (Thuiller et al., 2005; Nogués-Bravo et al., 2007), and the alpine zone specifically (EEA report warns of water overuse in Europe, 2009). The projected changes show a major threat to biodiversity in the alpine zone, and most future change research efforts try to understand how plant communities will respond. Plant microclimate and environmental data can be strongly disconnected. For instance, aerodynamic decoupling of microclimate air temperature from atmospheric circulation creates deviations from that in ambient air temperature (Körner, 2003; Larcher, 2012). How specific plants will respond to such examples of climate change effects is not entirely known, as not for all plants have the capacity for fast adaptation or population displacement, nor are adjacent temperature niches suited for all taxa equally, considering other environmental and ecophysiological factors. Another argument that large displacement scenarios in the alpine zone need not always be true, is given through the fact that various thermal niches are present in proximity due to the highly complex 3D high mountain environment (Körner and Hiltbrunner, 2018). However, the expected patterns of profit and loss among species are complex due to differing species responses to atmospheric changes. In addition, the overall suitable area gain through glacial retreat versus the loss through upslope movement of the treeline and other factors of encroaching habitat loss do not appear to be favourable (Körner and Hiltbrunner, 2018). Overall, it is still generally accepted that major contraction of alpine species range is to be expected, possibly preceded by notable population size decline (Cotto et al., 2017).

A better understanding of how alpine plant diversity has been generated through time could be achieved through genetically related functional groups that can be defined through combined phylogenies, functional trait data, and (environmental) ecophysiology data. Furthermore, it could be a tool to aid in predicting how climate change will impact plant communities and will give additional insights at affected taxa that are part of an at-risk functional group and additional conservation management goals.

1.2 Phylogenomics

Phylogenetics is the reconstruction of evolutionary relationships between organisms. Traditionally this was performed with morphological data, but since the onset of standardized and increasingly affordable DNA sequencing methods (Sanger et al., 1977; Schuster, 2008), molecular phylogenetic trees have been widely used in comparative research (Soltis and Soltis, 2003). As the limits of Sanger-sequencing for advancing phylogenetics became apparent, new techniques were explored with a higher throughput and lower sequencing cost per base (Schuster, 2008). Over the past decade, a range of innovative next-generation sequencing (NGS) methods have become available and increasingly more affordable, allowing for genome-scale data generation for non-model taxa (Ekblom and Galindo, 2011; de Sousa et al., 2014; Weitemier et al., 2014).

The available NGS methods are diverse and accommodate different approaches (Lemmon and Lemmon, 2013; Zimmer and Wen, 2015). Important variables to take into account when choosing a suitable method are the taxonomic application (taxa involved, non-model species), efforts in development (sequencing target identification, bait design) and cost efficiency. One technique known as targeted enrichment (Weitemier et al., 2014; Dodsworth et al., 2019), is particularly versatile as it allows for the acquisition of hundreds of single or low copy genes across the genome through in-solution hybridization of specific regions with biotinylated oligonucleotides (Albert et al., 2007; Lemmon et al., 2012; Barrett et al., 2016). It is also increasingly easy to select genomic regions of importance and test assumptions of orthologous descent (Lemmon et al., 2012; Struck, 2013, Johnson et al., 2016), which again provides increased utility setting up analysis pipelines not involving an established model clade.

1.3 Phylogenetics of *Saxifraga*

Previous efforts to build phylogenies for *Saxifraga* based on nuclear and plastid DNA markers clearly revealed relationships between the sections and resolved some historically pervasive taxonomic issues in the previously polyphyletic genus (Soltis et al., 1996; Conti et al., 1999; Vargas et al., 1999; Deng et al., 2015; Tkach et al., 2015a, 2015b; Ebersbach et al., 2017a). The phylogeny by Ebersbach et al., (2017a) included 312 taxa which takes the coverage to > 60% of extant species. Including all cited sources on *Saxifraga* phylogenetics in this text, a potent open-access database of *Saxifraga* sequence data is available (cDNA: *matK*, *trnL-trnF*, *rbcL*; nDNA: ITS) for future studies. Despite all available sequence data,

the phylogenetic studies on *Saxifraga* showed limitations, resulting in low node support values and topological incongruences among gene trees, where even the most thorough sampling will result in massive polytomies within species-rich clades and conflicting nuclear and chloroplast DNA gene trees (see Tkach et al., 2015b). Possible sources of these issues are polyploidy through ancient and recent hybridization (Soltis and Soltis, 1999), evolutionary radiation (Hughes and Atchison, 2015) and incomplete lineage sorting (ILS) (Degnan and Rosenberg, 2009) that obscure our ability to accurately reconstruct among-species relationships.

The occurrence of polyploids is a well-documented issue for resolving the evolutionary history of *Saxifraga*. It is now generally accepted that polyploidy facilitates rapid speciation (Soltis and Soltis, 1999), as copies of genes are released from their former constraints and allow for a higher rate of response to selection (Seehausen, 2004), even more so in case of ecological release. Over generations, some of the newly generated copies lose their function and are prone to rapid diversification (pseudogenes). The first problem this generates for gene trees is the chance that recently diverged paralogs might not be detected. Furthermore, both auto- and allopolyploids are common and drivers of species diversity (Soltis and Soltis, 1999), but as more adaptive radiations are thoroughly investigated, there is more evidence of the importance of hybridization coinciding with these events (Dunbar-Co et al., 2008; Joly et al., 2009a). Hybrids can be difficult to detect with few markers (Joly et al., 2009b), although it is known to occur widely throughout *Saxifraga* and is increasingly documented through molecular studies (Brochmann et al., 1998; Tkach et al., 2019). To avoid multi-copy loci of polyploid taxa, putative single-copy genes can be targeted for sequencing through the careful selection of baits based on transcriptomes (Weitemier et al., 2014; Ambrosino and Chiusano, 2017), after which any remaining paralogs can be detected and eliminated if needed (e.g., Nicholls et al., 2015).

For closely related species that resulted from evolutionary radiation, phylogenetic analysis often fails to resolve relationships due to a lack of informative characters (Hughes and Atchison, 2015). The occurrence of evolutionary radiations has been shown in sections in *Saxifraga* sections *Ciliatae* and *Porphyrion* through shifts in evolutionary rates (Ebersbach et al., 2017a) and the distribution of haplotypes (Li et al., 2018). In addition, radiation can coincide with ILS, causing further disagreement among gene trees (Degnan and Rosenberg, 2009). However, through NGS sequencing data we can infer phylogenies with a vast increase in informative sites, through methods that additionally consider discordant gene tree topologies under the multi species coalescent (MSC) (Struck, 2013; Hellmuth et al., 2015).

As an additional point to note, studies of alpine plant diversification are often suffering from incomplete coverage of extant species (Hughes and Atchison, 2015) and a low coverage of taxa can hamper phylogenetic studies on the relative importance of adaptive radiation, hybridization and dispersal events. Many available specimens from herbarium collections have fragmented DNA through degradation over time, due to which they are often unavailable for Sanger sequencing. Sequence capture techniques are also promising with fragmented DNA of herbarium collections (de Sousa et al., 2014; Nicholls et al., 2015; Hart et al., 2016), and could therefore provide access to a wealth of historical collections, leaving research projects less constrained by field collection investment and gaining access to populations and species that are no longer available in the present.

In summary, the abovementioned advances in phylogenomics provide us with the means to overcome phylogeny estimation issues encountered in *Saxifraga* specifically. The new opportunities with NGS look promising for future work on plant genomes (Schuster, 2008), and specifically the evolution of alpine plants (Hughes and Atchison, 2015). It is imperative that for future biogeographic studies on historically 'difficult-to-resolve' lineages we commit to NGS techniques to produce well-supported phylogenies for the advancement of taxonomy and study of evolutionary processes. Hence, we had decided to construct an NGS pipeline for this thesis.

1.4 *Saxifraga* L.: a model group for alpine plant diversity

With over 440 species, *Saxifraga* L. (Saxifragaceae) is the largest genus within Saxifragaceae (Folk et al., 2020). Recent estimates of total diversity have been variable due to frequent lumping and splitting of species complexes and varieties (e.g., Gornall et al., 2000; Winkler et al., 2013), new species descriptions (e.g., Gornall et al., 2012; Firat, 2016; Zhang et al., 2018; Zhang et al., 2021), and the recognition of former *Saxifraga* spp. as the separate genus *Micranthes* Haw. (Soltis et al., 1996; Tkach et al., 2015a). *Saxifraga* has a broad distribution throughout the northern hemisphere, with a few species south of the Tropic of Cancer **(Fig. 1.1**). Centers of diversity occur in the European Alpine System and the Himalayas and Hengduan mountains, where highly diverse species, from broad-leaved herbs to compact cushions, occupy a wide range of habitats. The species-richness of *Saxifraga*, and the many alpine specialists contained within, render it an ideal model system for studying alpine lineage evolution.

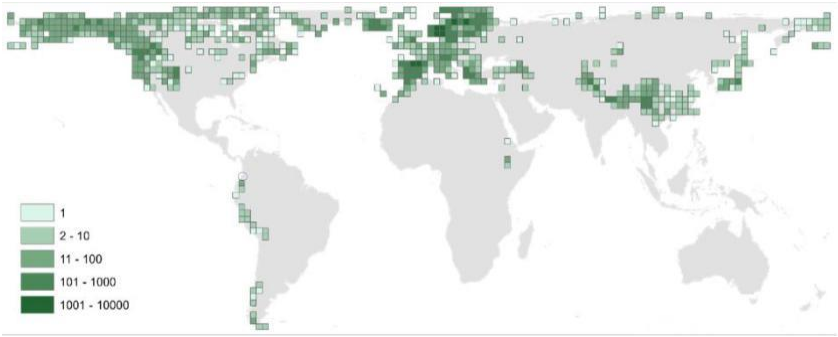

Fig. 1.1: World distribution map of Saxifraga*, based on cleaned occurrence data from GBIF (obtained and cleaned by Wolf Eiserhardt). Density of records shown in scale (number of records) is relatively high in Europe and North America, despite Asia containing the center of highest diversity*.

The shorthand description of *Saxifraga* would include that they are perennial (rarely annual or biennial) herbs with 10 (rarely 5-8) stamens with tetralocular, longitudinally dehiscing anthers, and 2 (rarely 3) carpels, and 2-valved capsule fruits (Engler and Irmscher, 1916; Folk et al., 2021). The morphological variation among *Saxifraga* sections is described in this thesis, albeit with a focus on morphological characters which are important for sectional delimitation as per Gornall (1989) and Tkach et al. (2015b) (chapter 3), and which are of importance in temperature regulation such as plant stature and leaf functional traits relating to the leaf economic spectrum (chapter 4).

Fig. 1.2: Examples of Saxifraga *spp. diversity. A,* S. squarrosa *(sect.* Porphyrion*), Italy; B,* S. moschata *(sect.* Saxifraga*), Italy; C,* S. *aff.* unguiculata *(sect.* Ciliatae*), China; D,* S. mutata *(sect.* Porphyrion*), Italy; E,* S. rotundifolia *(sect.* Cotylea*), Slovenia; F,* S. bryoides *(sect.* Trachyphyllum*), Switzerland; G,* S. paradoxa *(sect.* Saxifraga*), Slovenia; H,* S. diapensioides *(Sect.* Porphyrion*), Switzerland; I,* S. cernua *(Sect.* Mesogyne*), Scotland; J,* S. aizoides *(sect.* Porphyrion*), Slovenia; K,* S. nigroglandulifera *(sect.* Ciliatae*), China; L,* S. cuneifolia *(sect.* Gymnopera*), Slovenia.*

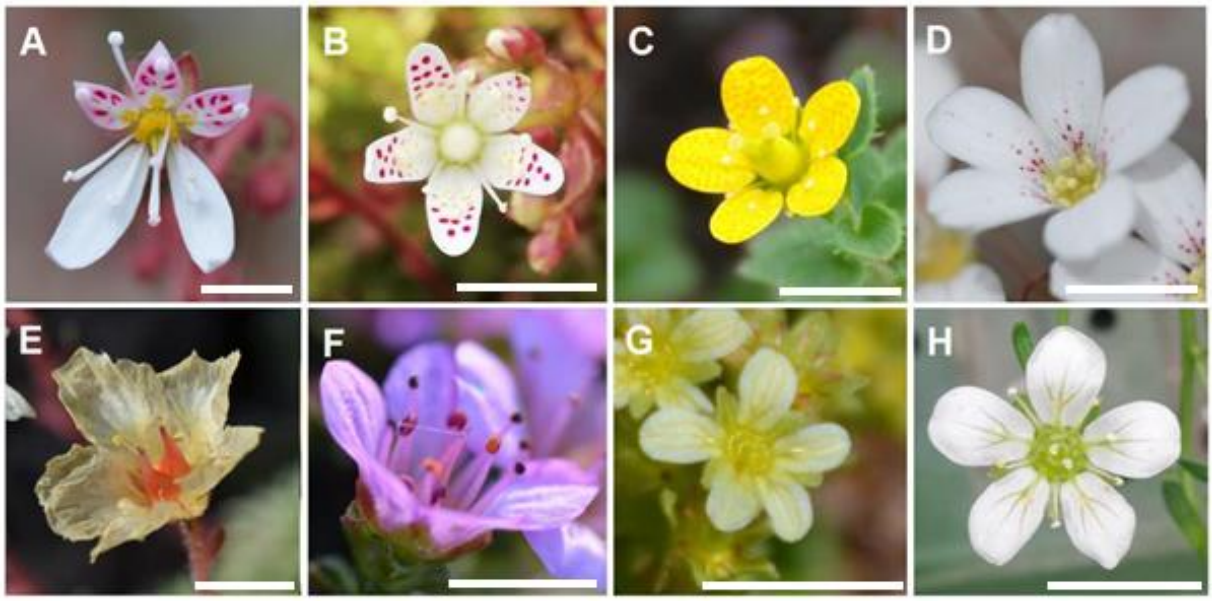

Fig. 1.3: Examples of floral morphology in Saxifraga *spp. A,* S. stolonifera *(sect.* Irregulares*); B,* S. bronchialis ssp. austromontana *(sect.* Bronchiales*); C,* S. *aff.* bulleyana *(sect.* Ciliatae*); D,* S. longifolia *(sect.* Ligulatae*); E,* S. burseriana *(sect.* Porphyrion*); F,* S. oppositifolia *(sect.* Porphyrion*); G,* S. carniolica *(sect.* Saxifraga*); H,* S. geranioides *(sect.* Saxifraga*). White bars correspond to ~10mm.*

The genus is remarkably diverse as it contains broad-leaved forest floor herbs and minute-leaved high-alpine cushion plants **(Fig. 1.2)**, with a leaf surface size difference of up to a factor 2,000 measured between living specimens available to this study. Various taxa have highly compact cushion growth form or fleshy leaved rosettes, which are typical for the alpine biome. Two clades have lime-secreting hydathodes which can form lime encrustation on leaf margins, likely aiding in releasing excess levels of calcium and forming a reflective rim to thrive under high solar radiation conditions. Various unique propagation methods occur, such as through stolons, various types of extending rhizomes and the formation of bulbils near the plant base under or near the ground or replacing flowers along the stem (sometimes replacing sexual reproduction altogether). Many taxa also have glandular or villous hairs along the flowering stem or leaves. Descriptions of the reproductive organs are relatively unreliable as they can vary to a great extent within the sections **(Fig. 1.3)**. For instance, petal colour can differ among closely related taxa between white, yellow, purple, orange, and green, and have various intricate patterns of petal spots and blotches or be absent altogether. Changes in floral merosity also occur (not regarding true zygomorphy in sect. *Irregulares*), as well as placement of the ovule. Various other reproduction-associated traits such as the number and organisation of flowers per plant or rosette also vary widely and can vary within species to a great degree (see Engler and Irmscher, 1916; Webb and Gornall, 1989), warranting the establishment of well-researched continuous traits per taxon. Pollen types, however, are likely to be a relatively

reliable key to discern between sections (Zhang et al., 2015), although inter- and infrasectional sampling is still relatively low.

There is long-standing interest in *Saxifraga* as a model to study alpine plant speciation, ecology, and biogeographic history. Work on *Saxifraga* DNA data has been undertaken to study the relative importance of outcrossing in alpine and arctic plant communities (Gabrielsen and Brochmann, 1998; Reisch, 2008; Pietilainen and Korpelainen, 2013), plant population contractions and colonisations during the glacials, and to determine the locations of arctic and alpine refugia (Bauert et al., 1998; Holderegger and Abbott, 2003; Reisch et al., 2003; Schönswetter et al., 2005; Winkler et al., 2012). Recent *Saxifraga*-focused studies with similar interests to this thesis have focused more on morphological and ecological differentiation. For instance, the driving forces of *Saxifraga* speciation in the alpine biome were studied through the occurrence of novel traits (Ebersbach et al., 2017b) and mountain uplift (Ebersbach et al., 2018; Li et al., 2018), and rates of speciation in and among biomes (de Casas et al., 2016; Folk et al., 2019). The results from various studies find consensus in that *Saxifraga* diversification has been driven by various intrinsic and extrinsic factors, such as through an increased rate of divergence of a clade coinciding with an interval of Hengduan Mountain uplift and climatological change (Ebersbach et al., 2017b, 2018), an increased rate of diversification likely resulting from the development of lime-secreting hydathodes (Ebersbach et al., 2017b), and higher rates of diversification after forest-dwelling ancestors switched to rock cliff and tundra habitats (associated with alpine biome sensu lato) (de Casas et al., 2016). In summary, *Saxifraga* has been widely used to study the eco-evolutionary assembly of alpine floras. To use the genus as a model group to study fundamental processes of alpine plant evolution, the available genetic material and phylogeny reconstruction success of previously applied methods need to be considered to advance.

This thesis focuses on the genus *Saxifraga* as a model group to study complex molecular evolutionary history and adaptation to the alpine biome. As would be expected of modern systematic studies (Marhold et al., 2013), I present work with a strong focus on phylogenetic analysis of DNA data and evolutionary processes.

1.5 Organisation and aims of the thesis

The research for this thesis is organised into three data chapters, all demonstrating the use of genome-scale sequence data for the construction of a comprehensive phylogeny of Saxifraga. The main aim is to construct a highly resolved phylogeny despite the high occurrence of paralogous copies due to the rich history of hybridization and introgression in Saxifraga. In turn, we use the new NGS phylogeny estimation pipeline to construct trees for taxonomic revision and divergence time estimation. Finally, the phylogeny is used to test leaf heating response to high solar radiation in an evolutionary framework. A summary of results, as well as views on future research, is presented in chapter 5.

Chapter 2: Paralog detection in museomics: a case study in the genus Saxifraga

In this chapter, newly designed target-capture baits for the genus Saxifraga are used to obtain up to 329 nuclear genes for plant material from silica-stored to museum specimens. We aim to test the overall performance of hybrid-capture on a secondary set of target sequences, derived from baits and sequencing results from previous studies. The pipeline for sequence extraction and phylogenetic inference contains paralog detection and exclusion steps that are used to test the effects of persistent paralogous copies in genomic data. In addition, the effect of degraded DNAs from museum specimens on paralog detection

Chapter 3: Phylogenomic analysis of the genus Saxifraga

In this chapter, the sequences from chapter 2 are used, and supplemented with available hybrid-capture data for *Saxifraga* and outgroups to build a well-supported species tree. Representatives from all accepted sections are included and taxonomic revisions are presented. The increased coverage of in- and outgroup taxa and nuclear DNA loci are used to estimate divergence times in *Saxifraga* with additional fossil calibration points. In addition, we use a ‘true’ species tree instead of a gene tree and use a selection of strongly congruent genes for the alignments, through both penalised likelihood and Bayesian divergence time estimation methods and the effect of divergence time estimation with a ‘true species tree’ and congruent gene alignment is assessed.

Chapter 4: Leaf temperature response to solar radiation in the genus Saxifraga

In this chapter, the leaf temperature response of *Saxifraga* spp. to solar radiation is measured in a common garden experiment and a functional trait database is constructed. The study explores which plant traits predict how taxa maintain their leaf temperature closer to an optimum to avoid damage from heat stress. The phylogeny from chapter 3 is used to explore the eco-evolutionary history of *Saxifraga* adaptation to high solar radiation environments representative of the alpine biome. In addition, in this chapter an assessment is made if closely related taxa show a similar leaf temperature response to increased solar radiation, and which functional traits have predictive value. Through this, we test if any functional groups can be identified that could be prone to climatic disturbance through future change.

Chapter 2:
Paralog detection in museomics: a case study in genus *Saxifraga*

2.1 Introduction

Next generation sequencing (NGS) methods have been revolutionising phylogenetic systematics, as they enabled higher rates of data retrieval by several orders of magnitude for a fraction of the cost of Sanger sequencing (Lemmon and Lemmon, 2013; McKain et al., 2016). Several methods of high-throughput sequencing are available, and among a variety of widely used approaches such as ddRAD, genome skimming, anchored enrichment (Davey and Blaxter, 2010; Lemmon et al., 2012; Dodsworth, 2015), hybrid-capture techniques are becoming widely established for phylogenetic studies (Dodsworth et al., 2019; Jones and Good, 2016). Here, genomic libraries are prepared and then selectively enriched using short RNA baits that hybridise with target loci, after which the enriched libraries are sequenced, typically using Illumina sequencing. The technique also enables use of highly fragmented DNA, for instance from museum specimens (e.g., Hart et al., 2016; McCormack et al., 2015; Forrest et al., 2019). Overall, hybrid-capture allows for flexible study design in terms of starting total DNA and locus selection and is considered cost-effective for studies at various phylogenetic depths (Lemmon and Lemmon, 2013; reviewed by Dodsworth et al., 2019).

Despite its popularity and promises, hybrid-capture techniques pose challenges for bioinformatic processing of the generated data that are incompletely understood. Most phylogenetic applications of hybrid-capture aim to use loci that are single-copy, that is, genomic loci that are related by descent between species (orthologous). If a locus is present more than once in a species and is related by duplication within a (ancestral) species, these are paralogous. Single-copy loci can be conveniently analysed, as the copy within individuals will be orthologous to the copy in each other individual. In contrast, for genes that are present with multiple paralogs in individuals, phylogenetic analysis requires to first establish orthology relations between the gene copies recovered from different species, requiring dedicated analysis pipelines (e.g., Moore et al., 2018; Gardner et al., 2019). A common goal is to use nuclear loci for which paralogy assessment is easy during the stage of bait design, for which popular methods include paralog detection through analysis of gene trees of potential target sequences (e.g., Kocot et al., 2013) or predicting orthology based on similarities of mRNA fragments in transcriptome references (e.g., Ambrosino and Chiusano, 2017). Typically, all genes from multiple transcriptomes are blasted all-by-all, and only those with a single reciprocal hit are retained for bait design (e.g., Weitemier et al., 2014).

However, assembling loci post-sequencing often reveals multiple contigs for a single locus, and a selection criterion (such as sequence length or similarity,) is applied in a second step to select the appropriate, orthologous sequence (e.g., Johnson et al., 2016). We refer to such loci as flagged with a "paralog warning" (following Johnson et al. 2016). Biological reasons underlying such paralog warnings include single gene duplications, whole genome duplications (WGD) and heterozygosity (Vallender, 2009; Gardner et al., 2019), but they may also result from assembly artefacts. Overall, there is no consensus as to how to deal with paralogs in phylogenetic studies, and solutions range from excluding all loci with suspected paralogs (e.g., Nicholls et al., 2015; Stubbs et al., 2018b; Villaverde et al., 2018), possibly omitting valuable phylogenetic information, to keeping all (e.g., Folk et al., 2019), possibly introducing noise or artifactual results.

NGS techniques have advanced our ability to utilise historical specimens (reviewed by Kistler et al., 2020). Previously available techniques already allowed for acquisition of aDNA (e.g., Rollo et al., 1988), although NGS methods have made it more efficient and affordable (Dodsworth et al., 2019). Phylogenomic analysis based on sequences obtained from, often degraded and low concentration, DNAs of historic collections is defined as museomics (Hart et al., 2016; Bakker, 2017). It is an excellent opportunity to access museum specimens for sequencing efforts. Specifically, acquiring many relatively fresh samples of geographically widespread taxa provides a logistical challenge in study design. Furthermore, taxa or populations are at times only known from limited locality descriptions or have been reported extinct. Various studies have also made a point of aiming to include type specimens if possible (Paer et al., 2016; Zedane et al., 2016; Malakasi et al., 2019), which prevents misidentification. Methods such as hybrid-capture sequencing proved specifically useful as they are able to amplify DNA from highly degraded museum specimens, although this affects target capture success rates (e.g., Nicholls et al., 2015; Hart et al., 2016). The acquired percentage of reads on target has been found to decline with sample age (e.g., Hart et al., 2016; Villaverde et al., 2018; e.g., Brewer et al., 2019; Malakasi et al., 2019; Shee et al. 2020), and collection conditions and preservation method (e.g., Brewer et al., 2019; Forrest et al., 2019, de Lima Ferreira et al., 2022).

Despite relatively old specimen age and low starting DNA amounts, one of the early hybrid-capture museomics studies by Hart et al. (2016) obtained sufficient capture success for herbarium samples up to 180 years old. However, while new studies continuously achieve a higher percentage of raw sequence reads that successfully map to a target genomic region (on-target rates) for phylogenetic inference, and the field

adopts new best practice advice for DNA extraction, cleaning, and library preparation steps, it is unclear what the full potential of the method is before effort spent, costs and museum specimen damage become limiting factors.

Despite major advances, museomics in practice routinely suffers from data quality issues, because it is challenging to obtain enough sequences on target to successfully detect paralogs, and thus we need to consider if we can reliably infer phylogenies when we expect hidden paralogy to be prevalent. As described above, we may miss paralogous copies due to the selection criteria employed during locus assembly. Sufficient length and coverage of contigs is needed to claim the presence of multi-copy loci (e.g., Johnson et al., 2016), and thus the presence of copies can be masked by a low on-target rate, in turn resulting from highly degraded DNA (Weiß et al., 2016). The sequences mistaken for single-copy orthologs then may cause conflicting gene-tree topologies. Gene-tree heterogeneity due to biological factors impacts species tree inference (Maddison, 1997), and thus we similarly need to account for the effects of paralogs in the method we employ (Smith and Hahn, 2020). Importantly, studies show that with species tree analysis under the multi species coalescent (MSC) the inclusion of paralogs in datasets does not necessarily have to impede phylogenetic inference (Struck, 2013; Hellmuth et al., 2015; Yan et al., 2020).

The genus *Saxifraga* L. (Saxifragaceae) is an ideal model for exploring the effects of paralogy as various occurrences of hybrid speciation and allopolyploidy are known throughout the genus (Tkach et al., 2015; Ebersbach et al., 2020), that are suspected to cause high degrees of gene tree heterogeneity. Early efforts of phylogenetic inference of *Saxifraga* were based on sequence data of few taxa and loci and revealed relationships between the different sections and resolved some historically pervasive taxonomic issues in the previously polyphyletic genus (e.g., Soltis et al., 1996; Conti et al., 1999; Vargas et al., 1999). Later, phylogenies were estimated based on more taxa and the delineation and topology of sections within the genus became well-understood (Deng et al., 2015; Tkach et al., 2015; Ebersbach et al., 2017). Nevertheless, species relationships show low support even in comprehensively sampled studies, possibly through the effect of various instances of hybridization (Brochmann et al., 1998; Brochmann and Håpnes, 2001; Li et al., 2018), and rapid diversification (Li et al., 2018). With polyploids occurring throughout (Ebersbach et al., 2020), *Saxifraga* is a well-suited model to explore how multi-copy loci affect bait design and data cleaning steps, and what their impact is on phylogenetic inference.

In this study we perform phylogenetic inference on data generated through a hybrid-capture NGS approach, aiming to evaluate the effects of low-quality DNAs and high persistence of paralogs. We redesigned a bait kit that was developed to target putative single-copy loci across the order Saxifragales, by updating bait sequences based on raw

sequencing results from *Saxifraga* species. We then used it to target a set of 329 loci from herbarium material and silica-preserved tissue. We test (1) the effect of sample age and preservation method on sequence retrieval and paralog detection, (2) the effect of different criteria for locus removal based on paralog warnings on tree topology, support and congruence with trees inferred in literature. We discuss how future work should consider the presence of hidden paralogous loci in NGS data resulting from degraded DNA.

2.2 Materials and methods

2.2.1 Selection of target loci for *Saxifraga*

A set of target loci was selected specifically for the genus *Saxifraga* by using the raw sequence data resulting from hybrid-capture NGS with two existing sets of target genomic regions (baits). Reference sequences were used for the order Saxifragales (Folk et al., 2019) and the genus *Micranthes* (Saxifragaceae) (Stubbs et al., 2018a). *Saxifraga* DNA data sequenced by Folk et al. (2019) showed that the target capture method with the Saxifragales bait set appeared not to be equally successful for all sections of *Saxifraga* (Ryan Folk, personal communication). Additionally, the conserved loci selected to elucidate backbone structure within the order Saxifragales may not be phylogenetically informative at the species level. Hence, targets from the *Micranthes* set were added, through which sequence data could be retrieved despite its origination from an outgroup. The *Micranthes* target sequences at the time of development contained 295 loci and were mapped against the consensus sequences of Saxifragales targets for 301 loci through the 'Map to reference' function in Geneious v8.0.5 (www.geneious.com). Between bait sets we found 101 loci were shared and 495 unique loci were identified.

To evaluate the performance of all loci from the Saxifragales and *Micranthes* bait sets in *Saxifraga*, and to select new target sequences, we used hybrid-capture data for six *Saxifraga* species representing different sections and spanning the phylogenetic diversity of the genus. We used data for *S. fortunei* Hook. (sect. *Irregulares*), *S. magellanica* Poir. (sect. *Saxifraga*), *S. parnassifolia* D. Don (sect. *Ciliatae*), *S. pulchra* Engl. & Irmsch. (sect. *Porphyrion*), *S. rebunshirensis* Sipliv. (sect. *Bronchiales*), and *S. rotundifolia* L. (sect. *Cotylea*). The sequence data were the sequencing result of DNA libraries enriched with the Saxifragales and *Micranthes* baits and trimmed of adapters and low-quality reads as per (Folk et al., 2019). We then used Hybpiper v1.3.1 (Johnson et al., 2016) to assemble the trimmed reads into contigs matching each of the target sequences from the combined 495 loci, using the standard options for mapping through BWA (Li, 2013) and assembly through SPAdes v3.11 (Bankevich et al., 2012). We used Hybpiper scripts to return only exon regions and flag loci with paralog warnings to identify potential paralogous copies.

Hybpiper selects if paralogs occur, as opposed to allelic variants, through steps that assess relative length and coverage in case more than one contig is retrieved against a reference sequence. In case multiple contigs are retrieved with 75% coverage of the target, Hybpiper selects the sequence with high % identity to the reference as the 'orthologous' copy. Paralog warnings were found for 36 loci, distributed over four of the six taxa. The origin of paralog-flagged loci was assessed to be a product of either ancient duplication or allelic variation through visual observation of all copies in a phylogenetic tree. Trees were made through sequence alignment with default settings in MAFFT v7 (--auto) (Katoh and Standley, 2013) and phylogenetic inference in FastTree v2.1.7 (using the options -nt -gtr) (Price et al., 2009). Tree topologies did not suggest ancient duplication within *Saxifraga* as paralogs within taxa formed well-defined clades. Hence, we did not employ additional measures to select which copies to use and continued using only the putatively orthologous copy selected through HybPiper. Exon sequences were aligned to the target loci with MAFFT. Sequences in the alignments were trimmed from the 5' or 3' end if they contained an insertion or deletion that resulted from a poor-quality sequence with less than 10x coverage on the contig resulting from SPAdes. Specifically, the entire length of the sequence between the indel and the nearest 5' or 3' end was removed. To guarantee overlap among sequences for a locus, sequences with a length of < 200 bases were omitted, and those of 200 to 400 bases were only kept in case additional longer sequences were available from other *Saxifraga* species. For each locus, we kept all remaining sequences of *Saxifraga* spp., including sequences of *Saxifraga stolonifera* Curtis already present in the target sequences of (Folk et al., 2019). Finally, loci were omitted if no *Saxifraga* spp. representatives remained, and if fewer than four Saxifraga spp. were available for a locus we included a maximum of four non-*Saxifraga* target sequences from (Folk et al., 2019) and (Stubbs et al., 2018a). Priority was given to taxa that were most closely related to *Saxifraga* and at least being placed within the Saxifragaceae alliance accepted by Jian et al. (2008). The taxa we included are *Itea virginica* L. (Saxifragaceae), *Micranthes caroliniana* (A. Gray) Small (Saxifragaceae), *Mitella pentandra* Hook. (Saxifragaceae), and *Ribes* aff. *giraldii* Janczewski. (Grossulariaceae). Finally, we ordered custom myBaits biotinylated baits which were designed and produced by Arbor Biosciences (Ann Arbor, Michigan, USA).

2.2.2 Sample collection and sequencing strategy

Taxa were selected for sequencing if listed as accepted by Plants of the World Online (POWO, 2019; retrieved 18-8-2018) and whether they were not sequenced by Folk et al. (2019). The checklist totalled 458 accepted species based on POWO, and 599 names when accounting for unresolved names and accepted intraspecific taxa. We were able to include samples of 44 specimens from wild populations collected between 2016 and 2018

in six countries (Austria, China, England, Italy, Slovenia, Switzerland) and 43 specimens from five living collections of botanic gardens **(Appendix 2.1)**. The vouchers for wild and ex hort material were stored at K or CDBI. However, most samples were collected from historic collections available from six herbaria (BASBG, CDBI, E, FIAF, K, LJU). A total of 227 unique species of *Saxifraga* were obtained for sequencing (289 total taxa including unresolved and intraspecific names). Leaf tissue samples were collected from living plants and desiccated in silica gel immediately after. The collection and drying method information was absent for the historic collections we sampled from herbarium sheets and could not be taken into consideration despite it affecting the amount and quality of sequence data one can retrieve through hybrid-capture methods (Forrest et al., 2019). Fourteen outgroup taxa were included from silica-dried and herbarium sources to broadly represent Saxifragaceae diversity. Finally, including some double accessions, a total of 322 DNA samples were available for sequencing, of which 63 were sourced from silica-dried samples and 258 from herbarium sheets.

Samples were ground in 2 ml tubes with two stainless steel beads in an MM400 mixer mill (Retsch Inc.). For silica-stored samples and some of the more recently collected herbarium accessions we performed DNA extractions with the DNeasy Plant Mini Kit (Qiagen, Manchester, UK), using the manufacturer's protocol with at least one hour of initial incubation time. For most herbarium specimens, we used an adapted CTAB extraction method (Doyle and Doyle, 1987), followed by an extra cleaning step of the total DNA with QIAamp DNA Mini Kit spin columns (Qiagen, Manchester, UK). All samples were run on a 1% agarose gel to estimate fragment size and sonicated with a Covaris ME220 Focused-ultrasonicator™ (Covaris Inc., Woburn, Massachusetts, USA). Sample shearing was implemented to produce fragment lengths of approximately 300 or 600 bp, depending on available fragment length distribution of total DNA and available sequencing platforms. Sonication was not performed on total DNA where the gel image indicated most fragments were already at or below a 300 bp threshold.

Library preparation was performed with the NEBNext® Ultra™ II Library Prep Kit and NEBNext® Multiplex Oligos for Illumina® (Dual Index Primers set 1 and 2) (New England BioLabs, Ipswich, MA, USA). The concentration of total DNA dilutions was measured with a Quantus™ Fluorometer (Promega Corporation, Madison, WI, USA). We started with 200 ng of total DNA following the protocol, or less if no more was available after extraction procedures (down to 11 ng). We cleaned and size-selected libraries to 300 bp with Agencourt AMPure XP Bead Clean-up (Beckman Coulter, Indianapolis, IN, USA), while only a cleaning step was performed for samples with highly degraded (peak of fragment length < 200 bp) and low total DNA (< 50 ng). A set of 96 ‘high-quality’ libraries with long mean total library length, predominantly including samples of silica-stored origin, was size-selected at

500-600 bp. Libraries were amplified through 8-12 PCR cycles, followed by bead clean-up. Library fragment length, DNA concentration and the presence of primer dimers were assessed with a 4200 TapeStation System (Agilent Technologies, Santa Clara, CA, USA). If library concentration was < 10 ng/µl, we performed additional PCR for 4-6 cycles followed by bead clean-up.

Enrichment of library pools was performed with our custom myBaits kit in pools of seven to seventeen DNA libraries. As much as possible samples were pooled with those that were (1) assumed to be closely related taxa and (2) of roughly similar library concentration after size selection (ng/µl). The MYbaits User Manual v3.02 was followed with the hybridization step set to 65°C for 20 hours. The pools were then amplified through PCR over 8-12 cycles with KAPA HiFi 2X HotStart ReadyMix PCR solution (Roche, Basel, Switzerland). We performed quality control for each pool through use of a TapeStation, after which pools were normalised to 4 nM, multiplexed, and denatured as preparation for sequencing on an in-house Illumina MiSeq machine (Illumina, San Diego, CA, USA) at the Jodrell Laboratory at the the Royal Botanic Gardens, Kew (Richmond, UK). Sequencing of most enriched libraries was run with four 2 x 150 bp v2 Illumina® MiSeq reagent kits. The 96 'high-quality' libraries containing longer insert lengths were pooled together and were sequenced with both a 2 x 250 bp v2 and a 2 x 300 bp v3 Illumina® MiSeq reagent kit.

2.2.3 Dataset assembly and phylogenetic analyses

The pipeline from raw sequences to phylogenetic inference is schematically portrayed in **Fig. 2.1**. Raw sequences were trimmed (removing adapters and low-quality bases) using Trimmomatic v0.36 (Bolger et al., 2014), employing recommended settings for Illumina® paired-end reads (ILLUMINACLIP:TruSeq3-PE.fa:2:30:10 LEADING:3 TRAILING:3 SLIDINGWINDOW:4:15 MINLEN:36). Before and after trimming we performed quality control steps through visualisation with FastQC v0.11.7 (Andrews, 2010).

Exon retrieval was performed using HybPiper v.1.3.1 (Johnson et al., 2016). Therein, the trimmed reads were mapped to target DNA sequences through the BWA mapper and assembled through SPAdes. Exon sequences were extracted without regions labeled by HybPiper as intronic and flanking regions. If multiple contigs are mapped against a reference, HybPiper discards all but the longest sequence by default unless multiple contigs cover over 85% of the target region. After this step, contigs are regarded as paralogous copies, where the true ortholog for further analysis is selected based on having a mean read

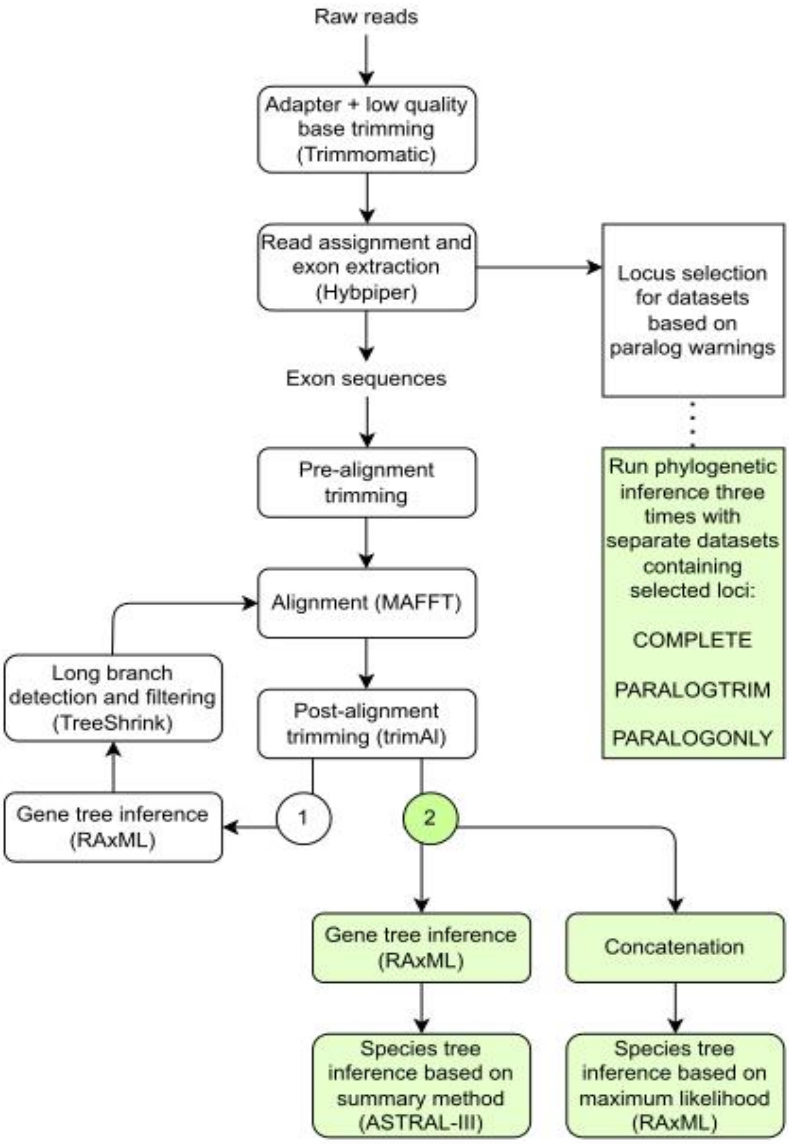

Fig. 2.1. Sequence data analysis flowchart from raw reads to phylogenies. The pre-alignment trimming consists of three separate steps: 1) removal of taxa with low number of reads on target 2) trimming of sequences shorter than basic threshold, and 3) removal of sequences shorter than percentage of median retrieved sequence length. The pipeline loops back once after long-branch detection in TreeShrink, after which the three datasets are constructed and separately analysed. Panels with green shading highlight where locus selection and final phylogenetic inference for the three distinct datasets occurs.

depth per base ten times higher than the others. If this is not the case the sequence with the highest percent identity to the reference is selected. In all downstream analyses we used the gene copies flagged as orthologs by HybPiper. The number of paralogous sequences that were retrieved per sample per locus was recorded using the “paralog_investigator.py” script of HybPiper.We used phylogenetic generalized least squares (pgls) mixed models through the ape package (Paradis and Schliep, 2019) in R (R Core Team, 2018) to further investigate the effect of the on-target rate on the efficiency of paralog detection. For the error term, we used as covariance structure a Brownian motion process of evolution based on the concatenated partitioned ML COMPLETE phylogeny (see Materials and Methods). For the loci that had paralog warnings issued by HybPiper for no more than ten taxa, we assessed their phylogenetic relationships by extracting all available sequences, including all paralogous copies, through the “paralog_retriever.py” script. Taxa with multiple copies of a locus were tested for monophyly through sequence alignment performed with MAFFT (--auto) with all retrieved copies included, followed by phylogenetic inference in FastTree (-nt -gtr) (Price et al., 2009). When duplicate sequences were monophyletic, it was assumed that they were allelic variants and not further considered as paralogs during dataset construction.

Samples were omitted from further steps if either < 12,000 reads were mapped to the targets or < 35 loci were retrieved through HybPiper. Additionally, samples for which any notes were taken on having any possibility of contamination were assessed through a preliminary analysis of alignments and phylogenies. Only samples noted to be potentially contaminated that also showed extreme heterogeneity or peaks of unexpected lengths on TapeStation images were omitted to not dismiss samples of which uncertainty of phylogenetic position is simply a result of stochastic error or reticulate evolution.

To investigate the effect of paralogous sequences on gene tree concordance, and topology and branch support for the species trees, three datasets were constructed from this point forward for phylogenetic inference. All 329 loci were used in the dataset COMPLETE, and based on the potential paralogs found within loci we constructed datasets PARALOGTRIM with 90 loci without detected paralogs, and PARALOGONLY with 239 loci that do contain paralogs.

Data cleaning steps were performed before and after alignment due to substantial variation in retrieved exon sequence lengths within loci causing alignment mismatch and long branch attraction. A two-step sequence exclusion step was implemented to remove short sequences from the sequence multi fasta files to prevent alignment errors. First, any

exon sequences were removed that were fewer than 300 bases in length. Then, sequences were removed when significantly shorter than the other available sequences for their respective locus, which was set to 40 percent of median sequence length to reduce the number of short sequences while not discarding too much data. The remaining sequences were aligned per locus with a speed-oriented run in MAFFT (--retree --maxiterate 200). Ragged ends of the alignments, which indicated intronic regions missed by the exon selection step in hybpiper were pruned using Phyutility (Smith and Dunn, 2008). We removed all sites for which more than 95% of the taxa had no information. Any remaining sequences that result in artificially long branches were removed using TreeShrink v1.3.3 (Mai and Mirarab, 2018). The maximum likelihood (ML) best trees for loci were generated with RAxML v8.2 (-f a -# 1 -m GTRGAMMA) (Stamatakis, 2006), and problematic sequences identified by TreeShrink using centroid rerooting and a false positive error rate below 0.05 were removed. Alignments for all loci were re-run with the same settings in MAFFT.

For all three datasets, phylogenetic inference was performed using both partitioned maximum likelihood and coalescent methods (i.e., estimating species trees using the summary statistics of a set of gene trees). For phylogenetic inference with a maximum likelihood method, alignments of separate loci were concatenated, partitioned (fasta_merge.py script from HybPiper), and run under a GTR-GAMMA model with 100 bootstraps (using the option -f a). For inference under a coalescent model, we ran RAxML with the same model and bootstraps to construct separate gene trees. Then, the RAxML "best trees" were used to estimate a species tree in ASTRAL-III v5.6.3 (Mirarab et al., 2014; Mirarab and Warnow, 2015) with local posterior probability (LPP) support values on branches. Robinson-Foulds (RF) distance values that count the number of splits that are unique to one of two trees were calculated through the Phytools (Robinson and Foulds, 1981; Revell, 2012) package in R. Concordance factor values for the species tree branches were calculated through IQ-TREE v2 (Minh et al., 2018, 2020), and more specifically obtained concordance factor values at the gene (gCF) and site (sCF) level (Nguyen et al., 2015; Minh et al., 2020).

We tested the number of mapped reads, and number of genes retrieved (any sequence and ≥ 50 %) between sections of *Saxifraga* through one-way analysis of variance (ANOVA). The percentage of reads on target and the sequence retrieval change with sample age were tested through ordinary least squares (OLS) linear models. We correlated the paralog warnings to the number of mapped reads, and therefore used mixed models through the ape package (Paradis and Schliep, 2019) in R (R Core Team, 2018),

employing phylogenetic generalized least squares (pgls). Both axes were log transformed to normalize data, and for the error term, we used as covariance structure a Brownian motion process of evolution based on the concatenated partitioned ML COMPLETE phylogeny.

2.3 Results

2.3.1 Target sequences for the RNA probes

The finalised dataset of target sequences contained 329 loci, of which 281 were present in the Saxifragales bait set and 48 were unique to the *Micranthes* bait set. Target length ranged from 318 to 4,017 bp, with a total length of 1,663,233 bp for all sequences combined. A total of 1,463 unique exon sequences were used by Arbor Biosciences for bait design to produce 38,731 bait sequences with 2x tiling.

2.3.2 Sequencing results

Total DNA extraction from herbarium sheets typically resulted in low starting concentrations of fragmented DNAs, but DNA libraries could successfully be made with starting amounts as low as 11.1 ng total DNA, opposed to the 200 ng suggested starting amount for the library preparation protocol. Year of collection from silica samples ranged from 2016 to 2018, while collection years from herbarium samples ranged from 1849 to 2018. For eight samples the exact year of collection could not be determined, including the oldest outgroup sample (*Telesonix heucheriformis* (Rydberg) Rydberg) that has been mounted on a herbarium sheet from at least 1832. The percentage of reads on target declined with collection age over all samples included (Adj. $R_2 = 0.096$, $P < 0.0001$), although the slope was less negative and non-significant when only regarding herbarium samples (Adj. $R_2 = 0.020$, $P = 0.063$) **(Fig. 2.2)**. Furthermore, the number of loci for which any sequence was retrieved declined with age (Adj. $R_2 = 0.027$, $P = 0.021$), or more than 50% of the target sequence was retrieved ($R_2 = 0.125$, $P = 0.000$).

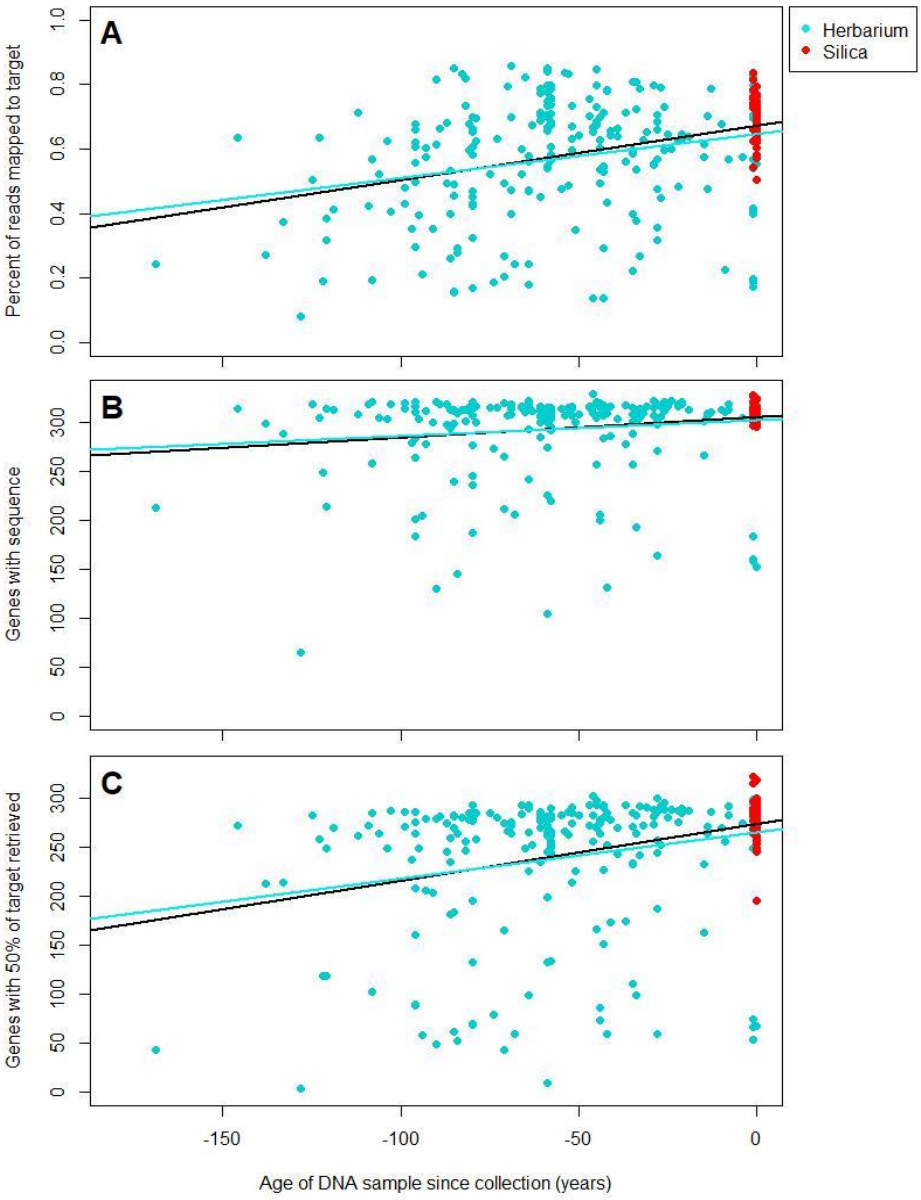

Fig. 2.2: Effect of age of DNA sample since collection in years on a) percent of reads that mapped to target, b) number of loci (out of total 329) for which a sequence was retrieved, and c) number of loci (out of total 329) with more than half of the target sequence retrieved. Regression lines shown are based on herbarium (blue lines) and all (black lines) data. Only ingroup taxa of Saxifraga are included.

Out of 322 sequenced accessions, 308 yielded enough and read data for further analysis. Of the samples retained for further analysis a median of 308 genes (min: 65, max: 329) had been recovered before short-sequence removal, and HybPiper was able to distribute a median 63% of trimmed reads to the targets (min: 6%, max: 86%). The total dataset included 59% of accepted species. Raw reads for 316 accessions (excluding contaminated and failed sequencing results) are available from the GenBank Sequence Read Archive (SRA) under BioProject number PRJNA672815 (http://www.ncbi.nlm.nih.gov/bioproject/PRJNA672815).

2.3.3 Sequencing success for taxonomic units

Sequence retrieval was variable but generally high throughout *Saxifraga* and the outgroups **(Fig. 2.3)**. The percentage of reads on target was lower in the outgroups than in *Saxifraga* (one-way ANOVA, $F_{(1, 306)} = 21.33$, $P = 0$), but the number of genes for which a sequence was retrieved did not differ between these groups (one-way ANOVA, $F_{(1, 306)} = 1.85$, $P = 0.176$). Nevertheless, the number of loci for which more than 50% of the target was retrieved did decrease in outgroup taxa (one-way ANOVA, $F_{(1, 306)} = 5.61$, $P = 0.012$). While we were able to use all loci for phylogenetic analyses, it is apparent some loci were retrieved only, or mostly, for specific clades **(Fig. 2.4)**. Within *Saxifraga*, especially the section *Irregulares* that is sister to the rest of the genus deviated, with three loci restricted to it and additional loci being sparsely retrieved in other sections.

2.3.4 Dataset construction with paralogous sequences

The total number of loci for which we recorded paralogs was a remarkably high 239 out of the total 329, and only after testing 20 loci with few paralog warnings for allelic variants a total of 90 loci remained without known paralogs. The average number of paralog warnings we obtained for our outgroups are lower than within the genus *Saxifraga* (one-way ANOVA; $F_{(1, 306)} = 5.85$, $P = 0.017$). Among sections we also find differences in the mean number of paralog warnings **(Fig. 2.5)**, although many present paralogs could be obscured since there was a positive relationship in paralog warnings retrieved with total reads on target (OLS; $R^2 = 0.212$, $P = 0$). The slope of the linear model of paralog warnings over reads on target was different depending on the use of herbarium or silica-dried material (one-way ANOVA; $F_{(1, 306)} = 5.84$, $P = 0$) **(Fig. 2.6)**. One outlier had been removed for the silica-sourced data in **Fig. 2.6**, which resulted in a better fit and marginal significance of the model. Nevertheless, silica samples with low total on-target reads are not available for a more thorough interpretation of a linear model. A mixed model with combined effect of section and source of DNA shows marginal support ($P < 0.1$) for a lower increase in paralog detection with reads on target for sections *Cilitae* and *Irregulares, compared to the other sections Bronchiales*, *Ligulatae*, *Porphyrion*, and *Saxifraga* that had a relatively high number of samples available as well as significant slopes (all $P < 0.05$).

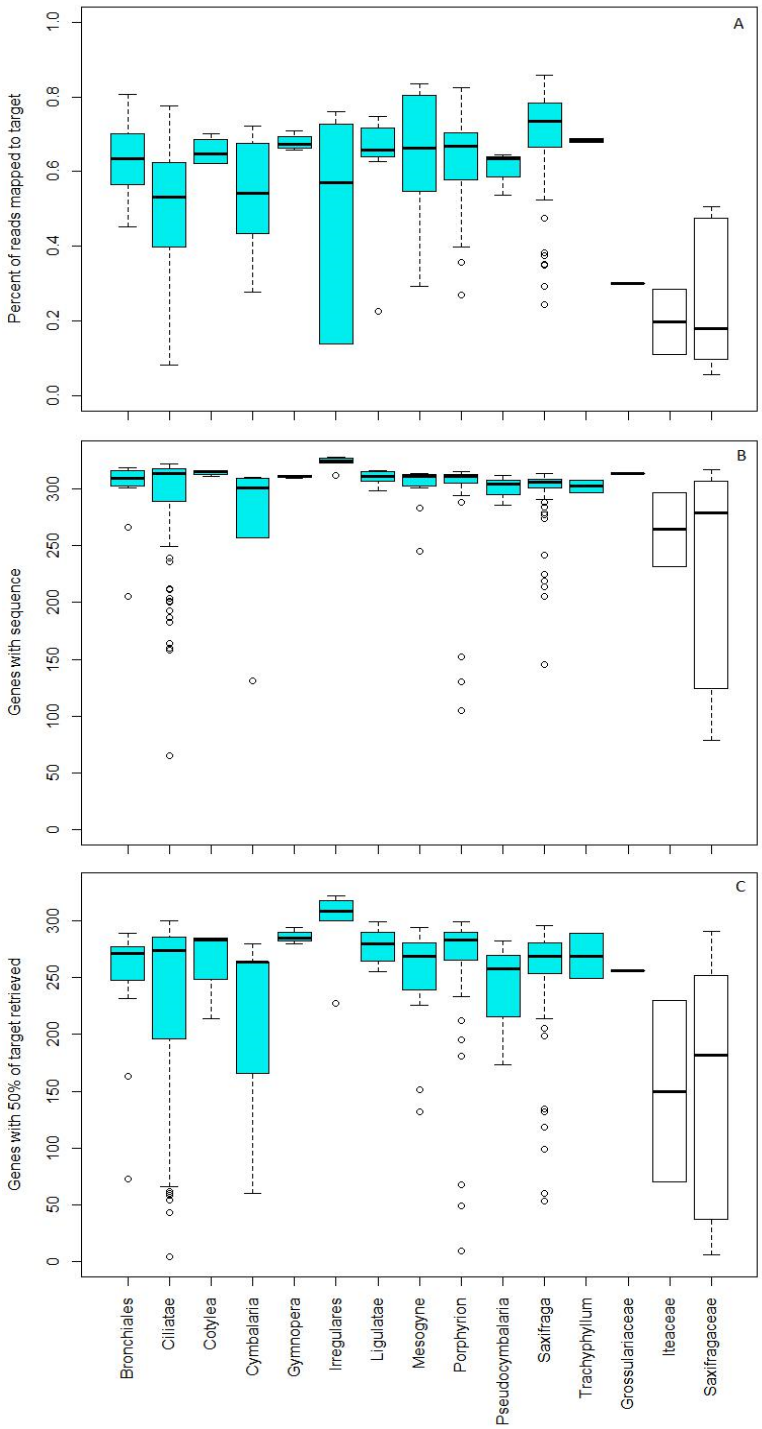

Fig. 2.3: Boxplots of sections of Saxifraga *and outgroups, for the a) percent of reads that mapped to target, b) the number of loci (out of 329) for which contigs resulted in a sequence, and c) the number of loci (out of 329) with more than half of the target sequence retrieved. Section names are shown with the number of included specimens.*

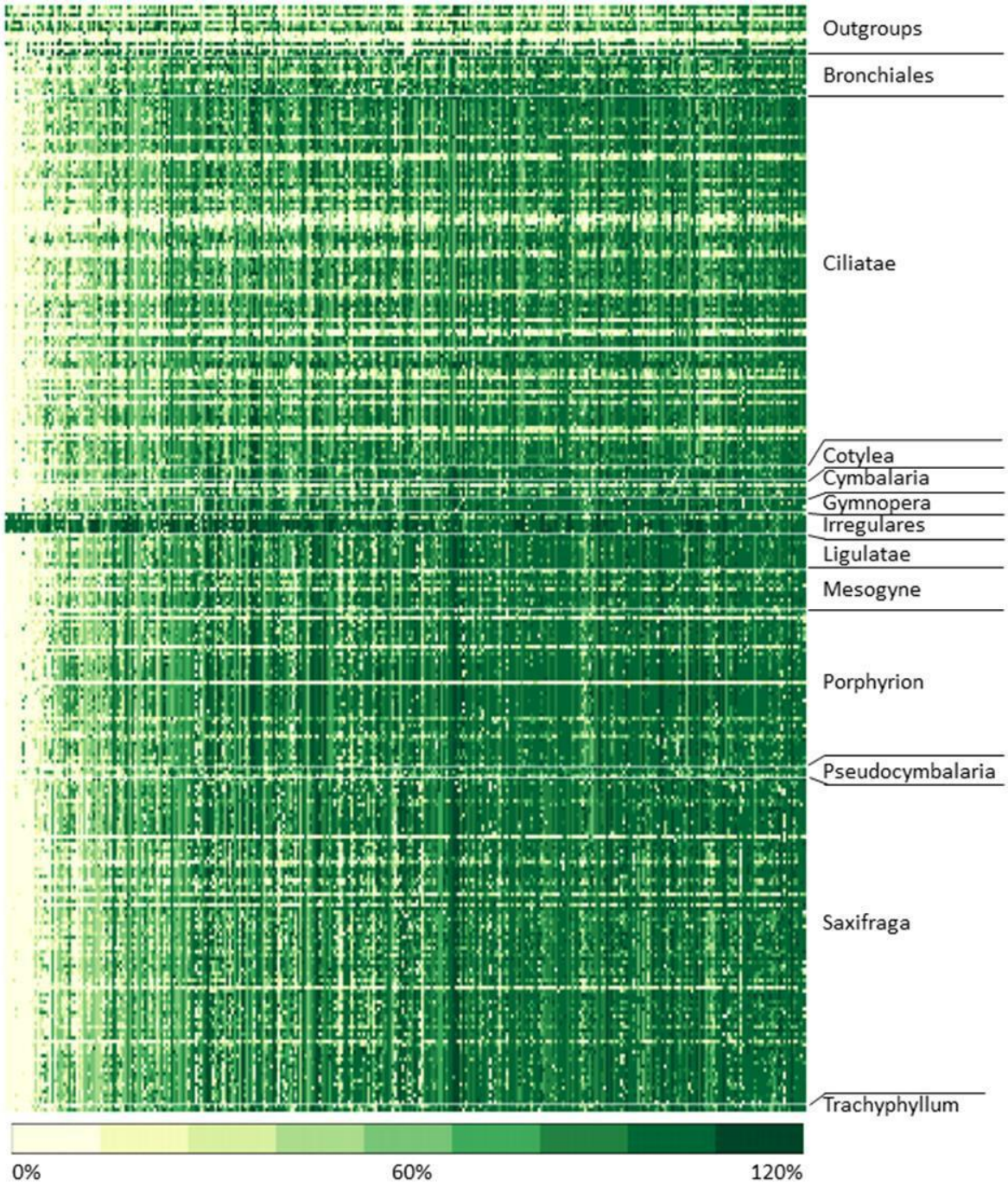

Fig. 2.4: Heatmap of retrieval rate of reference exon sequence length. Samples are shown on rows grouped as sections within Saxifraga *and columns represent locus ID's. Scale of retrieval rate is shown up to 1.2x target sequence length.*

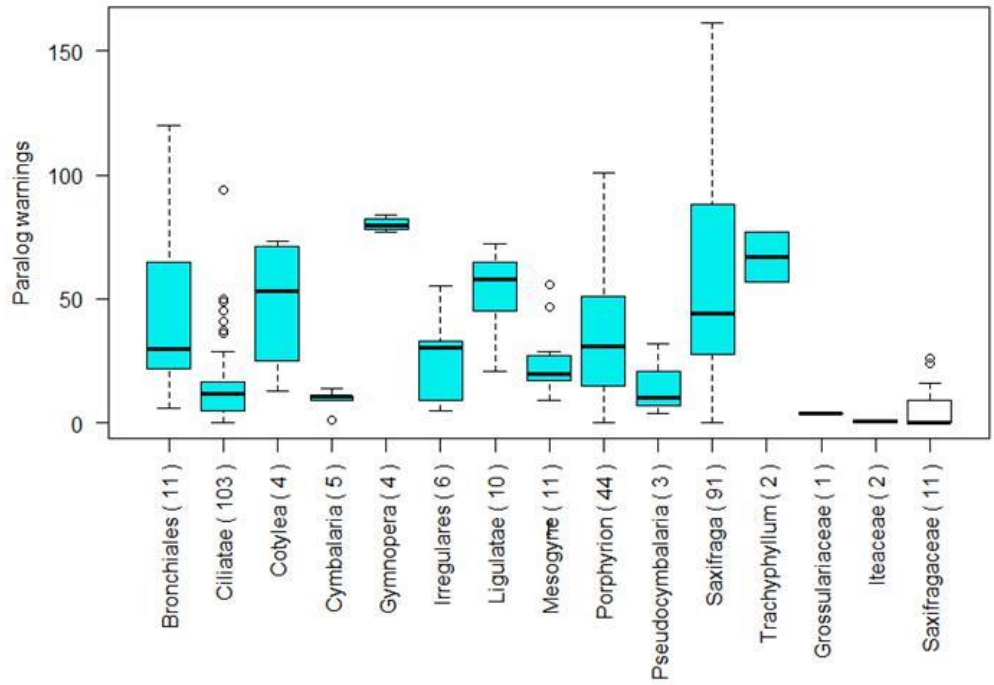

Fig. 2.5: Boxplots of sections of Saxifraga *and outgroups for the number of paralog warnings issued by HybPiper. The number of taxa included per taxonomic group are shown with names.*

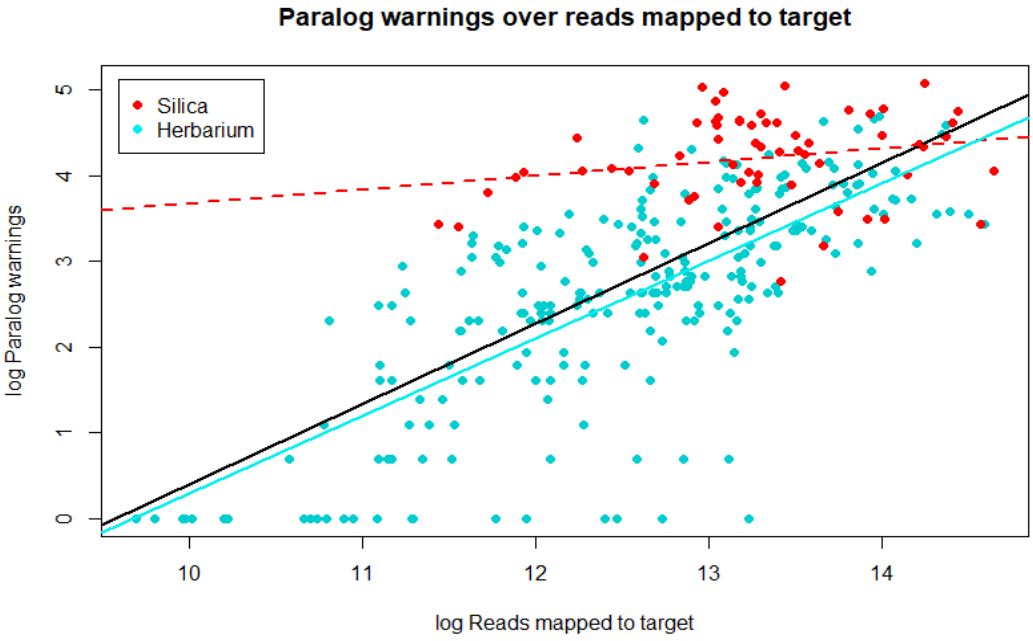

Fig. 2.6: Pgls analysis of log paralog warnings as a function of log reads mapped to target. Data points and regression lines are coloured by source of DNA. Only ingroup taxa of Saxifraga *are included. For the herbarium-sourced data there is a significant increase of paralog warnings with number of on-target reads (Adj. R^2 = 0.498, P < 0.0001), while only marginal significance is found for the silica stored samples (Adj. R^2 = 0.351, P = 0.079).*

With the average on-target rate for the six taxa from the reference bait sets (see section 2.2.1) being relatively low at 32%, the number of available raw reads per sample was an order of 10-100 times higher. Despite these facts, there were paralog warnings issued for only 36 out of 496 target loci, and only four out of the six taxa had any warnings at all, whereas the newly sequenced species had paralog warnings that were found not to be allelic variants in 298 out of 308.

The final exon sequence dataset of COMPLETE included all 329 loci, including those represented by few taxa as it has been shown that removal on basis of low sequence representation does not affect gene tree discordance (Molloy and Warnow, 2018). The datasets PARALOGTRIM and PARALOGONLY consisted of respectively 90 and 239 loci. Sequence removal after implementing TreeShrink resulted in a loss of 966 base positions throughout all data after realignment. The total aligned length of the final datasets before phylogenetic inference was 381,560 sites (COMPLETE), 113,541 sites (PARALOGTRIM) and 268,019 sites (PARALOGONLY).

2.3.5 Alignments

The total number of sequences and the average number of sequences per locus are given in **Table 2.1**. The PARALOGTRIM dataset was much smaller than PARALOGONLY, but more importantly it sequences available per locus was reduced more after all alignment trimming steps, resulting in 25% lower taxon availability per locus. Since the number of variable sites is barely lower in PARALOGTRIM in proportion to the number of loci, this results in relatively more gaps. The average GC content of the alignment consensus was 42.2% (min. 38.9% - max. 53.2% per locus).

		Untrimmed		Trimmed		
	Loci	Sequences	Taxa per locus	Sequences	Taxa per locus	Columns
COMPLETE	329	92,727	282	83,191	253	309,773
PARALOGONLY	239	70,318	294	64,869	271	227,096
PARALOGTRIM	90	22,409	249	18,322	204	94,269

Table 2.1: Alignment statistics for the three datasets. The number of sequences (each representing a taxon) and how many taxa are on average available per locus, is given for alignments before and after trimming steps as per Fig. 2.1. The total number of columns from the trimmed alignments are given for variable sites only.

2.3.6 Phylogenetics

We retrieved a 0.875 normalised quartet-score (Q-score) for the COMPLETE ASTRAL tree, and while it has overall high LPP support for the backbone of the phylogeny, many branches show strong discordance at the gene and site level **(Fig. 2.7)**. The PARALOGTRIM ASTRAL tree resulted in a Q-score of 0.886 and differed from COMPLETE ASTRAL by an RF-distance of 248. The PARALOGONLY ASTRAL tree was different from COMPLETE ASTRAL by a comparatively low RF-distance of 66, as well as a marginally lower Q-score of 0.884, showing an overall strong similarity in topology and support between COMPLETE and PARALOGTRIM datasets**.** For concatenated partitioned ML analyses of all datasets, we found high bootstrap support throughout the backbone of *Saxifraga*, while showing much lower support at shallow phylogenetic depth. When comparing topologies of concatenated ML and ASTRAL phylogenies of the same datasets, strong topological differences at shallow depths occur, with RF-distances of 293 (COMPLETE), 321 (PARALOGTRIM), and 297 (PARALOGONLY).

Further analysis of branch support provides more insight into the origin of the topological differences. Higher overall values of branch support were found in COMPLETE dataset branch LPP values compared to PARALOGTRIM (mean LPP = 0.86/0.77) and more nodes had an LPP above 50% (% nodes with LPP > 0.5 = 0.89/0.82). The mean gCF and sCF values were lower in COMPLETE (mean gCF = 25.06/25.74; mean sCF = 41.81/45.95). The relationship between gCF and sCF was plotted for both the COMPLETE and PARALOGTRIM datasets **(Appendix 2.2)** and revealed scattered data points in the gCF and sCF relationship, where some high gCF values coincide with a low sCF value and vice versa.

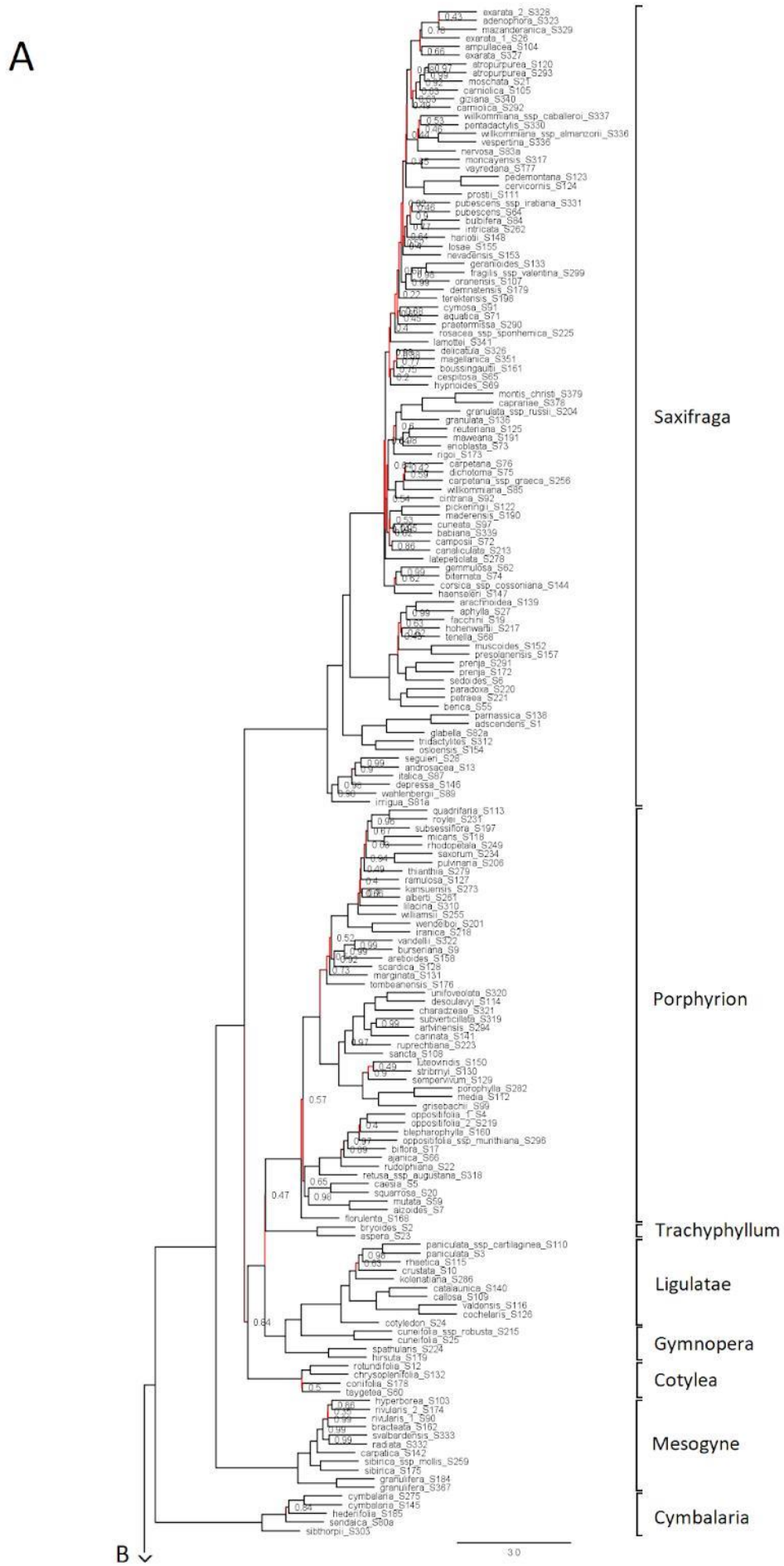
A
exarata_2_S328
adenophora_S323
mazanderanica_S329
exarata_1_S26
ampullacea_S104
exarata_S327
atropurpurea_S120
atropurpurea_S293
moschata_S21
carniolica_S105
gaziana_S30
carniolica_S292
willkommiana_ssp_caballeroi_S337
pentadactylis_S330
willkommiana_ssp_almanzorii_S336
vespertina_S336
nervosa_S83a
moncayensis_S317
vayredana_S177
pedemontana_S123
cervicornis_S124
prostii_S111
pubescens_ssp_irabana_S331
pubescens_S64
bubifera_S84
intricata_S262
hariotii_S148
losae_S155
nevadensis_S153
geranioides_S133
fragilis_ssp_valentina_S299
oranensis_S107
demnatensis_S179
terektensis_S198
cymosa_S91
equatica_S71
praetermissa_S290
rosacea_ssp_sponhemica_S225
lamottei_S341
delicatula_S326
magellanica_S351
boussingaultii_S161
cespitosa_S65
hyprioides_S69
montis_christi_S379
caprariae_S378
granulata_ssp_russii_S204
granulata_S135
reuteriana_S125
maweana_S191
androsacea_S73
rigoi_S173
carpetana_S76
dichotoma_S75
carpetana_ssp_graeca_S256
willkommiana_S85
cintrana_S92
pickeringii_S122
maderensis_S190
cuneata_S97
babiana_S339
camposii_S72
carialiculata_S213
latepetiolata_S278
gemmulosa_S62
biternata_S74
corsica_ssp_cossoniana_S144
haenseleri_S147
arachnoidea_S139
aphylla_S27
facchinii_S19
hohenwartii_S217
tenella_S68
muscoides_S152
presolanensis_S157
prenja_S291
prenja_S172
sedoides_S8
paradoxa_S220
petraea_S221
benca_S55
parnassica_S138
adscendens_S1
glabella_S82a
tridactylites_S312
osloensis_S154
seguieri_S28
androsacea_S13
italica_S87
depressa_S146
wahlenbergii_S89
irrigua_S81a
quadrifaria_S113
royle_S251
subaessiflora_S197
micans_S118
rhodopetala_S249
saxorum_S234
pulvinaria_S206
thianthla_S279
ramulosa_S127
kansuensis_S273
alberti_S261
lilacina_S310
williamsii_S255
wendelboi_S201
irranica_S218
vandellii_S322
burseriana_S9
aretioides_S158
scardica_S128
marginata_S131
tombeanensis_S176
unifoveolata_S320
desoulavyi_S114
charadzeae_S321
subverticillata_S319
artvinensis_S294
carinata_S141
ruprechtiana_S223
sancta_S108
luteovirldis_S150
stribrnyi_S130
sempervivum_S129
porophylla_S282
media_S172
grisebachii_S99
oppositifolia_1_S4
oppositifolia_2_S219
blepharophylla_S160
oppositifolia_ssp_murithiana_S296
biflora_S17
ajanica_S66
rudolphiana_S22
retusa_ssp_augustana_S318
caesia_S5
squarrosa_S20
mutata_S59
aizoides_S7
florulenta_S168
bryoides_S2
aspera_S23
paniculata_ssp_cartilaginea_S110
paniculata_S3
rhaetica_S115
crustata_S10
kolenatiana_S286
catalaunica_S140
callosa_S109
valdensis_S116
cochlearis_S126
cotyledon_S24
cuneifolia_ssp_robusta_S215
cuneifolia_S25
spathularis_S224
hirsuta_S119
rotundifolia_S12
chrysosplenifolia_S132
conifolia_S178
tsygetea_S60
hyperborea_S103
rivularis_2_S174
rivularis_1_S90
bracteata_S162
svalbardensis_S333
radiata_S332
carpatica_S142
sibirica_ssp_mollis_S259
sibirica_S175
granulifera_S184
granulifera_S367
cymbalaria_S275
cymbalaria_S145
hederifolia_S185
sendaica_S60a
sibthorpii_S303
Saxifraga
Porphyrion
Trachyphyllum
Ligulatae
Gymnopera
Cotylea
Mesogyne
Cymbalaria
B
3.0

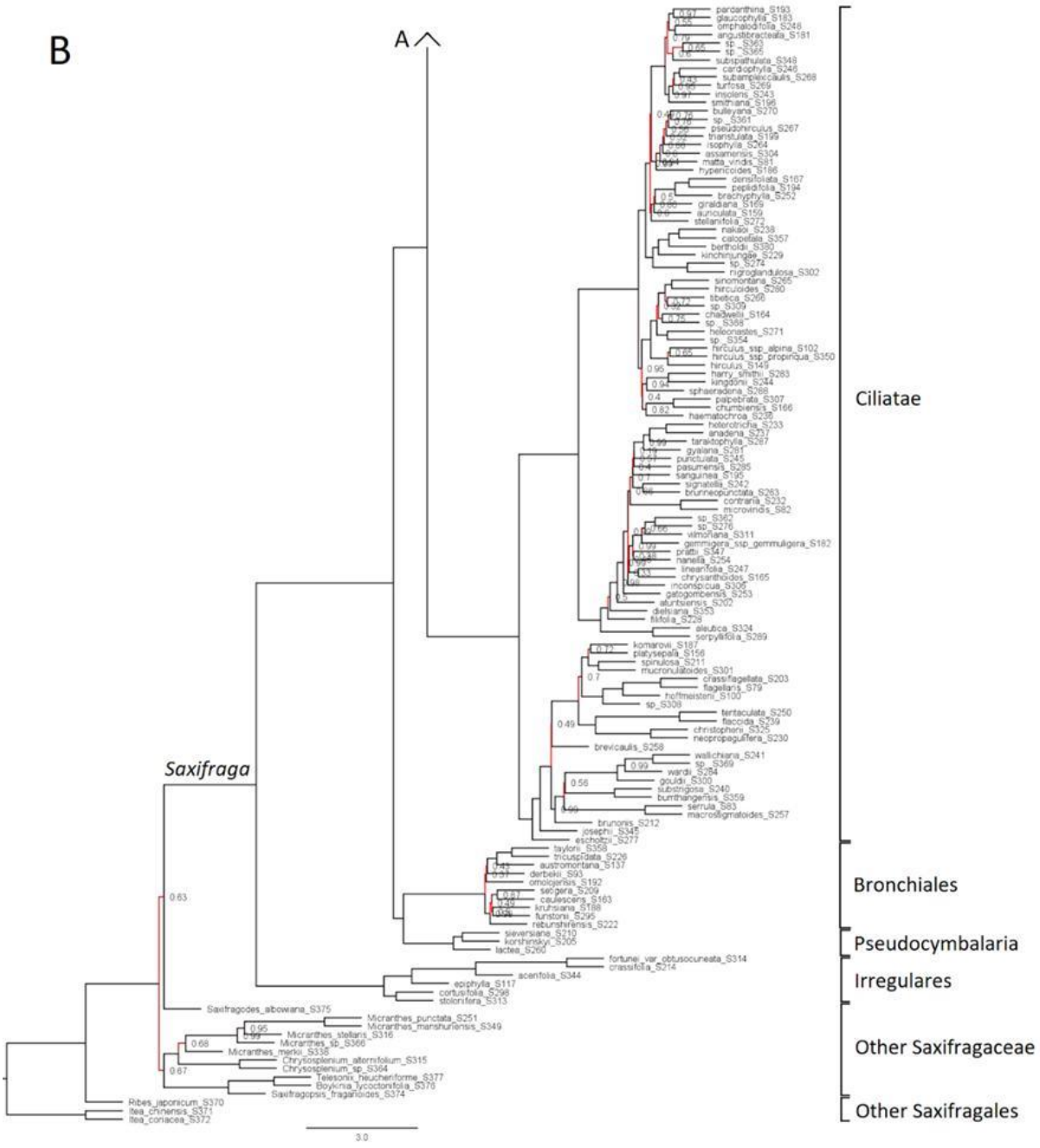

Fig. 2.7: ASTRAL species tree generated with the COMPLETE dataset (329 loci) with long branch filtering. Branch labels show ASTRAL local posterior probability (LPP) values below 100, and branches are coloured red if support is low (< 85 LPP). Branch lengths based on ASTRAL coalescent units, and terminal branches from ASTRAL output are unitless. Section names are shown to the right of the phylogeny.

2.4 Discussion

2.4.1 Museomics

In this study we find that target sequences for bait design specifically selected for a relatively closely related clade of plants provides a high percentage of reads on target overall (median 63%), while DNA starting material is available in much lower quantities than conventional protocols require. The reads on target obtained from our *Saxifraga* reference samples had nearly half the proportion of reads on target (average 31%). Compared to other hybrid-capture studies, we find that we obtain similar on-target rates as studies that use specialised baits for their respective clade (71 - 80%, Nicholls et al. (2015); median 48.61%, Villaverde et al. (2018)), while < 30% on target is more common in more universal probe sets (see Brewer et al., 2019), such as Angiosperms353 (Johnson et al., 2019; McLay et al., 2021). Of course, the percentage of reads that map to a target is affected not only by how well the baits match the targeted region (see McLay et al., 2021), but also by the quality of DNA starting material, lab procedures, stringency of assembly pipelines, and many other factors, and thus interpreting the efficiency of various bait sets is not at all straightforward. However, we find that using existing target sequences and previously generated raw read data provides a relatively cheap and efficient way of optimising target capture efforts for a taxonomic group of interest. Importantly, through this approach strong dataset compatibility is maintained through a high percentage of overlapping loci. In a situation where bait sets for target capture designed to cover a broad taxonomic group produce a dissatisfactory percentage of reads on target, selecting new bait sequences from existing data is a viable option as demonstrated here.

With the *Saxifraga* herbarium samples we show a less abrupt decline of sequence recovery with sample age than shown in other studies (Hart et al., 2016; Villaverde et al., 2018), especially for herbarium-sourced DNA. Previous publications give insight in the limits through time of museomics using hybrid-capture methods at various phylogenetic depths, specifically in herbarium specimens (e.g., Hart et al., 2016; Villaverde et al., 2018; Brewer et al., 2019; Folk et al., 2019; McLay et al., 2021). Through those papers we know increased age of herbarium samples (with associated DNA degradation and low total DNA after extraction) negatively affects the percentage of reads on target and total exon length that is effectively retrieved. While many confounding factors limit our ability to estimate the extent to which herbarium material can effectively be used with target capture techniques, highly specialized baits as used here could prove to extend the sample age range by decades.

2.4.3 Paralogy detection in target capture datasets

Paralogous copies of the targeted loci were found to be abundant throughout *Saxifraga*, while the putative low-copy loci were previously selected for on the higher taxonomic level of Saxifragales (Folk et al., 2019). The multi-step approach to assess paralogy that is employed throughout the data-retrieval process, acting from target locus selection to sequence retrieval, does not provide certainty of the absence of paralogs from the data (Conover et al., 2019; Stubbs et al., 2020). More so, multi-copy loci are expected to occur in groups such as *Saxifraga* as there are abundant indications of clade-specific polyploidy and ploidy levels varying within and among species (Webb and Gornall, 1989; Ebersbach et al., 2018; Ebersbach et al., 2020). Not as much strong evidence exists for polyploidy in the used outgroups, while this does occur in various families in Saxifragaceae (e.g., Visger et al., 2017; Stubbs et al., 2020). We clearly show an increased incidence of paralog warnings with number of reads on target, which in turn is negatively affected by the age and preservation method of the DNA sample. Hence, paralogy detection can be expected to decline when using increasingly old specimens in museomics and should be considered in data analysis steps. Nonetheless, the small difference in normalized Q-score between the COMPLETE and PARALOGTRIM datasets (Astral analysis) indicates that most gene tree-species tree incongruence is not due to failure to detect paralogy but rather due to incomplete lineage sorting or hybridization, both of which also affect orthologous loci. The topological disagreement among clades found between the PARALOGTRIM ASTRAL phylogeny and the topology established by Tkach et al. (2015) was limited to the placement of section *Trachyphyllum* and the subsections within section *Saxifraga*, as well as lowered LPP values for some nodes. On a shallow phylogenetic scale especially, species relationships show many incongruences (**Fig. 2.7**; branches with *< 85 LPP*).

Despite *Saxifraga*'s complex evolutionary history, we don't find detrimental effects of loci with non-orthologous copies for phylogeny estimation. Namely, despite high persistence of paralogous sequences in the untrimmed dataset we can build a phylogeny with lower stochastic error (low variance in gCF/sCF distribution) compared to the strict paralog trimmed dataset **(Appendix 2.2)**. Higher scatter in data points of gCF and sCF relationship would indicate more stochastic error affects the data than gene tree discordance from processes such as ILS (Minh et al., 2020). The higher normalised Q-score does also suggest that gene trees conflict compared to the species tree does not result from paralogy issues. The presence of paralogs does not necessarily have a detrimental impact on coalescent species tree inference, although they can potentially introduce more noise (Yan et al., 2020). As many taxonomists are moving towards NGS

and coalescent methods to better understand taxa with complex evolutionary histories, we need to consider not only establishing orthology, but we should always consider the presence of paralogy during tree building and analysis steps to clarify underlying gene tree conflict. Omitting loci expected to contain paralogs from large datasets is an easy and accepted option, although overcommitting to paralog removal can result in too high a loss of loci, while a certain threshold is needed to produce a high resolution species tree depending on the level of ILS and branch lengths (Sayyari and Mirarab, 2016; Shekhar et al., 2018). The loss of high amounts of informative data appears to impair phylogeny estimation more than inclusion of rampant paralogous sequences. Alternatively, when paralogs are found in the dataset after sequencing, loci can be grouped into gene families either through selection during the retrieval process by adding gene families to the target sequences (Johnson et al., 2016; Gardner et al., 2019) or after sequence retrieval (Moore et al., 2018).

2.5 Conclusion

The hybrid-capture target sequences that were designed specifically to maximise hybridization success for *Saxifraga* worked effectively. Throughout the sections of *Saxifraga* we were able to obtain a sequence for an average of 244 of the 329 target loci. A dozen loci were mainly obtained for the outgroups and sect. *Irregulares*, the sister clade to the rest of *Saxifraga,* possibly due to significant gene loss early in *Saxifraga* diversification. However, for other loci the phylogenetic density of retrieved sequences was high (i.e., sequence retrieval success was similar among phylogenetic clusters within the targeted range of genetic diversity). Overall, reads on target were approximately as high as in other studies focusing on genus to family level phylogenetic depth (Brewer et al., 2018; Villaverde et al., 2018).

For degraded DNAs from museum material, we find that a lower percentage of reads map back to targets with increased age of the sample. This issue is well known and depends on degradation of DNA over time and the collection and storage methods (Nicholls et al., 2015; Brewer et al., 2018; Forrest et al., 2018). Importantly, while for silica-stored DNA samples we find that the number of detected paralogous copies declines with the number of reads on target, the number of paralogous copies detected for museum DNA samples declines at a much faster rate. This suggests that sequences retrieved from degraded DNAs are less likely to meet the standards of common paralog detection pipelines that accept paralog status based on the relative sequence length and raw read coverage of contig positions (e.g., Hybpiper: Johnson et al., 2015). Hence, with museomics we should be cautious while interpreting the presence of multi-copy loci. Furthermore, paralog removal criteria have been in constant revision during the development of NGS analysis pipelines, although it is currently understood that the presence of paralogs does not impede species tree analysis under the multi-species coalescent (Hellmuth et al., 2015; Yan et al., 2020). We show that removal of loci with strong presence of paralogs in a group with a complex evolutionary history is detrimental to species tree inference, as stochastic error, and subsequent phylogenetic branch (and quartet) support are negatively affected.

Chapter 3: Phylogenomic analysis of the genus *Saxifraga*

3.1 Introduction

With over 440 species, *Saxifraga* is the largest genus within Saxifragaceae (Engler and Irmscher, 1916; Tkach et al., 2015b). *Saxifraga* has a broad distribution throughout the Northern Hemisphere, with a few disjunct species south of the Tropic of Cancer. Two centres of diversity occur, in the European Alpine system and in the Qinghai-Tibet plateau and surrounding systems (Webb and Gornall, 1989). Specifically, the most diverse clades in the genus consist of alpine specialists, with strong evidence of ecological shifts into the alpine biome and development of novel characters that contributed to extant high species diversity (Ebersbach et al., 2017b, 2018).

Saxifraga is morphologically diverse, and the only characters binding all taxa are floral structures; 3-colpate pollen, the (near) absence of a free hypanthium and stamens inserted near the ovary wall (Webb and Gornall, 1989). Defining clades has been historically difficult due to indeterminate characters within the genus (Engler and Irmscher, 1916; Gerschwitz-Eidt and Kadereit, 2020). For example, ovary position is nearly homogenous within families in Saxifragales, but varies among closely related species in *Saxifraga (Soltis et al., 2013)*. In addition, various unique characters that are otherwise rare throughout Saxifragales have evolved within *Saxifraga* once or in various sections independently, including bulbils (basal or on flowering stem), lime-secreting hydathodes, stolons and zygomorphic flowers (Zhang and Gornall 2011; Gornall 1987). After revisions by Gornall (1989) and Tkach et al. (2015b), the delineation of subgeneric sections and their determinate characters have been resolved to great extent. However, obtaining phylogenetic support to establish monophyly has been difficult due to conflict among genetic markers caused by hybridization (Brochmann et al., 1998; Steen et al., 2000; Brochmann and Håpnes, 2001; Ebersbach et al., 2020) and low genetic differentiation resulting from evolutionary radiations (Ebersbach et al., 2017b; Li et al., 2018).

Previous efforts to build phylogenies for *Saxifraga* based on nuclear and plastid DNA markers have incurred far-reaching taxonomic changes as compared to the fundamental morphological delineation of sections by Engler and Irmscher (1916). *Saxifraga* has long been a polyphyletic based on early phylogeny estimation within Saxifragaceae and was finally resolved as monophyletic after exclusion of sect. *Micranthes* (Haw.) D.Don as a distantly related separate genus (Soltis et al., 1996; Deng et al., 2015; Tkach et al., 2015b). Recently, the relationship of *Saxifraga* to other tribes of Saxifragaceae was further resolved through phylogeny estimation of genome-scale hybrid-capture data, placing the genus as sister to tribe Cascadieae R.A.Folk & D.E.Soltis (Folk et al., 2021),

and sections were revised and found monophyletic by Tkach et al. (2015a, 2015b), although nuclear and plastid markers show different evolutionary histories (Soltis et al., 1996; Conti et al., 1999; Vargas et al., 1999; Zhang et al., 2008; Deng et al., 2015; Tkach et al., 2015b).

The stem age of *Saxifraga* was estimated to be 73.63 million years (Ma) old by Ebersbach et al. (2017b), which corresponds to a Late Cretaceous origin, and the crown node was placed in the Paleocene at 61.75 Ma. *Saxifraga* is expected to have originated on the West of the American continent, after which it moved into Eurasia where high rates of diversification occurred in various episodes (Ebersbach et al., 2017a, 2017b), which are assumed to be associated with episodes of mountain uplift and climatological changes. Previous divergence time estimates for the stem of the genus are much younger (e.g., 38.45 Ma, Gao et al. 2015; 38.37 Ma, Deng et al., 2015) and are expected to be skewed to a younger age due to a lower available number of ingroup taxa, loci and fossil calibration data (Ebersbach et al., 2017a). To elucidate the origination of *Saxifraga* diversity and distribution in light of geological and climate change events, further corroboration of divergence times is needed.

In this chapter we aim to 1) infer a phylogenetic tree from target capture data for the genus *Saxifraga*, with a high coverage of species diversity and representatives from all established and tentative sections and subsections. We describe the difference in topology and support between phylogenetic inference from gene trees and our species tree, and further discuss revisions for *Saxifraga* taxonomy alongside two papers that shaped modern delineation of sections within *Saxifraga* (Gornall, 1987; Tkach et al., 2015b). In addition, we aim (2) to estimate divergence times of sections in *Saxifraga* through a highly resolved species tree and inclusion of more outgroup nodes for time calibration. We discuss the implications of phylogenomics and divergence time estimation on the study of *Saxifraga* evolutionary history.

3.2 Materials and methods

3.2.1 Taxon and locus selection

The sequence data generated in chapter 2 of this thesis was used, as well as *Saxifraga* target capture data from Folk et al. (2019). We defined (sub)sections as per the extensive revision by Gornall (Gornall, 1987), that was later confirmed by Tkach et al. (2015). Accepted species epithets were assigned to (sub)sections separately from accepted names

collected from Plants of the World Online (POWO, 2019; retrieved 18-8-2018). Selection of *Saxifraga* spp. for sequencing in chapter 2 was performed as to include taxa not available in Folk et al. (2019), with specific effort to include all known distinct sections and subsections. Additional outgroup sequence data from (Folk et al., 2019) was included to accommodate time calibration of the phylogeny (see further description for time calibration under "3.2.3 Divergence time estimation"), with broad sampling of clades within Saxifragales (see Fishbein et al., 2001; Jian et al., 2008; Soltis et al., 2013).

The same 329 target loci and reference sequences were used as in chapter 2. Since sequences generated by Folk et al. (2019) were the result of hybrid capture sequencing with both target sequences generated therein, as well as those from Stubbs et al. (2018), we could extract the same target loci.

3.2.2 Sequence alignment and phylogenetic inference

Raw sequences had adapters and low-quality bases removed through Trimmomatic v0.36 (Bolger et al., 2014), employing recommended settings for Illumina® paired-end reads (ILLUMINACLIP:TruSeq3-PE.fa:2:30:10 LEADING:3 TRAILING:3 SLIDINGWINDOW:4:15 MINLEN:36). Quality control steps were used before and after trimming through visualisation with FastQC v0.11.7 (Andrews, 2010). Exon retrieval was performed using HybPiper v.1.3.1 (Johnson et al., 2016). The trimmed reads were mapped to target DNA sequences through the BWA mapper (Li, 2013) and assembled through SPAdes v3.11 (Bankevich et al., 2012), after which exon sequences are extracted without intron and flanking regions.Before sequence alignment, short sequences were removed to prevent alignment errors. First, any exon sequences were removed that were fewer than 150 bases in length. Second, sequences were removed if below 25 percent of median sequence length. The sequences that remained were aligned per locus with a speed-oriented run in MAFFT (--retree -- maxiterate 200) (Katoh and Standley, 2013). Any potential intronic regions that remained were pruned using Phyutility (Smith and Dunn, 2008), by removing sites that were not represented by >99% of the taxa.

Maximum likelihood (ML) best trees were generated per locus with RAxML v8.2 (-f a -# 100 -m GTRGAMMA) (Stamatakis, 2006). Outlier long branches in gene trees were selected using TreeShrink v1.3.3 (Mai and Mirarab, 2018), using centroid rerooting and a false positive error rate below 0.05. Then, sequences that resulted in those long branches were removed and the other sequences were again aligned with the same settings in MAFFT, then pruned with Phyutility, and again we performed ML phylogeny estimation through RAxML for all loci. Finally, we collapsed branches in gene trees with ≤ 10% bootstrap support to lower

species-tree estimation error, which was suggested to be a reliable threshold by Zhang et al. (2018). Phylogeny inference under a coalescent model was performed with ASTRAL-III v5.6.3 (Mirarab et al., 2014; Mirarab and Warnow, 2015), generating local posterior probability (LPP) support values and quartet scores for branches (Sayyari and Mirarab, 2016). The pipeline from raw data to the species tree is summarised in **Fig. 3.1**.

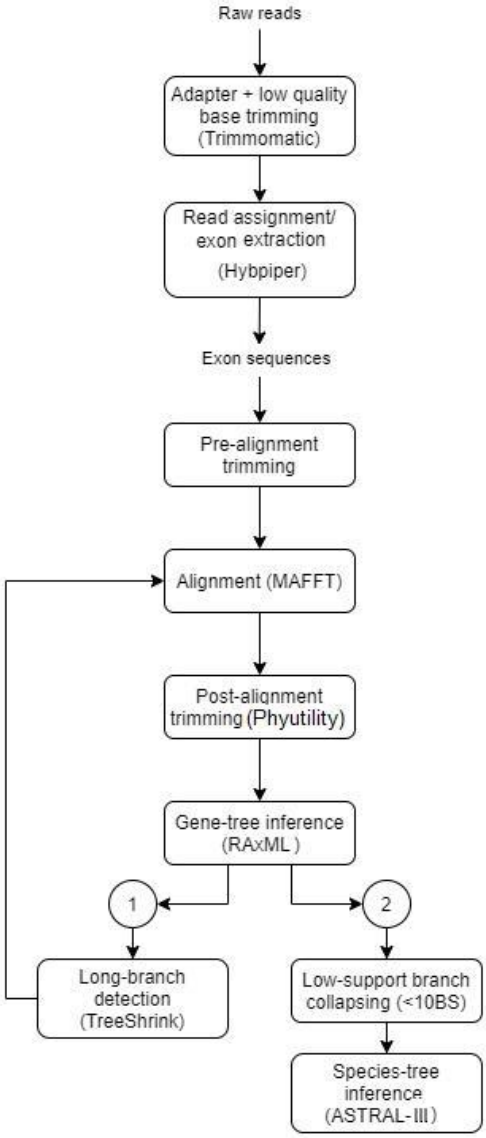

Fig. 3.1. Sequence data analysis flowchart from raw reads to phylogenies for exon and supercontig datasets. The pipeline loops back once after long-branch detection in TreeShrink. The pre-alignment trimming consists of three separate steps: 1) removal of taxa with low number of reads on target 2) trimming of sequences shorter than basic threshold, and 3) removal of sequences shorter than percentage of median retrieved sequence length.

3.2.3 Divergence time estimation

Since no fossils were available for Saxifragaceae, we included fossil calibrations for outgroups from within Saxifragales. We used an age estimate for the crown node of *Ribes* of 15.6 Ma (million years from present), which is older than the age used by Ebersbach et al. (2016a), because we use the species *Ribes barrowsae* described from the United States Buffalo Canyon flora (Hermsen, 2005). The stem node for Ribes was set to 48.9 Ma (Hermsen, 2005; Moss et al., 2005), complying with the younger age choice from Ebersbach et al. (2017a). For the Itea stem node, we set a constraint at 49 Ma, based on Eocene pollen from North America (Hermsen, 2013). The crown node of the Saxifragaceae alliance was constrained at 89 Ma, based on the characteristics of fossil genus *Divisestylus,* described in Hermsen et al. (2003). Here we follow Ebersbach et al. (2017a) to choose morphological resemblance of *Divisestylus* to both Saxifragaceae and Iteaceae over some evidence it could be placed as sister to Iteaceae, as this may need further corroboration (Hermsen et al., 2006). The Altingiaceae family stem was constrained at 89 Ma on the node of the most recent common ancestor of *Altingia siamensis* and *Distylopsis laurifolia*. This was based on floral structures from the upper Cretaceous (Zhou et al., 2001). For the Haloragaceae family stem, we used an age of 70.6 Ma, on the most recent common ancestor of *Penthorum chinense* and *Gonocarpus oreophilus*, which was derived from floral structures from the Cretaceous (Hernandez-Castillo and Cevallos-Ferriz, 1999).

Divergence time estimation was carried out through both a penalised likelihood and Bayesian method. The estimation through penalised likelihood was performed with treePL (Smith and O'Meara, 2012). The input phylogeny requires branch lengths indicating molecular change, which we generated while accounting for gene tree incongruence that can result in divergence time estimation errors. We first omitted loci that were represented by < 75% of all taxa in the species tree. Then, we used a novel script to cycle through branches in (exon) gene trees to test if all descendants in a clade are the same as in the species tree, irrespective of topology therein, to then produce a congruence score. Loci were not used further if more than 30% of well-supported clades (bootstrap support > 75) in the gene tree were incongruent with the species tree. The input phylogeny was estimated through RAxML for concatenated alignments of 46 selected loci as per the settings previously used for the gene trees while constraining (-g) by the topology of the coalescent species tree.

Compared to other divergence time estimation methods, treePL does not allow for much flexibility in manipulating priors. For instance, treePL assumes that substitution rates are inherited between ancestral and descendant branches and implements a smoothing parameter which describes how much rates should differ between branches that were selected through cross-validation (Sanderson, 1997, 2002). Though more importantly, calibration of node ages allows only for minimum and maximum age constraints. The minimum constraints are the only direct fossil evidence data we can implement, thereby inflating node ages. Hence, we use probability density to set a maximum constraint on the stem of *Ribes*, using the predictive distribution of fossil occurrences (see Donoghue and Yang, 2016). Importantly, we can use *Ribes* due to well-documented fossil records of many described taxa with similar propensity to fossilise (Hermsen, 2005; Moss et al., 2005). Various approaches exist to calculate a confidence interval for the distribution of the sampled fossils (Marshall,1997; Wang et al., 2016), though here we use the more conservative approach and set the maximum constraint at two times the largest time interval between the fossils used for minimum constraints in *Ribes*, added to the minimum constraint of the stem node (79 Ma).

Bayesian methods can have difficulty to converge when analysing large datasets in terms of tree tips and alignment length (Tamura et al., 2012; Höhna et al., 2016), and therefore we used a more rigid data selection process than used for treePL. We used 55 tips with relevance for setting priors on nodes and covering familial and infrageneric *Saxifraga* crown nodes. Taxa were chosen only if sequences were available for > 50% of all loci and the taxon had none or low recorded naturally occurring hybridization as summarised by Ebersbach et al. (2020). For locus selection, gene tree topologies were compared to the species tree topology, although trees were pruned down to the selected 64 tips. Loci were not used if more than 30% of well-supported branches (LPP > 80) in the gene tree were incongruent with the species tree. For the 28 loci that were subsequently selected, we realigned sequences with MAFFT (--retree --maxiterate 200) and performed post-alignment trimming of sites (Phyutility) if not represented by > 50% of taxa present in the alignment, leaving a combined alignment length of 51,293 sites.

For the Bayesian approach to divergence time estimation, we used BEAST v2.6.3 (Drummond et al., 2002; Bouckaert et al., 2019). The 64-tip exon tree was used as a topological constraint. Without the constrained phylogeny the run would have difficulty initializing or failed to converge. Two separate analyses were run with an uncorrelated relaxed clock model (Drummond et al., 2006) and a birth-death model of speciation. Nodes age priors were set as log-normal distributions and we used the conservative distribution shapes used by Ebersbach et al. (2017a) (m = 1.5, SD = 1.0). Initially, a uniform

distribution with a minimum constraint was tested for most nodes, along with a normal distribution prior for the Saxifragaceae alliance crown node, although the posterior distributions failed to converge under these priors. The alignments were partitioned, and fitting nucleotide substitution models were selected with ModelFinder (Kalyaanamoorthy et al., 2017). Analyses were run for 100 million generations with samples drawn every 5,000 generations and two independent analyses were run from different starting seeds. Visual inspection for convergence was performed in Tracer 1.6 (Rambaut et al., 2014), to test if effective sample size (ESS) values for each parameter had reached >200. LogCombiner and TreeAnnotator of the BEAST 2 package were used to summarise the runs after a burn-in of 20% and to generate a maximum clade credibility (MCC) tree.

Visualisation of time-calibrated, ultrametric trees from the treePL and BEAST runs was performed with FigTree v1.4.4 (Rambaut, 2010) and through R package geoscalePhylo (Gradstein et al., 2012).

3.3 Results

3.3.1 Alignments and phylogenetic analyses

We used 519 hybrid-capture DNA accessions that remained after all quality screening and data cleaning steps, of which 321 accessions from chapter 2, and 198 from Folk et al., (2019). All sections and subsections of *Saxifraga* were represented **(Table 3.1)**, not considering uncertainty of monophyly of subsections within section *Ciliatae*. The coverage of accepted species in the genus (disregarding infraspecific ranks) is 320 out of 462 (69%). The exon data after post-alignment trimming steps had a total of 400,638 sites of which 391,022 (97.60%) were variable, the supercontig data had 1,682,003 sites of which 1,679,850 (99.87%) were variable. The average number of genes available per alignment was 243.9 (SD: 68.0). The mean GC content in exon consensus sequences was 43.41% (SD = 0.019), and a lower mean of 38.36% (SD = 0.020) was found in supercontigs.

Table 3.1: Sections and subsections of genus Saxifraga *supported by phylogenetic analysis of Tkach et al. (2015) and subsections of sect.* Ciliatae *outlined by Gornall (1987). The diversity coverage shows number of accepted species (disregarding infraspecific ranks) as per POWO.*

Section	**Type**	**Diversity coverage**
Heterisia (Raf. ex Small) A.M.Johnson	*S. mertensiana Bong.*	1/1
Irregulares Haw.	*S. stolonifera Meerb.*	11/17
Saxifragella (Engl.) Gornall & Zhou-Xin Zhang	*S. bicuspidata (Hook.f.) Engl.*	1/1
Pseudocymbalaria Zhmylev	*S. sieversiana Sternb.*	3/4
Bronchiales DeChaine	*S. bronchialis L.*	7/11
Ciliatae Haw.	*S. hirculus L.*	130/214
subsect. *Flagellares* (C.B.Clarke) Engl. & Irmsch.	*S. flagellaris* Willd.	10/19
subsect. *Gemmiparae* Engl. & Irmsch.	*S. gemmipara* Franch.	15/24
subsect. *Hemisphaericae* (Engler & Irmscher)	*S. hemisphaerica* Hook.f.	2/3
subsect. *Hirculoideae* (Engler & Irmscher) Gornall	*S. nigroglandulosa* Engl. & Irmsch.	68/111
subsect. *Rosulares* Gornall	*S. sediformis* Engl. & Irmsch.	33/54
subsect. *Serpyllifoliae* Gornall	*S. serpyllifolia* Pursh.	2/3
Cymbalaria Griseb.	*S. cymbalaria L.*	4/4
Odontophyllae Gornall	*S. odontophylla Wall. ex Sternb.*	1/1
Mesogyne Sternb.	*S. sibirica L.*	7/9
Saxifraga Gornall	*S. granulata L.*	76/87
subsect. *Tridactylites* (Haw.) Gornall	*S. tridactylites* L.	4/4
subsect. *Androsaceae* (Engl. & Irmsch.) Tkach, Röser & M.H.Hoffm.	*S. androsacea* L.	7/8
subsect. *Arachnoideae* (Engl. & Irmsch.) Tkach, Röser & M.H.Hoffm.	*S. arachnoidea* Sternb.	11/11
subsect. *Saxifraga*	*S. granulata* L.	54/64
Cotylea Tausch	*S. rotundifolia L.*	4/5
Gymnopera D.Don	*S. hirsuta L.*	3/3
Incertae sedis	*S. cuneifolia L.*	1/1
Ligulatae Haw.	*S. cotyledon L.*	8/9
Trachyphyllum (Gaudin) W.D.J.Koch	*S. aspera L.*	2/2
Porphyrion Tausch	*S. oppositifolia L.*	62/93
subsect. *Squarrosae* (Engl. & Irmsch.) Tkach, Röser & M.H.Hoffm.	S. squrrosa Sieber	2/2
subsect. *Mutatae* (Engl. & Irmsch.) Gornall	*S. mutata* L.	2/2
subsect. *Oppositifoliae* Hayek	*S. oppositifolia* L.	3/3
subsect. *Florulentae* (Engl. & Irmsch.) Gornall	*S. florulenta* Moretti	1/1
subsect. *Kabschia* (Engl.) Rouy & Camus	*S. marginata* Sternb.	54/85

For the exon phylogeny we retrieved a normalised quartet-score (Q-score) of 0.893 **(Fig. 3.2),** slightly higher than for species trees generated in chapter 2. The gene trees therefore have a higher proportion of agreeing quartet trees, in part due to the imposed low-support branch contraction on gene trees, and despite the introduction of new sequences with a low number of retrieved sequences. For the supercontig analysis we found a Q-score of 0.930 **(Appendix 3.1)**, thus having less conflicting quartet trees after the introduction of non-coding sequences. While the normalised Q-score for the supercontig phylogeny is higher, we use the exon tree for the divergence time estimation pipeline since the backbone nodes have slightly higher support (Q-score and LPP) and the overall higher Q-score is likely attributed to species-level relationships.

Table 3.1: Sections and subsections of genus Saxifraga *supported by phylogenetic analysis of Tkach et al. (2015) and subsections of sect.* Ciliatae *outlined by Gornall (1987). The diversity coverage shows number of accepted species (disregarding infraspecific ranks) as per POWO.*

were monophyletic with sect. *Ligulatae*. Conflict among gene trees was relatively high, however, and we retrieved a Q-score of 57.12 for the quartet grouping sect. Ligulatae and *S. cuneifolia*. Among gene trees, high discordance was found for the placement of *S. cuneifolia* taxa, which could be grouped within sect. *Ligulatae* or sect. *Gymnopera*. In addition, within some gene trees the three accessions of *S. cuneifolia* could be placed within both sections. Despite the contended position of *S. cuneifolia*, overall the

3.3.2 Topology of major clades in *Saxifraga*

All non-monotypic sections within *Saxifraga* showed high branch support (LPP = 1), and a relatively high proportion of quartet trees that agree with the species tree (Q-score > 80) **(Fig. 3.2)**. However, since major clades have marginally higher support values in the exon phylogeny, we use exon tree branch support values to describe the topology. The branch leading to sect. *Irregulares* had slightly higher discordance among gene trees (Q-score = 77.60). The three specimens of *S. cuneifolia* L. were not grouped in sect. *Gymnopera* and phylogenies support for the sections established by Gornall (1987) and Tkach et al. (2015b) was high. We find support for 15 sections, and at least 15 subsections **(Table 3.1)**.

Various topological differences among sections as compared to Tkach et al. (2015b) were found in the estimated phylogeny. Here, we present the main differences in topology. We retrieved sect. *Bronchiales* and sect. *Pseudocymbalaria* as sister clades with high support and moderate gene tree conflict (LPP = 1, Q-score = 53.87). Where previously a large polytomy occurred, we found that the various sections that are sister to sect. *Cymbalaria*, first the sister groups sect. *Mesogyne* and sect. *Odontophyllae* were supported (LPP = 1, Q-score = 43.12), after which sect. *Saxifraga* diverged from a remainder of sections including species rich sect. *Porphyrion* and sect. *Ligulatae* that as a clade had

relatively low support (LPP = 0.93, Q-score = 40.80). For sect. *Ligulatae* and sect. *Gymnopera*, as well as undetermined *S. cuneifolia*, there is high support for their monophyletic grouping (LPP = 1, Q-score = 66.96). While sect. *Trachyphyllum* has been difficult to place in previous studies as it was found to be polyphyletic (Engler and Irmscher, 1916, Gornall, 1987), after changes to nomenclature (Gornall, 1987; DeChaine et al., 2013), the phylogeny by Tkach et al. (2015b) placed them as sister to sect. *Ligulatae* with low ML support based on ITS and trnL-trnF gene regions. With 329 loci, we could again not confidently place this section, as the quartet trees leading to sect. *Trachyphyllum* showed highly incongruent underlying gene trees in both the exon (LPP = 0.53, Q-score = 35.66) and supercontig phylogeny (LPP = 0.48, Q-score = 34.88). Within the framework of this study, we can consider sect. *Trachyphyllum* as part of a tripartion, along with sect. *Porphyrion* and the clade involving sect. *Ligulatae* and sect. *Gymnopera*.

3.3.3 Divergence times

Overall, the treePL and BEAST results show many differences between each other and other publications **(Table 3.2)**. Node ages in the outgroups and crown of *Saxifraga* in the treePL result are slightly younger than most other recent estimates (Ebersbach et al. 2017a; Gao et al., 2017) **(Fig. 3.3)**. Stem node ages of families in Saxifragales were estimated to be mostly in the Upper Cretaceous at approximately 75 Ma by studies with a broader taxon and fossil calibration sampling strategy (e.g., Magallon et al., 1999; Folk et al., 2021; Tarullo et al., 2021), and our estimates from treePL are quite close to these values (79 Ma). However, the *Saxifraga* stem (67.56 Ma) and crown (47.38 Ma) nodes we retrieved are much younger, placing these nodes in the Paleocene and Eocene, respectively.

The median divergence times estimated through BEAST are considerably older, while showing substantial highest posterior density (HPD) intervals **(Fig. 3.4)**. For the Saxifragacea alliance crown node and *Ribes* stem node priors we found an older age compared to Eberbach et al. (2017a) for the latter. However, ESS scores of < 100 would be common even if the analysis was re-run with model simplification steps, using a Yule model of speciation or a single-partition HKY substitution model (data not presented here). Therefore, the BEAST results may be considered dubious, although we do find strong similarity nodes found by Ebersbach et al. (2017a), as confidence intervals always overlap, except for the sect. *Cotylea* stem and crown node **(Table 3.2)**.

A

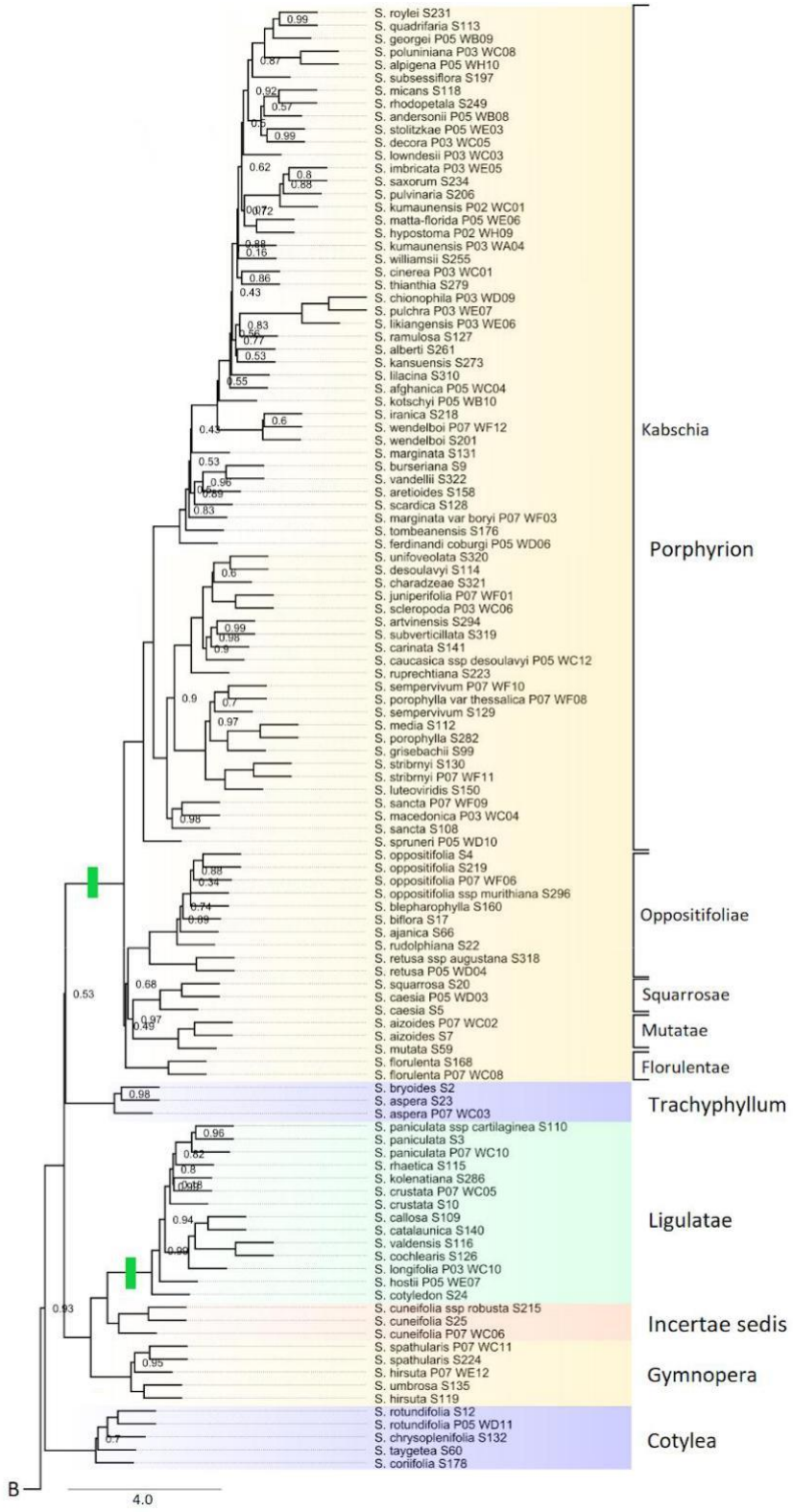
S. roylei S231
S. quadrifaria S113
S. georgei P05 WB09
S. poluniniana P03 WC08
S. alpigena P05 WH10
S. subsessiflora S197
S. micans S118
S. rhodopetala S249
S. andersonii P05 WB08
S. stolitzkae P05 WE03
S. decora P03 WC05
S. lowndesii P03 WC03
S. imbricata P03 WE05
S. saxorum S234
S. pulvinaria S206
S. kumaunensis P02 WC01
S. matta-florida P05 WE06
S. hypostoma P02 WH09
S. kumaunensis P03 WA04
S. williamsii S255
S. cinerea P03 WC01
S. thianthia S279
S. chionophila P03 WD09
S. pulchra P03 WE07
S. likiangensis P03 WE06
S. ramulosa S127
S. alberti S261
S. kansuensis S273
S. lilacina S310
S. afghanica P05 WC04
S. kotschyi P05 WB10
S. iranica S218
S. wendelboi P07 WF12
S. wendelboi S201
S. marginata S131
S. burseriana S9
S. vandellii S322
S. aretioides S158
S. scardica S128
S. marginata var boryi P07 WF03
S. tombeanensis S176
S. ferdinandi coburgi P05 WD06
S. unifoveolata S320
S. desoulavyi S114
S. charadzeae S321
S. juniperifolia P07 WF01
S. scleropoda P03 WC06
S. artvinensis S294
S. subverticillata S319
S. carinata S141
S. caucasica ssp desoulavyi P05 WC12
S. ruprechtiana S223
S. sempervivum P07 WF10
S. porophylla var thessalica P07 WF08
S. sempervivum S129
S. media S112
S. porophylla S282
S. grisebachii S99
S. stribrnyi S130
S. stribrnyi P07 WF11
S. luteoviridis S150
S. sancta P07 WF09
S. macedonica P03 WC04
S. sancta S108
S. sprunerii P05 WD10
S. oppositifolia S4
S. oppositifolia S219
S. oppositifolia P07 WF06
S. oppositifolia ssp murithiana S296
S. blepharophylla S160
S. biflora S17
S. ajanica S66
S. rudolphiana S22
S. retusa ssp augustana S318
S. retusa P05 WD04
S. squarrosa S20
S. caesia P05 WD03
S. caesia S5
S. aizoides P07 WC02
S. aizoides S7
S. mutata S59
S. florulenta S168
S. florulenta P07 WC08
S. bryoides S2
S. aspera S23
S. aspera P07 WC03
S. paniculata ssp cartilaginea S110
S. paniculata S3
S. paniculata P07 WC10
S. rhaetica S115
S. kolenatiana S286
S. crustata P07 WC05
S. crustata S10
S. callosa S109
S. catalaunica S140
S. valdensis S116
S. cochlearis S126
S. longifolia P03 WC10
S. hostii P05 WE07
S. cotyledon S24
S. cuneifolia ssp robusta S215
S. cuneifolia S25
S. cuneifolia P07 WC06
S. spathularis P07 WC11
S. spathularis S224
S. hirsuta P07 WE12
S. umbrosa S135
S. hirsuta S119
S. rotundifolia S12
S. rotundifolia P05 WD11
S. chrysoplenifolia S132
S. taygetea S60
S. coriifolia S178
Kabschia
Porphyrion
Oppositifoliae
Squarrosae
Mutatae
Florulentae
Trachyphyllum
Ligulatae
Incertae sedis
Gymnopera
Cotylea
B
4.0

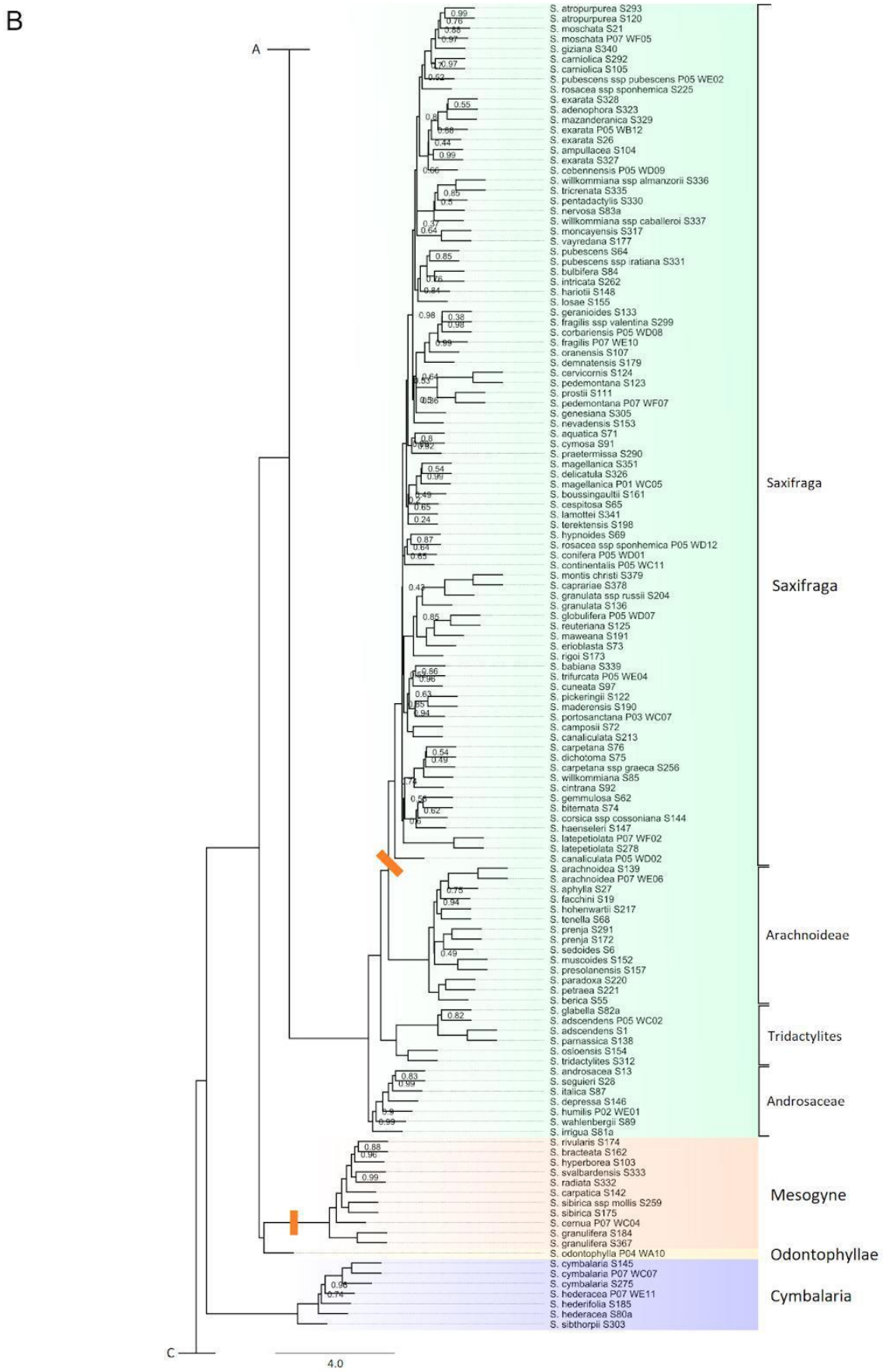
B
A
C
4.0
S. atropurpurea S293
S. atropurpurea S120
S. moschata S21
S. moschata P07 WF05
S. giziana S340
S. carniolica S292
S. carniolica S105
S. pubescens ssp pubescens P05 WE02
S. rosacea ssp sponhemica S225
S. exarata S328
S. adenophora S323
S. mazanderanica S329
S. exarata P05 WB12
S. exarata S26
S. ampullacea S104
S. exarata S327
S. cebennensis P05 WD09
S. willkommiana ssp almanzorii S336
S. tricrenata S335
S. pentadactylis S330
S. nervosa S83a
S. willkommiana ssp caballeroi S337
S. moncayensis S317
S. vayredana S177
S. pubescens S64
S. pubescens ssp iratiana S331
S. bulbifera S84
S. intricata S262
S. hariotii S148
S. losae S155
S. geranioides S133
S. fragilis ssp valentina S299
S. corbariensis P05 WD08
S. fragilis P07 WE10
S. oranensis S107
S. demnatensis S179
S. cervicornis S124
S. pedemontana S123
S. prostii S111
S. pedemontana P07 WF07
S. genesiana S305
S. nevadensis S153
S. aquatica S71
S. cymosa S91
S. praetermissa S290
S. magellanica S351
S. delicatula S326
S. magellanica P01 WC05
S. boussingaultii S161
S. cespitosa S65
S. lamottei S341
S. terektensis S198
S. hypnoides S69
S. rosacea ssp sponhemica P05 WD12
S. conifera P05 WD01
S. continentalis P05 WC11
S. montis christi S379
S. caprariae S378
S. granulata ssp russii S204
S. granulata S136
S. globulifera P05 WD07
S. reuteriana S125
S. maweana S191
S. erioblasta S73
S. rigoi S173
S. babiana S339
S. trifurcata P05 WE04
S. cuneata S97
S. pickeringii S122
S. maderensis S190
S. portosanctana P03 WC07
S. camposii S72
S. canaliculata S213
S. carpetana S76
S. dichotoma S75
S. carpetana ssp graeca S256
S. willkommiana S85
S. cintrana S92
S. gemmulosa S62
S. biternata S74
S. corsica ssp cossoniana S144
S. haenseleri S147
S. latepetiolata P07 WF02
S. latepetiolata S278
S. canaliculata P05 WD02
S. arachnoidea S139
S. arachnoidea P07 WE06
S. aphylla S27
S. facchini S19
S. hohenwartii S217
S. tenella S68
S. prenja S291
S. prenja S172
S. sedoides S6
S. muscoides S152
S. presolanensis S157
S. paradoxa S220
S. petraea S221
S. berica S55
S. glabella S82a
S. adscendens P05 WC02
S. adscendens S1
S. parnassica S138
S. osloensis S154
S. tridactylites S312
S. androsacea S13
S. seguieri S28
S. italica S87
S. depressa S146
S. humilis P02 WE01
S. wahlenbergii S89
S. irrigua S81a
S. rivularis S174
S. bracteata S162
S. hyperborea S103
S. svalbardensis S333
S. radiata S332
S. carpatica S142
S. sibirica ssp mollis S259
S. sibirica S175
S. cernua P07 WC04
S. granulifera S184
S. granulifera S367
S. odontophylla P04 WA10
S. cymbalaria S145
S. cymbalaria P07 WC07
S. cymbalaria S275
S. hederacea P07 WE11
S. hederifolia S185
S. hederacea S80a
S. sibthorpii S303
Saxifraga
Saxifraga
Arachnoideae
Tridactylites
Androsaceae
Mesogyne
Odontophyllae
Cymbalaria

C

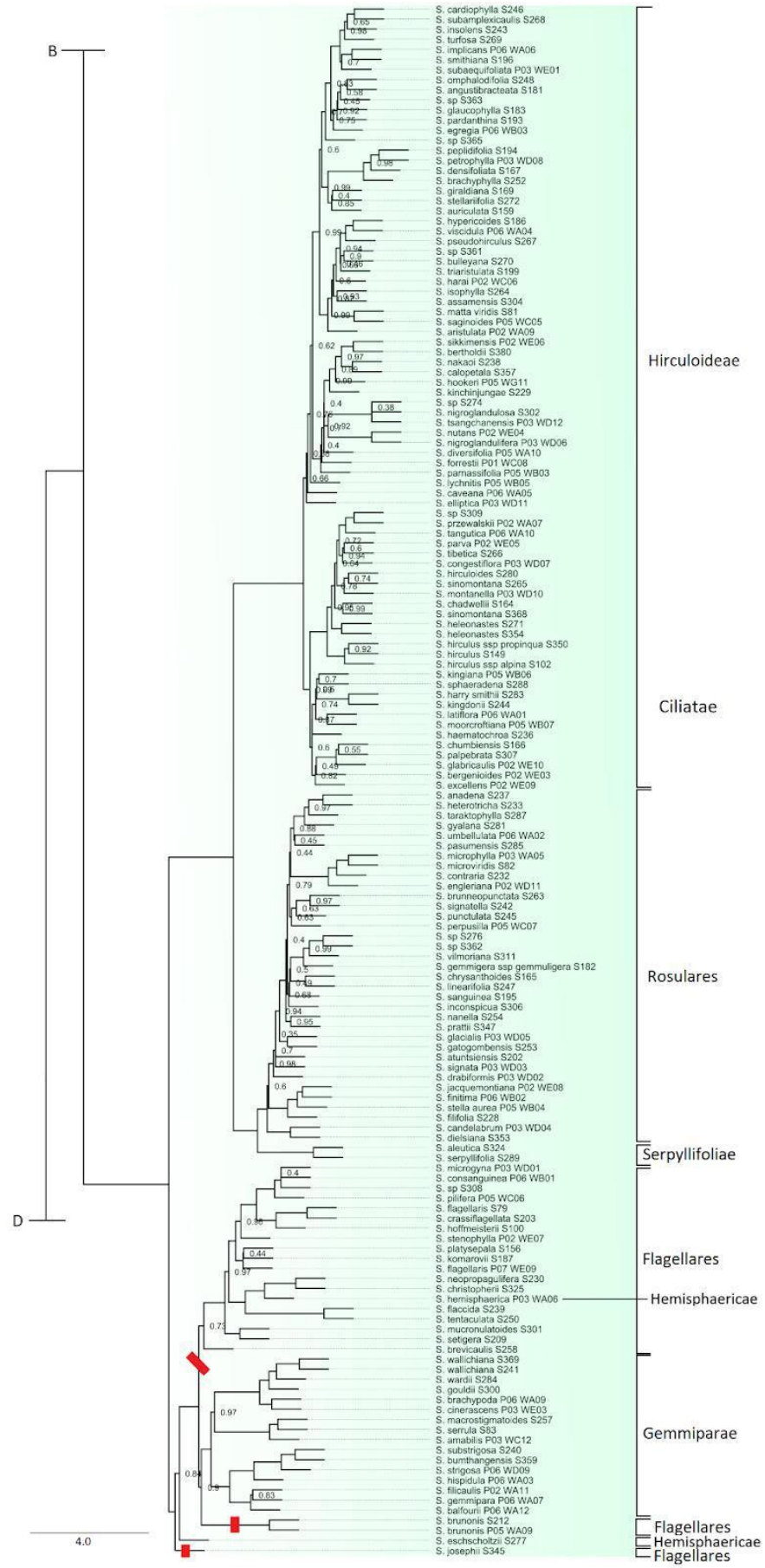
B
D
4.0
S. cardiophylla S246
S. subamplexicaulis S268
S. insolens S243
S. turfosa S269
S. implicans P06 WA06
S. smithiana S196
S. subaequifoliata P03 WE01
S. omphalodifolia S248
S. angustibracteata S181
S. sp S363
S. glaucophylla S183
S. pardanthina S193
S. egregia P06 WB03
S. sp S365
S. peplidifolia S194
S. petrophylla P03 WD08
S. densifoliata S167
S. brachyphylla S252
S. giraldiana S169
S. stellariifolia S272
S. auriculata S159
S. hypericoides S186
S. viscidula P06 WA04
S. pseudohirculus S267
S. sp S361
S. bulleyana S270
S. triaristulata S199
S. harai P02 WC06
S. isophylla S264
S. assamensis S304
S. matta viridis S81
S. saginoides P05 WC05
S. aristulata P02 WA09
S. sikkimensis P02 WE06
S. bertholdii S380
S. nakaoi S238
S. calopetala S357
S. hookeri P05 WG11
S. kinchinjungae S229
S. sp S274
S. nigroglandulosa S302
S. tsangchanensis P03 WD12
S. nutans P02 WE04
S. nigroglandulifera P03 WD06
S. diversifolia P05 WA10
S. forrestii P01 WC08
S. parnassifolia P05 WB03
S. lychnitis P05 WB05
S. caveana P06 WA05
S. elliptica P03 WD11
S. sp S309
S. przewalskii P02 WA07
S. tangutica P06 WA10
S. parva P02 WE05
S. tibetica S266
S. congestiflora P03 WD07
S. hirculoides S280
S. sinomontana S265
S. montanella P03 WD10
S. chadwellii S164
S. sinomontana S368
S. heleonastes S271
S. heleonastes S354
S. hirculus ssp propinqua S350
S. hirculus S149
S. hirculus ssp alpina S102
S. kingiana P05 WB06
S. sphaeradena S288
S. harry smithii S283
S. kingdonii S244
S. latiflora P06 WA01
S. moorcroftiana P05 WB07
S. haematochroa S236
S. chumbiensis S166
S. palpebrata S307
S. glabricaulis P02 WE10
S. bergenioides P02 WE03
S. excellens P02 WE09
S. anadena S237
S. heterotricha S233
S. taraktophylla S287
S. gyalana S281
S. umbellulata P06 WA02
S. pasumensis S285
S. microphylla P03 WA05
S. microviridis S82
S. contraria S232
S. engleriana P02 WD11
S. brunneopunctata S263
S. signatella S242
S. punctulata S245
S. perpusilla P05 WC07
S. sp S276
S. sp S362
S. vilmoriana S311
S. gemmigera ssp gemmuligera S182
S. chrysanthoides S165
S. linearifolia S247
S. sanguinea S195
S. inconspicua S306
S. nanella S254
S. prattii S347
S. glacialis P03 WD05
S. gatogombensis S253
S. atuntsiensis S202
S. signata P03 WD03
S. drabiformis P03 WD02
S. jacquemontiana P02 WE08
S. finitima P06 WB02
S. stella aurea P05 WB04
S. filifolia S228
S. candelabrum P03 WD04
S. dielsiana S353
S. aleutica S324
S. serpyllifolia S289
S. microgyna P03 WD01
S. consanguinea P06 WB01
S. sp S308
S. pilifera P05 WC06
S. flagellaris S79
S. crassiflagellata S203
S. hoffmeisterii S100
S. stenophylla P02 WE07
S. platysepala S156
S. komarovii S187
S. flagellaris P07 WE09
S. neopropagulifera S230
S. christopherii S325
S. hemisphaerica P03 WA06
S. flaccida S239
S. tentaculata S250
S. mucronulatoides S301
S. setigera S209
S. brevicaulis S258
S. wallichiana S369
S. wallichiana S241
S. wardii S284
S. gouldii S300
S. brachypoda P06 WA09
S. cinerascens P03 WE03
S. macrostigmatoides S257
S. serrula S83
S. amabilis P03 WC12
S. substrigosa S240
S. bumthangensis S359
S. strigosa P06 WD09
S. hispidula P06 WA03
S. filicaulis P02 WA11
S. gemmipara P06 WA07
S. balfourii P06 WA12
S. brunonis S212
S. brunonis P05 WA09
S. eschscholtzii S277
S. josephii S345
Hirculoideae
Ciliatae
Rosulares
Serpyllifoliae
Flagellares
Hemisphaericae
Gemmiparae
Flagellares
Hemisphaericae
Flagellares

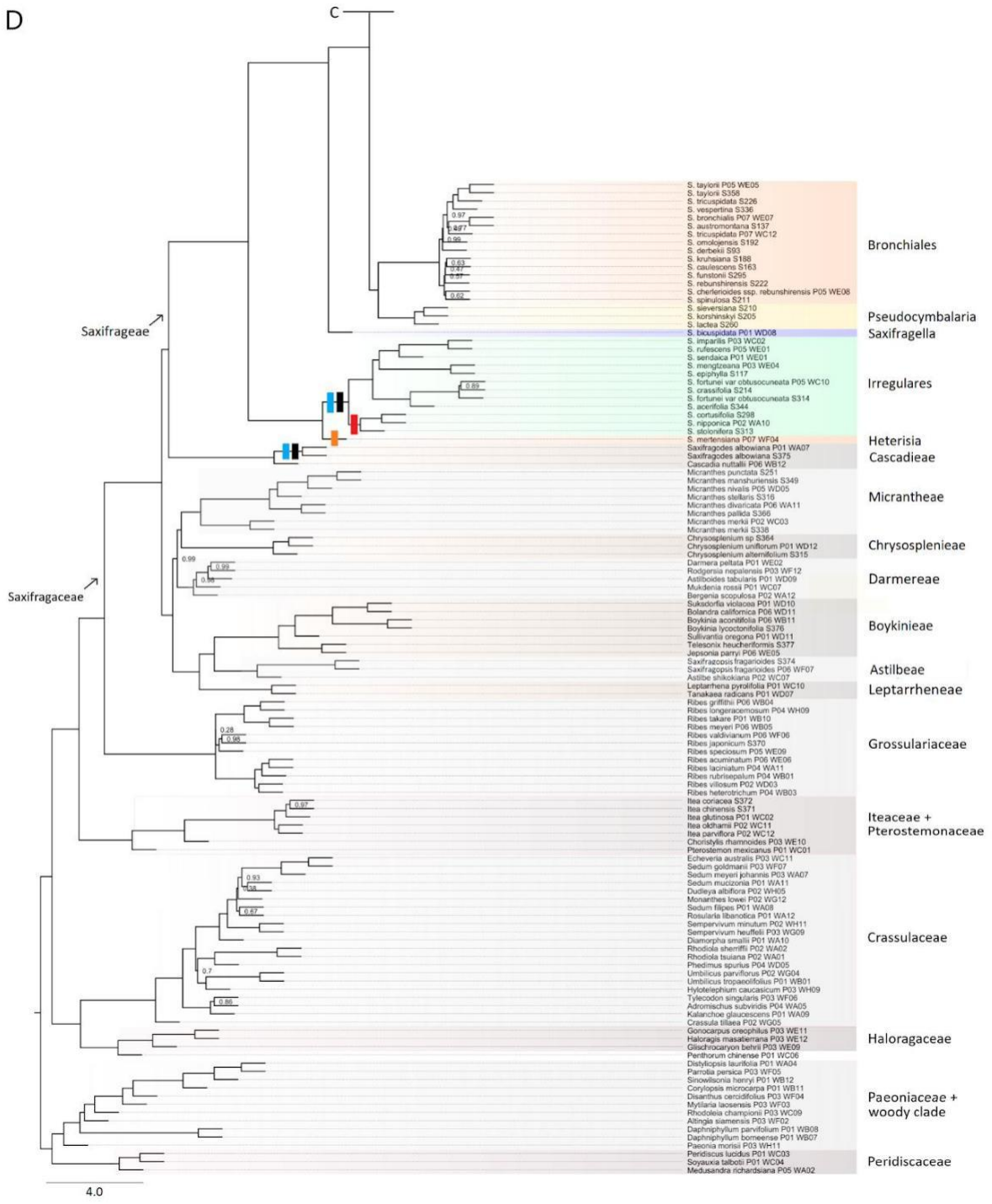

Fig. 3.2: ASTRAL species tree generated from 329 exon nDNA gene trees. Branch labels show ASTRAL local posterior probability (LPP) value, which are not reported when LPP = 1. Branch lengths are based on coalescent units and terminal branches are dimensionless. Connections between figure panels A,B,C,D are shown within figures. Occurrence (apomorphy) of key deterministic characters for section delimitation is shown on branches: red: stolons, green: lime-secreting hydathodes on leaf margins, blue: zygomorphic flowers, black: foliar calcium oxalate crystals, orange: bulbils (either replacing flowers or partially underground near base of stalk, secondary loss within subsect. Saxifraga*).*

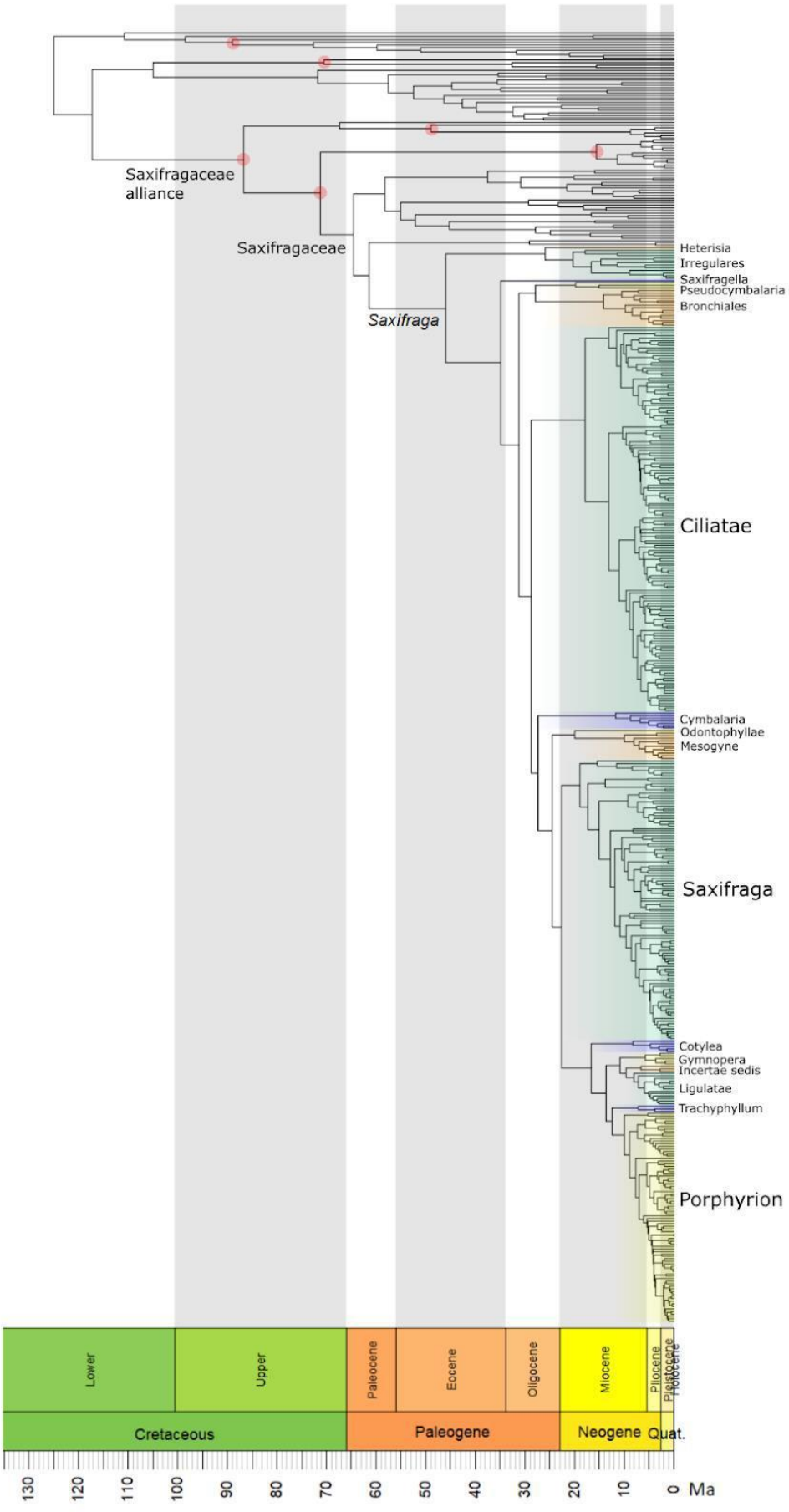
Saxifragaceae alliance
Saxifragaceae
Saxifraga
Heterisia
Irregulares
Saxifragella
Pseudocymbalaria
Bronchiales
Ciliatae
Cymbalaria
Odontophyllae
Mesogyne
Saxifraga
Cotylea
Gymnopera
Incertae sedis
Ligulatae
Trachyphyllum
Porphyrion
Lower
Upper
Paleocene
Eocene
Oligocene
Miocene
Pliocene
Pleistocene
Holocene
Cretaceous
Paleogene
Neogene
Quat.
130
120
110
100
90
80
70
60
50
40
30
20
10
0
Ma

Previous page: Fig. 3.3: treePL chronogram of Saxifragales. Sections of the genus Saxifraga *are indicated to the right of the tree, and other clades of importance are depicted under the branch leading to their crown node. The six nodes with minimum age priors are circled red. Specific stem and crown node ages are given in* ***Table 3.2.***

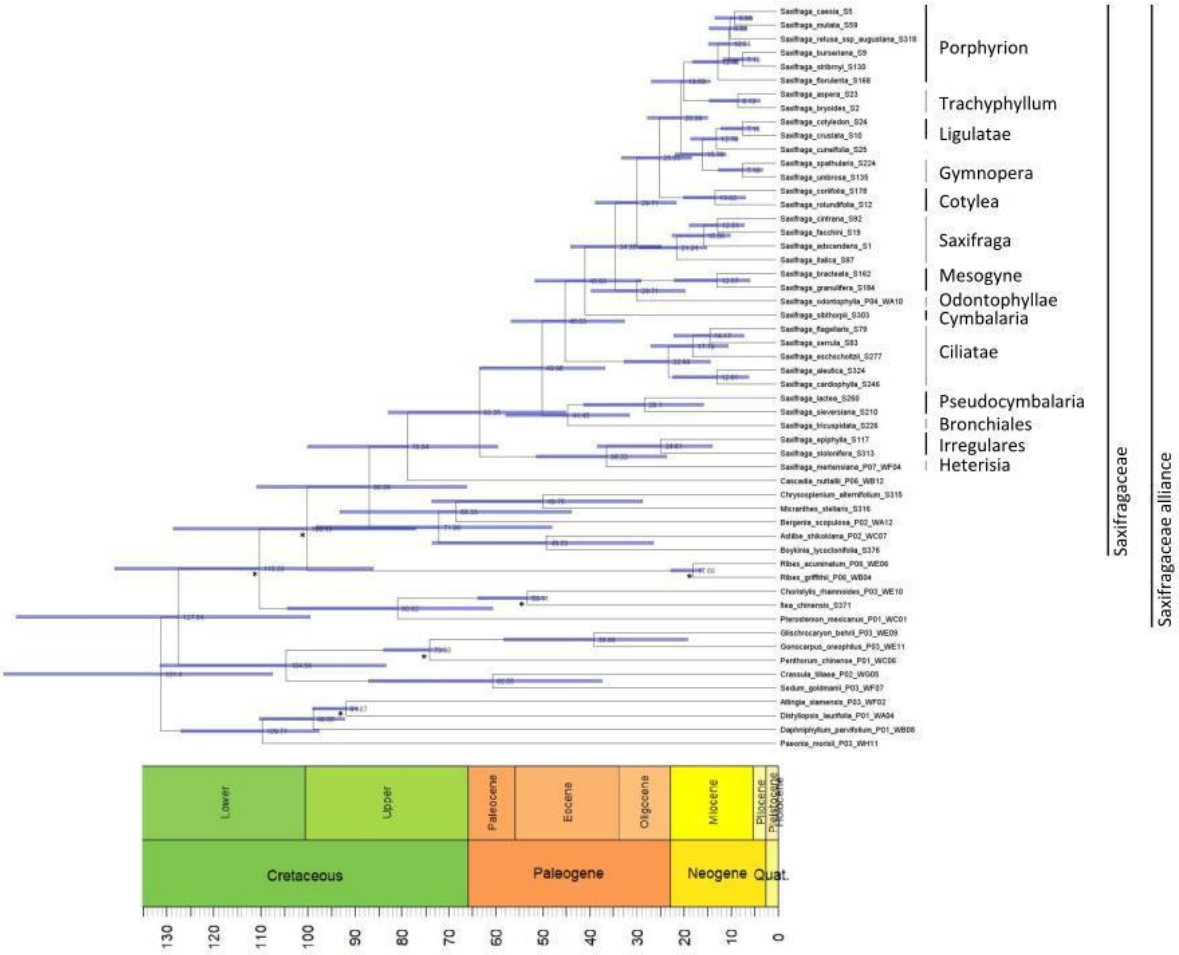

Fig. 3.4: BEAST chronogram of Saxifragales pruned to 55 tips. Clades of importance that are discussed in the text are indicated to the right of the tree. Numbers to the right of nodes represent median node age and the blue bars represent the 95% highest posterior density (HPD) of node ages. The six nodes with minimum age priors are indicated with an asterisk. Specific stem and crown node median age and HPD are given in ***Table 3.2***

*Table 3.2: Divergence time estimates for nodes as reported by Gao et al. (2017) and Ebersbach et al. (2017), compared to estimates from this study (green panels). Node ages are shown in million years from present (Ma). Support values for nodes are given as *: ≥ 0.90–0.93, **: ≥ 0.94–0.97, ***: 0.98– 1.0 for Bayesian posterior probability (PP) (Drummond et al., 2012), or the ASTRAL local posterior probability values (LPP) (Mirarab et al., 2014) based on the exon species tree. New node age estimates are the result of penalised likelihood (treePL; Smith and O'Meara, 2012), and Bayesian (BEAST 2; Bouckaert et al., 2019) divergence time estimation methods.*

	Gao et al., 2017		Ebersbach et al., 2017			treePL	BEAST		
	Mean age	95% HPD	Median age	95% HPD	PP	Node age	Median age	95% HPD	LPP
Saxifragaceae alliance crown			91.65	89.10–98.32	***	91.61	110.33	86.04-141.17	1
Saxifragaceae stem	88.09	78.22–92.82	83.96	74.35–92.85	***	79.00	100.13	76.99-128.74	1
Saxifragaceae crown			73.63	63.88–82.78	***	71.64	86.88	56.10-110.89	1
Saxifraga stem	69.83	58.14–80.29	73.63	63.88–82.78	***	67.56	78.64	59.43-100.05	1
Saxifraga crown	54.22	42.99–66.37	61.75	52.05–71.81	***	47.38	63.35	44.91-82.63	1
sect. Heterisia stem			32.58	22.44–44.43	***	25.16	36.22	23.32-51.22	1
sect. Irregulares stem			32.58	22.44–44.43	***	25.16	36.22	23.32-51.22	1
sect. Irregulares crown			26.71	18.55–36.68	***	18.70	24.61	13.66-38.22	1
sect. Saxifragella stem			52.51	44.60–61.83	***	33.81			1
sect. Pseudocymbalaria stem			40.01	29.02–50.29	**	27.13	44.45	31.31-57.70	1
sect. Pseudocymbalaria crown			17.83	9.49–27.36	***	18.37	28.10	15.49-41.09	1
sect. Bronchiales stem			40.01	29.02–50.30	**	27.13	44.45	31.31-57.70	1
sect. Bronchiales crown			10.59	6.81–15.10	***	9.16			1
sect. Ciliatae stem	32.4	24.29–41.24	40.92	33.99–48.55	***	27.24	45.03	32.33-56.57	1
sect. Ciliatae crown	19.79	13.41–27.92	26.21	19.95–34.00	***	16.91	22.99	14.03-32.47	1
sect. Cymbalaria stem			37.53	30.99–44.93	***	26.15	40.83	28.86-51.53	1
sect. Cymbalaria crown			10.92	5.53–18.32	***	9.19			1
sect. Odontophylla stem						19.46	29.71	19.44–39.48	1
sect. Mesogyne stem			24.32	18.05–31.03	-	19.46	29.71	19.44–39.48	1
sect. Mesogyne crown			7.54	4.80–10.82	***	8.11	12.57	5.62-21.71	1
sect. Saxifraga stem			31.31	25.55–37.91	***	20.01	29.71	21.31-38.60	1
sect. Saxifraga crown			23.73	19.03–29.36	***	14.88	21.24	14.82-29.38	1
sect. Cotylea stem			24.32	18.05–31.03	-	16.90	25.03	18.05-32.98	0.93
sect. Cotylea crown			1.55	0.40–3.46	***	7.00	13.02	6.53-19.80	1
sect. Gymnopera stem			18.97	14.33–24.72	**	11.59	15.78	10.72-21.54	1
sect. Gymnopera crown			13.64	8.26–19.30	**	6.08	7.18	2.88-12.34	1
S. cuneifolia L. stem						9.84	12.76	8.11-18.24	1
sect. Ligulatae stem			14	9.49–19.42	***	9.84	12.76	8.11-18.24	1
sect. Ligulatae crown			7.94	4.86–11.87	***	7.35	7.16	3.85-11.76	1
sect. Trachyphyllum stem			14	9.49–19.42	***	12.99	19.69	14.06-25.53	0.53
sect. Trachyphyllum crown			2.43	0.47–5.44	***	7.45	8.13	3.41-14.26	1
sect. Porphyrion stem			22.32	17.29–27.96	***	12.99	19.69	14.06-25.53	0.53
sect. Porphyrion crown			14.89	11.14–19.21	***	8.37	12.45	8.21-17.76	1

3.4 Discussion

3.4.1 Changes to classification of sections

We have included representatives of all sections discussed by Tkach et al. (2015b), as well as subsections **(Table 3.1)**. Descriptions of clades are used as presented by Tkach et al. (2015b) and in the discussion we aim to expand upon their findings or suggest taxonomic changes. The topology of sections and origin of key deterministic characters (apomorphy) discussed in the text are visualised in **Fig. 3.2**.

Saxifrageae and Cascadieae divergence

The exon and supercontig phylogenies support the placement of tribe Cascadieae R.A.Folk & D.E.Soltis as sister to *Saxifraga*. Previously, Folk al. (2019) recovered inconsistent placements of Cascadieae with only coalescent analyses agreeing with previous analyses that suggest a position within the heucheroids (e.g., Deng et al., 2015). Other studies found Cascadieae likely to be sister to the remainder of Saxifragaceae excluding *Saxifraga* (e.g., Tkach et al. 2015b; Tarullo et al., 2021). Based partly on the solitary flowers with white elongated petals, and 3-5-pronged leaves allocated only to the trailing stem, the South-American *Cascadia nuttallii* (Small) A.M.Johnson, was first described as a *Saxifraga* taxon related to *S. petraea* L. Currently, it is placed in tribe Casacadiae along with the rather dissimilar *Saxifragodes albowiana* (Kurtz ex Albov & Kurtz) D.M.Moore (Folk et al., 2021), sharing only the characteristics of two carpels, tetralocular anthers and the lack of rhizomes and basal leaves. Saxifrageae and Cascadieae have but few characteristics to delineate the clades, since these are highly indeterminate within both tribes. However, Cascadieae are different through their 6 to 10 stamens and echinate-tuberculate seeds (Kaplan, 1981; Folk et al., 2021). Interestingly, *S. albowiana* has foliar calcium oxalate crystals that are also found within *Saxifraga* sect. Irregulares (Gornall, 1987). Finally, regarding the geographic origin of *Saxifraga* that was estimated to be in North America (Ebersbach et al., 2017a), this topological development determined the same through the presence of Cascadieae in the Americas (Folk et al., 2020).

sect. *Heterisia*

The monotypic sect. *Heterisia* is here supported as sister to sect. *Irregulares*, a relationship already suggested by Zhmylev (2004), while Tkach et al. (2015b) reported it to be embedded within the latter. The key characters defining *Saxifraga mertensiana* Bong. from sect. *Irregulares* are the actinomorphic flowers, as opposed to zygomorphic flowers (Engler and Irmscher, 1916). In addition, bulbils can replace flowers along the flowering stem (Webb and Gornall,

1989), which is a rare occurrence in *Saxifraga* and otherwise only occurs in sect *Mesogyne* (Zhmylev, 1997). Opposed to sect. *Irregulares*, foliar calcium oxalate crystals do not occur in *S. mertensiana* (Gornall, 1987). Hence, based on our phylogeny and the strong morphological divergence, we do not accept the suggestion by Tkach et al. (2015) to merge (synonymise) sect. *Heterisia* with sect. *Irregulares*.

sect. *Irregulares*

We included 11 out of approximately 17 taxa and we found support (LPP = 1) for the two distinct series suggested by Pan (1992), where ser. *Stoloniferae* J.T. Pan includes the stoloniferous *S. cortusifolia*, *S. stolonifera* and *S. nipponica*, and the remainder of non-stoloniferous taxa are part of ser. *Rufescentes* J.T. Pan (Zhang et al., 2020). As sect. *Irregulares* is generally supported as monophyletic (Ebersbach et al., 2017b; Zhang et al., 2020), the zygomorphic flowers and foliar calcium oxalate crystals are defining synapomorphies (Pan et al., 2001; Zhang et al., 2020).

sect. *Saxifragella*

The monotypic sect. *Saxifragella* contains species *Saxifragella bicuspidata* (Hook.f.) Engl., that is morphologically unique within the genus due to absence of petals and hairs, as well as a reduced number of stamens (5 opposed to 10) (Gornall, 1986). Species tree support and topological placement are in line with previous findings (Tkach et al., 2015b; Zhang et al., 2015).

sect. *Pseudocymbalaria*

The section consists of only three species with leafless stems or stems with bract-like leaves (Engler and Irmscher, 1916). The new species tree supports sect. *Pseudocymbalaria* as monophyletic (Tkach et al., 2015b), and as a sister clade to sect. *Bronchiales* (Ebersbach et al., 2017b), while high disagreement between gene trees shows varying topologies in cited studies.

sect. *Bronchiales*

Circumscription of sect. *Bronchiales* has changed since DeChaine et al. (2013) recognized it as a different clade from sect. *Trachyphyllum*. The clade can be delineated based on morphology, consisting of cushion growth forms with stiff, pointed leaves, spotted petals and somewhat woody branchlets (DeChaine, 2014). However, inter-specific relationships and subspecies ranks are still obscure (Tkach et al., 2015b; Tamura et al., 2018). While the species tree presented here shows overall decently high LPP values, specifically for support of two main clades within the section **(Fig. 3.2D)**, many extra copies of loci were present,

and this varies strongly between taxa **(Fig. 2.4)**. Strong differences in occurrence of multi-copy loci in this section is further explained by Ebersbach et al. (2020), showing how diploidy, polyploidy and mixed-ploidy occurs among closely related taxa within the section. Molecular and cytological data does not support a straightforward hybrid origin (Tamura et al., 2018). Hence, interspecific relationships of sect. *Bronchiales* need further study to elucidate the potential effects of introgression, autopolyploidy and incomplete lineage sorting on speciation.

sect. *Ciliatae*

Sect. *Ciliatae* is the most species-rich section of Saxifraga with approximately 214 species, although this number is debatable due to many synonymised names in various sources, and therefore Tkach et al. (2015b) assumed about 175 species are currently accepted. The section has few characters shared among all taxa (Engler and Irmscher, 1916), as well as highly differing ploidy levels (Ebersbach et al., 2020), although trinucleate pollen with a lirate to striate surface occur in almost all taxa (Ferguson and Webb, 1970; Gornall, 1987; Zhang and Gornall, 2011; Zhang et al., 2015). Three main clades are recognized in sect. Ciliatae by various studies (Zhang et al., 2008; Gao et al., 2015; Tkach et al., 2015b; Ebersbach et al., 2018). Within these three clades, six to seven subsections occur (Gornall, 1987; Webb and Gornall, 1989), although phylogenetic analyses show evidence that sections are polyphyletic (Gao et al., 2015; Ebersbach et al., 2018).

In this study we find that the first clade within sect. *Ciliatae* that is sister to the others (LPP = 1) is the same as found in previous studies (e.g., Zhang et al., 2008; Gao et al., 2015; Ebersbach et al., 2018), and includes subsect. *Cinerascentes* Engl. & Irmsch., subsect. *Flagellares* (C.B.Clarke) Engl. & Irmsch., subsect. *Gemmiparae* Engl. & Irmsch., and subsect. *Hemisphaericae* Engl. & Irmsch. However, no phylogenetic support exists for the monotypic subsect. *Cinerascentes*, due to being nested within subsect. *Gemmiparae*. Opposed to its related taxa, *S. cinerascens* does not lose basal leaves before flowering and has few leaves along the flower stem, though it shared the key descriptive characters of buds in leaf axils and at the base of shoots (Engler and Irmscher, 1916). Hence, we agree with Gao et al. (2015) to abandon the use of subsect. *Cinerascentes* and recognize *S. cinerascens* as part of sect. *Gemmiparae*.

The subsect. *Flagellares* and subsect. *Hemisphaericae* are polyphyletic in the species tree. We found *S. hemisphaerica* Hook.f. & Thomson, as representative of subsect. *Hemisphaericae* nested within subsect. *Flagellares*, as was also found for *S. zhidoensis* J.T. Pan in previous studies (Gao et al., 2015; Ebersbach et al., 2018). While these taxa form characteristic cushions, have reduced length of (almost leafless) flowering stems, reflexed sepals, and produce no typical stolons as most taxa in subsect. *Flagellares* (Engler and Irmscher, 1916; McGregor and Harding, 1998), morphology of reproductive and vegetative structures is in line with the rest of the subsection (including the absence of buds in leaf axils in opposition of sect. *Gemmiparae*). However, *S. eschscholtzii* Sternberg of the subsect. *Hemisphaericae* (Engler and Irmscher, 1916) has generally been supported as sister to subsect. *Flagellares* and subsect. *Gemmiparae*, and shares all typical characters for the subsection with *S. hemisphaerica* and *S. zhidoensis*. Further study of subsect. *Hemisphaericae* is warranted due to the phylogenetic placement of the type species in our exon and supercontig trees and the findings by Tkach et al. (2015b), although we suggest to uphold the name based on the strong morphological evidence and the restricted sampling of the clade in this study. Finally, subsect. *Flagellares* does still appear to be paraphyletic, due to stoloniferous *S. brunonis* Wallich ex Seringe forming a moderately supported clade with subsect. *Gemmiparae* (LPP = 0.90, Q-score = 39.79), as has also been found by Gao et al. (2015). We also retrieved a well-supported (LPP = 1, Q-score = 42.85), though atypical placement of the *S. josephii* Engler as sister to the entire clade comprising subsect. Flagellares, subsect. Gemmiparae, and subsect. Hemisphaericae. One of the authors of the eFlora of Chinese Plant Names (Ohba H.; eFloras, 2008) regards this species as synonymous with *S. brunonis*. We consider subsect. Flagellares polyphyletic, although further study is warranted due to strong morphological similarity within the clade, as well as high underlying gene tree discordance that resulted in an otherwise well-supported topology in the phylogenetic summary method we employed.

For the remaining clades of sect *Ciliatae*, we find high support (LPP = 1) for existing well-defined subsections. One group diverges into subsect. *Rosulares* Gornall and subsect. *Serpyllifoliae*. Here, subsect. *Rosulares* is defined as having mostly basal leaf arrangements in rosettes with simple or branched flowering stems, and lacking stolons or buds in leaf axils (Gornall, 1987; McGregor, 1998). The subsect. *Serpyllifoliae* is defined by solitary flowers and mat-forming habits with creeping, and leaf-bearing shoots that grow from basal leaf axils (Gornall, 1987). The other group consists only of subsect. *Hirculoideae* (Engler and Irmscher) Gornall that is defined by crisped, mostly eglandular hairs on the basal stem nodes and the leaf petioles (Engler and Irmscher, 1916; Gornall, 1987). While subsect. *Hirculoideae* and subsect. *Rosulares* are well-supported in the phylogeny, the branches showing interspecific relationships show overall low quartet tree support (high precedence

of Q-score < 40). This could be the result of rapid diversification resulting in gene tree discordance. Studies have found fast and recent diversification in subsect. *Hirculoideae* through evolutionary rate change (Ebersbach et al., 2018) and population genetic structure (Li et al., 2018), and have also suggested effects of introgression from closely-related sympatric species (Li et al., 2018).

sect. *Cymbalaria*

All four species of this clade are included in this study and were monophyletic. Among congenerics, this section is unique in that it contains various annual or biennial taxa (Zhmylev, 2004), which is overall rare in *Saxifraga*.

sect. *Odontophyllae*

This monotypic section has been suggested to be related to various unrelated sections in *Saxifraga* and *Micranthes* through time (Tkach et al., 2015b, and references therein). In this study we estimate that *S. odontophylla* shared a last common ancestor with sect. *Mesogyne* at 28.81 Ma, which is over twice the crown age of sect. *Mesogyne* at 12.31 Ma. If we consider the long distance through time and difference in seed morphology with sect. *Mesogyne* (Kaplan, 1981), *we* can reliably support sect. *Odontophyllae*.

sect. *Mesogyne*

The relatively well-sampled sect. *Mesogyne* (7 out of 9 species) is strongly supported as monophyletic group (Conti et al., 1999; Tkach et al., 2015b). The section is marked by toothed or lobed, petiolate, and somewhat flimsy leaves occurring together with bulbils in cauline leaf axils (Zhmylev, 1997).

sect. *Saxifraga*

For sect. *Saxifraga* the morphological characters among subsections are often shared, making identification difficult (Engler and Irmscher, 1916; Gerschwitz-Eidt and Kadereit, 2020), and phylogenetic trees based on few plastid genes or ribosomal ITS often result in large polytomies (Mas De Xaxars et al., 2015; Tkach et al., 2015b; Gerschwitz-Eidt and Kadereit, 2020). In the phylogeny presented here we show the topology of subsections is well-supported (LPP = 1), with subsect. *Saxifraga* and subsect. *Arachnoideae* forming sister clades, and these are in turn sister to subsect. *Tridactylites*, which is then followed by sister clade subsect. *Androsaceae*. Studies have generally found different topologies (Tkach et al., 2015b; Ebersbach et al., 2020; Gerschwitz-Eidt and Kadereit, 2020), and depending on the locus we find that tree estimation places *S. irrugua* M.Bieb. and *S. wahlenbergii* Ball as outgroup to or embedded in either subsect. *Androsaceae* or subsect.

Tridactylites., likely due to introgression (Tkach et al., 2019). Gerschwitz-Eidt and Kadereit (2020) even found *S. irrigua* to be related to subsect. *Arachnoideae* based on plastid genes. Despite high branch support of the species tree reported in this study, delineation of subsections remains difficult within sect. *Saxifraga* due to gene tree conflict resulting from numerous occurrences of allo- and autopolyploids (Ebersbach et al., 2020), and a lack of key morphological characters to define clades (Gerschwitz-Eidt and Kadereit, 2020). Within subsect. *Saxifraga* various species have bulbils near the base of the stem, also stored underground, although this would be likely a character that has been repeatedly lost.

sect. *Cotylea*

The section has reniform leaves with petioles and superior ovaries (Engler and Irmscher, 1916). In addition to being morphologically distinct, sect. *Cotylea* is strongly supported as monophyletic (Tkach et al., 2015b), and its placement in *Saxifraga* is resolved in this study.

sect. *Gymnopera*

The key characters for this section are that their fleshy-leaved rosettes are connected by short rhizomes and that they have superior gynoecia (Engler and Irmscher, 1916). Various studies have found taxa from sect. *Gymnopera* were grouped with other sections or in polytomies (e.g., *Cotylea*, *Ligulatae*, *Mesogyne*, *Porphyrion*) based on plastid loci (Soltis et al., 1996; Conti et al., 1999; Tkach et al., 2015b). However, we find strong support for three species in the section to be monophyletic, although *S. cuneifolia* L. forms a clade with sect. *Ligulatae*. Other studies have reported either recent or ancient chloroplast capture in sect *Gymnopera* as it is known to hybridize with other sections often (Ebersbach et al., 2020).

Incertae sedis - *Saxifraga cuneifolia* L.

Opposed to sect. *Gymnopera*, we found that phylogenetic trees of the separate nDNA loci of *S. cuneifolia*, including paralogous copies, interchangeably could be placed as sister to, or embedded within, sections *Gymnopera* and *Ligulatae*. Although *S. cuneifolia* has generally been accepted as part of sect. *Gymnopera* (Engler & Irmscher, 1916), studies show a relationship with sect. *Ligulatae* through plastid markers (Soltis et al., 1996; Tkach et al., 2015b). It has been established that *S. cuneifolia* hybridises with various taxa from sect. *Ligulatae* (e.g., *S. cotyledon* L., *S. crustata* Vest and *S. paniculata* Mill.) (Engler and Irmscher, 1916), while it does not hybridise with the other species of the sect. *Gymnopera* (McGregor, 2008). Notably, all taxa in sect. *Gymnopera* and sect. *Ligulatae* are diploid (Ebersbach et al., 2020), so we suggest patterns of molecular evolution found in *S. cuneifolia* are the results of ancient intersectional introgression.

For S. *cuneifolia*, two subspecies are well-described S. *cuneifolia* subsp. *cuneifolia* and subsp. *robusta* Webb (Sanna et al., 2019). Morphology of S. *cuneifolia* is characterized by rosettes of fleshy leaves that are separated by stolons of 2 to 3 cm, a subglabrous peduncle and a small panicle of 5 to 10 flowers (Webb, 1988). Characters that are not shared (in combination) with all members of sect. *Gymnopera* are crenate to dentate, obovate to spathulate leaves that have actinodromous venation, and glandular trichomes on the pedicel are uniseriate (Engler and Irmscher, 1916; Zhang et al., 2015). No remarkable characters are shared with sect. *Ligulatae*, as opposed to sect. *Mesogyne*, except for a less-defined petiole (Engler and Irmscher, 1916).

sect. *Ligulatae*

The section is almost completely represented in this study, with 8 out of 9 known species. Sect. *Ligulatae* is defined by fleshy, finely toothed leaves that are arranged in rosettes and have lime-secreting hydathodes (Engler and Irmscher, 1916). We find strong support for monophyly, although the section is known to produce intra- and intersectional hybrids (Engler and Irmscher, 1916; Ebersbach et al., 2020).

sect. *Trachyphyllum*

This section is defined by ciliate leaf margins and white petals with dots and yellow blotches at the base of the petal. After Tkach et al. (2015b) established the current circumscription of sect. *Trachyphyllum* with only two representatives (*S. aspera* L. and *S. bryoides* L.), its placement within the genus has still been contested. However, the group is genetically and morphologically distinct, and has been placed along sect. *Ligulatae* and sect. *Porphyrion* with low support (Tkach et al., 2015b, this study). The sections it is associated with have lime-secreting hydathodes and slightly toothed leaf margins, while this section notably has not. Tkach et al. (2015) theorised that the ciliate hairs on leaf margins in sect. *Trachyphyllum* are homologous to the teeth in related sections, which could explain part of their striking dissimilarity from their presumed parentage. The topology estimated in this study further supports the theory of intersectional origination through sect. *Ligulatae* and *Porphyrion.*

sect. *Porphyrion*

The section is morphologically diverse, but overall has characteristic lime-secreting hydathodes, seeds with epidermal cells with notable cuticular folds, and 2-3 carpels (Engler and Irmscher, 1916; Kaplan, 1981; Tkach et al., 2015b). While Tkach et al. (2015b) established inclusion of various subsections within sect. *Porphyrion*, we corroborate the inclusion though find that subsection topology is very poorly supported due to high gene

tree conflict while intraspecific relationships are relatively well-resolved. The topology among subsection subsections *Florulentae*, *Kabschia* and *Oppositifoliae* is not supported, and only subsections. *Mutatae* and *Squarrosae* are highly supported as sister clades. However, all subsections are themselves strongly supported clades. Especially the enigmatic *S. florulenta* Moretti from monotypic subsect. *Florulentae* has been historically difficult to place based on morphology and molecular phylogenetics, though is expected to have formed close to the crown node of sect. *Porphyrion*.

3.4.2 Reliability of divergence time estimation methods

The Bayesian method of divergence time estimation used in this study resulted in convergence issues and unfavourably wide HPD intervals. Bayesian methods are known to have issues converging MCMC chains on large datasets with many terminals (Tamura et al., 2012; Höhna et al., 2016), and in addition to scalability of run times, the substitution rate prior has a stronger effect on posterior time estimates when many loci are analysed, and if the rate prior is not implemented correctly (substitution model selection), one can find divergence times converging on wrong values with small HPD intervals (Dos Reis et al., 2014). We also tested more simplified models to increase the chance of convergence of chains, however, convergence on incorrected values with small posterior confidence would be the opposite result of what we obtained in terms of non-convergence and wide intervals. While we constrained the analysis with what we consider to be the “true species tree”, the branch lengths are still strongly affected if loci are used as single concatenated gene without partitioning and selecting fitting partition rate priors (Degnan and Rosenberg, 2009; Mirarab et al., 2014; Hahn and Nakhleh, 2016). We can also perform Bayesian methods using a subsample of terminals without impacting accuracy (Luo et al., 2021), and excluding loci after which missing data effects on dating error are relatively minor (Zheng and Wiens, 2015). Importantly, selection of loci with congruent gene trees helps to reduce issues with unrealistic branch lengths (Carruthers et al., 2022). However, the fossil minimum age constraints on nodes caused issues in initiation steps of runs, as well as convergence issues, after careful selection of loci and priors. Corrections to fossil priors as carried out here are minor compared to other studies (Ebersbach et al., 2017a; Tarullo et al., 2021), including the new interpretation affecting the *Ribes* crown node. While this analysis was problematic, the estimated ages of *Saxifraga* ingroup crown nodes are realistic and in line with our treePL estimates and those found by Ebersbach et al. (2017a).

The treePL phylogeny results can’t be interpreted akin to posterior diagnostics as is available to BEAST, though it presents a result without strongly divergent node age estimates in the outgroups (Magallon et al., 1999; Tarullo et al., 2021). We implemented a slightly different selection of congruent loci and we set a single maximum constraint based on

probability densities for the *Ribes* stem node to have existed (Donoghue and Yang, 2016). This approach resulted in divergence times for the nodes under the Saxifragaceae alliance crown node to be in line with other studies with broad taxon and locus sampling, as well as broad and alternatively implemented range of fossil calibrations (Gao et al., 217; Ebersbach et al., 2017a; Tarullo et al., 2021). Divergence times within *Saxifraga* are generally found to be younger than estimated by Ebersbach et al. (2017a), although crown nodes of some particularly young sections and within sections are older. This could have been expected as we try to establish true speciation times, instead of latest coalescence times, which are often more recent (DeGiorgio and Degnan, 2014).

Differences in stem node ages of section are often a result of topological changes we established in our phylogeny, which must be interpreted carefully in some cases. For instance, the topological placement sect. *Trachyphyllum* and the relationship between sect. *Ligulatae* and sect. *Gymnopera* are likely affected by ancient introgression events.

3.4.3 Divergence times in *Saxifraga*

Saxifragales is thought to have undergone rapid early diversification (Fishbein et al., 2001) that resulted in an uncertain topology below the crown node of the order (Magallón et al., 1999; Jian et al., 2008; Soltis et al., 2011). However, most stem lineages of families were placed in the Upper Cretaceous at ca. 75 Ma in the most recent, complete reconstruction of the order (Tarullo et al., 2021). This supports the 79 Ma maximum constraint for the Saxifragaceae stem node we set through a relatively wide predictive distribution of fossil occurrences. The stem age of *Saxifraga* may be placed in the Paleocene (67.56 Ma), based on the treePL divergence time estimation, noting also that a topological shift occurred whereby *Saxifraga* is no longer sister to the rest of Saxifragaceae (Folk et al., 2019; 2020). It is important to note that other divergence time estimates for the stem of the genus are much younger (e.g., 38.45 Ma, Gao et al. 2015; 38.37 Ma, Deng et al., 2015), although these are based on single fossil node priors from within the Saxifragaceae alliance. The *Saxifraga* crown node age estimation in treePL is once more rather young at 47.38 Ma, thereby suggesting a start of diversification of extant *Saxifraga* in the mid-Eocene. The BEAST estimates are more akin to Ebersbach et al. (2017a) and suggest a crown age in the Paleocene (63.35 Ma, 95% HPD 44.91-82.63 Ma). However, the age estimate of the genus could be regarded as a tentative finding due to the prevailing conflict between our two approaches to divergence time estimation, although our analyses fall in the confidence intervals of the divergence time estimation performed by Ebersbach et al. (2017a). The constraints for BEAST that were set in this study, such as the tree topology, the fossil calibrations and speciation rate models, could have impacted the unrealistically wide HPDs. However, since we found these settings optimal given test runs with other

settings, future studies should find a different approach from an earlier point in the data preparation pipeline, such as the implementation of various other gene-shopping methods to counteract missing and multi-copy genes, while selecting for topological congruency.

Most crown nodes of *Saxifraga* (sub)sections have been established in the Miocene, according to both treePL and BEAST results. The epoch is known for the extreme climate events that caused (repeated) ice mass formation on land (Filippelli, 1997; Prista et al., 2015), and expansion of dry and cold temperate biomes became prominent (Herbert et al., 2016) where representatives from Saxifragales are now extremely diverse (Folk et al., 2019). Importantly, significant episodes of mountain uplift occurred during the Miocene in mountains systems where *Saxifraga* is now prominent. The Himalayas and Qinghai-Tibet plateau had various uplift events throughout the Miocene (Fang et al., 2005; Favre et al., 2015), followed by late-Miocene to Pliocene uplift of the Hengduan Mountains (Sun et al., 2011), and significant uplift also occurred throughout portions of the European Alpine System (Prista et al., 2015). In general, we find that the ingroup crown nodes presented here move towards the (mid-)Miocene, as even the mega-diverse clades such as sections *Ciliatae*, *Porphyrion*, and *Saxifraga*, were estimated to be younger than by Ebersbach et al. (2017a), and this supports theories of *Saxifraga* diversification being driven in part by a geographical context through mountain uplift and glaciation events (Gao et al., 2015; Ebersbach et al., 2017b).

We established older crown nodes for some of the *Saxifraga* sections that previously were estimated at remarkably young ages, leading to all most recent common ancestors for the sections accepted in this study being estimated older than 7.00 Ma. Some of the very young crown nodes, such as sect. *Trachyphyllum* and sect. *Cotylea* (Ebersbach et al., 2017a), could have been the result of the limited informativeness of loci affected by phylogeny estimation without consideration of the multi-species coalescent. Through processes such as introgression one would expect that the true divergence time of species would be older than the divergence time of (most) genes. Naturally, many nodes among taxa in species rich clades with a lot of documented introgression were also estimated to be older than found in other studies and this affects claims of speciation rates and the role of geographic events. Various studies have tried to explain distribution and speciation of *Saxifraga* spp. through co-occurrence of ancestral range estimates and diversification rate shifts with geographic and climatic events (e.g., Gao et al., 2015, 2017; Ebersbach et al., 2017b, 2018; Li et al., 2018). In the study by Li et al. (2018), the crown node for diversification of the species complex involving *S. sinomontana* J.T. Pan & Gornall was estimated at 1.19 Ma (0.85 -1.62 95% HPD). We estimated a much older (5.86 Ma) last common ancestor of the *S. sinomontana* species complex and closely related taxa (e.g., *S. heleonastes* H. Sm.*, S. hirculoides* Decne.). The discrepancies in estimates, from what is likely an artefactual result from introgression, results in loss of support for the theory that diversification for this clade occurred during the four most recent Quaternary glaciations on

the Qinghai-Tibet plateau that started at ca. 1.17 Ma (Zheng et al., 2002). Here, we argue that through the many known cases of introgression in *Saxifraga* any divergence times not generated under assumption of the coalescent are questionable.

3.5 Conclusion

The *Saxifraga* species tree retrieved in this study, either through the exon or supercontig data, has high overall branch support for accepted infrageneric sections (except for placement of sect. *Trachyphyllum*). In addition, it is one of the most complete phylogenies for *Saxifraga* to date with 320 out of approx. 462 taxa (69%). While the dataset includes many loci with paralogous copies, the data cleaning pipeline has minimised gene tree conflict. We find support for sections defined by Tkach et al. (2015), except for the establishment of sect. *Heterisia* and minor comments on clades within sect. *Ciliatae*. In addition, conflicting placement of *S. cuneifolia* in the gene trees which is likely the result of intersectional introgression, warrants future in-depth study to consider its relationship to sect. *Gymnopera* and sect. *Ligulatae*. We also explored the effect of using the “splash zones” of the 329 nDNA loci, which are the non-coding and trailing ends that are obtained during hybrid-capture sequencing and find high local posterior probability support and lower gene tree conflict for branches establishing species level relationships. We established that after the review of sectional delimitation by Tkach et al. (2015) very few changes are needed, though most progress in establishing the *Saxifraga* species tree and nomenclature would be achieved through further study of reticulate evolution within and among sections. In addition, as the characterization of some clades within sect. Ciliatae is still strenuous, further phylogenetic analysis with the inclusion of pollen characters and stolon types (development, placement, dissection) would be beneficial.

Divergence time estimation using the new species tree topology, as well as a broad inclusion of *Saxifraga* spp. and Saxifragales outgroups with additional fossil calibrations, shows a departure from previous well-sampled studies (e.g., Gao et al., 2015; Ebersbach et al., 2017a). Evidence is presented of a younger stem node for *Saxifraga* in the early Paleogene. We also establish a contraction within *Saxifraga* through both a penalised likelihood and Bayesian method, which show that all crown nodes of the sections we support fall within the Miocene and that all oldest common ancestors for the sections we support are not younger than 6 Ma. Generally, older divergence times were retrieved in more recent nodes, as topological constraints and a larger dataset of congruent loci help to estimate divergence times closer to true species tree divergence times than gene tree speciation.

Chapter 4:

Leaf temperature response to solar radiation in the genus *Saxifraga*

4.1 Introduction

In high-elevation climatic conditions above the natural treeline, also known as the alpine zone, low average temperatures occur, and this impacts plant leaf photosynthetic productivity, driving physiological adaptation (Körner, 2003; Testolin et al., 2020). Indeed, optimal temperature for photosynthesis in plants is often lower with higher altitude (Gates, 1965; Körner and Diemer, 1987; Terashima et al., 1993; Kleier and Rundel, 2009). However, the temperature of a leaf can be in part decoupled from the ambient air temperature through radiation. Direct solar irradiance generally increases with altitude (Blumthaler, 2012), thus creating a juxtaposition for plant temperatures, as the main source of heat load for a plant comes from direct short-wave radiation (Idso et al., 1966).

A theory of "limited leaf homeothermy" was suggested to occur among higher plants by Mahan and Upchurch (1988), where leaf characteristics influence the relation between ambient air temperature (T_{AIR}) and the temperature of photosynthetic leaf tissue (T_{LEAF}) ($T_{LEAF} - T_{AIR} = \Delta T$), such that leaf temperature is maintained closer to optimum temperature for photosynthesis (Michaletz et al., 2015). However, cushion plant habits, as specialist representatives of alpine or other high radiation habitats, are found to have a strong positive departure of T_{LEAF} over T_{AIR} (Michaletz et al., 2016; Blonder and Michaletz, 2018), which is described as megathermy (Blonder and Michaletz, 2018), which can lead to differences of over 20 °C (Salisbury and Spomer, 1964). The cushion growth form creates a strong decoupling from T_{AIR} as it reduces the boundary layer of the plant. Since ambient temperatures and solar radiation intensity in the alpine biome fluctuate greatly between seasons and between day and night (Rundel et al., 1994; Körner, 1999), alpine plants lacking the ability for effective temperature regulation risk irreversible damage, notably to the photosynthetic organs (Berry and Björkman, 1980).

Heat gain and loss in leaves is controlled by three main types of heat transfer, which are radiation by electromagnetic waves, convection by movement of air, and transpiration through stomata (Idso and Baker, 1967). Apart from a low average, but highly fluctuating air temperature and high maximum radiation, plants in high altitude habitats are subject to various other factors, including drought and strong winds, that impact heat transfer mechanics. Plant communities in high alpine ecosystems can be exposed to high wind speeds, which increases conductance of the leaf boundary layer (Idso and Baker, 1967). The boundary layer is the air layer in contact with the leaf surface

that affects heat transfer through convection (Schuepp, 1993), as well as transpiration (Daudet et al., 1999). In addition, through either short- or long-term increase in air temperature and decrease in air vapour pressure, the vapour pressure deficit increases (Shirke, 2004; Grossiord et al., 2020). Water availability strongly influences the capacity to actively regulate leaf temperature through transpiration, and a high deficit of air moisture and risk of hydraulic failure impacts plant productivity due to closure of stomata (Grossiord et al., 2020). How plant leaves experience and respond to temperature can only be fully understood through data on microhabitat level, because microhabitat temperature may greatly differ from the macroclimate (Körner and Hiltbrunner, 2018). Hence, environmental data that impacts the three main types of heat transfer are needed for evaluation of plant temperature response at microhabitat level.

Plant adaptations to alpine habitat have occurred through strict environmental selection, which has led to relatively low variation in plant stature and leaf traits among families (Billings, 1974). Functional traits that play a role in passive or active temperature regulation vary over elevational gradients, including leaf surface area, leaf margin dissection, leaf mass per area, leaf dry matter content, and leaf thickness (Gurevitch, 1988; Hüner et al., 1998; Streb et al., 1999; Pellissier et al., 2013). Overall, alpine plant leaves tend to be smaller in area while denser in mass, giving a smaller specific leaf area (SLA). The low SLA values of many alpine taxa represent the slow extreme end of the leaf economic spectrum, where leaves are costly, but hardy and slow on return of investment (Woodward, 1983; Donovan et al., 2011). While the overall trend shows that alpine plant leaf traits support a relatively limited ability to regulate leaf temperature compared to lowland taxa (Michaletz et al., 2016; Blonder and Michaletz, 2018), important differentiation still occurs among taxa. For instance, some taxa in high radiation habitats developed increased leaf hairiness to augment reflectance of solar radiation to maintain a T_{LEAF} closer to T_{AIR} (Ehleringer and Mooney, 1978). In another approach, leaves can possess succulent leaves with specific water-storage cells that can withstand water deficit conditions (Ehleringer and Mooney, 1978), increasing capacity for leaf heat storage while slowing heat dissipation (Lewis and Nobel, 1977). Overall, leaf thermal tolerance (i.e., T_{LEAF} that is lethal to 50 % of leaf surface) (e.g., Buchner and Neuner, 2003; Slot et al., 2021) tends to increase in species in high radiation habitat and with costly leaves that cannot rapidly cool down when heated (Idso and Baker, 1967; Slot et al., 2021). Despite the relatively narrow morphological range of alpine taxa, we find indications of divergence in ability to either avoid leaf heating or actively regulate leaf temperature.

The genus *Saxifraga* contains taxa from temperate lowlands as well as the coldest (Körner, 2011) and highest alpine habitats known for vascular plants (Oehl and Körner, 2014). Some of the lowland species with large, dissected leaves are deciduous and on the low-investment-end of the leaf economic spectrum, while alpine species that tend to be small-leaved represent the other end of the spectrum (Tkach et al., 2015b). As in most other alpine taxa, leaves of alpine *Saxifraga* are smaller, have lower mass and are less dissected in alpine habitats compared to related lowland species (Zhu et al., 2010; Jeffery, 2017). While leaf size changes systematically with elevation, diversity in leaf size within the alpine across phylogenetically distinct groups is still relatively large (Jeffery, 2017), indicating ecological differentiation among species. Traits in *Saxifraga* associated with elevation that have evolved once or more, include the cushion growth form and lime-secreting hydathodes on leaf margins (Wightman et al., 2018). Ebersbach et al. (2017b) recently found that evolution of these characters correlated with an increase in the rate of species diversification, although not universally across the genus. These findings suggested that leaf- and growth form evolution constitutes the building blocks of adaptive radiation. As these traits affect leaf heating through their effect of decreasing the boundary layer (cushion form) and increasing reflectance (hairs, waxy cuticle, and lime secreting hydathodes), it is likely that changes in leaf ecophysiology has played a major role in driving the diversification of alpine *Saxifraga*. Yet, the precise relation between leaf and growth form traits on the heating of leaves remains unclear.

In this study, we aim to investigate the functional implications of leaf trait and growth form evolution across *Saxifraga* species, focusing on the relation between air temperature (TAIR) and leaf temperature (TLEAF) under a wide range of solar incident radiation values. Specifically, we test the following hypotheses: 1) that the temperature offset of leaves compared to air temperature ($\Delta T = TLEAF - TAIR$) increases with solar radiation, reflecting ecophysiological expectations of $\Delta T > 1$ for alpine specialists , 2) that leaf and whole-plant functional traits predict temperature offset response to incident solar radiation ($\Delta T \sim SI$) (i.e., thermoregulation capacity), and 3) that closely related species will have a similar value of $\Delta T \sim SI$. Regarding traits, we expect leaf area and dry mass, among others, to affect $\Delta T \sim SI$, similarly for whole plants traits that represent cushion-likeness, such as rosette density. To control for heterogeneous environmental effects, we conducted the study in a common garden experiment measuring temperature responses across a broad sample of 44 *Saxifraga* taxa, collected functional trait from the experimental plants, and we use the newly inferred phylogeny from this thesis presented in the previous two chapters.

4.2 Materials and Methods

4.2.1 Set-up and species selection

The taxa for the study were selected to represent the taxonomic diversity (as many sections within *Saxifraga* as possible), and morphological variation of the genus, with growth forms ranging from broad-leaved herbs to compact cushion plants. However, not all sections or functional diversity could be included due availability in cultivation (e.g., Harding, 1976). A total of 44 taxa was used, from 8 clades as per established in chapter 3 and one outgroup (*Micranthes stellaris* - STEL). Species names are shown as 4 four letter abbreviations **(Table 4.1)**. The included taxa represent habitats ranging from temperate, lowland meadows to montane forests and alpine cliffs.

The plants for which we measured air-leaf temperature offset were sourced from living collections at Royal Botanic Gardens, Kew and Cambridge University Botanic Garden. Within the living collections we selected healthy single potted plants that were maintained in similar conditions within and among sites. Overall, plants were permanently kept in aerated, partially shaded greenhouses with daily watering regimes at two sites 80 km apart. Although potted plants were kept under similar regimes of care, the plants at Kew would likely experience higher temperatures year-round due to the London heat island (Bassett et al., 2021). However, for this study we assume it has reduced effect due to the controlled greenhouse conditions. The evening before measurements, plants were watered to avoid water stress effects on transpiration capacity (Grant et al., 2007). Photos were taken to assess plant health before and two weeks after measurements. If plants showed rosette browning/mortality or any other deterioration two weeks after measurements, they were labelled unfit for further inclusion in analyses. The measurements for the study were performed between 21-04-2019 and 26-07-2019.

Genus	Section	Species epithet	SpecID
Saxifraga	*Saxifraga*	*berica* (Bég.) D.A.Webb	**BERI**
Saxifraga	*Porphyrion*	*burseriana* L.	**BURS**
Saxifraga	*Ligulatae*	*callosa* Sm.	**CALL**
Saxifraga	*Saxifraga*	*canaliculata*	**CANA**
Saxifraga	*Saxifraga*	*catalaunica* Boiss. & Reut.	**CATA***
Saxifraga	*Porphyrion*	*caucasica* Sommier & Levier	**CAUC**
Saxifraga	*Saxifraga*	*cebennensis* Rouy & E.G.Camus	**CEBE**
Saxifraga	*Ligulatae*	*cochlearis* Rchb.	**COCH**
Saxifraga	*Ligulatae*	*cotyledon* L.	**COTY**
Saxifraga	*Gymnopera*	*cuneifolia* L.	**CUNE**
Saxifraga	*Cymbalaria*	*cymbalaria* L.	**CYMB**
Saxifraga	*Porphyrion*	*diapensioides* Bellardi	**DIAP***
Saxifraga	*Saxifraga*	*exarata* ssp. *carniolica* (Huter) Jalas	**EXCA**
Saxifraga	*Porphyrion*	*ferdinandi-coburgi* Kellerer & Sünd.	**FERD**
Saxifraga	*Ciliatae*	*flagellaris* Willd.	**FLAG**
Saxifraga	*Saxifraga*	*fragilis* Schrank	**FRAG***
Saxifraga	*Irregulares*	*fortunei* var. *obtusocuneata* Makino	**FOOB**
Saxifraga	*Porphyrion*	*georgei* J. Anthony	**GEOR**
Saxifraga	*Saxifraga*	*geranioides* L.	**GERA**
Saxifraga	*Saxifraga*	*granulata* L.	**GRAN**
Saxifraga	*Ligulatae*	*hostii* ssp. *rhaetica* (A.Kern. ex Engl.) Braun-Blanq.	**HORH**
Saxifraga	*Saxifraga*	*hypnoides* L.	**HYPN**
Saxifraga	*Saxifraga*	*latepetiolata* Willk.	**LATE**
Saxifraga	*Porphyrion*	*lilacina* Duthie	**LILA**
Saxifraga	*Saxifraga*	*maderensis* D.Don	**MADE**
Saxifraga	*Saxifraga*	*maderensis* ssp. *pickeringii* C.Simon	**MAPI**
Saxifraga	*Saxifraga*	*moncayensis* D.A.Webb	**MONC**
Saxifraga	*Porphyrion*	*oppositifolia* L.	**OPPO**
Saxifraga	*Porphyrion*	*paniculata* ssp. *cartilaginea* (Willd.) D. A. Webb	**PACA**
Saxifraga	*Ligulatae*	*paniculata* Mill.	**PANI**
Saxifraga	*Saxifraga*	*pedemontana* All.	**PEDE**
Saxifraga	*Saxifraga*	*pedemontana* ssp. *prostii* (Sternb.) D.A.Webb	**PEPR**
Saxifraga	*Porphyrion*	*sancta* Griseb.	**SANC**
Saxifraga	*Porphyrion*	*scardica* Griseb.	**SCAR**
Saxifraga	*Porphyrion*	*scleropoda* Sommier & Levier	**SCLE**
Saxifraga	*Porphyrion*	*sempervivum* K.Koch	**SEMP**
Saxifraga	*Gymnopera*	*spathularis* Brot.	**SPAT**
Saxifraga	*Porphyrion*	*spruneri* Boiss.	**SPRU**
Saxifraga	*Irregulares*	*stolonifera* Curtis	**STOL**
Saxifraga	*Porphyrion*	*stribrnyi* (Velen.) Podp.	**STRI**
Saxifraga	*Saxifraga*	*tridactylites* L.	**TRID**
Saxifraga	*Porphyrion*	*valdensis* DC.	**VALD**
Saxifraga	*Porphyrion*	*wendelboi* Schönb.-Tem.	**WEND**
Micranthes	*Outgroup*	*stellaris* (L.) Galasso, Banfi & Soldano	**STEL**

Table 4.1: Genus, section, and (sub)species names as identified by botanic gardens along with 4-letter "specID" codes used per taxon. Taxa with an asterisk are not included in analyses, due to absence in phylogenetic tree or sparse temperature data available above SI 600 W m^{-2}.

4.2.2 Plant temperature and environmental data measurement

Multiple plants were measured on a workbench throughout a day, approximately from sunrise to sunset, to obtain temperature measurements over at least a range of incident solar irradiance (SI) between 0 to 800 W m^{-2}. Three leaves were measured per plant, for one, two, or three plants depending on availability at the living collections. Measurements were made in cycles, where for each cycle every leaf in the set-up individually had its associated temperature under solar irradiance measured. Once for each cycle, other environmental variables were measured that were linked to all temperature measurements in the cycle.

During each cycle, for each individual leaf, leaf temperature in °C (T_{LEAF}) was measured on the adaxial side at the center of the lamina with a thermometer (TASI®, TASI-8620) with type-K thermocouples. Horizontally positioned leaves were measured to ensure the same angle of solar radiation toward the plane of incidence as that of that solar radiation meter, and the angle of the meter was changed accordingly. At the same time, the air temperature (T_{AIR}) at approximately 5 cm above the leaf surface was measured with another thermocouple on the same thermometer. Thermocouples were shaded between measurements to limit additional heating from solar radiation. Control measurements for T_{LEAF} were made with an infra-red laser thermometer (Etekcity, Lasergrip 1080) pointed at the same position on the leaf surface (T_{IR}). The incident solar irradiance in W m^{-2} (SI) was measured from a fixed location just above the plants on the workbench with a solar irradiance meter (Handyman, TEK1307), registering both direct and diffuse radiation. Finally, all previous measurements were taken at roughly the same time, which was additionally recorded (hour:minutes).

To control for the range of naturally fluctuating environmental factors that can strongly affect transpiration, and to a lesser degree convection (Idso and Baker, 1967), we measured wind speed and relative humidity at the start of each cycle. For wind effects on the boundary layer to be minimised throughout the dataset, we measured wind speed in m s^{-1} at plant height with an anemometer (Benetech, GM8902). Air flow was present at < 4 m s^{-1} during measurements (moderate breeze, Beaufort number 4), and all processes were halted during stronger wind speed at plant level. Overall, the work benches were partially sheltered and deviations in wind speed above 4 m s^{-1} were strongly limited. The relative humidity in % (RH) was measured with a hygrometer (Ehdis, LH500) and its effect on temperature regulation was not controlled during measurements but further assessed during data analysis.

4.2.3 Temperature response analysis

An initial test of water vapour pressure deficit (VPD) values for all temperature measurements was done to visualise the range of VPD occurring in the data. The VPD shows the deficit between air moisture and maximum moisture that can be contained when saturated. Low VPD values strongly affect stomatal conductance (Shirke, 2004; Grossiord et al., 2020), and are an extreme form of plant stress resulting in stomatal closure and thus the ability to actively regulate leaf temperature. Therefore, an initial removal of data points was performed for all data from days with outlier VPD values > 5 kPa. To this end, saturation vapour pressure in millibar (SVP) was first calculated for T_{AIR} (Monteith and Unsworth, 2013), through the formula

$$SVP = 610.7 * 10\text{^}(\frac{7.5*Tair}{(237.3+Tair}))$$

Then, the VPD was calculated in in kPa through

$$VPD = \frac{100 - RH}{100 - SVP}$$

The temperature response of T_{LEAF} to changing T_{AIR} was tested through linear models, both for the complete dataset (using a PGLS regression), as well as for separate taxa and individuals (using OLS regression) measured therein. Then, the leaf temperature offset (ΔT) was calculated by subtracting T_{AIR} from T_{LEAF}, and additionally ΔT was calculated through T_{IR} instead of T_{LEAF}. The temperature response of leaves to solar radiation was defined as the slope of the linear model of ΔT as a function of SI. The linear ∆T~SI models were made for all taxa and individuals using OLS regression.

4.2.4 Functional trait measurements

General attributes of plant morphology were recorded for every plant included in the temperature study. Plant height and maximum diameter as seen from above (cm) were measured, as well as diameter of individual rosettes, taking the mean for up to ten rosettes (depending on availability and growth form). For these rosettes, the average internode length (mm) was measured between fully grown, healthy leaves. Rosette density per cm2 was measured by counting all rosettes that were present with more than half of their surface within a frame of 5x5 or 10x10 cm depending on plant size. A leaf area index (LAI) was calculated by counting the number of living leaves that overlap each other perpendicular to

the ground, averaged from five to ten random points on the plant canopy. Here, LAI can be defined as a unit of (stacked) leaf area (see Gholz et al., 1976). While LAI is usually an effective trait to define processes at a community level (Violle et al., 2012), in this case it is a proxy for plant compactness and effects on the boundary layer.

Leaf functional traits were measured through averaging measurements of five to ten leaves from one or multiple individual plants. Leaves were collected from healthy plants approximately one hour after watering. The leaf thickness was measured with an analog thickness gauge (x 0.01mm) and M_w was measured for all leaves for a taxon at the same time on a weighing scale (x 0.1 mg) (Sartorius Lab Instruments GmbH and Co., SECURA225D-1S). Next, leaves were scanned (adaxial) using a flatbed scanner (HP, Scanjet 200). Size measurements were made from scanned images in ImageJ (Abràmoff et al., 2004; Rasband, 2012). We measured leaf length, leaf width, leaf thickness, wet leaf mass (M_w), leaf area of fresh leaves including petiole (A_l), leaf perimeter including petiole (P_l), largest circle size on leaf surface (LC_l) (methods reviewed by Perez-Harguindeguy et al., 2016). Afterwards, leaves were left to dry in an oven at 60 °C for seven days, followed by measurement of dry leaf mass (M_d).

With the measured leaf functional traits, we calculated composite traits related to the leaf economic spectrum. Importantly, they portray life strategies and predict resistance to eco-physiological sources of stress (Donovan et al., 2011; Pérez-Harguindeguy et al., 2016). The specific leaf area (SLA) ($mm^2\ mg^{-1}$) predicts resource investment in leaves, as well as respiratory rate, resistance to drought and other perturbations, and is defined as

$$SLA = \frac{Al}{Md}$$

Leaf dry matter content (LDMC) ($kg\ kg^{-1}$) as an important predictor of net primary production (Smart et al., 2017) is defined as

$$SLA = \frac{Md}{Mw}$$

We tested for each functional trait whether it predicted the ∆T ~ SI slopes (hypothesis 2), using a phylogenetic generalized least square regression (with correlation structure of the error term based on a Brownian evolution model) implemented in the R package Caper (Orme et al., 2012). We then visualized their relation through the phylomorphospace function in phytools 0.7-47 (Revell, 2012). To additionally visualise differences in traits across species and temperature response groups, we performed principal coordinate analysis (PCoA).

4.2.5 Evolutionary signal

The presence of a phylogenetic signal for the slope of the ∆T~SI models was tested through the fitContinuous function in Geiger 2.0.7 (Pennell et al., 2014) under a lambda model of evolution (Pagel, 1999) that had the lowest AIC-score when constrained (lambda > 0). All functional traits were log-transformed to improve normality; for internode length we added 1 before log-transforming, as this trait includes the value zero. The phylogeny used for all purposes was the maximum likelihood phylogeny that was constrained by the Astral species tree topology, as described in chapter 3 of this thesis. We also mapped the functional traits separately on the phylogeny (ultrametric presentation) to test for phylogenetic signal, as here we analyse more species and traits than have been included by Jeffery (2017).

4.3 Results

4.3.1 Environmental effects on leaf temperature response

Overall, the leaf temperature (TLEAF) data shows a strong relation with TAIR for the complete dataset **(Fig. 4.1A; Fig. 4.2)** (Adj. R_2: 0.8154, F: 11440, df: 2589, $P < 0.0001$). The relationship between TLEAF and TAIR additionally was found to be positive ($b > 1$, $P < 0.05$) for all 44 taxa **(Appendix 4.1),** including species with lowland, montane and alpine habitat origins.

The vapour pressure deficit (VPD) had extreme outlier values **(Fig. 4.1B)**, especially around midday on a few of the warmest days. Thus, a breakdown of the linear relationship of T_{LEAF} and T_{AIR} with high VPD is suggested. For two specific days during a heat wave (22-04-2019 and 26-05-2019) the VPD for multiple data points was above the threshold that was set at 5 kPa (see **Fig. 4.1B**). Removal of all data for these days resulted in a loss of 4 taxa for further analyses (down to 40).

The linear relationship between temperature offset (∆T) and solar irradiance (SI) for the complete temperature dataset (before removal of high VPD values) was again strongly positive both when measuring leaf temperature using thermocouples (TLEAF; Adj. R_2 =0.6879, F = 5709, df = 2589, P = 0) and using infrared thermometers (TIR; Adj. R_2 = 0.2189, F = 726.6, df = 2589, P = 0) **(Fig. 4.2)**. An analysis of variance (ANOVA) found that TIR is more noisy than TLEAF and therefore we only consider TLEAF for further analyses (F(1, 2589) = 5709.1, P = 0). Further using ∆T based on TLEAF, a significant correlation between ∆T and SI was present for all taxa (b > 1, P < 0.05), and slopes were found to be different among taxa **(Appendix 4.2)**.

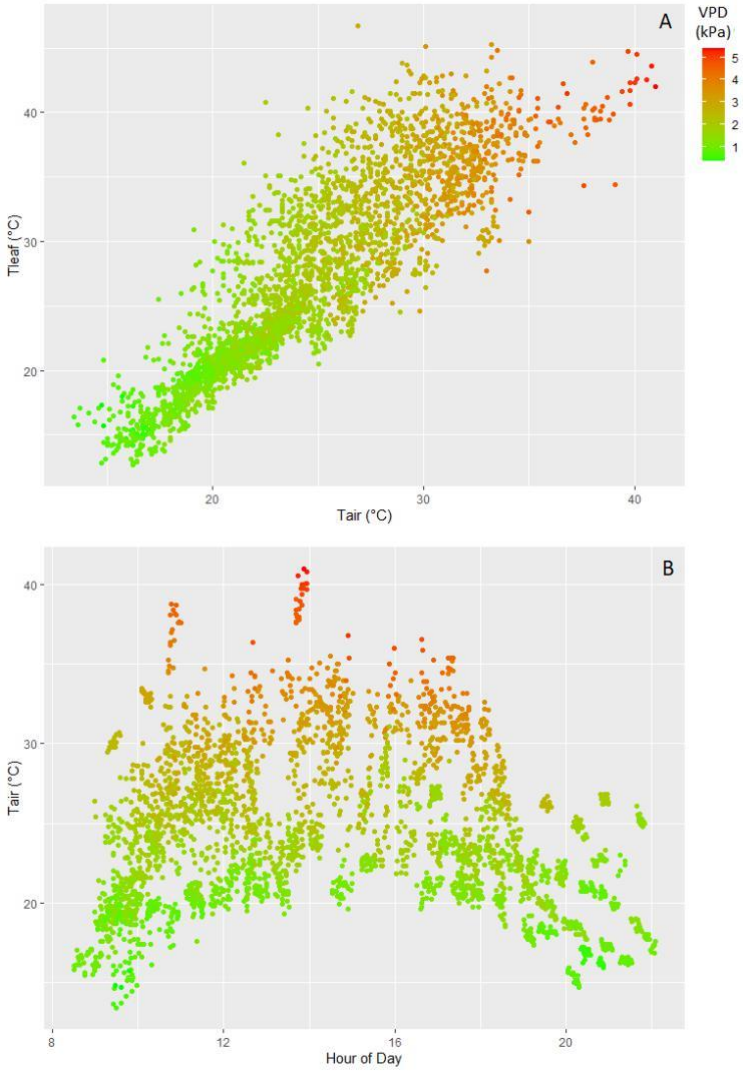

Fig. 4.1: The (A) leaf temperature (T_{LEAF}) set out against air temperature (T_{AIR}), and (B) T_{AIR} plotted over the time of day. Data points are coloured by vapour pressure deficit (VPD), which shows higher values with increased T_{AIR}, with highest outlier values close to midday, due to temporary high T_{AIR} and low relative humidity.

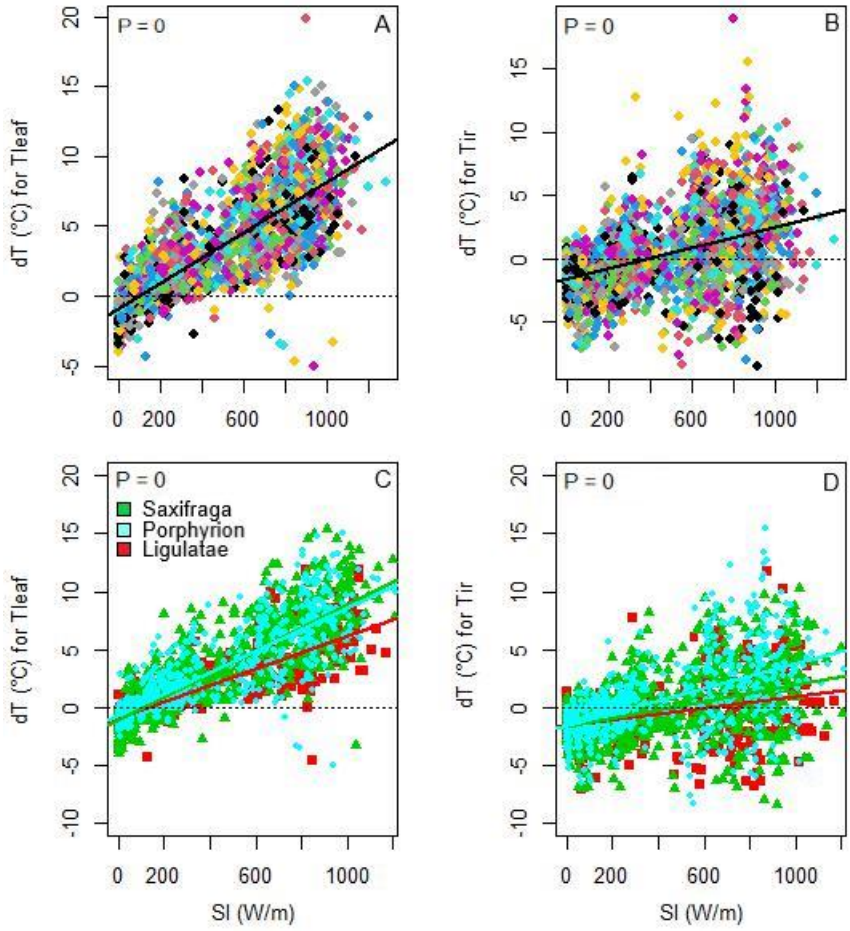

Fig. 4.2: The leaf temperature offset (∆T) is plotted against solar irradiance (SI) (where the former is measured using thermocouples (T_{LEAF}) (A); or infrared thermometer (T_{IR}) (B) across all species. Data points are coloured by species ID; see ***Appendix 4.2*** *for analogous plots for individual species, which all have a significant positive slope. The three sections with a high number of taxa present in the dataset have been plotted to compare effects among major clades. Again ∆T is based on T_{LEAF} (C) and T_{IR} (D) and data points and regression lines are coloured by clade While all slopes were significant, those for Tleaf had the highest fit (*Saxifraga; *Adj.* $R_2 = 0.6552$, $P = 0$, Porphyrion; *Adj.* $R_2 = 0.5892$, $P = 0$, Ligulatae; *Adj.* $R_2 = 0.4181$, $P < 0.001$*). For m For this figure and subsequent analyses, values obtained during periods of extreme VPD (>5 kPa) were excluded.*

Next page: Table 4.2: Leaf and whole plant trait values, given as average value of leaves (shown in column) or 1-4 plants used in temperature response measurements. Leaf trait values shown are wet mass (M_w), dry mass (M_d), thickness, length, width, leaf area (A_l), leaf perimeter (P_l), leaf largest circle area (LC_l), specific leaf area (SLA), and leaf dry matter content (LDMC). Whole plant trait values shown are height and diameter for the entire plant and individual rosettes, leaf area index (LAI), and the internode length. Missing values (NA) occur if any value was uncertain due to any issues in the trait measurement process.

		Leaf traits										Whole plant traits					
SpecID	Leaf Nr.	M_w (g)	M_d (g)	thickness (mm)	length (mm)	width (mm)	A_l (mm^2)	P_l (mm)	LC_l (mm^2)	SLA ($mm^2 mg^{-1}$)	LDMC ($kg kg^{-1}$)	Height (cm)	Diam. (cm)	$Height_{rosette}$ (mm)	$Diam_{rosette}$ (mm)	LAI	Internode (mm)
BERI	5	0.0458	0.0050	0.37	35.68	17.59	196.69	132.45	53.34	39.34	10.93%	4.75	8.65	33.00	47.15	2.70	9.0
BURS	10	0.0014	0.0004	NA	5.28	1.32	5.05	11.24	1.65	11.85	30.89%	2.00	15.00	7.30	7.10	3.60	0.0
CALL	5	0.0776	0.0143	0.62	63.84	3.11	129.57	106.36	8.00	9.09	18.39%	6.40	17.00	32.30	79.50	3.15	0.0
CANA	5	0.0559	0.0146	0.96	22.38	16.26	96.12	99.85	11.15	6.59	26.07%	6.50	17.50	33.10	44.70	3.00	0.8
CAUC	10	0.0005	0.0002	0.14	3.85	1.04	2.96	8.59	0.95	12.35	53.31%	2.90	7.25	3.65	6.40	2.60	0.0
CEBE	5	0.0067	0.0007	0.29	10.95	4.54	24.84	27.92	7.28	36.53	10.17%	2.80	13.75	3.90	11.60	3.75	0.0
COCH	5	0.0163	0.0029	NA	NA	NA	24.98	26.35	10.06	8.57	17.88%	4.00	11.30	13.40	36.70	4.70	0.0
COTY	5	0.2716	0.0619	1.32	62.93	15.95	239.91	64.82	103.15	3.88	22.78%	6.80	20.67	48.00	124.67	4.20	0.0
CUNE	5	0.0514	0.0091	0.37	26.38	10.34	113.85	61.99	67.98	12.54	17.68%	NA	NA	NA	NA	NA	NA
CYMB	15	0.0694	0.0052	0.63	27.53	17.45	201.02	91.42	86.40	38.76	7.47%	2.90	6.40	29.00	64.00	2.00	10.7
DIAP	10	0.0020	0.0004	0.28	4.03	1.60	5.40	9.53	2.28	12.56	22.05%	2.00	6.00	4.00	6.60	2.70	0.0
EXCA	5	0.0119	0.0013	0.32	13.24	4.65	28.09	38.63	6.92	21.28	11.07%	4.00	11.30	13.40	36.70	4.70	0.0
FERD	10	0.0022	0.0007	NA	NA	NA	6.70	9.95	2.86	10.24	29.12%	3.90	15.00	7.70	10.90	3.25	0.0
FLAG	5	0.0577	0.0082	0.53	30.94	3.47	9.62	87.04	65.45	1.18	14.17%	4.50	9.00	31.30	46.30	3.30	0.1
FOOB	3	0.0825	0.0096	0.54	46.10	15.99	171.83	131.25	50.43	17.96	11.60%	3.00	11.00	30.00	110.00	2.60	0.0
FRAG	5	NA	0.0095	0.99	30.50	14.32	97.51	103.91	9.44	10.22	NA	7.00	18.00	51.10	93.00	2.60	0.4
GEOR	10	0.0008	0.0002	0.13	2.77	1.57	3.31	7.27	2.04	13.80	31.58%	2.00	7.50	3.85	3.90	2.10	0.2
GERA	5	0.0775	0.0146	0.79	27.79	14.69	119.86	94.74	14.55	8.19	18.87%	7.50	17.50	40.90	75.70	3.90	0.0
GRAN	5	0.1410	0.0179	NA	68.06	25.65	412.01	214.19	83.90	23.02	12.69%	3.75	7.93	27.00	101.00	0.90	1.5
HORH	5	0.1662	NA	1.05	53.13	5.30	267.10	126.93	22.46	NA	NA	8.50	19.00	39.85	77.70	4.25	0.0
HOST	5	0.9725	0.1913	1.55	114.65	10.48	1137.44	313.96	90.29	5.95	19.67%	NA	NA	NA	NA	NA	NA
HYPN	6	NA	NA	0.34	11.76	8.57	30.59	46.69	5.38	NA	NA	3.25	11.25	25.65	22.00	4.40	0.7
LATE	5	0.0787	NA	0.80	74.49	31.69	672.66	271.33	70.48	NA	NA	7.80	25.00	69.30	123.60	3.50	0.0
LILA	10	0.0020	NA	0.26	5.57	1.29	6.44	12.53	1.35	NA	NA	1.50	7.00	4.00	9.90	2.30	0.0
MADE	5	0.3011	0.0659	1.03	NA	NA	484.83	260.83	60.50	7.36	21.88%	14.50	30.00	64.60	87.70	1.70	0.9
MONC	5	0.0091	0.0014	0.40	19.10	12.19	40.76	77.02	2.30	28.42	15.75%	NA	NA	NA	NA	NA	NA
OPPO	10	0.0008	0.0002	0.27	2.56	1.48	3.47	6.25	1.89	19.05	21.88%	5.10	25.00	56.35	10.20	2.60	1.9
PACA	2	0.0699	NA	0.94	24.94	6.95	113.44	60.11	36.55	NA	NA	5.70	17.67	20.23	32.30	4.33	0.0
PANI	5	0.0393	0.0075	NA	NA	NA	53.42	27.60	23.82	7.11	19.11%	7.00	17.30	20.00	30.00	1.90	0.0
PEDE	5	0.0325	NA	0.56	15.58	12.33	70.88	67.72	12.60	NA	NA	7.80	25.50	23.55	20.55	4.00	0.4
PEPR	5	0.0095	0.0011	0.57	16.69	12.13	29.64	35.30	5.22	26.14	11.93%	9.67	23.00	25.50	26.80	4.45	0.2
SANC	6	0.0048	0.0013	0.55	8.45	2.01	12.09	18.53	3.12	9.30	27.13%	8.20	17.75	9.70	12.75	4.25	0.0
SCAR	10	0.0144	0.0032	0.72	10.70	3.24	30.85	23.13	8.68	9.77	21.87%	7.80	27.50	19.40	20.20	3.70	0.0
SCLE	10	0.0029	0.0008	0.37	8.28	1.47	10.59	16.77	1.81	12.69	28.66%	4.50	13.00	10.30	13.90	2.70	0.0
SEMP	5	0.0124	0.0029	0.64	NA	NA	25.41	26.15	5.26	8.80	23.26%	6.00	15.00	15.10	24.70	3.70	0.0
SPAT	5	0.1225	NA	0.94	33.03	16.36	260.48	92.93	147.31	NA	NA	7.00	38.50	57.15	87.70	2.70	1.0
SPRU	10	0.0022	0.0006	0.38	5.94	2.07	9.48	14.72	3.53	16.64	25.93%	5.30	16.00	4.60	9.60	2.70	0.0
STOL	3	2.7707	0.3439	1.41	124.79	79.14	4266.20	255.14	3198.89	12.40	12.41%	6.00	21.00	43.80	120.00	2.30	0.0
STRI	5	0.0286	0.0085	0.37	NA	NA	44.40	29.99	14.60	5.24	29.60%	3.45	8.25	13.65	21.40	3.80	0.0
TRID	10	0.0152	0.0015	NA	14.19	8.22	42.10	46.09	10.21	28.64	9.66%	NA	NA	NA	NA	NA	NA
VALD	5	0.0103	0.0022	1.14	8.87	2.43	14.29	21.18	4.62	6.62	21.01%	5.75	12.00	5.75	11.00	2.55	0.0
WEND	10	0.0039	0.0010	0.51	4.45	2.16	9.96	11.68	4.94	9.62	26.81%	4.00	12.00	5.90	8.60	2.10	0.0
STEL	6	0.0134	0.0020	0.27	10.46	5.69	38.86	28.24	20.52	19.76	14.66%	1.40	5.25	7.25	19.20	2.40	0.3

4.3.2 Functional trait predictions of leaf temperature offset

Trait data is presented in **Table 4.2**, where averages are used per taxon. The relationship between functional traits, and the slope and intercept of the ΔT~SI models was first tested on data without removal of the two days with high VPD outlier data. This resulted in no significant relationships between any of the leaf and whole plant traits. After high VPD outlier removal, no significant trends for a correlation with ΔT~SI slopes emerged for any of the traits **(Appendix 4.3).** However, sect. *Porphyrion* clustered together in phylomorphospace, and was clearly distinct from the rest of the genus, forming a morphologically distinct cluster despite divergent ΔT~SI values **(Fig. 4.3).** Additional multivariate analysis through principal coordinate analysis (PCoA) did not reveal any further grouping of ΔT~SI values or clades **(Fig. 4.3)**. The eigenvalues from the PCoA are presented in **Appendix 4.4.**

4.3.3 Phylogenetic signal

After removing data measured on days with outlier high VPD (>5 kPa), we find phylogenetic signal under a lambda model (ʎ = 0.744296). Thus, closely related species are more likely to have a similar response of ΔT to increasing SI. Overall, trends in the phylogeny revealed that sections *Saxifraga* and *Porphyrion* **(Fig. 4.5)** incline towards high degree of leaf heating from radiation (higher ΔT with increasing SI, thus steeper slopes), despite some outliers. The other well-represented section in the phylogeny, *Ligulatae*, showed a lesser degree of heating from radiation, revealing a tendency to remain close to T_{AIR} with increasing through either active or passive means.

Phylogenetic signal under lambda model (ʎ) was also found in most of the leaf and whole plant traits. Lambda values show phylogenetic signal for all traits except plant height and leaf area index (LAI). A rather low value for signal was found for leaf wet mass (Mw), specific leaf area (SLA) and rosette diameter. Notably, most traits that lack signal or have lower phylogenetic signal are strongly affected by plant growing conditions and long-term water availability that we could not control within the scope of this study. Apart from ʎ values and continuous traits imposed on phylogenies, the computed values for model selection through Akaike's information criterion (AIC) are given in **Appendix 4.4** and **Appendix 4.5.**

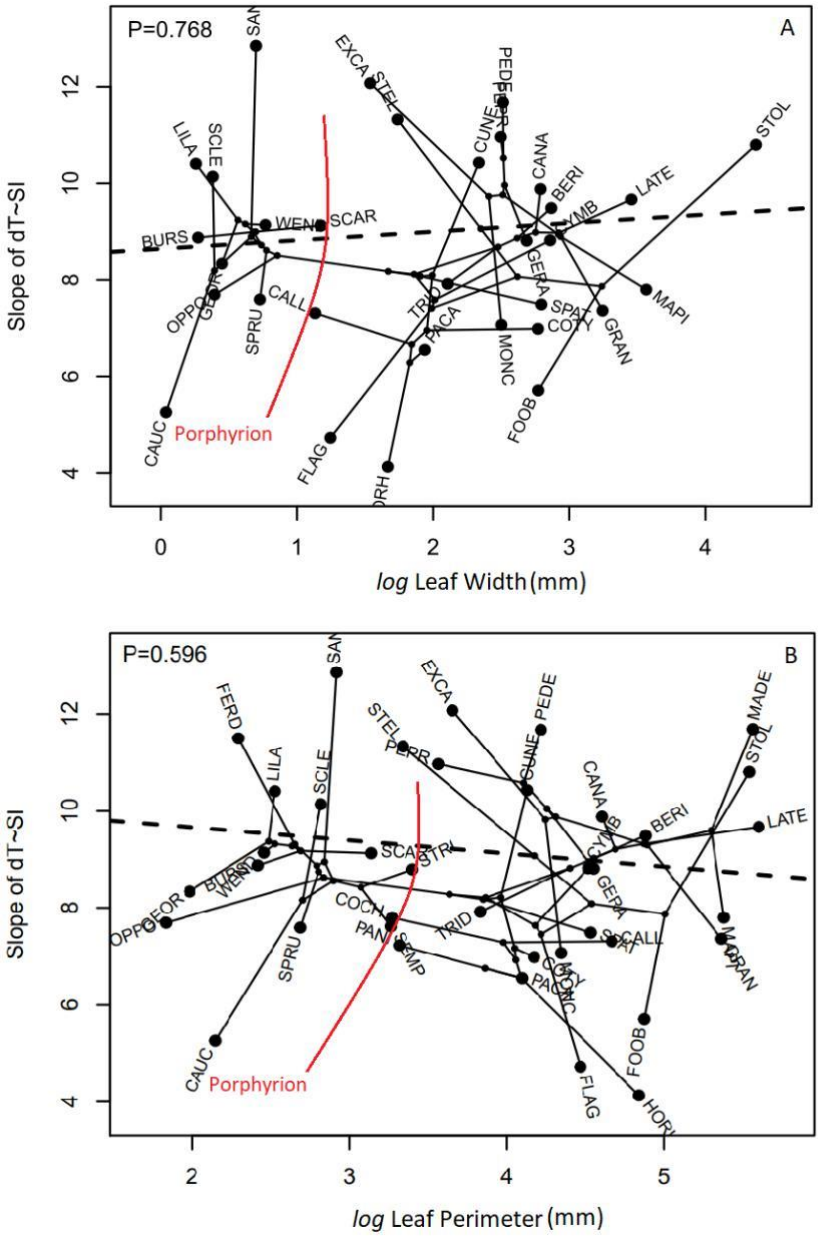

Fig. 4.3: Phylomorphospace plots of the slope of ΔT~SI as a function of plant morphological variables. Variables shown here on the x-axis are (A) leaf width (mm) and (B) leaf perimeter (mm), for which clear differentiation in section Porphyrion *is visible (red barrier). The species identities are indicated by four letter abbreviations (large dots), and the ancestral states are reconstructed for each internal node (small dots). None of the slopes are significant.*

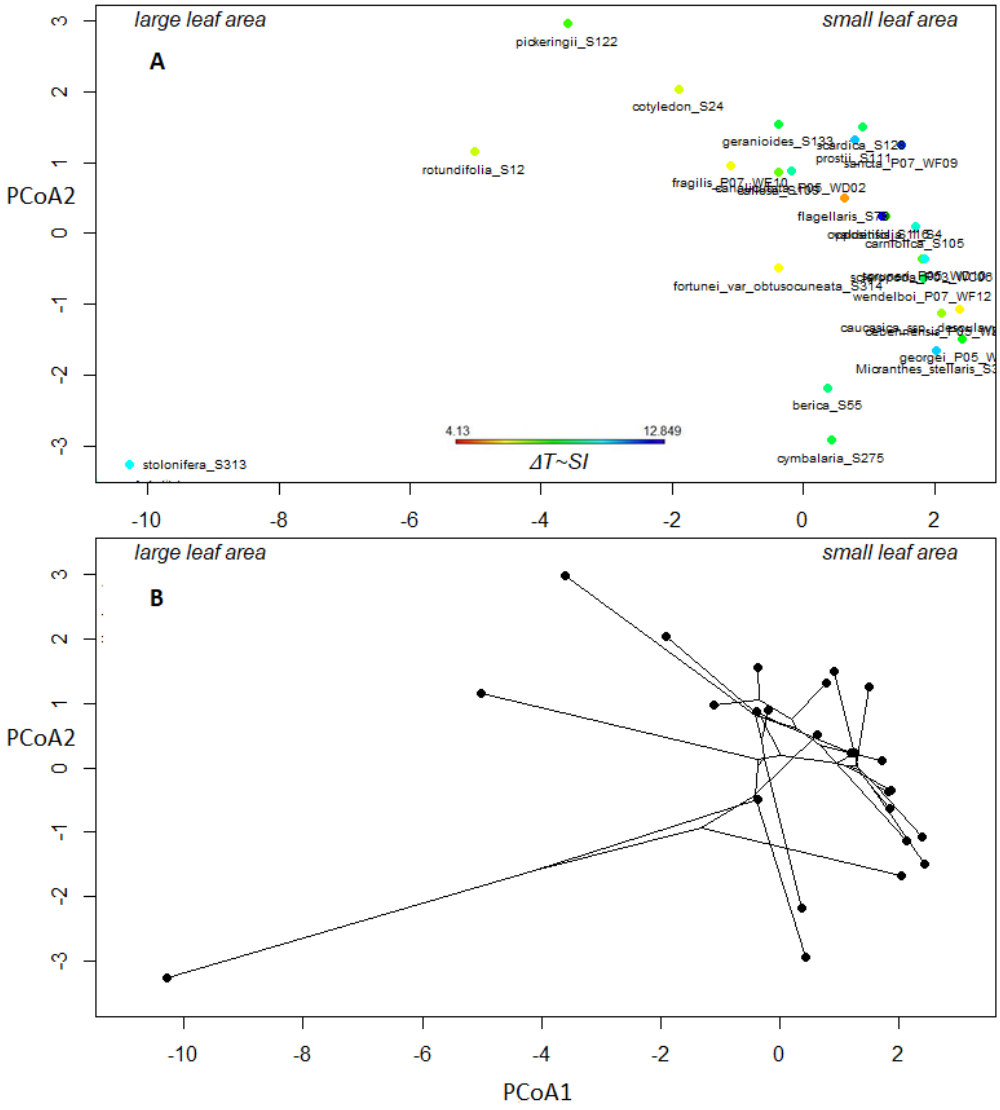

Fig. 4.4: (A) PCoA ordination plot showing distances among 25 Saxifraga *species and* Micranthes nivalis *outgroup for which all trait values are present. The data points are coloured as per the value of the slope of ΔT~SI, for which a legend is embedded. Principal component 1 is mostly affected by traits relating to leaf size, and component 2 is mostly affected by whole plant dimensions and leaf density. Phylomorphospace plot (B) of the same taxa and axes is also given. As no significant correlations were found between ΔT~SI slopes and individual traits, so again do no patterns emerge from the PCA matrix. Individual PCoA values are presented in Appendix 4.4.*

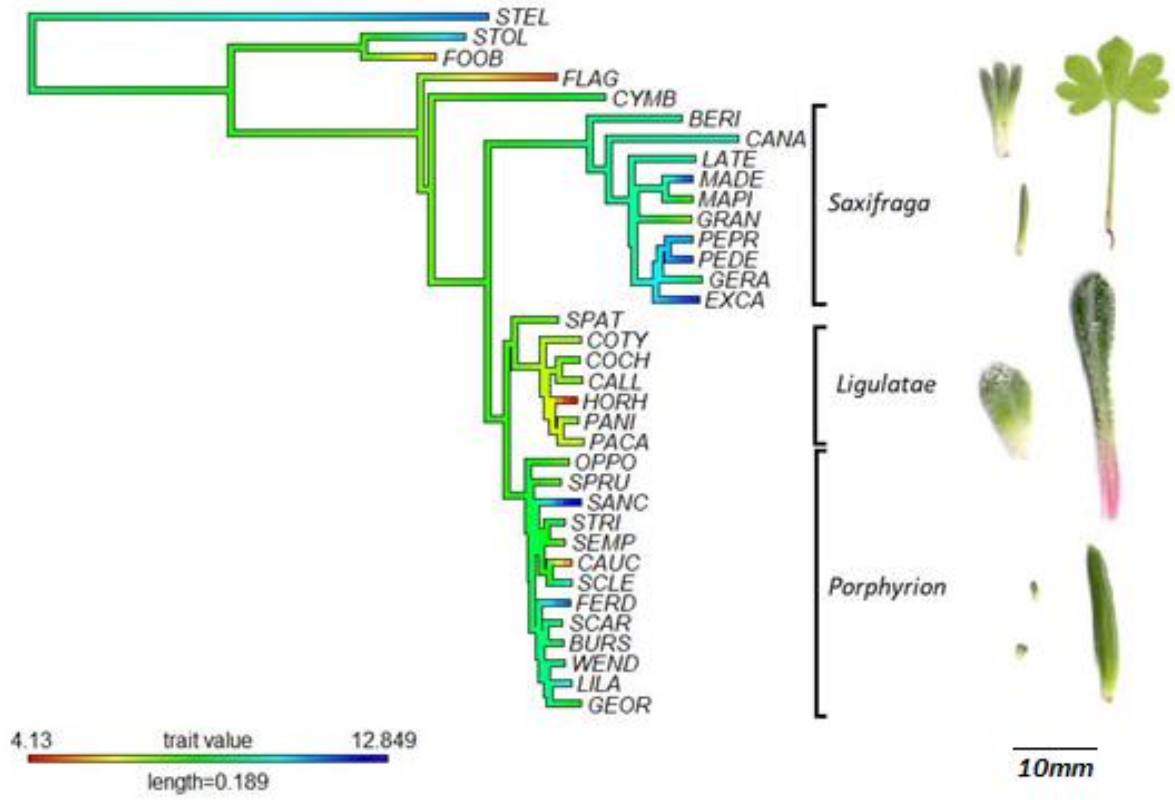

Fig. 4.5: Phylogenetic tree of Saxifraga with slope of ΔT~SI estimated on branches. The species identities are indicated by four letter abbreviations. Closely related species have more similar values (λ = 0.744296).

4.4 Discussion

4.4.1 Leaf temperature response to air temperature and radiation

We found a positive relation of T_{LEAF} with T_{AIR} for all data combined, among sections, and for each taxon individually. Importantly, the positive relationship for the full dataset with a slope > 1 (megathermy) is in line with the relationship found for alpine cushion plants (Michaletz et al., 2016; Blonder and Michaletz, 2018). Megathermy occurs naturally when convective resistance is high (e.g., in cushion plants) or stomatal conductance is low, and notably under conditions with high environmental temperatures and incident radiation (Blonder and Michaletz, 2018). Most species of *Saxifraga* we included in temperature measurements are considered to have a cushion growth form, creating a morphological constraint for effective temperature regulation, partially explaining megathermy. However, we found the same megatherm temperature response in lowland and montane herb and rosette growth forms, likely due to the overall high temperatures and radiation conditions included in our measurements (Blonder and Michaletz, 2018), which may alter leaf temperature response compared to when it would be measured in their natural environment.

The linear positive relationship between temperature offset (ΔT) and solar irradiance (SI) was also significant for the full dataset, per section, and per species. This was the expected effect of SI on leaf heating (Ehleringer and Mooney, 1978). Finally, we did not proceed using the infrared leaf temperature measurements, due to high variance in the data and the strong divergence of the linear models obtained when compared to the thermocouple measurements. Possibly, infrared measurements are so variable due to reflective properties of the surrounding, difficulty in obtaining the exact distance and angle per measurement, and the structure of the leaf, such as reflective properties of thick cuticles, waxy leaf surfaces, lime encrustations (missing here due to minerals lacking from soil), and glandular hairs. While these traits are also likely to impact leaf heating through reflection (Ehleringer and Mooney, 1978), it hampers accuracy of measurements.

To control for environmental factors that affect leaf thermoregulation, we limited effects from wind speed and soil drought during measurements, while water vapour pressure deficit varied naturally with changing air relative humidity and temperature during measurements. Data was omitted from days during which VPD reached extreme drought values of > 5 kPa (i.e., well above the 3 kPa that some authors consider drought (e.g., Bobich et al., 2010). It is difficult to differentiate VPD effects on T_{LEAF} from co-occurring effects of T_{AIR}, SI and other climatic factors (Novick et al., 2016). In most species, leaf thermal tolerance decreases in plants growing under high VPD conditions, while other authors suggested that *Saxifraga paniculata* Mill. has increased heat tolerance when

growing in drought stress conditions (Buchner and Neuner, 2003). Due to the simultaneous effects of multiple environmental variables on plant temperature, it is difficult to assess temperature regulation data on plants without additional information on the physical environment.

4.4.2 Leaf trait prediction for leaf heating

We expected the slope of the ΔT~SI models to correlate with leaf and whole plant traits. However, none of the traits included here produced a significant relationship. Notably, leaf area and dry mass are the main predictors of how quickly a leaf responds and manages ΔT (i.e., thermal stability of a leaf; Michaletz et al., 2016) but also did not predict the ΔT~SI slopes. One explanation could be that there is a mixed effect of traits, or that traits aiding in reflection have a stronger effect overall, e.g., a reflective waxy cuticle, lime-secretion, or the presence of a layer of epidermal hairs. However, within phylomorphospace we see sect. *Porphyrion* clustering together based on their conserved small leaf size, suggesting that the relative importance of leaf traits on ΔT~SI slopes can also vary among plant clades (Monteiro et al., 2016).

4.4.3 Phylogenetic trends in leaf temperature response

We hypothesised that closely related *Saxifraga* species are more likely to have a similar ΔT response to radiation, which would be in line with similarity of related taxa in ecology and morphological traits related to temperature regulation (Jeffery, 2017), and active temperature regulation ability specifically through high variation in leaf surface (Michaletz et al., 2016). Indeed, we retrieved a phylogenetic effect for ΔT~SI slopes, despite not finding any explanatory power of functional traits. Other studies on evolution of heat tolerance show a generally weak phylogenetic signal (Lancaster and Humphreys, 2020; Perez and Feeley, 2020; Slot et al., 2021). The three well-sampled clades (sections *Ligulatae*, *Porphyrion*, and *Saxifraga*) show trends toward similar ΔT~SI slopes among closely related taxa, and possibly an even stronger phylogenetic effect would be retrieved through inclusion of more than one to three individual plants in measurements and stronger control of other environmental variables during measurements, for instance using experiments in walk-in growth chambers.

Leaves that are structurally costly to produce need to last long enough for a return on investment, and therefore are generally more resistant to biotic (Coley, 2008) and abiotic stressors (Nardini et al., 2012). Within a clade such as sect. *Porphyrion*, leaf thermal tolerance should generally be higher due to its relatively costly leaves on the leaf economic spectrum with high leaf mass per area (Jeffery, 2017), resulting in a slow cooldown response after heating up (Michaletz et al., 2016; Slot et al., 2021). Since sect. *Saxifraga*

contains many taxa with high SLA (Jeffery, 2017), and similarly high ∆T~SI, we would expect that this clade is rather prone to high SI (low thermal tolerance) so it can shed leaves at low cost. A low ∆T~SI, or fast leaf thermal response, was noted for sect. *Ligulatae*, and with such costly leaves (Jeffery, 2017) they efficiently maintain leaf temperatures near air temperature when submitted to high radiation. Therefore, some evidence is given that the three sections have adapted three distinct coping mechanisms in their respective habitats to avoid or tolerate heat stress.

The response to increased high radiation and temperature perturbations in alpine habitat can be expected to be similar among closely related *Saxifraga* species based on our finding that related taxa tend to have more similar leaf temperature response and functional traits. Thereby, species at risk from future climate change would likely be phylogenetically related, and, by extension, likely share distribution and conserved niches (de Casas et al., 2016).

4.5 Conclusion

Leaf temperature offset ($\Delta T = T_{LEAF} - T_{AIR}$) was higher as T_{AIR} increased, as thermoregulation theory suggests for alpine cushion plants (Michaletz et al., 2016), which are predominant in our data. The ΔT linear increase from heating through solar irradiance (SI) is higher in some taxa than others, although we did not find a relationship between leaf functional traits and leaf heating rate with increasing solar irradiance. Likely, various conditions are at play that prevent one variable from explaining the temperature response, and various traits have not been considered in this study also, e.g., reflectance (albedo) through leaf lime encrustation and hairs.

The representatives from some major clades in *Saxifraga* are more likely to overheat with high radiation than those in others and a phylogenetic signal suggests that this response is phylogenetically conserved, and likely still driven by leaf traits shared by closely related taxa to suit their niche in montane or alpine habitat. Extreme climate perturbations would likely act differently on species success and suitable distribution among phylogenetic clusters. However, the data set in this study could not answer which traits, or trait combinations, are the main predictors of leaf temperature response, and warrants further study.

Chapter 5: General conclusion and future research

5.1 Considerations for phylogenomic analysis and herbariomics

Next generation sequencing (NGS) methods such as hybrid-capture have been revolutionising phylogenetic systematics, as they outperform Sanger sequencing for a fraction of the cost per nucleotide sequenced (Lemmon and Lemmon, 2013; Weitemier et al., 2014; McKain et al., 2016). Clades such as *Saxifraga* have been of long-standing interest for genetic research into polyploidy and other complex phenomena of molecular evolution (Soltis and Soltis, 1999). For this study we decided to develop a new set of baits specifically targeting *Saxifraga*, targeting 329 loci that were selected from pre-existing target sequences for Saxifragales, to increase target capture success rate with the perspective of sequencing degraded herbarium DNAs. Target sequences for hybrid-capture can be selected to work specifically on a clade of interest or be more universal to obtain reads on target throughout the plant tree of life (Johnson et al., 2019; McLay et al., 2021). Capture rate will depend on the selected loci, and how specific the reference sequences are constructed. Another option is finding new target sequences through transcriptomics, though this avenue is much more expensive and time-consuming. Hence, it might be possible that researchers will use universal targets, or redesign existing baits, which is increasingly convenient with the large amount of open-access sequence data available (Gaffney et al. 2020). The method we employed was effective in that target capture rate improved upon the hybrid capture bait sets that were used as reference, and that reads on target are as high as other approximately genus-specific hybrid capture baits (Nicholls et al., 2015; Villaverde et al., 2018). Importantly, we found that degraded DNAs from herbarium material was effective, even with decreasing capture success with sample age (Brewer et al., 2018; Forrest et al., 2018).

An important consideration is that during target sequence selection it is common to select single-copy loci, as to not violate the that a gene would have an alternate evolutionary history to the species tree give wrong estimations of topology and branch lengths (Mirarab et al., 2014; Hahn and Nakhleh, 2016). However, studies show that with species tree analysis under the multi-species coalescent the inclusion of paralogs in datasets does not necessarily have to impede phylogenetic inference (Hellmuth et al., 2015; Yan et al., 2020). Yet we must account for the effect paralogs have on the method we use (Smith and Hahn, 2020), and options are being developed to conveniently test for their presence post-sequencing (Johnson et al., 2016), to effectively report on it to aid in visualising and understanding the discordance in phylogenetic inference.

A point of consideration we bring forward through this study is that the number of paralogous copies detected for museum DNA samples declines at a much faster rate with the number of loci on target. That is, while loci on target decline with age due to fragmentation of DNA and associated issues, paralog detection pipelines that use gene lengths and contig coverage metrics fall short of the ability to detect multi-copy sequences. Such processes must be considered when making assumptions about newly generated sequence data from herbarium specimens. As ploidy levels are known to be more stable in some sections of *Saxifraga*, it is logical to find fewer multi-copy loci, and the effect of the on-target rate on paralog detection can thus vary among clades. Further analysis should compare the interaction of on-target rates or sequencing depth on paralog detection through closely related species with few auto- or allopolyploid occurrences. Finally, it is not recommended to target nuclear and organellar DNA regions during bait design as it results in low coverage of nuclear targets due to higher per-locus organellar DNA (Andermann et al., 2020), though we open the possibility of obtaining mixed coverage among targets when using highly degraded DNAs. Through using low starting DNA and inflated PCR cycles the sequencing depth remains low for many target regions, resulting in lower chances of identifying paralogs. However, for the goals of most studies that employ hybrid-capture sequencing, the (unknown) presence of paralogs does not affect results as discussed previously, and therefore it is rarely needed to increase coverage through excessive sequencing.

5.2 *Saxifraga* in the age of phylogenomics

The new species tree presented in this thesis is the most densely sampled (ca. 70%) tree for *Saxifraga* and includes an extended Saxifragales outgroup sampling for increased possibilities for calibration of nodes divergence times with fossil data. A phylogeny was reconstructed with both exon (target sequence) data and supercontigs (exons plus non-coding splash sites) (Johnson et al., 2016). Previous studies showed species relationships with rather low support, even in comprehensively sampled studies (Tkach et al., 2015b), possibly through the effect of hybridization and introgression (Brochmann et al., 1998; Brochmann and Håpnes, 2001; Li et al., 2018), and rapid diversification (Li et al., 2018). We found that through employing both the exon and supercontig sequence data, one could pursue a certain level of precision on either the older or younger nodes. For instance, the exon data was able to confidently resolve the *Saxifraga* backbone and topology of sections, while the supercontig tree had overall lower gene tree conflict that results from the relatively recent processes radiations and introgression. This shows the degree of customisability of hybrid-capture data even after sequencing.

We obtained a well-supported (LPP) phylogeny and relatively low gene tree discordance among sections and established 15 sections and 15 subsections as per Gornall (1987) and Tkach et al. (2015b). One subsection was synonymised, and one section was reinstated after changes by Tkach et al. (2015b). For future research in taxonomic relationships, it would be interesting to determine where introgression and hybridisation cause gene tree conflict and what parentage hybrid taxa have through e.g., phylogenetic network analysis (Than et al., 2008). However, due to scalability and the algorithm of network analysis likely only detecting a certain amount gene exchange from within the many separate putative cases throughout *Saxifraga*, ideally a carefully selected subset of data would be constructed.

Divergence time estimation was performed with the new species tree topology, as well as a broad inclusion of *Saxifraga* spp. and Saxifragales outgroups with additional fossil calibrations, and notable differences occurred from previous well-sampled studies (e.g., Gao et al., 2015; Ebersbach et al., 2017a). In addition, both a penalised likelihood (Smith and O'Meara, 2012) and Bayesian method (Drummond et al., 2012)) were employed. The fossil data was relatively extensive, considering how little is available in literature for representatives from Saxifragales. In addition, a maximum node constraint was used based on probabilistic prediction of fossil occurrence distribution (Donoghue and Yang, 2016) of *Ribes* stem node, which approximate placement in time was corroborated by divergence time estimates from other studies (Gao et al., 217; Ebersbach et al., 2017b; Tarullo et al., 2021). The divergence times for the genus *Saxifraga* were contracted towards the mid-Miocene. Specifically, the crown node was estimated to be of Miocene origin, and crown nodes of section are not younger than 6 Ma. Hence, most bursts of *Saxifraga* diversification into ecologically and morphologically distinct sections happened in a relatively short time interval compared to other studies (47-6 Ma). In addition, using a multi-locus high throughput dataset and well-supported species tree topology in divergence time estimation resulted in older node ages within the last ca. 6 Ma, likely due to most analyses finding more recent divergence times among taxa with a long history of introgression, which results in gene trees diverging remarkably recent compared to the species tree (Gao et al., 2015, 2017; Ebersbach et al., 2017b, 2018; Li et al., 2018).

5.3 Niche evolution and future change in light of species trees and leaf functional traits

Far-reaching changes have been predicted for mountain areas across all latitudes due to human induced climate change (Nogués-Bravo et al., 2007; Buytaert et al., 2010), as well as a changing frequency and intensity of extreme climatic events (Pachauri et al., 2007). A disproportionate degree of habitat displacement is expected to occur in mountain regions (Thuiller et al., 2005; Nogués-Bravo et al., 2007), and the alpine zone specifically (EEA, 2009; IPCC, 2022). In the arctic-alpine climatic extremes for vascular plant life, plant lineages have adopted a relatively narrow range of morphological characteristics, causing strong convergence of optimal states (Hughes and Atchison, 2015). Most arctic-alpine representatives of *Saxifraga* occur as rosettes with fleshy leaves or tightly packed cushion plants. However, analyses of leaf functional traits show rather large differences among species (Jeffery, 2017), and unique adaptation in alpine taxa (Ebersbach et al., 2017b), resulting in profound differences in how alpine taxa experience the short bursts of high radiation and temperatures in climates with otherwise lower averages than their lowland counterparts experience. Overall, high heat tolerance tends to increase in species in high radiation habitat (e.g., Buchner and Neuner, 2003; Slot et al., 2021), temperatures are on average lower than photosynthetic optima in the alpine zone (Huang et al., 2019) and later decoupling of photosynthesis and transpiration at high temperatures can occur as a last cooling effort (Drake et al., 2018), though when higher temperatures and radiation occur it will cause irreversible damage (Berry and Björkman, 1980). Alpine taxa have adapted structurally and physiologically to mitigating bursts of high radiation, though the extent to which they can is finite and likely sensitive to climate change.

Based on our temperature response analysis, we find that closely related taxa are more likely to have a similar leaf heating response to higher incident solar radiation. While various sections in *Saxifraga* adapted to the alpine biome, their specific niche therein varies, as well as the naturally occurring average and highest daily level of exposure to solar radiation (e.g., cliff faces, scree fields, or alpine meadows). However, closely related species in sections *Saxifraga* and *Porphyrion* tend to ‘overheat’. It is likely that through future change these taxa respond earliest and with more species or populations affected by temperature and solar radiation regimes. *Saxifraga* species at risk would be phylogenetically related, and by extension, likely share conserved morphological characteristic (Jeffery, 2017), and conserved niches (de Casas et al., 2016).

Finally, effects of future change can also be studied through phylogenetics. We already know some arctic-alpine taxa have distributions based on climate-dependent haplotypes (Wessely et al., 2022) and ploidy levels in populations of *Saxifraga* change

according to niche occupation (Decanter et al., 2020). Furthermore, while population contraction occurs among alpine taxa, possibly followed by mountaintop extinction (Watts et al., 2022), upward movement of all biomes results in more contact areas among populations of montane-alpine sister taxa that could result in hybridisation-mediated extinction (Gomez et al., 2015), especially in groups with relatively high gene flow between species such as *Saxifraga*. Hopefully, the hybrid-capture bait set described in this thesis, along with further insights on phylogenomic analysis in the presence of paralogs and implementation of environmental and function trait variables in an eco-evolutionary framework, will form a basis for future studies.

5.4 Emerging questions and future research

5.4.1 Herbaria as repository for the study of plant climate change response

Herbaria are multi-purpose repositories that have growing functionality as a source for DNA data. While methods for effectively obtaining high quality DNAs through wet lab protocols to methods for manipulation and analysis of sequence data are still being advanced every year, there are already boundless possibilities. Apart from phylogenetic reconstruction of a species tree, there are opportunities to study temporal changes of genetic diversity in populations and identifying genes under selection (Bieker and Martin, 2018). Furthermore, herbaria are a store for data on various other types of information that can elucidate various processes such as distribution shifts (Meineke et al., 2018; Davis, 2022) or changes to phenology (Meineke et al., 2018). In addition, herbarium specimens can be used to find plant functional trait changes over space and time (Jaroszynska et al., 2023). Trait changes can not only be studied within species, but also in populations through time, given enough material is available. As discussed in the thesis, the study of functional group response to climatic perturbations within the context of a phylogeny can help model trends in species diversity and population displacement, as well as provide a basis for climate change at-risk species assessments for targeted conservation action. Hence, I hope for increased integration of phylogenetics and ecophysiology methods to understand alpine plant biodiversity through time and space, and an expanding role of herbarium collections in this endeavor (Davis, 2022).

5.4.2 Drivers of *Saxifraga* speciation in the alpine biome

To answer the question of how evolutionary processes relatively contribute to the diversification of alpine plant lineages through time, we have constructed more time-calibrated phylogenies and species and constructed a dataset to indicate the status of lowland, alpine or mixed for all taxa. Specifically, we test how much upslope evolution and mountain hopping between major mountain ranges worldwide contribute to the emergence of alpine lineages through time, through ancestral state reconstruction and Preliminary results indicate that upslope evolution contributes to alpine diversity notably more than long-distance mountain hopping. Interestingly, while in this thesis it is shown that all crown nodes for accepted sections in *Saxifraga* are older than 6 Ma, implying the pre-existence of important taxonomic clades and functional groups, we find that new species adaptation into the alpine zone notably increases after this time. As the alpine biome extended and climate instability increased during the mid-Miocene cooling (Zachos et al., 2001), plenty of opportunity arose for alpine specialists to emerge. Within the alpine zone we find that speciation rates do not increase, as high rates of evolution preliminary occur in generalist species that partially occur above the natural treeline. This research helps to show what processes contribute to the species-rich alpine zone and future studies can further contribute how much pre-existing states of microhabitats, functional traits and leaf temperature regulation capacity contributed to alpine plant evolutionary patterns.

References

Abràmoff, M. D., Magalhães, P. J., and Ram, S. J. (2004). Image processing with ImageJ. *Biophotonics international* 11, 36–42.

Aeschimann, D., and Lauber, K. (2004). *Flora alpina: ein Atlas sämtlicher 4500 Gefäßpflanzen der Alpen.Register*. Haupt.

Albert, T. J., Molla, M. N., Muzny, D. M., Nazareth, L., Wheeler, D., Song, X., et al. (2007). Direct selection of human genomic loci by microarray hybridization. *Nat. Methods* 4, 903–905.

Ambrosino, L., and Chiusano, M. L. (2017). Transcriptologs: A Transcriptome-Based Approach to Predict Orthology Relationships. *Bioinform. Biol. Insights* 11, 1177932217690136.

Andrews, S. (2010). Babraham bioinformatics-FastQC a quality control tool for high throughput sequence data. *URL: https://www. bioinformatics. babraham. ac. uk/projects/fastqc/(accessed 06. 12. 2018)*.

Bakker, F. T. (2017). Herbarium genomics: skimming and plastomics from archival specimens. *Webbia* 72, 35–45.

Bankevich, A., Nurk, S., Antipov, D., Gurevich, A. A., Dvorkin, M., Kulikov, A. S., et al. (2012). SPAdes: a new genome assembly algorithm and its applications to single-cell sequencing. *J. Comput. Biol.* 19, 455– 477.

Barrett, C. F., Bacon, C. D., Antonelli, A., Cano, Á., and Hofmann, T. (2016). An introduction to plant phylogenomics with a focus on palms. *Bot. J. Linn. Soc.* 182, 234–255.

Bauert, M. R., Kälin, M., Baltisberger, M., and Edwards, P. J. (1998). No genetic variation detected within isolated relict populations of Saxifraga cernua in the Alps using RAPD markers. *Mol. Ecol.* 7, 1519– 1527.

Berry, J., and Björkman, O. (1980). Photosynthetic Response and Adaptation to Temperature in Higher Plants. *Annual Review of Plant Physiology* 31, 491–543. doi:10.1146/annurev.pp.31.060180.002423.

Billings, W. D. (1974). Adaptations and Origins of Alpine Plants. *Arct. Alp. Res.* 6, 129–142.

Blonder, B., and Michaletz, S. T. (2018). A model for leaf temperature decoupling from air temperature. *Agric. For. Meteorol.* 262, 354–360.

Blumthaler, M. (2012). “Solar Radiation of the High Alps,” in *Plants in Alpine Regions: Cell Physiology of Adaption and Survival Strategies*, ed. C. Lütz (Vienna: Springer Vienna), 11–20.

Bobich, E. G., Barron-Gafford, G. A., Rascher, K. G., and Murthy, R. (2010). Effects of drought and changes in vapour pressure deficit on water relations of Populusdeltoides growing in ambient and elevated CO2. *Tree Physiol.* 30, 866–875.

Bolger, A. M., Lohse, M., and Usadel, B. (2014). Trimmomatic: a flexible trimmer for Illumina sequence data. *Bioinformatics* 30, 2114–2120.

Bouckaert R., Vaughan T.G., Barido-Sottani J., Duchêne S., Fourment M., Gavryushkina A., et al. (2019) BEAST 2.5: An advanced software platform for Bayesian evolutionary analysis. PLoS computational biology, 15(4), e1006650.

Brewer, G. E., Clarkson, J. J., Maurin, O., Zuntini, A. R., Barber, V., Bellot, S., et al. (2019). Factors Affecting Targeted Sequencing of 353 Nuclear Genes From Herbarium Specimens Spanning the Diversity of Angiosperms. *Front. Plant Sci.* 10, 1102.

Brochmann, C., and Håpnes, A. (2001). Reproductive strategies in some arctic Saxifraga (Saxifragaceae), with emphasis on the narrow endemic S. svalbardensis and its parental species. *Bot. J. Linn. Soc.* 137, 31–49.

Brochmann, C., Xiang, Q., Brunsfeld, S., Soltis, D., and Soltis, P. (1998). Molecular evidence for polyploid origins in Saxifraga (Saxifragaceae): the narrow arctic endemic S. svalbardensis and its widespread allies. *Am. J. Bot.* 85, 135.

Buchner, O., and Neuner, G. (2003). Variability of Heat Tolerance in Alpine Plant Species Measured at Different Altitudes. *Arct. Antarct. Alp. Res.* 35, 411–420.

Buytaert, W., Tovar Ingar, C., and Arnillas, C. (2010). A regional assessment of climate change impact on water resources in the tropical Andes. *Role of hydrology in managing consequences of a changing global environment*. *doi:10.7558/bhs.2010.ic05.*

Carruthers, T., Sun, M., Baker, W. J., Smith, S. A., de Vos, J. M., and Eiserhardt, W. L. (2022). The Implications of Incongruence between Gene Tree and Species Tree Topologies for Divergence Time Estimation. Syst. Biol., syac012.

Coley, P. D. (2008). Interspecific variation in plant anti-herbivore properties: The role of habitat quality and rate of disturbance. *New Phytol.* 106, 251–263.

Comes, H. P., and Kadereit, J. W. (2003). Spatial and temporal patterns in the evolution of the flora of the European Alpine System. *TAXON* 52, 451–462. doi:10.2307/3647382.

Conover, J. L., Karimi, N., Stenz, N., Ané, C., Grover, C. E., Skema, C., et al. (2019). A Malvaceae mystery: A mallow maelstrom of genome multiplications and maybe misleading methods? *J. Integr. Plant Biol.* 61, 12–31.

Conti, E., Soltis, D. E., Hardig, T. M., and Schneider, J. (1999). Phylogenetic Relationships of the Silver Saxifrages (Saxifraga, Sect. Ligulatae Haworth): Implications for the Evolution of Substrate Specificity, Life Histories, and Biogeography. *Mol. Phylogenet. Evol.* 13, 536–555.

Daudet, F. A., Le Roux, X., Sinoquet, H., and Adam, B. (1999). Wind speed and leaf boundary layer conductance variation within tree crown: Consequences on leaf-to-atmosphere coupling and tree functions. *Agric. For. Meteorol.* 97, 171–185.

Davey, J. W., and Blaxter, M. L. (2010). RADSeq: next-generation population genetics. *Brief. Funct. Genomics* 9, 416–423.

Davis C.C. (2022). The herbarium of the future. *Trends in Ecology & Evolution*, 38, 5.

de Casas, R. R., Mort, M. E., and Soltis, D. E. (2016). The influence of habitat on the evolution of plants: a case study across Saxifragales. *Ann. Bot.* 118, 1317–1328.

DeChaine, E. G. (2014). Introducing the Spotted Saxifrages: Saxifraga Sect. Bronchiales, Syan et al.ect. Nov. (Saxifragaceae). *Rhodora* 116, 25–40.

DeChaine, E. G., Anderson, S. A., McNew, J. M., and Wendling, B. M. (2013). On the evolutionary and biogeographic history of Saxifraga sect. Trachyphyllum (Gaud.) Koch (Saxifragaceae Juss.). *PLoS One* 8, e69814.

Degnan, J. H., and Rosenberg, N. A. (2009). Gene tree discordance, phylogenetic inference and the multispecies coalescent. *Trends in Ecology & Evolution* 24, 332–340. doi:10.1016/j.tree.2009.01.009.

Deng, J.-B., Drew, B. T., Mavrodiev, E. V., Gitzendanner, M. A., Soltis, P. S., and Soltis, D. E. (2015). Phylogeny, divergence times, and historical biogeography of the angiosperm family Saxifragaceae. *Mol. Phylogenet. Evol.* 83, 86–98.

de Sousa, F., Bertrand, Y. J. K., Nylinder, S., Oxelman, B., Eriksson, J. S., and Pfeil, B. E. (2014). Phylogenetic properties of 50 nuclear loci in Medicago (Leguminosae) generated using multiplexed sequence capture and next-generation sequencing. *PLoS One* 9, e109704.

Dodsworth, S. (2015). Genome skimming for next-generation biodiversity analysis. *Trends Plant Sci.* 20, 525–527.

Dodsworth, S., Pokorny, L., Johnson, M. G., Kim, J. T., Maurin, O., Wickett, N. J., et al. (2019). Hyb-Seq for Flowering Plant Systematics. *Trends Plant Sci.* 24, 887–891.

Donoghue, P. C. J., and Yang, Z. (2016). The evolution of methods for establishing evolutionary timescales. Philos. Trans. R. Soc. Lond. B Biol. Sci. 371. doi: 10.1098/rstb.2016.0020.

Donovan, L. A., Maherali, H., Caruso, C. M., Huber, H., and de Kroon, H. (2011). The evolution of the worldwide leaf economics spectrum. *Trends Ecol. Evol.* 26, 88–95.

Dos Reis, M., Zhu, T., and Yang, Z. (2014). The impact of the rate prior on Bayesian estimation of divergence times with multiple Loci. Syst. Biol. 63, 555–565.

Doyle, J., and Doyle, J. L. (1987). Genomic plant DNA preparation from fresh tissue-CTAB method. *Phytochem Bull* 19, 11–15.

Drake, J. E., Tjoelker, M. G., Vårhammar, A., Medlyn, B. E., Reich, P. B., Leigh, A., et al. (2018). Trees tolerate an extreme heatwave via sustained transpirational cooling and increased leaf thermal tolerance. Glob. Chang. Biol. 24, 2390–2402.

Drummond, A. J., Ho, S. Y. W., Phillips, M. J., and Rambaut, A. (2006). Relaxed phylogenetics and dating with confidence. PLoS Biol. 4, e88.

Drummond, A. J., Nicholls, G. K., Rodrigo, A. G., and Solomon, W. (2002). Estimating mutation parameters, population history and genealogy simultaneously from temporally spaced sequence data. Genetics 161, 1307–1320.

Drummond, A. J., Suchard, M. A., Xie, D., and Rambaut, A. (2012). Bayesian phylogenetics with BEAUti and the BEAST 1.7. *Mol. Biol. Evol.* 29, 1969–1973.

Dunbar-Co, S., Wieczorek, A. M., and Morden, C. W. (2008). Molecular phylogeny and adaptive radiation of the endemic Hawaiian Plantago species (Plantaginaceae). *Am. J. Bot.* 95, 1177–1188.

Ebersbach, J., Muellner-Riehl, A. N., Favre, A., Paule, J., Winterfeld, G., and Schnitzler, J. (2018). Driving forces behind evolutionary radiations: Saxifraga section Ciliatae (Saxifragaceae) in the region of the Qinghai–Tibet Plateau. *Bot. J. Linn. Soc.* 186, 304–320.

Ebersbach, J., Muellner-Riehl, A. N., Michalak, I., Tkach, N., Hoffmann, M. H., Röser, M., et al. (2017a). In and out of the Qinghai-Tibet Plateau: divergence time estimation and historical biogeography of the large arctic-alpine genusSaxifragaL. *Journal of Biogeography* 44, 900–910. doi:10.1111/jbi.12899.

Ebersbach, J., Schnitzler, J., Favre, A., and Muellner-Riehl, A. N. (2017b). Evolutionary radiations in the species-rich mountain genus Saxifraga L. *BMC Evolutionary Biology* 17. doi:10.1186/s12862-017-0967-2.

Ebersbach, J., Tkach, N., Röser, M., and Favre, A. (2020). The Role of Hybridisation in the Making of the Species-Rich Arctic-Alpine Genus Saxifraga (Saxifragaceae). *Diversity* 12, 440.

EEA report warns of water overuse in Europe (2009). *Membr. Technol.* 2009, 4.

Ehleringer, J. R., and Mooney, H. A. (1978). Leaf hairs: Effects on physiological activity and adaptive value to a desert shrub. *Oecologia* 37, 183–200. doi:10.1007/bf00344990.

Ekblom, R., and Galindo, J. (2011). Applications of next generation sequencing in molecular ecology of non-model organisms. *Heredity* 107, 1–15.

Engler, H.G.A. and Irmscher, E. (1916) (“1919”). Saxifragaceae – Saxifraga. Pp. 1–448 in: Engler, H.G.A. (ed.), Das Pflanzenreich, vol. 67 (IV, 117). Leipzig: Engelmann.

Fang, X., Yan, M., Van der Voo, R., Rea, D. K., Song, C., Parés, J. M., et al. (2005). Late Cenozoic deformation and uplift of the NE Tibetan Plateau: evidence from high-resolution magnetostratigraphy of the Guide Basin, Qinghai Province, China. *GSA Bulletin* 117, 1208–1225.

Favre, A., Päckert, M., Pauls, S. U., Jähnig, S. C., Uhl, D., Michalak, I., et al. (2015). The role of the uplift of the Qinghai-Tibetan Plateau for the evolution of Tibetan biotas. Biol. Rev. Camb. Philos. Soc. 90, 236–253.

Ferguson, I. K., and Webb, D. A. (1970). Pollen morphology in the genus Saxifraga and its taxonomic significance. *Bot. J. Linn. Soc.* 63, 295–311.

Ferreira, P. de L., Batista, R., Andermann, T., Groppo, M., Bacon, C. D., and Antonelli, A. (2022). Target sequence capture of Barnadesioideae (Compositae) demonstrates the utility of low coverage loci in phylogenomic analyses. Mol. Phylogenet. Evol. 169, 107432.

Firat, M. (2016). Saxifraga hakkariensis (Saxifragaceae), a new species from Hakkâri province (Turkey) belonging to section Porphyrion. *Phytotaxa* 289, 181–187.

Fishbein, M., Hibsch-Jetter, C., Soltis, D. E., and Hufford, L. (2001). Phylogeny of Saxifragales (angiosperms, eudicots): analysis of a rapid, ancient radiation. *Syst. Biol.* 50, 817–847.

Folk, R. A., Stubbs, R. L., Engle-Wrye, N. J., Soltis, D. E., and Okuyama, Y. (2021). Biogeography and habitat evolution of Saxifragaceae, with a revision of generic limits and a new tribal system. *Taxon* 70, 263– 285.

Folk, R. A., Stubbs, R. L., Mort, M. E., Cellinese, N., Allen, J. M., Soltis, P. S., et al. (2019). Rates of niche and phenotype evolution lag behind diversification in a temperate radiation. *Proc. Natl. Acad. Sci. U. S. A.* 116, 10874–10882.

Forrest, L. L., Hart, M. L., Hughes, M., Wilson, H. P., Chung, K.-F., Tseng, Y.-H., et al. (2019). The Limits of Hyb-Seq for Herbarium Specimens: Impact of Preservation Techniques. *Frontiers in Ecology and Evolution* 7, 439.

Gabrielsen, T. M., and Brochmann, C. (1998). Sex after all: high levels of diversity detected in the arctic clonal plantSaxifraga cernuausing RAPD markers: GENETIC DIVERSITY IN AN ARCTIC CLONAL PLANT. *Mol. Ecol.* 7, 1701–1708.

Gao, Q.-B., Li, Y., Gengji, Z.-M., Gornall, R. J., Wang, J.-L., Liu, H.-R., et al. (2017). Population Genetic Differentiation and Taxonomy of Three Closely Related Species of Saxifraga (Saxifragaceae) from Southern Tibet and the Hengduan Mountains. *Front. Plant Sci.* 8, 1325.

Gao, Q.-B., Li, Y.-H., Gornall, R. J., Zhang, Z.-X., Zhang, F.-Q., Xing, R., et al. (2015). Phylogeny and speciation in Saxifraga sect. Ciliatae (Saxifragaceae): Evidence from psbA-trnH, trnL-F and ITS sequences. *Taxon* 64, 703–713.

Gardner, E. M., Johnson, M. G., Pereira, J. T., Puad, A. S. A., Arifiani, D., Sahromi, et al. (2019). Paralogs and off-target sequences improve phylogenetic resolution in a densely-sampled study of the breadfruit genus (Artocarpus, Moraceae). *bioRxiv*, 854232. doi:10.1101/854232.

Gates, D. M. (1965). Energy, Plants, and Ecology. *Ecology* 46, 1–13.

Gerschwitz-Eidt, M. A., and Kadereit, J. W. (2020). Species composition of Saxifraga sect. Saxifraga subsect. Arachnoideae (Saxifragaceae) based on DNA sequence evidence. *Willdenowia* 50, 225–233.

Gholz, H. L., Fitz, F. K., and Waring, R. H. (1976). Leaf area differences associated with old-growth forest communities in the western Oregon Cascades. *Can. J. For. Res.* 6, 49–57.

Gornall, R. J. (1987). An outline of a revised classification of Saxifraga L. *Bot. J. Linn. Soc.* 95, 273–292.

Gornall, R. J., Ohba, H., and Jintang, P. (2000). New Taxa, Names, and Combinations in Saxifraga (Saxifragaceae) for the Flora of China. *Novon St. Louis Mo* 10, 375–377.

Gornall, R. J., Rawat, D. S., and Zhang, Z. (2012). SAXIFRAGA MINUTISSIMA, A NEW SPECIES FROM THE GARHWAL HIMALAYA, INDIA, AND ITS IMPLICATIONS FOR THE TAXONOMY OF THE GENUS SAXIFRAGA (SAXIFRAGACEAE). *Edinburgh Journal of Botany* 69, 211–217. doi:10.1017/s0960428612000054.

Gradstein, F. M., Ogg, J. G., Schmitz, M., and Ogg, G. (2012). The Geologic Time Scale 2012. Elsevier.

Grant, O. M., Tronina, L., Jones, H. G., and Chaves, M. M. (2007). Exploring thermal imaging variables for the detection of stress responses in grapevine under different irrigation regimes. *J. Exp. Bot.* 58, 815–825.

Grossiord, C., Buckley, T. N., Cernusak, L. A., Novick, K. A., Poulter, B., Siegwolf, R. T. W., et al. (2020). Plant responses to rising vapor pressure deficit. *New Phytol.* 226, 1550–1566.

Gurevitch, J. (1988). Variation in leaf dissection and leaf energy budgets among populations of Achillea from an altitudinal gradient. *Am. J. Bot.* 75, 1298–1306.

Hahn, M. W., and Nakhleh, L. (2016). Irrational exuberance for resolved species trees. *Evolution* 70, 7–17.

Harding, W. (1976). *Saxifrages: The Genus Saxifraga in the Wild and in Cultivation*. Lye End Link.

Hart, M. L., Forrest, L. L., Nicholls, J. A., and Kidner, C. A. (2016). Retrieval of hundreds of nuclear loci from herbarium specimens. *Taxon* 65, 1081–1092.

Hellmuth, M., Wieseke, N., Lechner, M., Lenhof, H.-P., Middendorf, M., and Stadler, P. F. (2015). Phylogenomics with paralogs. *Proc. Natl. Acad. Sci. U. S. A.* 112, 2058–2063.

Herbert, T. D., Lawrence, K. T., Tzanova, A., Peterson, L. C., Caballero-Gill, R., and Kelly, C. S. (2016). Late Miocene global cooling and the rise of modern ecosystems. Nat. Geosci. 9, 843–847.

Hermsen, E. J. (2003). ITEA-LIKE LEAVES FROM THE MIDDLE EOCENE REPUBLIC FLORA, WASHINGTON, USA. in *2003 Seattle Annual Meeting*.

Hermsen, E. J. (2005). The fossil record of Iteaceae and Grossulariaceae in the Cretaceous and Tertiary of the United States and Canada. Available at: https://elibrary.ru/item.asp?id=9371274.

Hermsen, E. J., Nixon, K. C., and Crepet, W. L. (2006). The impact of extinct taxa on understanding the early evolution of Angiosperm clades: an example incorporating fossil reproductive structures of Saxifragales. Osterr. bot. Z. 260, 141–169.

Hermsen, E. J. (2013). A review of the fossil record of the genus Itea (iteaceae, Saxifragales) with comments on its historical biogeography. *Bot. Rev.* 79, 1–47.

Hernandez-Castillo, G. R., and Cevallos-Ferriz, S. R. S. (1999). Reproductive and Vegetative Organs with Affinities to Haloragaceae from the Upper Cretaceous Huepac Chert Locality of Sonora, Mexico. *American Journal of Botany* 86, 1717. *doi:10.2307/2656670.*

Höhna, S., Landis, M. J., Heath, T. A., Boussau, B., Lartillot, N., Moore, B. R., et al. (2016). RevBayes: Bayesian Phylogenetic Inference Using Graphical Models and an Interactive Model-Specification Language. *Syst. Biol.* 65, 726–736.

Holderegger, R., and Abbott, R. J. (2003). Phylogeography of the Arctic-Alpine Saxifraga oppositifolia (Saxifragaceae) and some related taxa based on cpDNA and ITS sequence variation. *American Journal of Botany* 90, 931–936. *doi:10.3732/ajb.90.6.931.*

Huang, M., Piao, S., Ciais, P., Peñuelas, J., Wang, X., Keenan, T. F., et al. (2019). Air temperature optima of vegetation productivity across global biomes. Nature Ecology & Evolution 3, 772–779. doi: 10.1038/s41559-019-0838-x.

Hughes, C. E., and Atchison, G. W. (2015). The ubiquity of alpine plant radiations: from the Andes to the Hengduan Mountains. *New Phytol.* 207, 275–282.

Huner, N. P. A., Öquist, G., and Sarhan, F. (1998). Energy balance and acclimation to light and cold. *Trends Plant Sci.* 3, 224–230.

Idso, S. B., and Baker, D. G. (1967). Relative importance of reradiation, convection, and transpiration in heat transfer from plants. *Plant Physiol.* 42, 631–640.

Idso, S. B., Baker, D. G., and Gates, D. M. (1966). “The energy environment of plants,” in *Advances in Agronomy* (Elsevier), 171–218.

Jaccard, P. (1912). The distribution of the flora in the alpine zone.1. *New Phytol.* 11, 37–50.

Jeffery, M. (2017). From Lush Lowlands to the Roof of the World: Leaf Economics and Habitat Evolution in Saxifrages (Genus Saxifraga L.). BSc Thesis, Royal Botanic Gardens, Kew.

Jian, S., Soltis, P. S., Gitzendanner, M. A., Moore, M. J., Li, R., Hendry, T. A., et al. (2008). Resolving an ancient, rapid radiation in Saxifragales. *Syst. Biol.* 57, 38–57.

Johnson, M. G., Gardner, E. M., Liu, Y., Medina, R., Goffinet, B., Shaw, A. J., et al. (2016). HybPiper: Extracting coding sequence and introns for phylogenetics from high-throughput sequencing reads using target enrichment. *Appl. Plant Sci.* 4. Available at: https://onlinelibrary.wiley.com/doi/abs/10.3732/apps.1600016%4010.1111/%28ISSN%29136 5-313X.plants_day_collection.

Johnson, M. G., Pokorny, L., Dodsworth, S., Botigué, L. R., Cowan, R. S., Devault, A., et al. (2019). A Universal Probe Set for Targeted Sequencing of 353 Nuclear Genes from Any Flowering Plant Designed Using k-Medoids Clustering. *Syst. Biol.* 68, 594–606.

Joly, S., Heenan, P. B., and Lockhart, P. J. (2009a). A Pleistocene inter-tribal allopolyploidization event precedes the species radiation of Pachycladon (Brassicaceae) in New Zealand. *Mol. Phylogenet. Evol.* 51, 365–372.

Joly, S., McLenachan, P. A., and Lockhart, P. J. (2009b). A statistical approach for distinguishing hybridization and incomplete lineage sorting. *Am. Nat.* 174, E54–70.

Jones, M. R., and Good, J. M. (2016). Targeted capture in evolutionary and ecological genomics. *Molecular Ecology* 25, 185–202. *doi:10.1111/mec.13304.*

Kalyaanamoorthy, S., Minh, B. Q., Wong, T. K. F., von Haeseler, A., and Jermiin, L. S. (2017). ModelFinder: fast model selection for accurate phylogenetic estimates. Nat. Methods 14, 587–589.

Kaplan, K. (1981). *Embryologische, pollen- und samenmorphologische Untersuchungen zur Systematik von Saxifraga (Syxifragaceae)*. Stuttgart, Germany: Schweizerbart'sche, E.

Katoh, K., and Standley, D. M. (2013). MAFFT multiple sequence alignment software version 7: improvements in performance and usability. *Mol. Biol. Evol.* 30, 772–780.

Kistler, L., Bieker, V. C., Martin, M. D., Pedersen, M. W., Ramos Madrigal, J., and Wales, N. (2020). Ancient Plant Genomics in Archaeology, Herbaria, and the Environment. *Annu. Rev. Plant Biol.* 71, 605–629.

Kleier, C., and Rundel, P. (2009). Energy balance and temperature relations of Azorella compacta, a high-elevation cushion plant of the central Andes. *Plant Biol.* 11, 351–358.

Kocot, K. M., Citarella, M. R., Moroz, L. L., and Halanych, K. M. (2013). PhyloTreePruner: A Phylogenetic Tree-Based Approach for Selection of Orthologous Sequences for Phylogenomics. *Evol. Bioinform. Online* 9, 429–435.

Körner, C. (1999). Alpine treelines. *Alpine Plant Life*, 77–100. doi:10.1007/978-3-642-98018-3_7.

Körner, C. (2003). Alpine Plant Life. doi:10.1007/978-3-642-18970-8.

Körner, C. (2007). Alpine Ecosystems. *Encyclopedia of Life Sciences*. doi:10.1002/9780470015902.a0003492.pub2.

Körner, C., and Diemer, M. (1987). In situ Photosynthetic Responses to Light, Temperature and Carbon Dioxide in Herbaceous Plants from Low and High Altitude. Funct. Ecol. 1, 179–194.

Körner, C., and Hiltbrunner, E. (2018). The 90 ways to describe plant temperature. *Perspect. Plant Ecol. Evol. Syst.* 30, 16–21.

Körner, C., & Hiltbrunner, E. (2021). Why is the alpine flora comparatively robust against climatic warming? *Diversity*, 13, 383.

Lancaster, L. T., and Humphreys, A. M. (2020). Global variation in the thermal tolerances of plants. *Proc. Natl. Acad. Sci. U. S. A.* 117, 13580–13587.

Landolt, E., and Urbanska, K. M. (2003). *Our Alpine Flora*.

Lanfear, R., Frandsen, P. B., Wright, A. M., Senfeld, T., and Calcott, B. (2016). PartitionFinder 2: New Methods for Selecting Partitioned Models of Evolution for Molecular and Morphological

Phylogenetic Analyses. Molecular Biology and Evolution, msw260. doi: 10.1093/molbev/msw260.

Larcher, W. (2012). “Bioclimatic Temperatures in the High Alps,” in *Plants in Alpine Regions: Cell Physiology of Adaption and Survival Strategies*, ed. C. Lütz (Vienna: Springer Vienna), 21–27.

Lemmon, A. R., Emme, S. A., and Lemmon, E. M. (2012). Anchored hybrid enrichment for massively high-throughput phylogenomics. *Syst. Biol.* 61, 727–744.

Lemmon, E. M., and Lemmon, A. R. (2013). High-Throughput Genomic Data in Systematics and Phylogenetics. doi:10.1146/annurev-ecolsys-110512-135822.

Lewis, D. A., and Nobel, P. S. (1977). Thermal Energy Exchange Model and Water Loss of a Barrel Cactus, Ferocactus acanthodes. *Plant Physiol.* 60, 609–616.

Li, H. (2013). Aligning sequence reads, clone sequences and assembly contigs with BWA-MEM. *arXiv [q-bio.GN]*. Available at: *http://arxiv.org/abs/1303.3997.*

Li, Y., Gao, Q.-B., Gengji, Z.-M., Jia, L.-K., Wang, Z.-H., and Chen, S.-L. (2018). Rapid Intraspecific Diversification of the Alpine Species Saxifraga sinomontana (Saxifragaceae) in the Qinghai-Tibetan Plateau and Himalayas. *Front. Genet.* 9, 381.

Lütz, C. (2010). Cell physiology of plants growing in cold environments. *Protoplasma* 244, 53–73.

Maddison, W. P. (1997). Gene Trees in Species Trees. *Syst. Biol.* 46, 523–536.

Mahan, J. R., and Upchurch, D. R. (1988). Maintenance of constant leaf temperature by plants—I. Hypothesis-limited homeothermy. *Environ. Exp. Bot.* 28, 351–357.

Mai, U., and Mirarab, S. (2018). TreeShrink: fast and accurate detection of outlier long branches in collections of phylogenetic trees. *BMC Genomics* 19, 272.

Magallon, S., Crane, P. R., and Herendeen, P. S. (1999). Phylogenetic Pattern, Diversity, and Diversification of Eudicots. Ann. Mo. Bot. Gard. 86, 297–372.

Malakasi, P., Bellot, S., Dee, R., and Grace, O. M. (2019). Museomics Clarifies the Classification of Aloidendron (Asphodelaceae), the Iconic African Tree Aloes. *Front. Plant Sci.* 10, 1227.

Marhold, K., Stuessy, T., Agababian, M., Agosti, D., Alford, M. H., Crespo, A., et al. (2013). The Future of Botanical Monography: Report from an international workshop, 12-16 March 2012, Smolenice, Slovak Republic. *Taxon* 62, 4–20.

Mas De Xaxars, G., García-Fernández, A., Barnola, P., Martín, J., Mercadé, A., Vallès, J., et al. (2015). Phylogenetic and cytogenetic studies reveal hybrid speciation in Saxifraga subsect. Triplinervium (Saxifragaceae). *J. Syst. Evol.* 53, 53–62.

McCormack, J., Tsai, W. L. E., and Faircloth, B. C. Sequence capture of ultraconserved elements from bird museum specimens. doi:10.1101/020271.

McGregor, M., and Harding, W. (1998). *Saxifrages: the complete list of species*. Saxifrage Society.

McGregor, M. (2008). *Saxifrages: A definitive guide to the 2000 species, hybrids & cultivars*. Timber Press.

McKain, M. R., Tang, H., McNeal, J. R., Ayyampalayam, S., Davis, J. I., dePamphilis, C. W., et al. (2016). A phylogenomic assessment of ancient polyploidy and genome evolution across the Poales. *Genome Biology and Evolution*, evw060. *doi:10.1093/gbe/evw060.*

McLay, T. G. B., Birch, J. L., Gunn, B. F., Ning, W., Tate, J. A., Nauheimer, L., et al. (2021). New targets acquired: Improving locus recovery from the Angiosperms353 probe set. Appl. Plant Sci. 9. doi: 10.1002/aps3.11420.

Michaletz, S. T., Weiser, M. D., McDowell, N. G., Zhou, J., Kaspari, M., Helliker, B. R., et al. (2016). The energetic and carbon economic origins of leaf thermoregulation. *Nat Plants* 2, 16129.

Michaletz, S. T., Weiser, M. D., Zhou, J., Kaspari, M., Helliker, B. R., and Enquist, B. J. (2015). Plant Thermoregulation: Energetics, Trait-Environment Interactions, and Carbon Economics. *Trends Ecol. Evol.* 30, 714–724.

Minh, B. Q., Hahn, M. W., and Lanfear, R. (2018). New methods to calculate concordance factors for phylogenomic datasets. *bioRxiv*, 487801. doi:10.1101/487801.

Minh, B. Q., Schmidt, H. A., Chernomor, O., Schrempf, D., Woodhams, M. D., von Haeseler, A., et al. (2020). IQ-TREE 2: New models and efficient methods for phylogenetic inference in the genomic era. *Mol. Biol. Evol.* doi:10.1093/molbev/msaa015.

Mirarab, S., Reaz, R., Bayzid, M. S., Zimmermann, T., Swenson, M. S., and Warnow, T. (2014). ASTRAL:

genome-scale coalescent-based species tree estimation. *Bioinformatics* 30, i541–8.

Mirarab, S., and Warnow, T. (2015). ASTRAL-II: coalescent-based species tree estimation with many hundreds of taxa and thousands of genes. *Bioinformatics* 31, i44–52.

Molloy, E. K., and Warnow, T. (2018). To Include or Not to Include: The Impact of Gene Filtering on Species Tree Estimation Methods. *Syst. Biol.* 67, 285–303.

Monteiro, M. V., Blanuša, T., Verhoef, A., Hadley, P., and Cameron, R. W. F. (2016). Relative importance of transpiration rate and leaf morphological traits for the regulation of leaf temperature. *Aust. J. Bot.* 64, 32–44.

Monteith, J., and Unsworth, M. (2013). *Principles of Environmental Physics: Plants, Animals, and the Atmosphere*. Academic Press.

Moore, A. J., Vos, J. M. D., Hancock, L. P., Goolsby, E., and Edwards, E. J. (2018). Targeted Enrichment of Large Gene Families for Phylogenetic Inference: Phylogeny and Molecular Evolution of Photosynthesis Genes in the Portullugo Clade (Caryophyllales). *Syst. Biol.* 67, 367–383.

Moss, P.T., Greenwood, D.R. & Archibald, S.B. (2005) Regional and local vegetation community dynamics of the Eocene Okanagan Highlands (British Columbia Washington State) from palynology. Canadian Journal of Earth Sciences, 42, 187–204

Nardini, A., Pedà, G., and Rocca, N. L. (2012). Trade-offs between leaf hydraulic capacity and drought vulnerability: morpho-anatomical bases, carbon costs and ecological consequences. *New Phytol.* 196, 788–798.

Nguyen, L.-T., Schmidt, H. A., von Haeseler, A., and Minh, B. Q. (2015). IQ-TREE: a fast and effective stochastic algorithm for estimating maximum-likelihood phylogenies. *Mol. Biol. Evol.* 32, 268–274.

Nicholls, J. A., Pennington, R. T., Koenen, E. J., Hughes, C. E., Hearn, J., Bunnefeld, L., et al. (2015a). Using targeted enrichment of nuclear genes to increase phylogenetic resolution in the neotropical rain forest genus Inga (Leguminosae: Mimosoideae). *Front. Plant Sci.* 6, 710.

Nicholls, J. A., Pennington, R. T., Koenen, E. J. M., Hughes, C. E., Hearn, J., Bunnefeld, L., et al. (2015b). Using targeted enrichment of nuclear genes to increase phylogenetic resolution in the neotropical rain forest genus Inga (Leguminosae: Mimosoideae). *Front. Plant Sci.* 6, 710.

Nogués-Bravo, D., Araújo, M. B., Errea, M. P., and Martínez-Rica, J. P. (2007). Exposure of global mountain systems to climate warming during the 21st Century. *Global Environmental Change* 17, 420–428. doi:10.1016/j.gloenvcha.2006.11.007.

Novick, K. A., Oishi, A. C., and Miniat, C. F. (2016). Cold air drainage flows subsidize montane valley ecosystem productivity. *Glob. Chang. Biol.* 22, 4014–4027.

Oehl, F., and Körner, C. (2014). Multiple mycorrhization at the coldest place known for Angiosperm plant life. *Alp. Bot.* 124, 193–198.

Pachauri, R. K., Reisinger, A., and Others (2007). IPCC fourth assessment report. *IPCC, Geneva* 2007. Available at: https://archive.ipcc.ch/pdf/presentations/valencia-2007-11/pachauri-17-november-2007.pdf.

Paer, C. V. de, Van de Paer, C., Hong-Wa, C., Jeziorski, C., and Besnard, G. (2016). Mitogenomics of Hesperelaea, an extinct genus of Oleaceae. *Gene* 594, 197–202. doi:10.1016/j.gene.2016.09.007.

Pagel, M. (1999). Inferring the historical patterns of biological evolution. *Nature* 401, 877–884.

Pan, J.T. (1992). Saxifraga L. Pp. 35–231 in: Pan, J.T. (ed.), Flora Reipublicae Popularis Sinicae, vol. 34(2), Saxifragaceae (1). Beijing: Science Press.

Pan, J., Gornall, R. & Ohba, H. (2001). Saxifraga L. Pp. 280–344 in: Zhengyi, W. & Raven, P.H. (eds.), Flora of China, vol. 8, Brassicaceae–Saxifragaceae. Beijing: Science Press; Saint Louis: Missouri Botanical Garden Press. Paradis, E., and Schliep, K. (2019). ape 5.0: an environment for modern phylogenetics and evolutionary analyses in R. *Bioinformatics* 35, 526–528.

Pellissier, L., Bråthen, K. A., Vittoz, P., Yoccoz, N. G., Dubuis, A., Meier, E. S., et al. (2013). Thermal niches are more conserved at cold than warm limits in arctic-alpine plant species. *Glob. Ecol. Biogeogr.* 22, 933–941.

Pennell, M. W., Eastman, J. M., Slater, G. J., Brown, J. W., Uyeda, J. C., FitzJohn, R. G., et al. (2014). geiger v2.0: an expanded suite of methods for fitting macroevolutionary models to phylogenetic trees. *Bioinformatics* 30, 2216–2218.

Perez-Harguindeguy, N., Diaz, S., Garnier, E., Lavorel, S., Poorter, H., Jaureguiberry, P., et al. (2016).Corrigendum to: new handbook for standardised measurement of plant functional traits worldwide. *Aust. J. Bot.* 64, 715–716.

Pérez-Harguindeguy, N., Díaz, S., Garnier, E., Lavorel, S., Poorter, H., Jaureguiberry, P., et al. (2016).Corrigendum to: New handbook for standardised measurement of plant functional traits worldwide. *Aust. J. Bot.* 64, 715.

Perez, T. M., and Feeley, K. J. (2020). Photosynthetic heat tolerances and extreme leaf temperatures. *Funct. Ecol.* 34, 2236–2245.

Pietilainen, M., and Korpelainen, H. (2013). Population genetics of purple saxifrage (Saxifraga oppositifolia) in the high Arctic archipelago of Svalbard. *AoB Plants* 5, lt024–plt024. doi:10.1093/aobpla/plt024.

POWO (2019). "Plants of the World Online. Facilitated by the Royal Botanic Gardens, Kew. Published on the Internet; http://www.plantsoftheworldonline.org/ Retrieved 18-8-2018."

Price, M. N., Dehal, P. S., and Arkin, A. P. (2009). FastTree: computing large minimum evolution trees with profiles instead of a distance matrix. *Mol. Biol. Evol.* 26, 1641–1650.

Rambaut, A. (2010) FigTree v1.3.1. Institute of Evolutionary Biology, University of Edinburgh, Edinburgh. http://tree.bio.ed.ac.uk/software/figtree/

Rasband, W. S. (2012). ImageJ: Image processing and analysis in Java. *Astrophysics Source Code Library*,
ascl:1206.013. Available at: https://ui.adsabs.harvard.edu/abs/2012ascl.soft06013R.

Reisch, C. (2008). Glacial history of Saxifraga paniculata (Saxifragaceae): molecular biogeography of a disjunct arctic-alpine species from Europe and North America. *Biol. J. Linn. Soc. Lond.* 93, 385–398.

Reisch, C., Poschlod, P., and Wingender, R. (2003). Genetic variation of Saxifraga paniculata Mill. (Saxifragaceae): molecular evidence for glacial relict endemism in central Europe. *Biol. J. Linn. Soc. Lond.* 80, 11–21.

Reisigl, H., and Keller, R. (1987). Alpenpflanzen im Lebensraum. *Alpine Rasen, Schutt-und Felsvegetation.* *Fischer, Stuttgart*. Available at: *https://doc1.bibliothek.li/abd/FLML300940.pdf.*

Revell, L. J. (2012). phytools: an R package for phylogenetic comparative biology (and other things): phytools: R package. *Methods Ecol. Evol.* 3, 217–223.

Rollo, F., Amici, A., Salvi, R., and Garbuglia, A. (1988). Short but faithful pieces of ancient DNA. *Nature* 335, 774–774. doi:10.1038/335774a0.

Rundel, P. W., Smith, A. P., and Meinzer, F. C. (1994). *Tropical Alpine Environments: Plant Form and Function*. Cambridge University Press.

Salisbury, F. B., and Spomer, G. G. (1964). Leaf temperatures of alpine plants in the field. *Planta* 60, 497– 505. doi:10.1007/bf01894807.

Sanderson, M. J. (1997). A nonparametric approach to estimating divergence times in the absence of rate constancy. *Mol. Biol. Evol.* 14, 1218–1231.

Sanderson, M. J. (2002). Estimating absolute rates of molecular evolution and divergence times: a penalized likelihood approach. *Mol. Biol. Evol.* 19, 101–109.

Sanger, F., Nicklen, S., and Coulson, A. R. (1977). DNA sequencing with chain-terminating inhibitors. *Proc.Natl. Acad. Sci. U. S. A.* 74, 5463–5467.

Sanna, M., Cires, E., Pérez-Haase, A., and Fernández Prieto, J. A. (2019). Haplotype and ribotype diversity of Saxifraga cuneifolia sl (Saxifragaceae). *System. Biodivers.* 17, 402–411.

Sauquet, H., Ho, S. Y. W., Gandolfo, M. A., Jordan, G. J., Wilf, P., Cantrill, D. J., et al. (2012). Testing the impact of calibration on molecular divergence times using a fossil-rich group: the case of Nothofagus (Fagales). *Syst. Biol.* 61, 289–313.

Sayyari, E., and Mirarab, S. (2016a). Anchoring quartet-based phylogenetic distances and applications to species tree reconstruction. *BMC Genomics* 17, 783.

Sayyari, E., and Mirarab, S. (2016b). Fast Coalescent-Based Computation of Local Branch Support from Quartet Frequencies. *Mol. Biol. Evol.* 33, 1654–1668.

Schonswetter, P., Stehlik, I., Holderegger, R., and Tribsch, A. (2005). Molecular evidence for glacial refugia of mountain plants in the European Alps. *Molecular Ecology* 14, 3547–3555. doi:10.1111/j.1365-294x.2005.02683.x.

Schuepp, P. H. (1993). Tansley Review No. 59 Leaf boundary layers. *New Phytologist* 125, 477–507. doi:10.1111/j.1469-8137.1993.tb03898.x.

Schuster, S. C. (2008). Next-generation sequencing transforms today's biology. *Nat. Methods* 5, 16–18.

Seehausen, O. (2004). Hybridization and adaptive radiation. *Trends Ecol. Evol.* 19, 198–207.

Shee, Z. Q., Frodin, D. G., Cámara-Leret, R., and Pokorny, L. (2020). Reconstructing the Complex Evolutionary History of the Papuasian Schefflera Radiation Through Herbariomics. *Front. Plant Sci.* 11, 258.

Shekhar, S., Roch, S., and Mirarab, S. (2018). Species Tree Estimation Using ASTRAL: How Many Genes Are Enough? *IEEE/ACM Trans. Comput. Biol. Bioinform.* 15, 1738–1747.

Shirke, P. A. (2004). Influence of leaf-to-air vapour pressure deficit (VPD) on the biochemistry and physiology of photosynthesis in Prosopis juliflora. *Journal of Experimental Botany* 55, 2111–2120. doi:10.1093/jxb/erh229.

Slot, M., and Winter, K. (2017). In situ temperature response of photosynthesis of 42 tree and liana species in the canopy of two Panamanian lowland tropical forests with contrasting rainfall regimes. New Phytol. 214, 1103–1117.

Slot, M., Cala, D., Aranda, J., Virgo, A., Michaletz, S. T., and Winter, K. (2021). Leaf heat tolerance of 147 tropical forest species varies with elevation and leaf functional traits, but not with phylogeny. *Plant Cell Environ.* doi:10.1111/pce.14060.

Smart, S. M., Glanville, H. C., Blanes, M. del C., Mercado, L. M., Emmett, B. A., Jones, D. L., et al. (2017). Leaf dry matter content is better at predicting above-ground net primary production than specific leaf area. *Funct. Ecol.* 31, 1336–1344.

Smith, M. L., and Hahn, M. W. (2020). New Approaches for Inferring Phylogenies in the Presence of Paralogs. *Trends Genet.* doi:10.1016/j.tig.2020.08.012.

Smith, S. A., and Dunn, C. W. (2008). Phyutility: a phyloinformatics tool for trees, alignments and molecular data. *Bioinformatics* 24, 715–716.

Smith, S. A., and O'Meara, B. C. (2012). treePL: divergence time estimation using penalized likelihood for large phylogenies. *Bioinformatics* 28, 2689–2690.

Soltis, D. E., Kuzoff, R. K., Conti, E., Gornall, R., and Ferguson, K. (1996). matK and rbcL gene sequence data indicate that Saxifraga (Saxifragaceae) is polyphyletic. *Am. J. Bot.* 83, 371–382.

Soltis, D. E., Mort, M. E., Latvis, M., Mavrodiev, E. V., O'Meara, B. C., Soltis, P. S., et al. (2013). Phylogenetic relationships and character evolution analysis of Saxifragales using a supermatrix approach. *Am. J. Bot.* 100, 916–929.

Soltis, D. E., and Soltis, P. S. (1999). Polyploidy: recurrent formation and genome evolution. *Trends Ecol. Evol.* 14, 348–352.

Soltis, D. E., and Soltis, P. S. (2003). The role of phylogenetics in comparative genetics. *Plant Physiol.* 132, 1790–1800.

Stamatakis, A. (2006). RAxML-VI-HPC: maximum likelihood-based phylogenetic analyses with thousands of taxa and mixed models. *Bioinformatics* 22, 2688–2690.

Steen, S. W., Gielly, L., Taberlet, P., and Brochmann, C. (2000). Same parental species, but different taxa: molecular evidence for hybrid origins of the rare endemics Saxifraga opdalensis and S. svalbardensis (Saxifragaceae). *Botanical Journal of the Linnean Society* 132, 153–164. doi:10.1111/j.1095-8339.2000.tb01211.x.

Streb, P., Shang, W., and Feierabend, J. (1999). Resistance of cold-hardened winter rye leaves (Secale cerealeL.) to photo-oxidative stress. *Plant Cell Environ.* 22, 1211–1223.

Struck, T. H. (2013). The impact of paralogy on phylogenomic studies - a case study on annelid relationships. *PLoS One* 8, e62892.

Stubbs, R. L., Folk, R. A., Xiang, C.-L., Chen, S., Soltis, D. E., and Cellinese, N. (2020). A Phylogenomic Perspective on Evolution and Discordance in the Alpine-Arctic Plant Clade Micranthes (Saxifragaceae). *Front. Plant Sci.* 10, 1773.

Stubbs, R. L., Folk, R. A., Xiang, C.-L., Soltis, D. E., and Cellinese, N. (2018a). Pseudo-parallel patterns of disjunctions in an Arctic-alpine plant lineage. *Mol. Phylogenet. Evol.* 123, 88–100.

Stubbs, R. L., Soltis, D. E., and Cellinese, N. (2018b). The future of cold-adapted plants in changing climates: Micranthes (Saxifragaceae) as a case study. *Ecol. Evol.* 8, 7164–7177.

Tamura, K., Battistuzzi, F. U., Billing-Ross, P., Murillo, O., Filipski, A., and Kumar, S. (2012). Estimating divergence times in large molecular phylogenies. *Proc. Natl. Acad. Sci. U. S. A.* 109, 19333–19338.

Tamura, S., Fukuda, T., Pimenova, E. A., Petrunenko, E. A., Krestov, P. V., Bondarchuk, S. N., et al. (2018). Molecular and cytological evidences denied the immediate-hybrid hypothesis for Saxifraga yuparensis (sect. Bronchiales, Saxifragaceae) endemic to Mt. Yubari in Hokkaido, northern Japan. *Phytotaxa* 373, 53–70.

Team, R. C. (2018). R: a language and environment for statistical computing. R Foundation for Statistical Computing, Vienna. http s. *www. R-proje ct. org*.

Terashima, I., Masuzawa, T., and Ohba, H. (1993). Photosynthetic characteristics of a giant alpine plant, Rheum nobile Hook. f. et Thoms. and of some other alpine species measured at 4300 m, in the Eastern Himalaya, Nepal. *Oecologia* 95, 194–201.

Testolin, R., Attorre, F., and Jiménez-Alfaro, B. (2020). Global distribution and bioclimatic characterization of alpine biomes. *Ecography* 43, 779–788.

Thuiller, W., Lavorel, S., Araújo, M. B., Sykes, M. T., and Prentice, I. C. (2005). Climate change threats to plant diversity in Europe. *Proc. Natl. Acad. Sci. U. S. A.* 102, 8245–8250.

Tkach, N., Röser, M., and Hoffmann, M. H. (2015a). Molecular phylogenetics, character evolution and systematics of the genus Micranthes (Saxifragaceae). *Bot. J. Linn. Soc.* 178, 47–66.

Tkach, N., Röser, M., Miehe, G., Muellner-Riehl, A. N., Ebersbach, J., Favre, A., et al. (2015b). Molecular phylogenetics, morphology and a revised classification of the complex genus Saxifraga (Saxifragaceae). *Taxon* 64, 1159–1187.

Tkach, N., Röser, M., Suchan, T., Cieślak, E., Schönswetter, P., and Ronikier, M. (2019). Contrasting evolutionary origins of two mountain endemics: Saxifraga wahlenbergii (Western Carpathians) and S. styriaca (Eastern Alps). *BMC Evol. Biol.* 19, 18.

Vallender, E. J. (2009). Bioinformatic approaches to identifying orthologs and assessing evolutionary relationships. *Methods* 49, 50–55.

Vargas, P., Morton, C. M., and Jury, S. L. (1999). Biogeographic patterns in Mediterranean and Macaronesian species of Saxifraga (Saxifragaceae) inferred from phylogenetic analyses of ITS sequences. *Am. J. Bot.* 86, 724–734.

Villaverde, T., Pokorny, L., Olsson, S., Rincón-Barrado, M., Johnson, M. G., Gardner, E. M., et al. (2018). Bridging the micro-and macroevolutionary levels in phylogenomics: Hyb-Seq solves relationships from populations to species and above. *New Phytol.* 220, 636–650.

Violle C, Brian J. Enquist, McGill BJ, Jiang L., Albert CH, Hulshof C, Jung V, Messier J (2012) The return of the variance: intraspecific variability in community ecology, Trends in Ecology & Evolution, 27- 4.

Visger, C., Wong, G. K. S., Zhang, Y., Soltis, P. S., and Soltis, D. E. (2017). Divergent gene expression levels between diploid and autotetraploid Tolmiea (Saxifragaceae) relative to the total transcriptome, the cell, and biomass. *bioRxiv*. Available at: https://www.biorxiv.org/content/10.1101/169367v1.abstract.

Wallis, G. P., Waters, J. M., Upton, P., and Craw, D. (2016). Transverse Alpine Speciation Driven by Glaciation. *Trends Ecol. Evol.* 31, 916–926.

Webb, D. A. (1988). new subspecies of Saxifraga cuneifolia L. *Bot. J. Linn. Soc.* Available at: https://agris.fao.org/agris-search/search.do?recordID=US201301408762.

Webb, D. A., and Gornall, R. J. (1989). *Saxifrages of Europe: With Notes on African, American and Some Asiatic Species*. Christopher Helm.

Weiß, C. L., Schuenemann, V. J., Devos, J., Shirsekar, G., Reiter, E., Gould, B. A., et al. (2016). Temporal patterns of damage and decay kinetics of DNA retrieved from plant herbarium specimens. *R Soc Open Sci* 3, 160239.

Weitemier, K., Straub, S. C. K., Cronn, R. C., Fishbein, M., Schmickl, R., McDonnell, A., et al. (2014). Hyb-Seq: Combining target enrichment and genome skimming for plant phylogenomics. *Appl. Plant Sci.* 2. doi:10.3732/apps.1400042.

Wightman, R., Wallis, S., and Aston, P. (2018). Leaf margin organisation and the existence of vaterite-producing hydathodes in the alpine plant Saxifraga scardica. *Flora* 241, 27–34.

Winkler, M., Tribsch, A., Schneeweiss, G. M., Brodbeck, S., Gugerli, F., Holderegger, R., et al. (2012). Tales of the unexpected: Phylogeography of the arctic-alpine model plant Saxifraga oppositifolia (Saxifragaceae) revisited. *Mol. Ecol.* 21, 4618–4630.

Winkler, M., Tribsch, A., Schneeweiss, G. M., Brodbeck, S., Gugerli, F., Holderegger, R., et al. (2013). Strong nuclear differentiation contrasts with widespread sharing of plastid DNA haplotypes across taxa in European purple saxifrages (Saxifraga section Porphyrion subsection Oppositifoliae). *Bot. J. Linn. Soc.* 173, 622–636.

Woodward, F. I. (1983). The Significance of Interspecific Differences in Specific Leaf Area to the Growth of Selected Herbaceous Species from Different Altitudes. *New Phytol.* 95, 313–323.

Su X., Liu T., Liu Y.P., Harris A.J., Chen J.Y. (2022) Adaptive radiation in Orinus, an endemic alpine grass of the Qinghai-Tibet Plateau, based on comparative transcriptomic analysis. *Journal of Plant Physiology*, 277.

Yan Z., Du P., Hahn M.W., Nakhleh L. (2020). Species tree inference under the multispecies coalescent on data with paralogs is accurate. bioRxiv:498378.

Zedane, L., Hong-Wa, C., and Murienne, J. (2016). Museomics illuminate the history of an extinct, paleoendemic plant lineage (Hesperelaea, Oleaceae) known from an 1875 collection from Guadalupe Island, Mexico. *Biol. J. Linn. Soc. Lond.* Available at: https://academic.oup.com/biolinnean/article-abstract/117/1/44/2440216.

Zachos J., Pagani M., Sloan L., Thomas E., Billups K. (2001) Trends, rhythms, and aberrations in global climate 65 Ma to present. *Science*. 292, 686-693.

Zhang, C., Rabiee, M., Sayyari, E., and Mirarab, S. (2018a). ASTRAL-III: polynomial time species tree reconstruction from partially resolved gene trees. *BMC Bioinformatics* 19, 153.

Zhang, D.-J., Sheng-Yun, C., Qing-Bo, G. A. O., Yi-Zhong, D., and Shi-Long, C. (2008). Circumscription and phylogeny of Saxifraga sect. Ciliatae: Evidence from nrDNA ITS sequences. *J. Syst. Evol.* 46, 667.

Zhang, M., Wang, C., Zhang, C., Zhang, D., Li, K., Nie, Z., et al. (2020). Phylogenetic relationships and biogeographic history of the unique Saxifraga sect. Irregulares (Saxifragaceae) from eastern Asia. *J. Syst. Evol.* 58, 958–971.

Zhang, X.-J., Liu, Z.-C., Meng, K.-K., Ding, Q.-L., Wang, L., and Liao, W.-B. (2018b). Saxifraga luoxiaoensis (Saxifragaceae), a new species from Hunan and Jiangxi, China. *Phytotaxa* 350, 291. doi:10.11646/phytotaxa.350.3.8.

Zhang, Z., Chen, S., and Gornall, R. J. (2015). Morphology and anatomy of the exine in Saxifraga (Saxifragaceae). *Phytotaxa* 212, 105–132.

Zhang, Z.-X., and Gornall, R. J. (2011). Systematic significance of pollen nucleus number in the genus Saxifraga (Saxifragaceae). *Plant Systematics and Evolution* 295, 13–22. doi:10.1007/s00606-011-0456-9.

Zheng, B., Xu, Q., and Shen, Y. (2002). The relationship between climate change and Quaternary glacial cycles on the Qinghai–Tibetan Plateau: review and speculation. *Quat. Int.* 97-98, 93–101.

Zhou, Z. K., Crepet, W. L., and Nixon, K. C. (2001). The earliest fossil evidence of the Hamamelidaceae: Late Cretaceous (Turonian) inflorescences and fruits of Altingioideae. *Am. J. Bot.* 88, 753–766.

Zhmylev, P.Y. (2004). Rod Saxifraga L. (Saxifragaceae): Biomorfologia, sistematika i evolutsia zhiznennykh form. [Genus Saxifraga L. (Saxifragaceae): Biomorphology, systematics and evolution of the life forms.] Dissertation, Moscow State University.

Zimmer, E. A., and Wen, J. (2015). Using nuclear gene data for plant phylogenetics: Progress and prospects II. Next-gen approaches: Nuclear data for plant phylogenetics II. *J. Syst. Evol.* 53, 371–379.

APPENDIX 1.1: Simplified sample list of all sequenced accessions. Species names from herbarium sheets are given, as well as collector and herbarium IDs, based on standardised herbarium identifiers or other codes if available.

Genus	Taxon	Extr_Nr	Source	Herb_Index	Herbarium_ID	Collector_ID	Coll_Year
Saxifraga	*acerifolia*	S344	Herbarium	K	K000732236	Wakabayashi M. 695	1972
Saxifraga	*adenophora*	S323	Herbarium	K	NA	Watson J.M. 343	1964
Saxifraga	*adscendens*	S1	Silica	K	K000618563	Moerland M.S. 1	2016
Saxifraga	*aizoides*	S7	Silica	K	K000618571	Moerland M.S. 9	2016
Saxifraga	*ajanica*	S66	Herbarium	K	NA	Kharkevich S.	1989
Saxifraga	*alberti*	S261	Herbarium	E	E00714856	Philippe L.R.	1999
Saxifragodes	*albowiana*	S375	Herbarium	K	K000961728	Gatley E.J. 911	1959
Saxifraga	*aleutica*	S324	Herbarium	K	NA	Schaack, v G.B.	1945
Chrysosplenium	*alternifolium*	S315	Silica	K	NA	Vos, de J.M. 362	2016
Saxifraga	*ampullacea*	S104	Herbarium	K	NA	Guadagno M.	1905
Saxifraga	*anadena*	S237	Herbarium	E	E00850116	Ludlow F.	1947
Saxifraga	*androsacea*	S13	Silica	K	K000618577	Moerland M.S. 16	2016
Saxifraga	*angustibracteata*	S181	Herbarium	K	NA	Alp. G. Soc. Exp. 1593	1994
Saxifraga	*aphylla*	S27	Silica	K	NA	Vos, de J.M. 381	2016
Saxifraga	*aquatica*	S71	Herbarium	K	NA	Grey-Wilson C.	1975
Saxifraga	*arachnoidea*	S139	Herbarium	K	NA	Webb D.A.	1959
Saxifraga	*aretioides*	S158	Herbarium	K	NA	Meebold A.	1928
Saxifraga	*artvinensis*	S294	Herbarium	K	NA	Davis 29957	1957
Saxifraga	*aspera*	S23	Silica	K	K000618608	Moerland M.S. 47	2016
Saxifraga	*assamensis*	S304	Herbarium	K	NA	Kingdon Ward F.	1928
Saxifraga	*atropurpurea*	S120	Silica	K	NA	Jeffery M.J. 104	2017
Saxifraga	*atropurpurea*	S293	Herbarium	LJU	LJU10050627	Wraber T. 9748/1	1986
Saxifraga	*atuntsiensis*	S202	Herbarium	K	NA	Smith H.	1922
Saxifraga	*auriculata*	S159	Herbarium	K	K000961687	Smith H. 4064	1922
Saxifraga	*austromontana*	S137	Herbarium	K	1980-155	Jeffery M.J. 67	2017
Saxifraga	*babiana*	S339	Herbarium	BASBG	BASBG-00161309	Aexdo 2525PV	NA
Saxifraga	*berica*	S55	Herbarium	K	NA	Webb D.A.	1959
Saxifraga	*bertholdii*	S380	Herbarium	K	NA	Starling B.N. 391	1983
Saxifraga	*biflora*	S17	Silica	K	K000618585	Moerland M.S. 34	2016
Saxifraga	*biternata*	S74	Herbarium	K	NA	Webb D.A.	1959
Saxifraga	*blepharophylla*	S160	Herbarium	K	NA	Wyatt J.W.	1932
Saxifraga	*boussingaultii*	S161	Herbarium	K	NA	Grubb P.J. 587	1960
Saxifraga	*brachyphylla*	S252	Herbarium	E	E00850109	Rock J.F. 10873	1923
Saxifraga	*bracteata*	S162	Herbarium	K	NA	Kharkevich S.	1975
Saxifraga	*brevicaulis*	S258	Herbarium	E	E00850117	Ludlow F.	1944
Saxifraga	*brunneopunctata*	S263	Herbarium	E	E00850115	Ludlow F. 9750	1943
Saxifraga	*brunonis*	S212	Silica	K	2006BL00206	Moerland M.S. 100	2017
Saxifraga	*bryoides*	S2	Silica	K	K000618564	Moerland M.S. 2	2016
Saxifraga	*bulbifera*	S84	Herbarium	K	NA	Webb D.A.	1959
Saxifraga	*bulleyana*	S270	Herbarium	E	E00850111	Rock J.F. 6112	1922
Saxifraga	*bumthangensis*	S359	Herbarium	K	NA	Kingdon Ward F. 6058	1924
Saxifraga	*burseriana*	S9	Silica	K	K000618573	Moerland M.S. 11	2016
Saxifraga	*caesia*	S5	Silica	K	K000618568	Moerland M.S. 6	2016
Saxifraga	*callosa*	S109	Silica	K	1959-33327	Jeffery M.J. 39	2017
Saxifraga	*calopetala*	S357	Herbarium	K	NA	Wigram C.	1927
Saxifraga	*camposii*	S72	Herbarium	K	NA	Webb D.A.	1959
Saxifraga	*canaliculata*	S213	Silica	K	1958-27704	Jeffery M.J. 29	2017
Saxifraga	*caprariae*	S378	Herbarium	FIAF	FIO18364	Mannocci	2004
Saxifraga	*cardiophylla*	S246	Herbarium	E	E00850106	McLaren 284	NA
Saxifraga	*carinata*	S141	Herbarium	K	NA	Kudrjaschova G.	1965
Saxifraga	*carniolica*	S105	Silica	K	NA	Moerland M.S. 64	2017
Saxifraga	*carniolica*	S292	Herbarium	LJU	LJU10050658	Wraber T. 9548/4	1966
Saxifraga	*carpatica*	S142	Herbarium	K	NA	Środoń S.	1936
Saxifraga	*carpetana*	S76	Herbarium	K	E00635119	Webb D.A.	1959
Saxifraga	*carpetana _ssp_ graeca*	S256	Herbarium	E	NA	Greuter W.	1979
Saxifraga	*catalaunica*	S140	Herbarium	K	NA	Webb D.A.	1959
Saxifraga	*caulescens*	S163	Herbarium	K	NA	Brummit R.K.	2003
Saxifraga	*cervicornis*	S124	Silica	K	1969-51328	Jeffery M.J. 31	2017
Saxifraga	*cespitosa*	S65	Herbarium	K	NA	Rygg L.	1930
Saxifraga	*chadwellii*	S164	Herbarium	K	K000732316	Chadwell C.H.	1981
Saxifraga	*charadzeae*	S321	Herbarium	K	2012/1619	Groeger A.	2017
Itea	*chinensis*	S371	Herbarium	K	NA	Zhen-Yu L. 892471	1989
Saxifraga	*christopherii*	S325	Herbarium	K	NA	Grey-Wilson 558	1973
Saxifraga	*chrysanthoides*	S165	Herbarium	K	NA	Schneider C. 1964	1914
Saxifraga	*chrysoplenifolia*	S132	Silica	K	1975-2944	Jeffery M.J. 56	2017
Saxifraga	*chumbiensis*	S166	Herbarium	K	NA	Gould B.J. 1105	1938
Saxifraga	*cintrana*	S92	Herbarium	K	NA	Webb D.A.	1959
Saxifraga	*clivorum*	S235	Herbarium	E	E00170932	Cooper R.E. 3848	1915
Saxifraga	*cochlearis*	S126	Herbarium	K	1984-944	Jeffery M.J. 49	2017
Saxifraga	*contraria*	S232	Herbarium	E	E00578730	Stainton J.D.A. 995	1991
Itea	*coriacea*	S372	Herbarium	K	NA	Baishong X. 3716	2004
Saxifraga	*coriifolia*	S178	Herbarium	K	NA	Cheese M.J.	1966
Saxifraga	*corsica _ssp_ cossoniana*	S144	Herbarium	K	NA	Pau 4359	1921
Saxifraga	*cortusifolia*	S298	Herbarium	K	NA	Furuse M. 9894	1975
Saxifraga	*cotyledon*	S24	Silica	K	NA	Vos, de J.M. 348	2016
Saxifraga	*crassiflagellata*	S203	Herbarium	K	NA	Sidigi	1966
Saxifraga	*crassifolia*	S214	Silica	K	NA	Jeffery M.J.	2017
Saxifraga	*crustata*	S10	Silica	K	K000618574	Moerland M.S. 12	2016
Saxifraga	*cuneata*	S97	Herbarium	K	NA	Amich F.D.	1988
Saxifraga	*cuneifolia*	S25	Silica	K	NA	Vos, de J.M. 358	2016
Saxifraga	*cuneifolia _ssp_ robusta*	S215	Silica	K	NA	Jeffery M.J.	2017
Saxifraga	*cymbalaria*	S145	Herbarium	K	NA	Bock J.H. 929761	1976
Saxifraga	*cymbalaria*	S275	Herbarium	E	E00363492	Akuian Y. 4012	1975
Saxifraga	*cymosa*	S91	Herbarium	K	NA	Grobb. P.J.	1956

Saxifraga	*delicatula*	S326	Herbarium	K	NA	Ewan J. 18142	1949
Saxifraga	*demnatensis*	S179	Herbarium	K	NA	Balls E.K.	1936
Saxifraga	*densifoliata*	S167	Herbarium	K	NA	Flora of Yunnan Chunglien-Lijiang-Dali Expedition 743 CLD-90	1990
Saxifraga	*depressa*	S146	Herbarium	K	NA	Webb D.A.	1959
Saxifraga	*derbekii*	S93	Herbarium	K	NA	McDonald S. 20	2003
Saxifraga	*desoulavyi*	S114	Silica	K	20130472_	Jeffery M.J. 76	2017
Saxifraga	*dichotoma*	S75	Herbarium	K	NA	Fdez.-Suarez	1956
Saxifraga	*dielsiana*	S353	Herbarium	K	NA	E.H. Wilson 3614	1933
Saxifraga	*epiphylla*	S117	Silica	K	1992-0418	Jeffery M.J. 80	2017
Saxifraga	*erioblasta*	S73	Herbarium	K	NA	Halliwell 1106	1975
Saxifraga	*eschscholtzii*	S277	Herbarium	E	E00505760	Halliday G. 413/75	1975
Saxifraga	*exarata*	S327	Herbarium	K	NA	Webb D.A.	1959
Saxifraga	*exarata*	S26	Silica	K	NA	Vos, de J.M. 380	2016
Saxifraga	*exarata*	S328	Herbarium	K	NA	Reveal J. 8576	2005
Saxifraga	*facchini*	S19	Silica	K	K000618599	Moerland M.S. 38	2016
Saxifraga	*filifolia*	S228	Herbarium	E	E00850095	NA 1126	1919
Saxifraga	*flaccida*	S239	Herbarium	E	E00578801	Stainton J.D.A. 1826	1954
Saxifraga	*flagellaris*	S79	Herbarium	K	NA	Grey-Wilson C. 1590	1971
Saxifraga	*florulenta*	S168	Herbarium	K	NA	C.P.	1880
Saxifragopsis	*fragarioides*	S374	Herbarium	K	NA	Alexander A.M. 5434	1948
Saxifraga	*fragilis _ssp_valentina*	S299	Herbarium	K	NA	Sandwi* N.Y. 4859	1957
Saxifraga	*funstonii*	S295	Herbarium	K	NA	Kharkevich S.	1974
Saxifraga	*gatogombensis*	S253	Herbarium	E	E00850108	Smith H.	1922
Saxifraga	*gemmigera _ssp_gemmuligera*	S182	Herbarium	K	NA	Smith H.	1922
Saxifraga	*gemmulosa*	S62	Herbarium	K	NA	Webb D.A.	1959
Saxifraga	*genesiana*	S305	Herbarium	K	K000732262	Vargas P. MA562362	1959
Saxifraga	*geranioides*	S133	Herbarium	K	2011-80	Jeffery M.J. 59	2017
Saxifraga	*giraldiana*	S169	Herbarium	K	NA	Smith H.	1922
Saxifraga	*giziana*	S340	Herbarium	BASBG	BASBG-00162094	Bouchar*	1953
Saxifraga	*glabella*	S82a	Herbarium	K	NA	Rechinger	1933
Saxifraga	*glaucophylla*	S183	Herbarium	K	NA	Flora of Yunnan Chunglien-Lijiang-Dali Expedition 988 CLD-90	1990
Saxifraga	*gouldii*	S300	Herbarium	K	NA	Gould B.J. 1310	1938
Saxifraga	*graeca*	S143	Herbarium	K	NA	Webb D.A.	1959
Saxifraga	*granulata*	S136	Silica	K	2000-1403	Moerland M.S. 102	2018
Saxifraga	*granulata _ssp_russii*	S204	Herbarium	K	NA	Webb D.A.	1959
Saxifraga	*granulifera*	S184	Herbarium	K	NA	Zhang T.	2010
Saxifraga	*grisebachii*	S99	Herbarium	K	NA	Rechinger K.H.	1936
Saxifraga	*gyalana*	S281	Herbarium	E	E00850094	Ludlow F. 5361	1938
Saxifraga	*haematochroa*	S236	Herbarium	E	E00170891	Ludlow F. 445	1933
Saxifraga	*haenseleri*	S147	Herbarium	K	NA	NA	1925
Saxifraga	*hariotii*	S148	Herbarium	K	NA	Webb D.A.	1959
Saxifraga	*harry_smithii*	S283	Herbarium	E	E00170889	Ludlow F. 21149	1949
Saxifraga	*hederifolia*	S185	Herbarium	K	NA	Hedberg O.	1973
Saxifraga	*heleonastes*	S271	Herbarium	K	NA	Chungtien-Lijiang-Dali Expedition CLD90 470	1990
Saxifraga	*heterotricha*	S233	Herbarium	E	E00850091	F. Ludlow, G. Sherriff, G. Taylor 5219	1938
Telesonix	*heucheriforme*	S377	Herbarium	K	NA	Drummond	1832
Saxifraga	*hirculoides*	S280	Herbarium	E	E00850098	McBeath R.J.D. 1527	1983
Saxifraga	*hirculus*	S149	Herbarium	K	NA	Fijałkowski D.	1954
Saxifraga	*hirculus _ssp_alpina*	S102	Herbarium	K	NA	Budenberg W.J.	1982
Saxifraga	*hirculus _ssp_propinqua*	S350	Herbarium	K	NA	Komarov V. 821	1896
Saxifraga	*hirsuta*	S119	Silica	K	20090707_	Jeffery M.J. 83	2017
Saxifraga	*hoffmeisterii*	S100	Herbarium	K	NA	Grey-Wilson 686	1973
Saxifraga	*hohenwartii*	S217	Silica	K	NA	Moerland M.S. 65	2017
Saxifraga	*hyperborea*	S103	Herbarium	K	NA	Kharkevich S.	1974
Saxifraga	*hypericoides*	S186	Herbarium	K	NA	Sinclair I.W.J.	1984
Saxifraga	*hypnoides*	S69	Silica	K	1978BL00054 A	Moerland M.S. 97	2017
Saxifraga	*inconspicua*	S306	Herbarium	K	K00073230	Smith 1524	1909
Saxifraga	*insolens*	S243	Herbarium	E	E00850101	Gaoling Shan Expedition 1996 7767	1996
Saxifraga	*intricata*	S262	Herbarium	E	NA	Timbal-Lagrave E.	1885
Saxifraga	*iranica*	S218	Silica	K	20140135_	Moerland M.S.	2018
Saxifraga	*irrigua*	S81a	Herbarium	K	NA	Davis 33390	1959
Saxifraga	*isophylla*	S264	Herbarium	E	E00850114	Ludlow F. 6159	1938
Saxifraga	*italica*	S87	Herbarium	LJU	LJU10106812	Feoli E.	1971
Ribes	*japonicum*	S370	Herbarium	K	K000809013	Murata G. 376	1982
Saxifraga	*josephii*	S345	Herbarium	K	NA	Giraldi J.	1897
Saxifraga	*kansuensis*	S273	Herbarium	K	NA	Rock J.F. 12525	1925
Saxifraga	*kinchinjungae*	S229	Herbarium	E	E00170860	Ludlow F. 21081	1949
Saxifraga	*kingdonii*	S244	Herbarium	E	E00850087	Ludlow F. 14413	1947
Saxifraga	*kolenatiana*	S286	Herbarium	E	E00348303	Mitchell J. 194	2009
Saxifraga	*komarovii*	S187	Herbarium	K	K000493581	Osborne J.	2008
Saxifraga	*korshinskyi*	S205	Herbarium	K	NA	Komaròv V. 822	1895
Saxifraga	*kruhsiana*	S188	Herbarium	K	NA	Brummit N.A.	2003
Saxifraga	*lactea*	S260	Herbarium	E	E00505481	Petrovsky V. 6570	1984
Saxifraga	*lamottei*	S341	Herbarium	BASBG	BASBG-00162387	D'Alleizette	1950
Saxifraga	*latepetiolata*	S278	Herbarium	K	NA	B.M.T. 756	1912
Saxifraga	*lepida*	S189	Herbarium	K	NA	Sinclair I.W.J.	1984
Saxifraga	*lilacina*	S310	Herbarium	K	NA	Duthie J.F.	1899
Saxifraga	*limprichtii*	S355	Herbarium	K	NA	Licent A.E. 8966	1929
Saxifraga	*linearifolia*	S247	Herbarium	E	E00850107	Kingdon Ward J. 4091	1915
Saxifraga	*losae*	S155	Herbarium	K	NA	Rodriguez A. 30TWM7266	1985
Saxifraga	*luteoviridis*	S150	Herbarium	K	NA	Pawłowski B.	1933
Boykinia	*lycoctonifolia*	S376	Herbarium	K	NA	Furuse M. 9679	1975
Saxifraga	*macrostigmatoides*	S257	Herbarium	E	E00099502	Yü T.T.	1938

Saxifraga	*maderensis*	S190	Herbarium	K	NA	Pickering C.H.C.	1957
Saxifraga	*magellanica*	S351	Herbarium	K	NA	Chambers K.L.	NA
Micranthes	*manshuriensis*	S349	Herbarium	K	K000732458	Duthie J.F. 557	1887
Saxifraga	*marginata*	S131	Herbarium	K	1985-950	Jeffery M.J. 55	2017
Saxifraga	*matta-viridis*	S81	Herbarium	K	NA	Starling B.N.	NA
Saxifraga	*maweana*	S191	Herbarium	K	NA	Davis P. 431	1939
Saxifraga	*mazanderanica*	S329	Herbarium	K	K000732251	Rechinger K.H.	1948
Saxifraga	*media*	S112	Silica	K	20130471_	Jeffery M.J. 66	2017
Micranthes	*merkii*	S338	Herbarium	K	NA	Furuse M. 9250	1975
Saxifraga	*micans*	S118	Silica	K	20140511_	Jeffery M.J. 82	2017
Saxifraga	*microviridis*	S82	Herbarium	K	NA	Townsend C.C. 89/292	1989
Saxifraga	*moncayensis*	S317	Herbarium	K	ES-0M-1974/0144	Groeger A.	2017
Saxifraga	*montis_christi*	S379	Herbarium	FIAF	FIO18369	Ferretti	2014
Saxifraga	*moschata*	S21	Silica	K	K000618593	Moerland M.S. 32	2016
Saxifraga	*mucronulatoides*	S301	Herbarium	K	NA	Grey-Wilson C. 4310	1981
Saxifraga	*muscoides*	S152	Herbarium	K	NA	Webb D.A.	1959
Saxifraga	*mutata*	S59	Silica	K	K000618599	Moerland M.S. 38	1959
Saxifraga	*nakaoi*	S238	Herbarium	E	E00144942	Wu S.K. 8581123	1985
Saxifraga	*nanella*	S254	Herbarium	E	E00850096	Stainton J.D.A. 1284	1954
Saxifraga	*neopropagulifera*	S230	Herbarium	E	E00578719	Polunin 47	1952
Saxifraga	*nervosa*	S83a	Herbarium	K	NA	Webb D.A.	1959
Saxifraga	*nevadensis*	S153	Herbarium	K	NA	Szafranski F.	1973
Saxifraga	*nigroglandulosa*	S302	Herbarium	K	NA	Rock J.F. 22393	1932
Saxifraga	*omolojensis*	S192	Herbarium	K	NA	Kharkevich S.	1974
Saxifraga	*omphalodifolia*	S248	Herbarium	E	E00850103	Kingdon Ward J. 4696	1931
Saxifraga	*oppositifolia*	S4	Silica	K	K000618567	Moerland M.S. 5	2016
Saxifraga	*oppositifolia*	S219	Silica	K	NA	Jeffery M.J.	2017
Saxifraga	*oppositifolia _ssp_glandulifera*	S342	Herbarium	BASBG	BASBG-00162806	Simon C.	1964
Saxifraga	*oppositifolia _ssp_murithiana*	S296	Herbarium	K	NA	Bordere	1872
Saxifraga	*oranensis*	S107	Silica	K	1961-29909	Jeffery M.J. 23	2017
Saxifraga	*osloensis*	S154	Herbarium	K	NA	Jorgen Knaben	1954
Micranthes	*pallida*	S366	Herbarium	CDBI	NA	Moerland M.S. 81	2017
Saxifraga	*palpebrata*	S307	Herbarium	K	K000732304	Strackey R.	1849
Saxifraga	*paniculata*	S3	Silica	K	K000618565	Moerland M.S. 3	2016
Saxifraga	*paniculata _ssp_cartilaginea*	S110	Silica	K	1961-29904	Jeffery M.J. 42	2017
Saxifraga	*paradoxa*	S220	Silica	K	NA	Moerland M.S. 73	2017
Saxifraga	*pardanthina*	S193	Herbarium	K	NA	K.W. 4610	NA
Saxifraga	*parnassica*	S138	Herbarium	K	NA	Grey-Wilson C.	1968
Saxifraga	*pasumensis*	S285	Herbarium	E	E00850088	Ludlow F. 5692	1938
Saxifraga	*pavonii*	S171	Herbarium	K	NA	Boelcke O. 1786	1946
Saxifraga	*pedemontana*	S123	Silica	K	1994-1279	Jeffery M.J. 22	2017
Saxifraga	*pentadactylis*	S330	Herbarium	K	NA	Gomez S.	1973
Saxifraga	*peplidifolia*	S194	Herbarium	K	NA	Flora of Yunnan Chunglien-Lijiang-Dali Expedition 1200 CLD-90	1990
Saxifraga	*petraea*	S221	Silica	K	NA	Moerland M.S. 56	2017
Saxifraga	*pickeringii*	S122	Silica	K	1971-2387	Jeffery M.J. 24	2017
Saxifraga	*platysepala*	S156	Herbarium	K	NA	Max. S.	1973
Saxifraga	*porophylla*	S282	Herbarium	K	NA	Webb D.A.	1959
Saxifraga	*praetermissa*	S290	Herbarium	LJU	LJU10106974	Mettesics H.	1967
Saxifraga	*prattii*	S347	Herbarium	K	NA	Purdom W.	1910
Saxifraga	*prenja*	S172	Herbarium	K	NA	Loschuig. V.	1933
Saxifraga	*prenja*	S291	Herbarium	LJU	LJU10106975	Kofol A.	1979
Saxifraga	*presolanensis*	S157	Herbarium	K	NA	Webb D.A.	1960
Saxifraga	*prostii*	S111	Silica	K	NA	Jeffery M.J. 44	2017
Saxifraga	*pseudohirculus*	S267	Herbarium	E	E00136644	Long D.G.	1997
Saxifraga	*pubescens*	S64	Herbarium	K	NA	Webb D.A.	1959
Saxifraga	*pubescens _ssp_iratiana*	S331	Herbarium	K	NA	Webb D.A.	1959
Saxifraga	*pulvinaria*	S206	Herbarium	K	NA	Starling B.N.	1983
Micranthes	*punctata*	S251	Herbarium	E	E00258088	Bridger M.A. 2	2003
Saxifraga	*punctulata*	S245	Herbarium	E	E00850093	Cave G.H. 22/47	1947
Saxifraga	*quadrifaria*	S113	Silica	K	20150926_	Jeffery M.J. 72	2017
Saxifraga	*radiata*	S332	Herbarium	K	NA	Hutchinson S.W. 654	1933
Saxifraga	*ramulosa*	S127	Herbarium	K	1983-5902	Jeffery M.J. 51	2017
Saxifraga	*rebunshirensis*	S222	Silica	K	1997BL00485	Moerland M.S. 101	2017
Saxifraga	*retusa _ssp_augustana*	S318	Herbarium	K	G/1640	Groeger A.	2017
Saxifraga	*reuteriana*	S125	Herbarium	K	1976-2040	Jeffery M.J. 45	2017
Saxifraga	*rhaetica*	S115	Silica	K	20080359_	Jeffery M.J. 77	2017
Saxifraga	*rhodopetala*	S249	Herbarium	E	E00852960	Polunin 3472	1952
Saxifraga	*rigoi*	S173	Herbarium	K	NA	Webb D.A.	1959
Saxifraga	*rivularis*	S90	Herbarium	K	NA	Levi Rygg.	1930
Saxifraga	*rivularis*	S174	Herbarium	K	NA	Blakelock R.H. 46	1938
Saxifraga	*rosacea _ssp_sponhemica*	S225	Silica	K	MJG-198055520	Gerschwitz-Eidt M.	2017
Saxifraga	*rotundifolia*	S12	Silica	K	K000618575	Moerland M.S. 14	2016
Saxifraga	*roylei*	S231	Herbarium	E	E00578734	Stainton J.D.A. 4256	1963
Saxifraga	*rudolphiana*	S22	Silica	K	K000618605	Moerland M.S. 44	2016
Saxifraga	*ruprechtiana*	S223	Silica	K	19822800_	Moerland M.S.	2018
Saxifraga	*sancta*	S108	Silica	K	1958-23408	Jeffery M.J. 38	2017
Saxifraga	*sanguinea*	S195	Herbarium	K	NA	Soulié J.-A. 674	1893
Saxifraga	*saxorum*	S234	Herbarium	E	E00850098	Long D.J. 581	1992
Saxifraga	*scardica*	S128	Herbarium	K	1984-3742	Jeffery M.J. 52	2017
Saxifraga	*sedoides*	S6	Silica	K	K000618569	Moerland M.S. 7	2016
Saxifraga	*seguieri*	S28	Silica	K	NA	Vos, de J.M. 382	2016
Saxifraga	*sempervivum*	S129	Herbarium	K	1984-3743	Jeffery M.J. 53	2017
Saxifraga	*hederacea*	S80a	Herbarium	K	NA	Townsend C.C. 83/82	1983
Saxifraga	*serotina*	S207	Herbarium	K	NA	Kharkevich S.	1982
Saxifraga	*serpyllifolia*	S208	Herbarium	K	NA	Eyerdam W.J.	1932
Saxifraga	*serpyllifolia*	S289	Herbarium	E	E00505479	Maximova M.	1971
Saxifraga	*serrula*	S83	Herbarium	K	NA	Grey-Wilson C. 735	1973
Saxifraga	*setigera*	S209	Herbarium	K	NA	Kharkevich S.	1974

Saxifraga	*sibirica*	S175	Herbarium	K	NA	Davis P.H.	1965
Saxifraga	*sibirica _ssp_mollis*	S259	Herbarium	E	E00505481	Prima V.	1971
Saxifraga	*sibthorpii*	S303	Herbarium	K	NA	Atchley S.C. 2320	1934
Saxifraga	*sieversiana*	S210	Herbarium	K	NA	Kharkevich S.	1977
Saxifraga	*signatella*	S242	Herbarium	E	E00850089	Ludlow F. 6046	1938
Saxifraga	*sinomontana*	S265	Herbarium	E	E00061060	Ho T.N. 2831	1996
Saxifraga	*smithiana*	S196	Herbarium	K	NA	Flora of Yunnan Chunglien-Lijiang-Dali Expedition	1990
Saxifraga	*sp*	S274	Herbarium	E	E00850102	Forrest G. 22135	1919
Saxifraga	*sp*	S276	Herbarium	E	E00424887	Kunming & Edinburgh University Expedition to Sichuan 48	2010
Saxifraga	*sp*	S308	Herbarium	K	NA	Dickore B. 3884	1989
Saxifraga	*sp*	S309	Herbarium	K	NA	Dickore B. 3968	1989
Saxifraga	*sp*	S354	Herbarium	CDBI	NA	Moerland M.S. 85_2	2017
Saxifraga	*sp*	S360	Herbarium	CDBI	NA	Moerland M.S. 74	2017
Saxifraga	*sp*	S361	Herbarium	CDBI	NA	Moerland M.S. 75	2017
Saxifraga	*sp*	S362	Herbarium	CDBI	NA	Moerland M.S. 76	2017
Saxifraga	*sp*	S363	Herbarium	CDBI	NA	Moerland M.S. 77	2017
Chrysosplenium	*sp*	S364	Herbarium	CDBI	NA	Moerland M.S. 79	2017
Saxifraga	*sp*	S365	Herbarium	CDBI	NA	Moerland M.S. 80	2017
Saxifraga	*sp*	S367	Herbarium	CDBI	NA	Moerland M.S. 83	2017
Saxifraga	*sp*	S368	Herbarium	CDBI	NA	Moerland M.S. 85_1	2017
Saxifraga	*spathularis*	S224	Silica	K	19781920_	Moerland M.S.	2018
Saxifraga	*speciosa*	S343	Herbarium	BASBG	BASBG-00163275	Černoch s.n. 18162	1968
Saxifraga	*sphaeradena*	S288	Herbarium	E	NA	Long D.G. 556	1992
Saxifraga	*spinulosa*	S211	Herbarium	K	NA	H.B.M. 1889	1977
Saxifraga	*squarrosa*	S20	Silica	K	K000618591	Moerland M.S. 30	2016
Saxifraga	*stellariifolia*	S272	Herbarium	E	E00850105	Smith H.	1922
Micranthes	*stellaris*	S316	Silica	K	K000618566	Moerland M.S. 4	2016
Saxifraga	*stolonifera*	S313	Silica	K	1978-6242	Moerland M.S. 103	2018
Saxifraga	*stribrnyi*	S130	Herbarium	K	1960-13604	Jeffery M.J. 54	2017
Saxifraga	*subamplexicaulis*	S268	Herbarium	E	E00850113	Forrest G. 27946	1929
Saxifraga	*subsessiflora*	S197	Herbarium	K	NA	Grey-Wilson	1975
Saxifraga	*subspathulata*	S348	Herbarium	K	NA	Pratt A.E.	1890
Saxifraga	*substrigosa*	S240	Herbarium	E	E00850099	Ludlow F. 16938	1949
Saxifraga	*subverticillata*	S319	Herbarium	K	GE-M-2009/2412	Groeger A.	2017
Saxifraga	*svalbardensis*	S333	Herbarium	K	NA	Schuhwerk F. 91/898	1991
Saxifraga	*taraktophylla*	S287	Herbarium	E	NA	Ludlow F. 5398	1938
Saxifraga	*taygetea*	S60	Herbarium	K	NA	Chreb. V.	1938
Saxifraga	*taylorii*	S358	Herbarium	K	NA	Calder J.A.	1957
Saxifraga	*tenella*	S68	Silica	K	1992BL00387	Moerland M.S. 99	2017
Saxifraga	*tentaculata*	S250	Herbarium	E	E00578799	Stainton J.D.A. 1352	1954
Saxifraga	*terektensis*	S198	Herbarium	K	NA	NA	1955
Saxifraga	*thianthia*	S279	Herbarium	E	E00172012	Ludlow F. 3210	1937
Saxifraga	*tibetica*	S266	Herbarium	E	E00136636	Long D.G.	1997
Saxifraga	*tombeanensis*	S176	Herbarium	K	NA	Webb D.A.	1959
Saxifraga	*triaristulata*	S199	Herbarium	K	NA	Rock J.F.	1932
Saxifraga	*tricrenata*	S335	Herbarium	K	NA	Jacquemont F.	1980
Saxifraga	*tricuspidata*	S226	Silica	K	19860587_	Moerland M.S.	2018
Saxifraga	*tridactylites*	S312	Herbarium	K	NA	Vos, de J.M.	2018
Saxifraga	*turfosa*	S269	Herbarium	E	E00850112	McLaren 255	1993
Saxifraga	*umbrosa*	S135	Herbarium	K	1975-5326	Jeffery M.J. 64	2017
Saxifraga	*unifoveolata*	S320	Herbarium	K	2000/1128	Groeger A.	2017
Saxifraga	*valdensis*	S116	Silica	K	20130773_	Jeffery M.J. 79	2017
Saxifraga	*vandellii*	S322	Herbarium	K	2002/0789	Groeger A.	2017
Saxifraga	*vayredana*	S177	Herbarium	K	NA	Webb D.A.	1959
Saxifraga	*vespertina*	S336	Herbarium	K	NA	Rivas-Martinez	1983
Saxifraga	*vilmoriana*	S311	Herbarium	K	NA	C.M.A. Roberts 544	1987
Saxifraga	*wahlenbergii*	S89	Herbarium	K	NA	Woloszczak E.	1896
Saxifraga	*wallichiana*	S241	Herbarium	E	E00850100	Forrest G. 6627	1910
Saxifraga	*wallichiana*	S369	Herbarium	CDBI	NA	Moerland M.S. 86	2017
Saxifraga	*wardii*	S284	Herbarium	E	E00850090	Ludlow F. 5949	1938
Saxifraga	*wendelboi*	S201	Herbarium	K	NA	Archibald J.C.	1966
Saxifraga	*williamsii_b*	S255	Herbarium	E	E00393018	Stainton J.D.A. 7250	1954
Saxifraga	*willkommiana*	S85	Herbarium	K	NA	Halliwell B. 1037	NA
Saxifraga	*willkommiana _ssp_almanzorii*	S336	Herbarium	K	NA	Calder J.A.	1957
Saxifraga	*willkommiana _ssp_caballeroi*	S337	Herbarium	K	NA	Rivas-Martinez	1984

APPENDIX 2.2

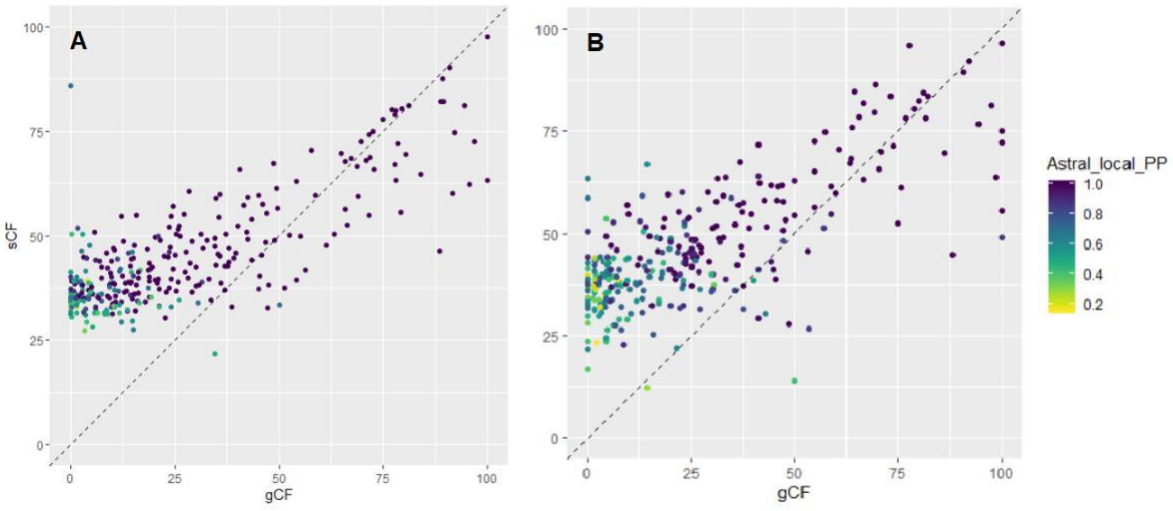

Appendix 2.2: Gene and site concordance factor calculated for branches in IQ-tree for datasets A) COMPLETE and B) PARALOGTRIM. Data points are coloured by ASTRAL local posterior probability value.

APPENDIX 3.1


A
Saxifraga_quadrifaria_S113
Saxifraga_roylei_S23T
Saxifraga_georgei_P05_WB09
Saxifraga_poluniniana_P03_WC08
Saxifraga_alpigena_P05_WH10
Saxifraga_subsessiflora_S197
Saxifraga_cinerea_P03_WC01
Saxifraga_micans_S118
Saxifraga_rhodopetala_S249
Saxifraga_andersonii_P05_WB08
Saxifraga_stolitzkae_P05_WE03
Saxifraga_decora_P03_WC05
Saxifraga_williamsii_b_S255
Saxifraga_saxorum_S234
Saxifraga_pulvinaria_S206
Saxifraga_kumaunensis_P02_WC01
Saxifraga_imbricata_P03_WE05
Saxifraga_matta_florida_P05_WE06
Saxifraga_hypostoma_P02_WH09
Saxifraga_lowndesii_P03_WC03
Saxifraga_thianthia_S279
Saxifraga_kumaunensis_P03_WA04
Saxifraga_pulchra_P03_WE07
Saxifraga_chionophila_P03_WD09
Saxifraga_likiangensis_P03_WE06
Saxifraga_ramulosa_ST27
Saxifraga_kansuensis_S273
Saxifraga_afghanica_P05_WC04
Saxifraga_alberti_S261
Saxifraga_lilacina_S310
Saxifraga_kotschyi_P05_WB10
Saxifraga_wendelboi_S201
Saxifraga_wendelboi_P07_WF12
Saxifraga_iranica_S218
Saxifraga_marginata_S131
Saxifraga_scardica_S128
Saxifraga_vandellii_S322
Saxifraga_burseriana_S9
Saxifraga_aretioides_S158
Saxifraga_tombeanensis_S176
Saxifraga_marginata_var_boryi_P07_WF03
Saxifraga_ferdinandi_coburgi_P05_WD06
Saxifraga_juniperifolia_P07_WF01
Saxifraga_scleropoda_P03_WC06
Saxifraga_unifoveolata_S320
Saxifraga_desoulavyi_S114
Saxifraga_charadzeae_S321
Saxifraga_subverticillata_S319
Saxifraga_artvinensis_S294
Saxifraga_carinata_ST41
Saxifraga_caucasica_ssp._desoulavyi_P05_WC12
Saxifraga_ruprechtiana_S223
Saxifraga_media_S112
Saxifraga_porophylla_S282
Saxifraga_grisebachii_S99
Saxifraga_porophylla_var_thessalica_P07_WF08
Saxifraga_sempervivum_P07_WF10
Saxifraga_stribrnyi_S130
Saxifraga_stribrnyi_P07_WF11
Saxifraga_luteoviridis_ST50
Saxifraga_sempervivum_S129
Saxifraga_macedonica_P03_WC04
Saxifraga_sancta_P07_WF09
Saxifraga_sancta_S108
Saxifraga_spruneri_P05_WD10
Saxifraga_oppositifolia_T_S4
Saxifraga_oppositifolia_2_S219
Saxifraga_oppositifolia_P07_WF06
Saxifraga_oppositifolia_ssp_murithiana_S296
Saxifraga_blepharophylla_S160
Saxifraga_biflora_S17
Saxifraga_ajanica_S66
Saxifraga_rudolphiana_S22
Saxifraga_retusa_ssp_augustana_S318
Saxifraga_retusa_P05_WD04
Saxifraga_aizoides_S7
Saxifraga_aizoides_P07_WC02
Saxifraga_mutata_S59
Saxifraga_squarrosa_S20
Saxifraga_caesia_P05_WD03
Saxifraga_caesia_S5
Saxifraga_florulenta_S168
Saxifraga_florulenta_P07_WC08
Saxifraga_paniculata_P07_WC10
Saxifraga_paniculata_S3
Saxifraga_paniculata_ssp._cartilaginea_S110
Saxifraga_rhaetica_S115
Saxifraga_kolenatiana_S286
Saxifraga_crustata_S10
Saxifraga_crustata_P07_WC05
Saxifraga_hostii_P05_WE07
Saxifraga_valdensis_S116
Saxifraga_cochlearis_S126
Saxifraga_callosa_S109
Saxifraga_catalaunica_S140
Saxifraga_longifolia_P03_WC10
Saxifraga_cotyledon_S24
Saxifraga_cuneifolia_S25
Saxifraga_cuneifolia_ssp_robusta_S215
Saxifraga_cuneifolia_P07_WC06
Saxifraga_spathularis_S224
Saxifraga_spathularis_P07_WC11
Saxifraga_hirsuta_P07_WE12
Saxifraga_hirsuta_S119
Saxifraga_umbrosa_S135
Saxifraga_aspera_S23
Saxifraga_bryoides_S2
Saxifraga_aspera_P07_WC03
Saxifraga_rotundifolia_P05_WD11
Saxifraga_rotundifolia_S12
Saxifraga_chrysoplenifolia_S132
Saxifraga_corifolia_S178
Saxifraga_taygetea_S60
3.0
B

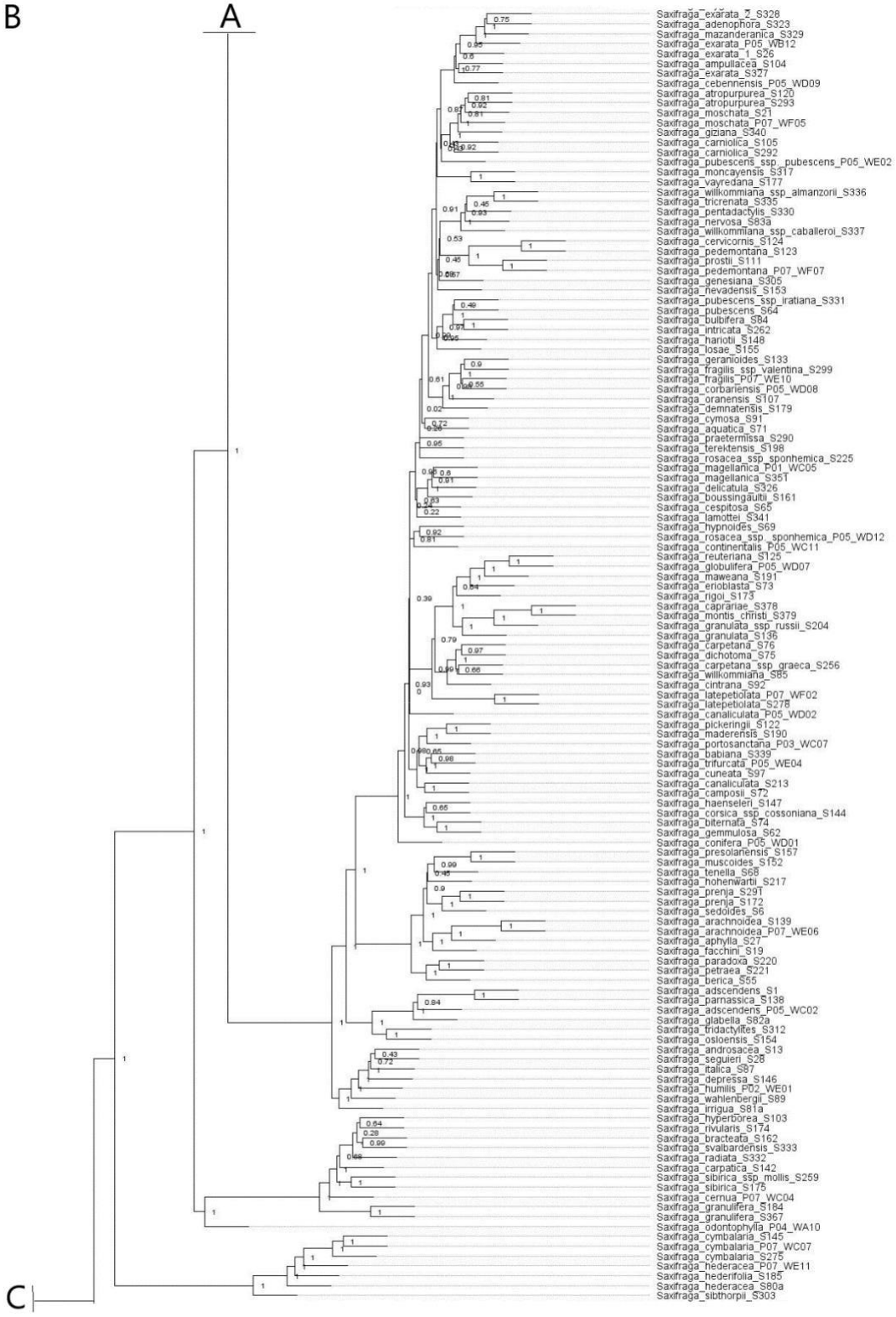
B
A
C
Saxifraga_exarata_2_S328
Saxifraga_adenophora_S323
Saxifraga_mazanderanica_S329
Saxifraga_exarata_P05_WB12
Saxifraga_exarata_1_S26
Saxifraga_ampullacea_S104
Saxifraga_exarata_S327
Saxifraga_cebennensis_P05_WD09
Saxifraga_atropurpurea_S120
Saxifraga_atropurpurea_S293
Saxifraga_moschata_S21
Saxifraga_moschata_P07_WF05
Saxifraga_giziana_S340
Saxifraga_carniolica_S105
Saxifraga_carniolica_S292
Saxifraga_pubescens_ssp._pubescens_P05_WE02
Saxifraga_moncayensis_S317
Saxifraga_vayredana_S177
Saxifraga_willkommiana_ssp._almanzorii_S336
Saxifraga_tricrenata_S335
Saxifraga_pentadactylis_S330
Saxifraga_nervosa_S63a
Saxifraga_willkommiana_ssp._caballeroi_S337
Saxifraga_cervicornis_S124
Saxifraga_pedemontana_S123
Saxifraga_prostii_S111
Saxifraga_pedemontana_P07_WF07
Saxifraga_genesiana_S305
Saxifraga_nevadensis_S153
Saxifraga_pubescens_ssp._iratiana_S331
Saxifraga_pubescens_S64
Saxifraga_bulbifera_S84
Saxifraga_intricata_S262
Saxifraga_hariotii_S148
Saxifraga_losae_S155
Saxifraga_geranioides_S133
Saxifraga_fragilis_ssp._valentina_S299
Saxifraga_fragilis_P07_WE10
Saxifraga_corbariensis_P05_WD08
Saxifraga_oranensis_S107
Saxifraga_demnatensis_S179
Saxifraga_cymosa_S91
Saxifraga_aquatica_S71
Saxifraga_praetermissa_S290
Saxifraga_terektensis_S198
Saxifraga_rosacea_ssp._sponhemica_S225
Saxifraga_magellanica_P01_WC05
Saxifraga_magellanica_S351
Saxifraga_delicatula_S326
Saxifraga_boussingaultii_S161
Saxifraga_cespitosa_S65
Saxifraga_lamottei_S341
Saxifraga_hypnoides_S69
Saxifraga_rosacea_ssp._sponhemica_P05_WD12
Saxifraga_continentalis_P05_WC11
Saxifraga_reuteriana_S125
Saxifraga_globulifera_P05_WD07
Saxifraga_maweana_S191
Saxifraga_erioblasta_S73
Saxifraga_rigoi_S173
Saxifraga_caprariae_S378
Saxifraga_montis_christi_S379
Saxifraga_granulata_ssp._russii_S204
Saxifraga_granulata_S136
Saxifraga_carpetana_S76
Saxifraga_dichotoma_S75
Saxifraga_carpetana_ssp._graeca_S256
Saxifraga_willkommiana_S85
Saxifraga_cintrana_S92
Saxifraga_latepetiolata_P07_WF02
Saxifraga_latepetiolata_S278
Saxifraga_canaliculata_P05_WD02
Saxifraga_pickeringii_S122
Saxifraga_maderensis_S190
Saxifraga_portosanctana_P03_WC07
Saxifraga_babiana_S339
Saxifraga_trifurcata_P05_WE04
Saxifraga_cuneata_S97
Saxifraga_canaliculata_S213
Saxifraga_camposii_S72
Saxifraga_haenseleri_S147
Saxifraga_corsica_ssp._cossoniana_S144
Saxifraga_biternata_S74
Saxifraga_gemmulosa_S62
Saxifraga_conifera_P05_WD01
Saxifraga_presolanensis_S157
Saxifraga_muscoides_S152
Saxifraga_tenella_S68
Saxifraga_hohenwartii_S217
Saxifraga_prenja_S291
Saxifraga_prenja_S172
Saxifraga_sedoides_S6
Saxifraga_arachnoidea_S139
Saxifraga_arachnoidea_P07_WE06
Saxifraga_aphylla_S27
Saxifraga_facchinii_S19
Saxifraga_paradoxa_S220
Saxifraga_petraea_S221
Saxifraga_berica_S55
Saxifraga_adscendens_S1
Saxifraga_parnassica_S138
Saxifraga_adscendens_P05_WC02
Saxifraga_glabella_S82a
Saxifraga_tridactylites_S312
Saxifraga_osloensis_S154
Saxifraga_androsacea_S13
Saxifraga_seguieri_S28
Saxifraga_italica_S87
Saxifraga_depressa_S146
Saxifraga_humilis_P02_WE01
Saxifraga_wahlenbergii_S89
Saxifraga_irrigua_S81a
Saxifraga_hyperborea_S103
Saxifraga_rivularis_S174
Saxifraga_bracteata_S162
Saxifraga_svalbardensis_S333
Saxifraga_radiata_S332
Saxifraga_carpatica_S142
Saxifraga_sibirica_ssp._mollis_S259
Saxifraga_sibirica_S175
Saxifraga_cernua_P07_WC04
Saxifraga_granulifera_S184
Saxifraga_granulifera_S367
Saxifraga_odontophylla_P04_WA10
Saxifraga_cymbalaria_S145
Saxifraga_cymbalaria_P07_WC07
Saxifraga_cymbalaria_S275
Saxifraga_hederacea_P07_WE11
Saxifraga_hederifolia_S185
Saxifraga_hederacea_S80a
Saxifraga_sibthorpii_S303

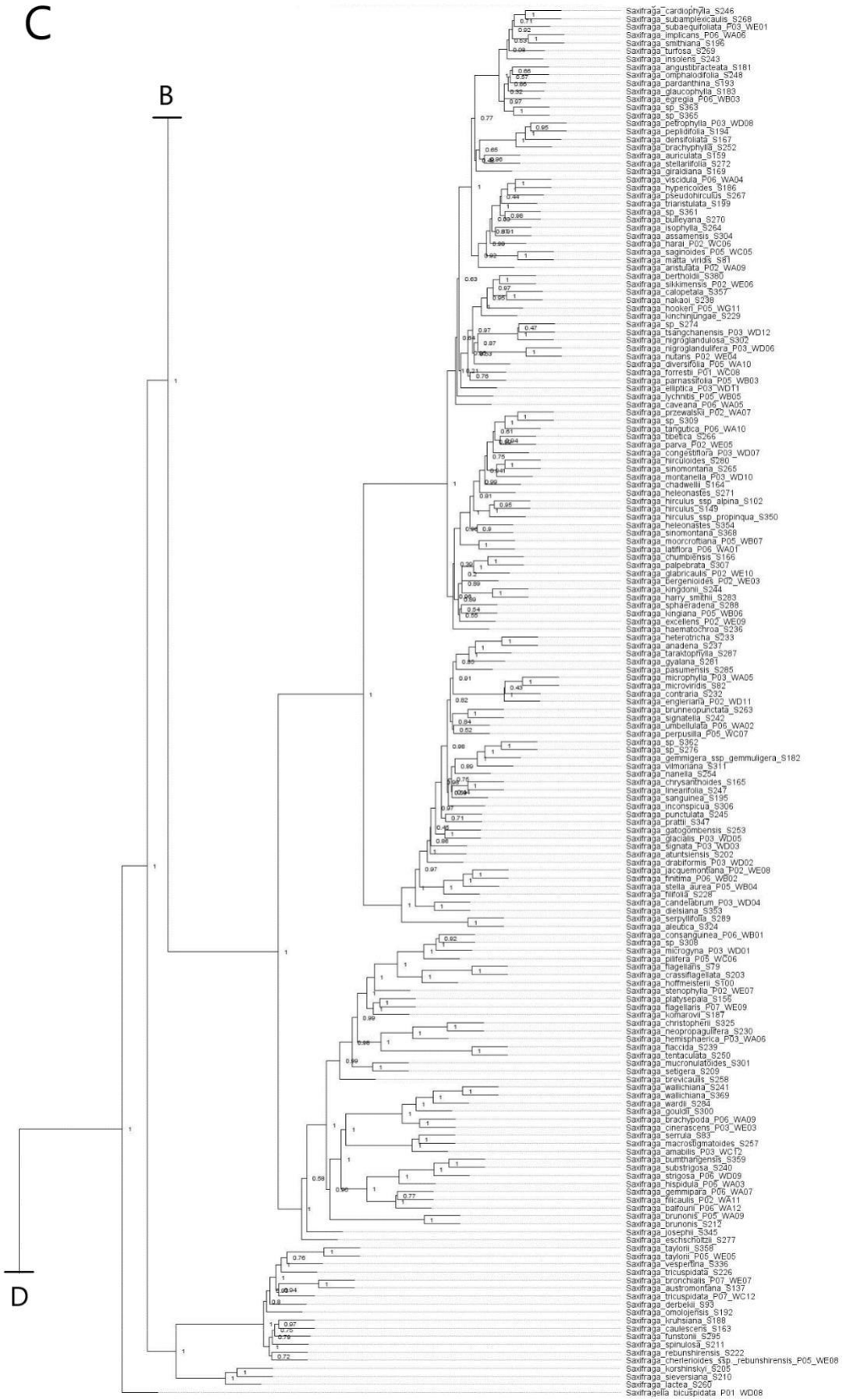
C
B
D
Saxifraga_cardiophylla_S246
Saxifraga_subamplexicaulis_S268
Saxifraga_subaequifoliata_P03_WE01
Saxifraga_implicans_P06_WA06
Saxifraga_smithiana_S196
Saxifraga_turfosa_S269
Saxifraga_insolens_S243
Saxifraga_angustibracteata_S181
Saxifraga_omphalodifolia_S248
Saxifraga_pardanthina_S193
Saxifraga_glaucophylla_S183
Saxifraga_egregia_P06_WB03
Saxifraga_sp_S363
Saxifraga_sp_S365
Saxifraga_petrophylla_P03_WD08
Saxifraga_pepidifolia_S194
Saxifraga_densifoliata_S167
Saxifraga_brachyphylla_S252
Saxifraga_auriculata_S159
Saxifraga_stellarifolia_S272
Saxifraga_giraldiana_S169
Saxifraga_viscidula_P06_WA04
Saxifraga_hypericoides_S186
Saxifraga_pseudohirculus_S267
Saxifraga_triaristulata_S199
Saxifraga_sp_S361
Saxifraga_bulleyana_S270
Saxifraga_isophylla_S264
Saxifraga_assamensis_S304
Saxifraga_harai_P02_WC06
Saxifraga_saginoides_P05_WC05
Saxifraga_matta_viridis_S81
Saxifraga_aristulata_P02_WA09
Saxifraga_bertholdii_S380
Saxifraga_sikkimensis_P02_WE06
Saxifraga_calopetala_S357
Saxifraga_nakaoi_S238
Saxifraga_hookeri_P05_WG11
Saxifraga_linchinjungae_S229
Saxifraga_sp_S274
Saxifraga_tsangchanensis_P03_WD12
Saxifraga_nigroglandulosa_S302
Saxifraga_nigroglandulifera_P03_WD06
Saxifraga_nutans_P02_WE04
Saxifraga_diversifolia_P05_WA10
Saxifraga_forrestii_P01_WC08
Saxifraga_parnassifolia_P05_WB03
Saxifraga_elliptica_P03_WD11
Saxifraga_lychnitis_P05_WB05
Saxifraga_caveana_P06_WA05
Saxifraga_przewalskii_P02_WA07
Saxifraga_sp_S309
Saxifraga_tangutica_P06_WA10
Saxifraga_tibetica_S266
Saxifraga_parva_P02_WE05
Saxifraga_congestiflora_P03_WD07
Saxifraga_hirculoides_S260
Saxifraga_sinomontana_S265
Saxifraga_montanella_P03_WD10
Saxifraga_chadwellii_S164
Saxifraga_heleonastes_S271
Saxifraga_hirculus_ssp_alpina_S102
Saxifraga_hirculus_S149
Saxifraga_hirculus_ssp_propinqua_S350
Saxifraga_heleonastes_S354
Saxifraga_sinomontana_S368
Saxifraga_moorcroftiana_P05_WB07
Saxifraga_latiflora_P06_WA01
Saxifraga_chumbiensis_S166
Saxifraga_palpebrata_S307
Saxifraga_glabricaulis_P02_WE10
Saxifraga_bergenioides_P02_WE03
Saxifraga_kingdonii_S244
Saxifraga_harry_smithii_S283
Saxifraga_sphaeradena_S289
Saxifraga_kingiana_P05_WB06
Saxifraga_excellens_P02_WE09
Saxifraga_haematochroa_S236
Saxifraga_heterotricha_S233
Saxifraga_anadena_S237
Saxifraga_taraktophylla_S287
Saxifraga_gyalana_S281
Saxifraga_pasumensis_S285
Saxifraga_microphylla_P03_WA05
Saxifraga_microviridis_S82
Saxifraga_contraria_S232
Saxifraga_engleriana_P02_WD11
Saxifraga_brunneopunctata_S263
Saxifraga_signatella_S242
Saxifraga_umbellulata_P06_WA02
Saxifraga_perpusilla_P06_WC07
Saxifraga_sp_S362
Saxifraga_sp_S276
Saxifraga_gemmigera_ssp_gemmuligera_S182
Saxifraga_vilmoriana_S311
Saxifraga_nanella_S254
Saxifraga_chrysanthoides_S165
Saxifraga_linearifolia_S247
Saxifraga_sanguinea_S195
Saxifraga_inconspicua_S306
Saxifraga_punctulata_S245
Saxifraga_prattii_S347
Saxifraga_gatogombensis_S263
Saxifraga_glacialis_P03_WD05
Saxifraga_signata_P03_WD03
Saxifraga_atuntsiensis_S202
Saxifraga_drabiformis_P03_WD02
Saxifraga_jacquemontiana_P02_WE08
Saxifraga_finitima_P06_WB02
Saxifraga_stella_aurea_P05_WB04
Saxifraga_filifolia_S228
Saxifraga_candelabrum_P03_WD04
Saxifraga_dielsiana_S353
Saxifraga_serpyllifolia_S289
Saxifraga_aleutica_S324
Saxifraga_consanguinea_P06_WB01
Saxifraga_sp_S308
Saxifraga_microgyna_P03_WD01
Saxifraga_pilifera_P05_WC06
Saxifraga_flagellaris_S79
Saxifraga_crassiflagellata_S203
Saxifraga_hoffmeisterii_ST00
Saxifraga_stenophylla_P02_WE07
Saxifraga_platysepala_S156
Saxifraga_flagellaris_P07_WE09
Saxifraga_komarovii_S187
Saxifraga_christophérii_S325
Saxifraga_neopropagulifera_S230
Saxifraga_hemisphaerica_P03_WA06
Saxifraga_flaccida_S239
Saxifraga_tentaculata_S250
Saxifraga_mucronulatoides_S301
Saxifraga_setigera_S209
Saxifraga_brevicaulis_S258
Saxifraga_wallichiana_S241
Saxifraga_wallichiana_S369
Saxifraga_wardii_S284
Saxifraga_gouldii_S300
Saxifraga_brachypoda_P06_WA09
Saxifraga_cinerascens_P03_WE03
Saxifraga_serrula_S83
Saxifraga_macrostigmatoides_S257
Saxifraga_amabilis_P03_WC12
Saxifraga_bumthangensis_S359
Saxifraga_substrigosa_S240
Saxifraga_strigosa_P06_WD09
Saxifraga_hispidula_P05_WA03
Saxifraga_gemmipara_P06_WA07
Saxifraga_filicaulis_P02_WA11
Saxifraga_balfourii_P06_WA12
Saxifraga_brunonis_P05_WA09
Saxifraga_brunonis_S212
Saxifraga_josephii_S345
Saxifraga_eschscholtzii_S277
Saxifraga_taylorii_S358
Saxifraga_taylorii_P05_WE05
Saxifraga_vespertina_S336
Saxifraga_tricuspidata_S226
Saxifraga_bronchialis_P07_WE07
Saxifraga_austromontana_S137
Saxifraga_tricuspidata_P07_WC12
Saxifraga_derbekii_S93
Saxifraga_omoloiensis_S192
Saxifraga_kruhsiana_S188
Saxifraga_caulescens_S163
Saxifraga_funstonii_S296
Saxifraga_spinulosa_S211
Saxifraga_rebunshirensis_S222
Saxifraga_cherlerioides_ssp._rebunshirensis_P05_WE08
Saxifraga_korshinskyi_S205
Saxifraga_sieversiana_S210
Saxifraga_lactea_S260
Saxifragella_bicuspidata_P01_WD08

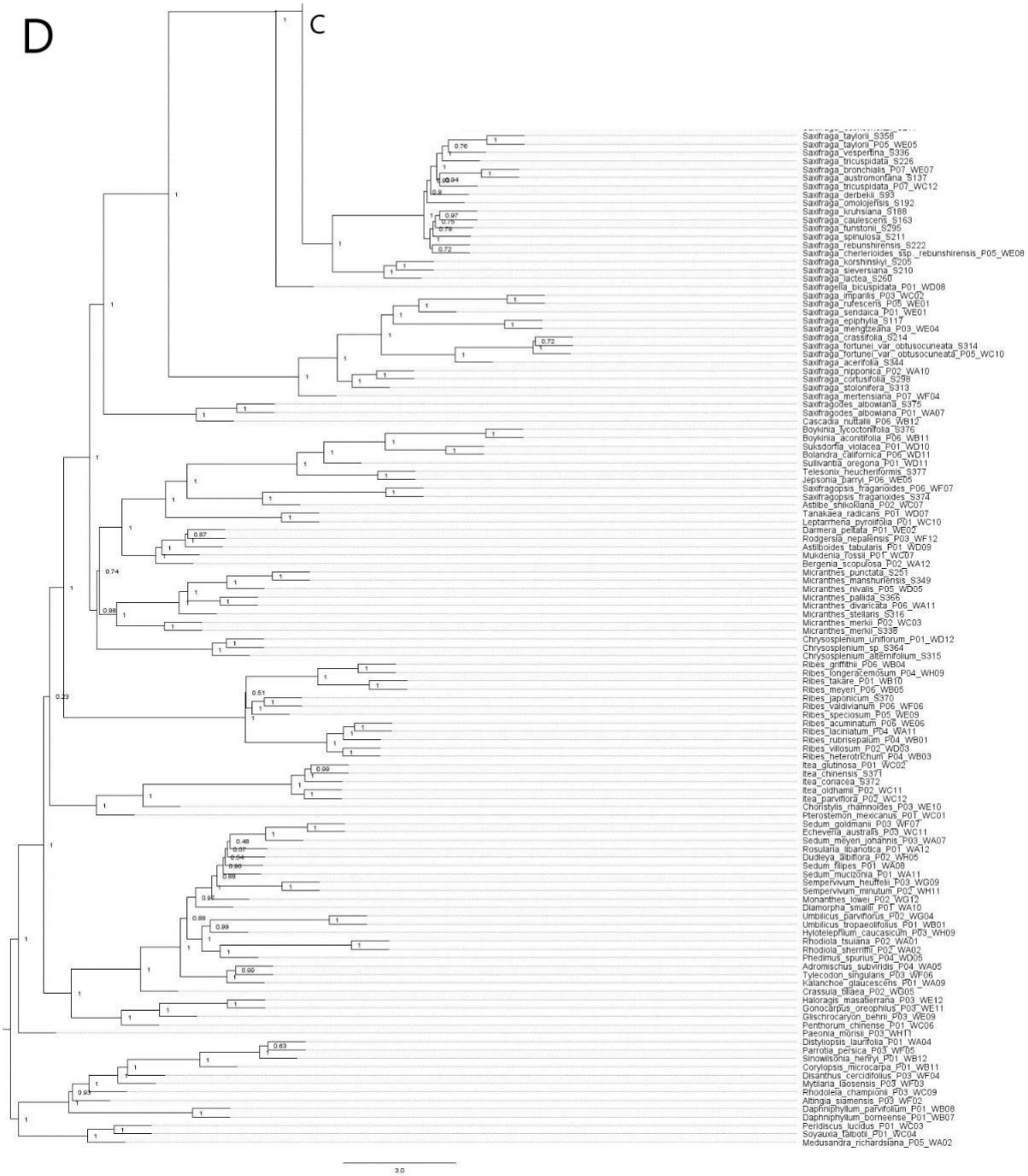

Appendix 3.1: Species tree generated from 329 supercontig nDNA gene trees. Branch labels show ASTRAL local posterior probability (LPP) value. Branch lengths are based on coalescent units and terminal branches are dimensionless. Connections between figure panels A,B,C,D are shown within figures.

APPENDIX 4.1

Residuals:

Min	1Q	Median	3Q	Max
- 11.5709	-1.8118	-0.5113	1.3674	15.8417

Coefficients:

	Estimate	Std. Error	t value	Pr(>|t|)	
(Intercept)	-9.625727	1.750069	-5.500	4.12e-08	***
Dat$Tair	1.464871	0.073446	19.945	< 2e-16	***
Dat$SpecIDBURS	3.039545	2.517250	1.207	0.227342	
Dat$SpecIDCALL	0.780629	2.485679	0.314	0.753505	
Dat$SpecIDCANA	8.001389	2.612089	3.063	0.002210	**
Dat$SpecIDCATA	10.727707	2.855736	3.757	0.000176	***
Dat$SpecIDCAUC	5.022152	2.603235	1.929	0.053803	.
Dat$SpecIDCEBE	1.149168	3.184074	0.361	0.718192	
Dat$SpecIDCOCH	13.187046	2.721906	4.845	1.33e-06	***
Dat$SpecIDCOTY	2.355590	2.287048	1.030	0.303109	
Dat$SpecIDCUNE	-7.979267	2.983836	-2.674	0.007533	**
Dat$SpecIDCYMB	4.887326	2.117108	2.308	0.021041	*
Dat$SpecIDDIAP	-7.429868	2.992110	-2.483	0.013078	*
Dat$SpecIDEXCA	5.802208	2.456704	2.362	0.018252	*
Dat$SpecIDFERD	-0.725894	4.184149	-0.173	0.862281	
Dat$SpecIDFLAG	3.946390	3.120087	1.265	0.206032	
Dat$SpecIDFOOB	1.125140	3.256040	0.346	0.729702	
Dat$SpecIDFRAG	0.076180	4.211780	0.018	0.985570	
Dat$SpecIDGEOR	2.339396	2.348283	0.996	0.319228	
Dat$SpecIDGERA	3.074835	2.644228	1.163	0.244986	
Dat$SpecIDGRAN	1.993207	2.830624	0.704	0.481390	
Dat$SpecIDHORH	6.700868	2.556830	2.621	0.008818	**
Dat$SpecIDLATE	-2.098253	2.555986	-0.821	0.411760	
Dat$SpecIDLILA	-0.908142	2.985480	-0.304	0.761008	
Dat$SpecIDMADE	-19.585898	4.461577	-4.390	1.17e-05	***
Dat$SpecIDMAPI	0.477781	2.647919	0.180	0.856822	
Dat$SpecIDMONC	3.128774	2.413738	1.296	0.194996	
Dat$SpecIDOPPO	-0.210741	2.687018	-0.078	0.937492	
Dat$SpecIDPACA	7.228619	2.318276	3.118	0.001838	**
Dat$SpecIDPANI	1.300129	5.020806	0.259	0.795693	
Dat$SpecIDPEDE	-5.607182	2.164413	-2.591	0.009628	**
Dat$SpecIDPEPR	-3.180442	2.475898	-1.285	0.199047	
Dat$SpecIDSANC	-1.134358	2.995654	-0.379	0.704962	
Dat$SpecIDSCAR	3.667811	2.631182	1.394	0.163430	
Dat$SpecIDSCLE	11.053622	2.667494	4.144	3.51e-05	***
Dat$SpecIDSEMP	0.067594	2.878925	0.023	0.981270	
Dat$SpecIDSPAT	1.891156	2.932260	0.645	0.519011	
Dat$SpecIDSPRU	7.645797	2.598475	2.942	0.003282	**
Dat$SpecIDSTEL	0.281520	2.817834	0.100	0.920425	
Dat$SpecIDSTOL	0.617113	3.181774	0.194	0.846226	
Dat$SpecIDSTRI	-2.890143	2.805239	-1.030	0.302970	
Dat$SpecIDTRID	7.650318	2.767035	2.765	0.005731	**
Dat$SpecIDWEND	5.137581	2.470514	2.080	0.037653	*
Dat$Tair:Dat$SpecIDBURS	-0.074699	0.099620	-0.750	0.453407	
Dat$Tair:Dat$SpecIDCALL	-0.017416	0.106120	-0.164	0.869651	
Dat$Tair:Dat$SpecIDCANA	-0.290561	0.103434	-2.809	0.005000	**
Dat$Tair:Dat$SpecIDCATA	-0.379942	0.113502	-3.347	0.000826	***
Dat$Tair:Dat$SpecIDCAUC	-0.225654	0.108225	-2.085	0.037151	*
Dat$Tair:Dat$SpecIDCEBE	-0.212159	0.112258	-1.890	0.058866	.
Dat$Tair:Dat$SpecIDCOCH	-0.467769	0.108371	-4.316	1.64e-05	***
Dat$Tair:Dat$SpecIDCOTY	-0.094934	0.094578	-1.004	0.315579	
Dat$Tair:Dat$SpecIDCUNE	0.496705	0.128631	3.861	0.000115	***

```
Dat$Tair:Dat$SpecIDCYMB -0.141574 0.087792 -1.613 0.106939
Dat$Tair:Dat$SpecIDDIAP 0.427581 0.127589 3.351 0.000815 ***
Dat$Tair:Dat$SpecIDEXCA -0.188796 0.097401 -1.938 0.052678 .
Dat$Tair:Dat$SpecIDFERD   0.264675   0.189935   1.394 0.163574
Dat$Tair:Dat$SpecIDFLAG  -0.192072   0.129035  -1.489 0.136721
Dat$Tair:Dat$SpecIDFOOB  -0.057095   0.125779  -0.454 0.649912
Dat$Tair:Dat$SpecIDFRAG  -0.140846   0.141608  -0.995 0.320005
Dat$Tair:Dat$SpecIDGEOR  -0.068951   0.099129  -0.696 0.486753
Dat$Tair:Dat$SpecIDGERA  -0.098316   0.106526  -0.923 0.356122
Dat$Tair:Dat$SpecIDGRAN   0.023611   0.118452   0.199 0.842020
Dat$Tair:Dat$SpecIDHORH  -0.316870   0.106559  -2.974 0.002967 **
Dat$Tair:Dat$SpecIDLATE   0.144218   0.106068   1.360 0.174037
Dat$Tair:Dat$SpecIDLILA   0.091673   0.127558   0.719 0.472398
Dat$Tair:Dat$SpecIDMADE 0.923133 0.186724 4.944 8.09e-07 ***
Dat$Tair:Dat$SpecIDMAPI 0.003210 0.107090 0.030 0.976089
Dat$Tair:Dat$SpecIDMONC -0.083750 0.098420 -0.851 0.394868
Dat$Tair:Dat$SpecIDOPPO 0.042678 0.110701 0.386 0.699875
Dat$Tair:Dat$SpecIDPACA -0.287372 0.095535 -3.008 0.002652 **
Dat$Tair:Dat$SpecIDPANI 0.091863 0.232532 0.395 0.692830
Dat$Tair:Dat$SpecIDPEDE 0.314279 0.093354 3.367 0.000771 ***
Dat$Tair:Dat$SpecIDPEPR 0.254715 0.105528 2.414 0.015852 *
Dat$Tair:Dat$SpecIDSANC 0.078464 0.116554 0.673 0.500876
Dat$Tair:Dat$SpecIDSCAR -0.120560 0.105482 -1.143 0.253158
Dat$Tair:Dat$SpecIDSCLE -0.480593 0.102672 -4.681 2.99e-06 ***
Dat$Tair:Dat$SpecIDSEMP 0.039639 0.117089 0.339 0.734986
Dat$Tair:Dat$SpecIDSPAT -0.064593 0.125457 -0.515 0.606687
Dat$Tair:Dat$SpecIDSPRU -0.288501 0.099832 -2.890 0.003882 **
Dat$Tair:Dat$SpecIDSTEL 0.008628 0.110941 0.078 0.938014
Dat$Tair:Dat$SpecIDSTOL -0.006691 0.131361 -0.051 0.959379
Dat$Tair:Dat$SpecIDSTRI 0.244232 0.120641 2.024 0.043014 *
Dat$Tair:Dat$SpecIDTRID -0.210669 0.124236 -1.696 0.090046 .
Dat$Tair:Dat$SpecIDWEND -0.166047 0.100632 -1.650 0.099041 . --
-

Signif. codes:  0 '***' 0.001 '**' 0.01 '*' 0.05 '.' 0.1 ' ' 1

Residual standard error: 3.006 on 2931 degrees of
  freedom (1 observation deleted due to missingness)
Multiple R-squared:  0.8326,  Adjusted R-squared:  0.8279
F-statistic: 175.7 on 83 and 2931 DF,  p-value: < 2.2e-16
```

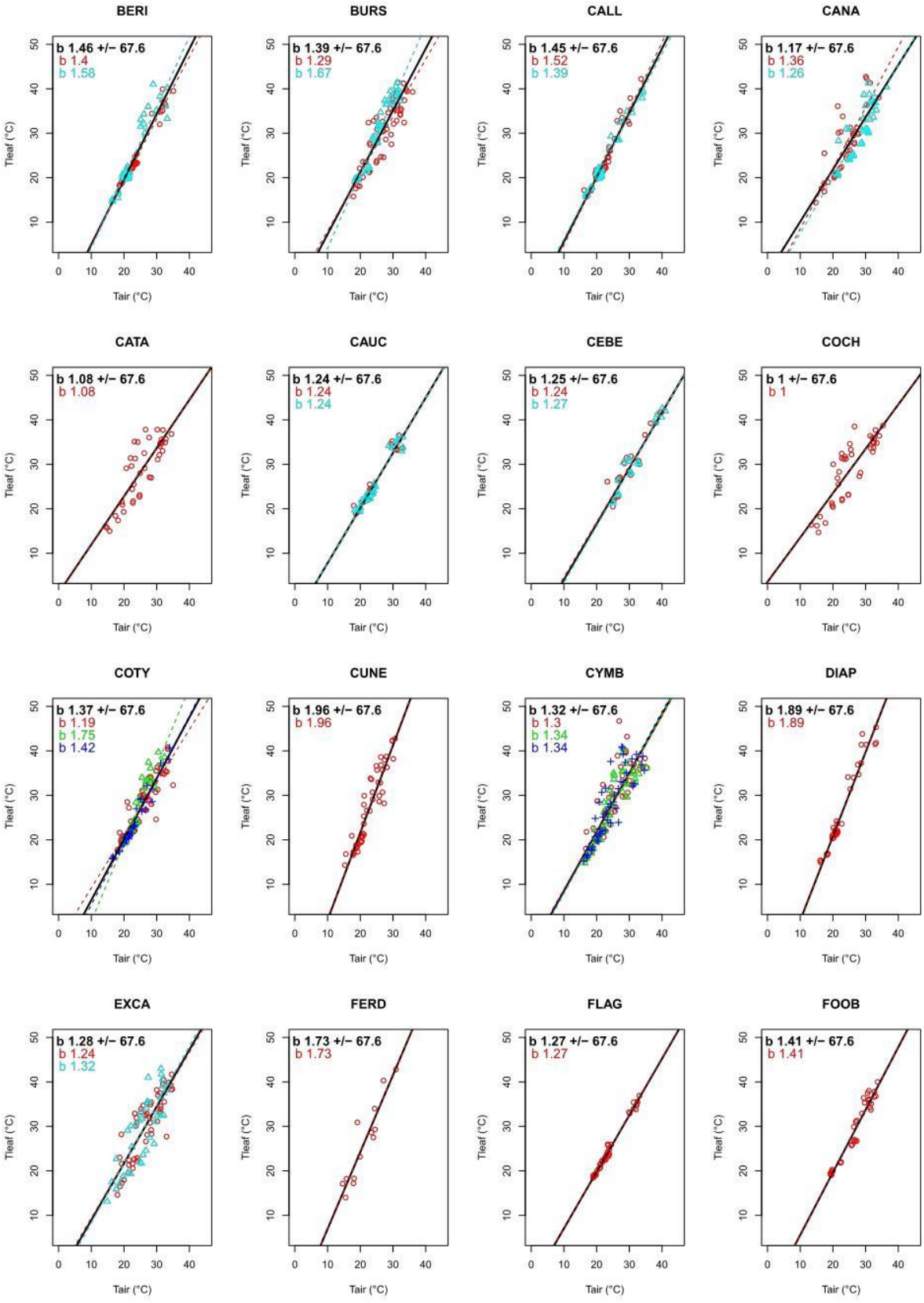
BERI
b 1.46 +/− 67.6
b 1.4
b 1.58
BURS
b 1.39 +/− 67.6
b 1.29
b 1.67
CALL
b 1.45 +/− 67.6
b 1.52
b 1.39
CANA
b 1.17 +/− 67.6
b 1.36
b 1.26
CATA
b 1.08 +/− 67.6
b 1.08
CAUC
b 1.24 +/− 67.6
b 1.24
b 1.24
CEBE
b 1.25 +/− 67.6
b 1.24
b 1.27
COCH
b 1 +/− 67.6
b 1
COTY
b 1.37 +/− 67.6
b 1.19
b 1.75
b 1.42
CUNE
b 1.96 +/− 67.6
b 1.96
CYMB
b 1.32 +/− 67.6
b 1.3
b 1.34
b 1.34
DIAP
b 1.89 +/− 67.6
b 1.89
EXCA
b 1.28 +/− 67.6
b 1.24
b 1.32
FERD
b 1.73 +/− 67.6
b 1.73
FLAG
b 1.27 +/− 67.6
b 1.27
FOOB
b 1.41 +/− 67.6
b 1.41
Tleaf (°C)
Tair (°C)

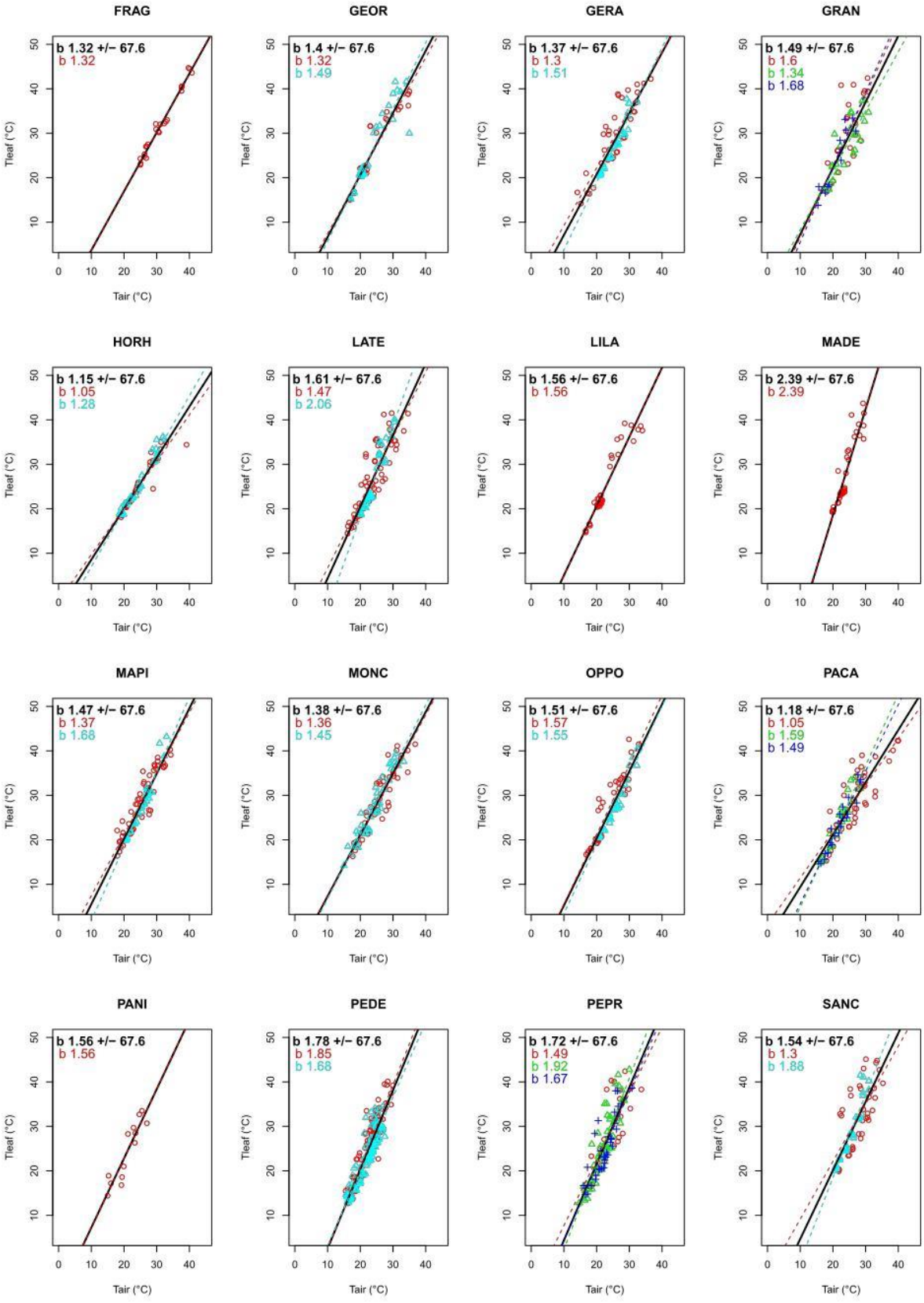
FRAG
b 1.32 +/− 67.6
b 1.32
GEOR
b 1.4 +/− 67.6
b 1.32
b 1.49
GERA
b 1.37 +/− 67.6
b 1.3
b 1.51
GRAN
b 1.49 +/− 67.6
b 1.6
b 1.34
b 1.68
HORH
b 1.15 +/− 67.6
b 1.05
b 1.28
LATE
b 1.61 +/− 67.6
b 1.47
b 2.06
LILA
b 1.56 +/− 67.6
b 1.56
MADE
b 2.39 +/− 67.6
b 2.39
MAPI
b 1.47 +/− 67.6
b 1.37
b 1.68
MONC
b 1.38 +/− 67.6
b 1.36
b 1.45
OPPO
b 1.51 +/− 67.6
b 1.57
b 1.55
PACA
b 1.18 +/− 67.6
b 1.05
b 1.59
b 1.49
PANI
b 1.56 +/− 67.6
b 1.56
PEDE
b 1.78 +/− 67.6
b 1.85
b 1.68
PEPR
b 1.72 +/− 67.6
b 1.49
b 1.92
b 1.67
SANC
b 1.54 +/− 67.6
b 1.3
b 1.88
Tleaf (°C)
Tair (°C)

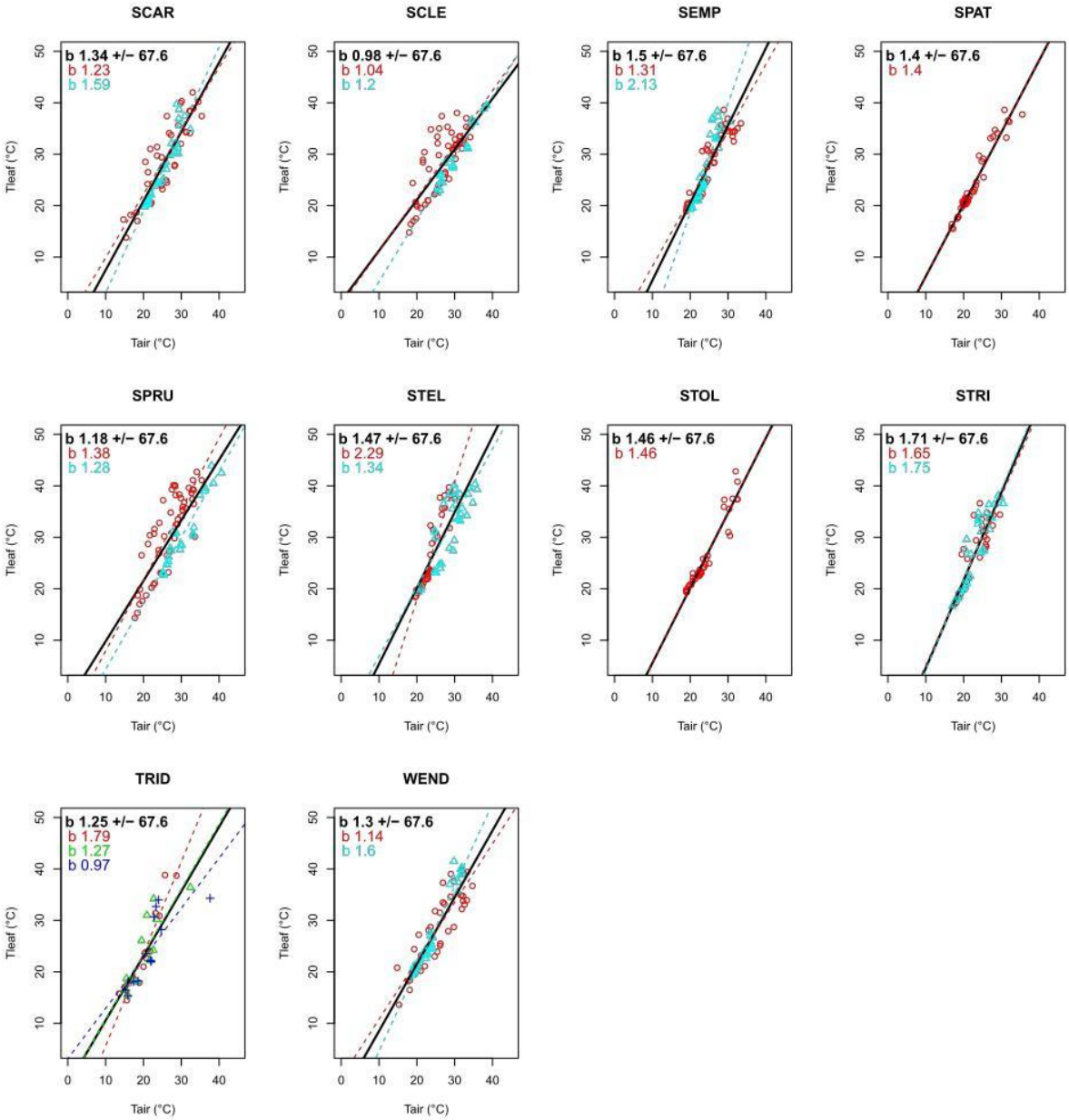

Appendix 4.1: Slope of T_{LEAF} (°C) measured by T_{AIR} (°C). Black point and line colours depict entire dataset for a taxon, while other colours depict individual plants. Inset numbers show slope values (b). Includes species removed due to being marked as unfit due to leaf deterioration.

APPENDIX 4.2

Residuals:

Min	1Q	Median	3Q	Max
- 13.3340	-0.8579	-0.1043	0.7301	12.2335

Coefficients:

	Estimate	Std. Error	t value	Pr(>|t|)	
(Intercept)	-1.7633781	0.3299483	-5.344	9.77e-08	***
Dat$RAD	0.0094882	0.0007887	12.030	< 2e-16	***
Dat$SpecIDBURS	0.9842088	0.4811271	2.046	0.040882	*
Dat$SpecIDCALL	0.7026355	0.4568887	1.538	0.124188	
Dat$SpecIDCANA	1.1125571	0.4676119	2.379	0.017412	*
Dat$SpecIDCATA	0.7268880	0.6343918	1.146	0.251970	
Dat$SpecIDCAUC	1.2110521	0.4873755	2.485	0.013016	*
Dat$SpecIDCEBE	-0.7023267	0.5018817	-1.399	0.161803	
Dat$SpecIDCOCH	0.9816204	0.6427992	1.527	0.126843	
Dat$SpecIDCOTY	1.0093611	0.4126005	2.446	0.014490	*
Dat$SpecIDCUNE	1.6011339	0.5020582	3.189	0.001442	**
Dat$SpecIDCYMB	1.3557960	0.4023210	3.370	0.000762	***
Dat$SpecIDDIAP	-0.2279360	0.5835025	-0.391	0.696096	
Dat$SpecIDEXCA	0.3810144	0.4758858	0.801	0.423404	
Dat$SpecIDFERD	1.7570023	0.8582405	2.047	0.040726	*
Dat$SpecIDFLAG	1.0525484	0.5993956	1.756	0.079190	.
Dat$SpecIDFOOB	1.0408374	0.6076599	1.713	0.086844	.
Dat$SpecIDFRAG	0.6994843	0.6212115	1.126	0.260258	
Dat$SpecIDGEOR	0.6445310	0.4717588	1.366	0.171972	
Dat$SpecIDGERA	1.2849132	0.4682492	2.744	0.006105	**
Dat$SpecIDGRAN	0.8316752	0.5141334	1.618	0.105851	
Dat$SpecIDHORH	0.9815294	0.4888756	2.008	0.044764	*
Dat$SpecIDLATE	0.5117363	0.4374019	1.170	0.242118	
Dat$SpecIDLILA	0.1862551	0.5892082	0.316	0.751941	
Dat$SpecIDMADE	0.7115285	0.5602347	1.270	0.204166	
Dat$SpecIDMAPI	1.5278307	0.4461544	3.424	0.000625	***
Dat$SpecIDMONC	1.2143145	0.4680215	2.595	0.009518	**
Dat$SpecIDOPPO	1.3904029	0.4517197	3.078	0.002103	**
Dat$SpecIDPACA	0.9454823	0.4383553	2.157	0.031096	*
Dat$SpecIDPANI	1.2756293	0.8975709	1.421	0.155365	
Dat$SpecIDPEDE	-0.0327073	0.3799554	-0.086	0.931407	
Dat$SpecIDPEPR	0.8862808	0.4256707	2.082	0.037422	*
Dat$SpecIDSANC	1.0464266	0.4630581	2.260	0.023906	*
Dat$SpecIDSCAR	1.3204273	0.4647229	2.841	0.004524	**
Dat$SpecIDSCLE	-0.4188655	0.4822691	-0.869	0.385175	
Dat$SpecIDSEMP	1.5037215	0.4621949	3.253	0.001153	**
Dat$SpecIDSPAT	0.8169899	0.5464854	1.495	0.135025	
Dat$SpecIDSPRU	0.3199682	0.4823184	0.663	0.507129	
Dat$SpecIDSTEL	0.3683878	0.4695845	0.784	0.432812	
Dat$SpecIDSTOL	0.5612447	0.6039222	0.929	0.352793	
Dat$SpecIDSTRI	1.9576325	0.4488703	4.361	1.34e-05	***
Dat$SpecIDTRID	1.6868205	0.5616556	3.003	0.002693	**
Dat$SpecIDWEND	1.1905615	0.4761460	2.500	0.012459	*
Dat$RAD:Dat$SpecIDBURS	-0.0004379	0.0009779	-0.448	0.654349	
Dat$RAD:Dat$SpecIDCALL	-0.0021775	0.0010876	-2.002	0.045367	*
Dat$RAD:Dat$SpecIDCANA	0.0003946	0.0010378	0.380	0.703817	
Dat$RAD:Dat$SpecIDCATA	-0.0013581	0.0011633	-1.167	0.243153	
Dat$RAD:Dat$SpecIDCAUC	-0.0042298	0.0012036	-3.514	0.000447	***
Dat$RAD:Dat$SpecIDCEBE	-0.0027101	0.0012555	-2.159	0.030961	*
Dat$RAD:Dat$SpecIDCOCH	-0.0016908	0.0011552	-1.464	0.143393	
Dat$RAD:Dat$SpecIDCOTY	-0.0033237	0.0009142	-3.636	0.000282	***
Dat$RAD:Dat$SpecIDCUNE	0.0009413	0.0010331	0.911	0.362312	

```
Dat$RAD:Dat$SpecIDCYMB -0.0006673 0.0009011 -0.741 0.459002
Dat$RAD:Dat$SpecIDDIAP 0.0056668 0.0013272 4.270 2.02e-05 ***
Dat$RAD:Dat$SpecIDEXCA 0.0009282 0.0009865 0.941 0.346843
Dat$RAD:Dat$SpecIDFERD 0.0020133 0.0015476 1.301 0.193380
Dat$RAD:Dat$SpecIDFLAG -0.0047590 0.0014399 -3.305 0.000961 ***
Dat$RAD:Dat$SpecIDFOOB -0.0037333 0.0010990 -3.397 0.000691 ***
Dat$RAD:Dat$SpecIDFRAG -0.0035813 0.0015046 -2.380 0.017369 *
Dat$RAD:Dat$SpecIDGEOR -0.0011501 0.0010812 -1.064 0.287530
Dat$RAD:Dat$SpecIDGERA -0.0006765 0.0010409 -0.650 0.515816
Dat$RAD:Dat$SpecIDGRAN 0.0013293 0.0010516 1.264 0.206311
Dat$RAD:Dat$SpecIDHORH -0.0053582 0.0011753 -4.559 5.35e-06 ***
Dat$RAD:Dat$SpecIDLATE 0.0011214 0.0009592 1.169 0.242462
Dat$RAD:Dat$SpecIDLILA 0.0009185 0.0013324 0.689 0.490647
Dat$RAD:Dat$SpecIDMADE 0.0022040 0.0011349 1.942 0.052230 .
Dat$RAD:Dat$SpecIDMAPI -0.0017963 0.0009871 -1.820 0.068912 .
Dat$RAD:Dat$SpecIDMONC -0.0020083 0.0009675 -2.076 0.038009 *
Dat$RAD:Dat$SpecIDOPPO -0.0017947 0.0009793 -1.833 0.066964 .
Dat$RAD:Dat$SpecIDPACA -0.0013511 0.0009926 -1.361 0.173560
Dat$RAD:Dat$SpecIDPANI -0.0022600 0.0014471 -1.562 0.118464
Dat$RAD:Dat$SpecIDPEDE 0.0021915 0.0009125 2.402 0.016388 *
Dat$RAD:Dat$SpecIDPEPR 0.0019795 0.0009371 2.112 0.034735 *
Dat$RAD:Dat$SpecIDSANC 0.0033607 0.0010453 3.215 0.001319 **
Dat$RAD:Dat$SpecIDSCAR -0.0003615 0.0010331 -0.350 0.726397
Dat$RAD:Dat$SpecIDSCLE -0.0019552 0.0010226 -1.912 0.055985 .
Dat$RAD:Dat$SpecIDSEMP -0.0018701 0.0009793 -1.910 0.056277 .
Dat$RAD:Dat$SpecIDSPAT -0.0019978 0.0013389 -1.492 0.135770
Dat$RAD:Dat$SpecIDSPRU 0.0012265 0.0010365 1.183 0.236773
Dat$RAD:Dat$SpecIDSTEL 0.0018365 0.0010138 1.812 0.070151 .
Dat$RAD:Dat$SpecIDSTOL 0.0013116 0.0015848 0.828 0.407969
Dat$RAD:Dat$SpecIDSTRI -0.0006927 0.0009707 -0.714 0.475501
Dat$RAD:Dat$SpecIDTRID -0.0015697 0.0011126 -1.411 0.158367
Dat$RAD:Dat$SpecIDWEND -0.0003497 0.0010474 -0.334 0.738533 --
-
Signif. codes:  0 ‘***’ 0.001 ‘**’ 0.01 ‘*’ 0.05 ‘.’ 0.1 ‘ ’ 1

 Residual standard error: 1.905 on 2931 degrees of
   freedom (1 observation deleted due to missingness)
Multiple R-squared:  0.7439,  Adjusted R-squared:  0.7366
F-statistic: 102.6 on 83 and 2931 DF,  p-value: < 2.2e-16
```

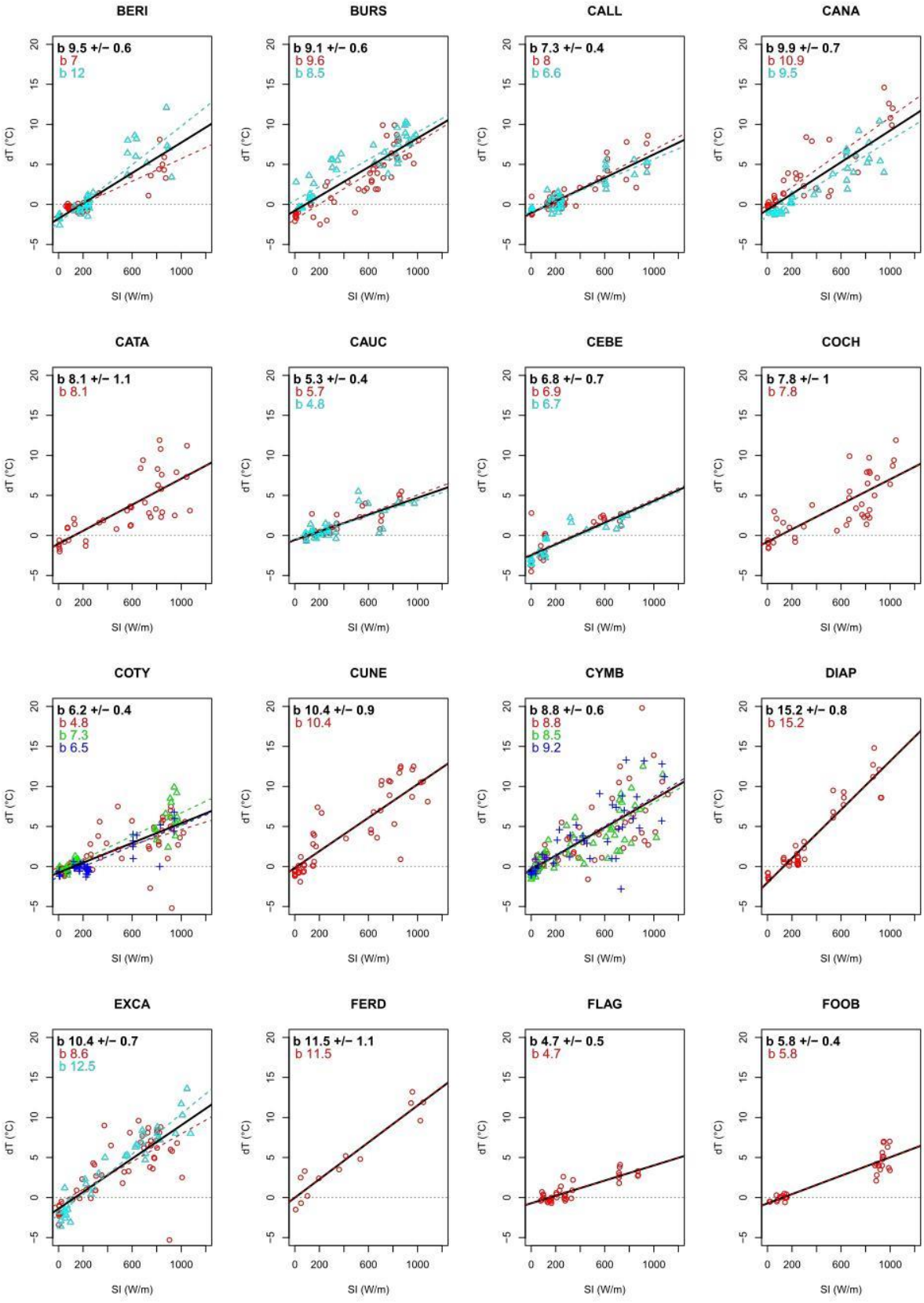
BERI
b 9.5 +/− 0.6
b 7
b 12
BURS
b 9.1 +/− 0.6
b 9.6
b 8.5
CALL
b 7.3 +/− 0.4
b 8
b 6.6
CANA
b 9.9 +/− 0.7
b 10.9
b 9.5
CATA
b 8.1 +/− 1.1
b 8.1
CAUC
b 5.3 +/− 0.4
b 5.7
b 4.8
CEBE
b 6.8 +/− 0.7
b 6.9
b 6.7
COCH
b 7.8 +/− 1
b 7.8
COTY
b 6.2 +/− 0.4
b 4.8
b 7.3
b 6.5
CUNE
b 10.4 +/− 0.9
b 10.4
CYMB
b 8.8 +/− 0.6
b 8.8
b 8.5
b 9.2
DIAP
b 15.2 +/− 0.8
b 15.2
EXCA
b 10.4 +/− 0.7
b 8.6
b 12.5
FERD
b 11.5 +/− 1.1
b 11.5
FLAG
b 4.7 +/− 0.5
b 4.7
FOOB
b 5.8 +/− 0.4
b 5.8
dT (°C)
SI (W/m)

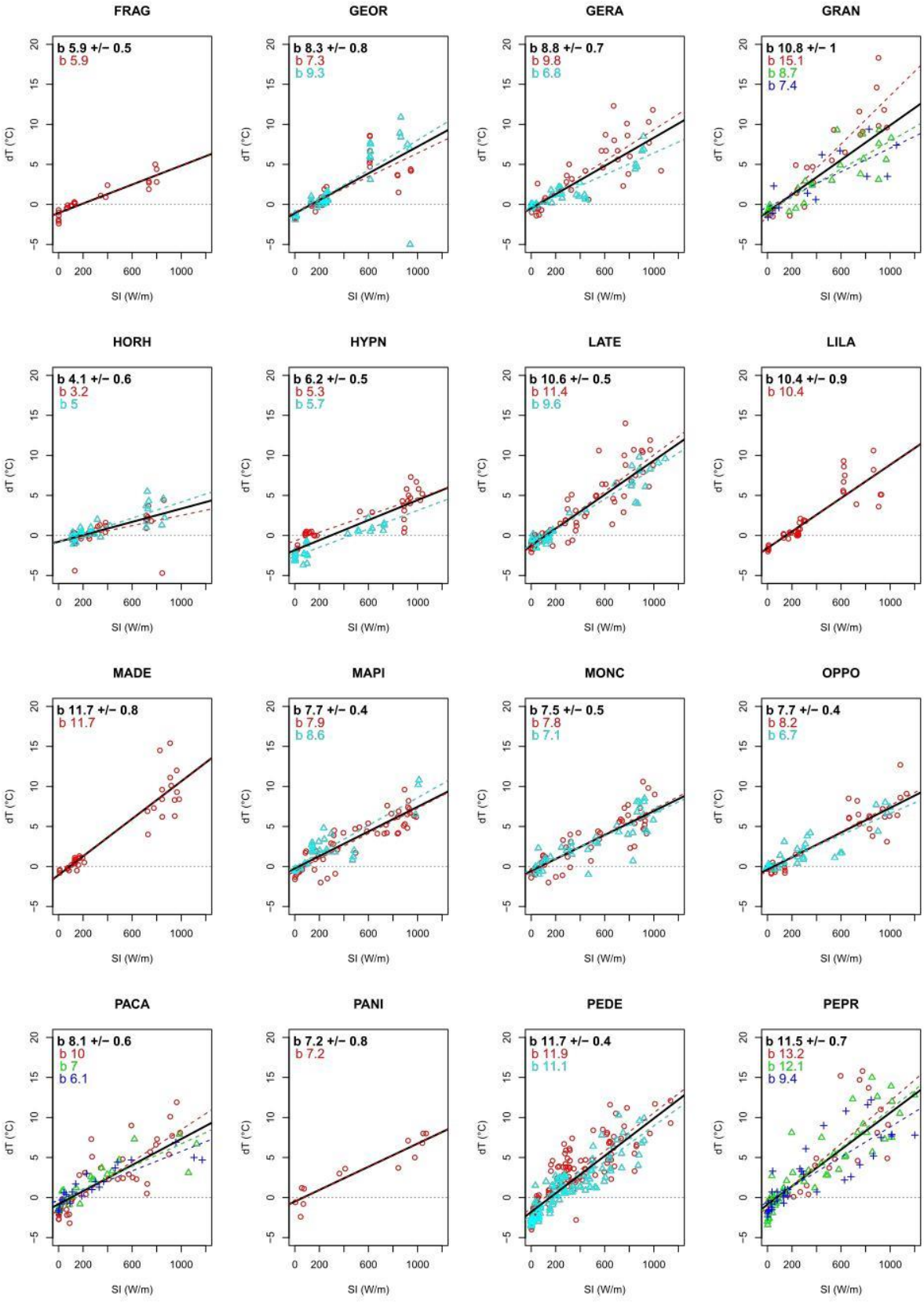
FRAG
b 5.9 +/− 0.5
b 5.9
GEOR
b 8.3 +/− 0.8
b 7.3
b 9.3
GERA
b 8.8 +/− 0.7
b 9.8
b 6.8
GRAN
b 10.8 +/− 1
b 15.1
b 8.7
b 7.4
HORH
b 4.1 +/− 0.6
b 3.2
b 5
HYPN
b 6.2 +/− 0.5
b 5.3
b 5.7
LATE
b 10.6 +/− 0.5
b 11.4
b 9.6
LILA
b 10.4 +/− 0.9
b 10.4
MADE
b 11.7 +/− 0.8
b 11.7
MAPI
b 7.7 +/− 0.4
b 7.9
b 8.6
MONC
b 7.5 +/− 0.5
b 7.8
b 7.1
OPPO
b 7.7 +/− 0.4
b 8.2
b 6.7
PACA
b 8.1 +/− 0.6
b 10
b 7
b 6.1
PANI
b 7.2 +/− 0.8
b 7.2
PEDE
b 11.7 +/− 0.4
b 11.9
b 11.1
PEPR
b 11.5 +/− 0.7
b 13.2
b 12.1
b 9.4
dT (°C)
SI (W/m)

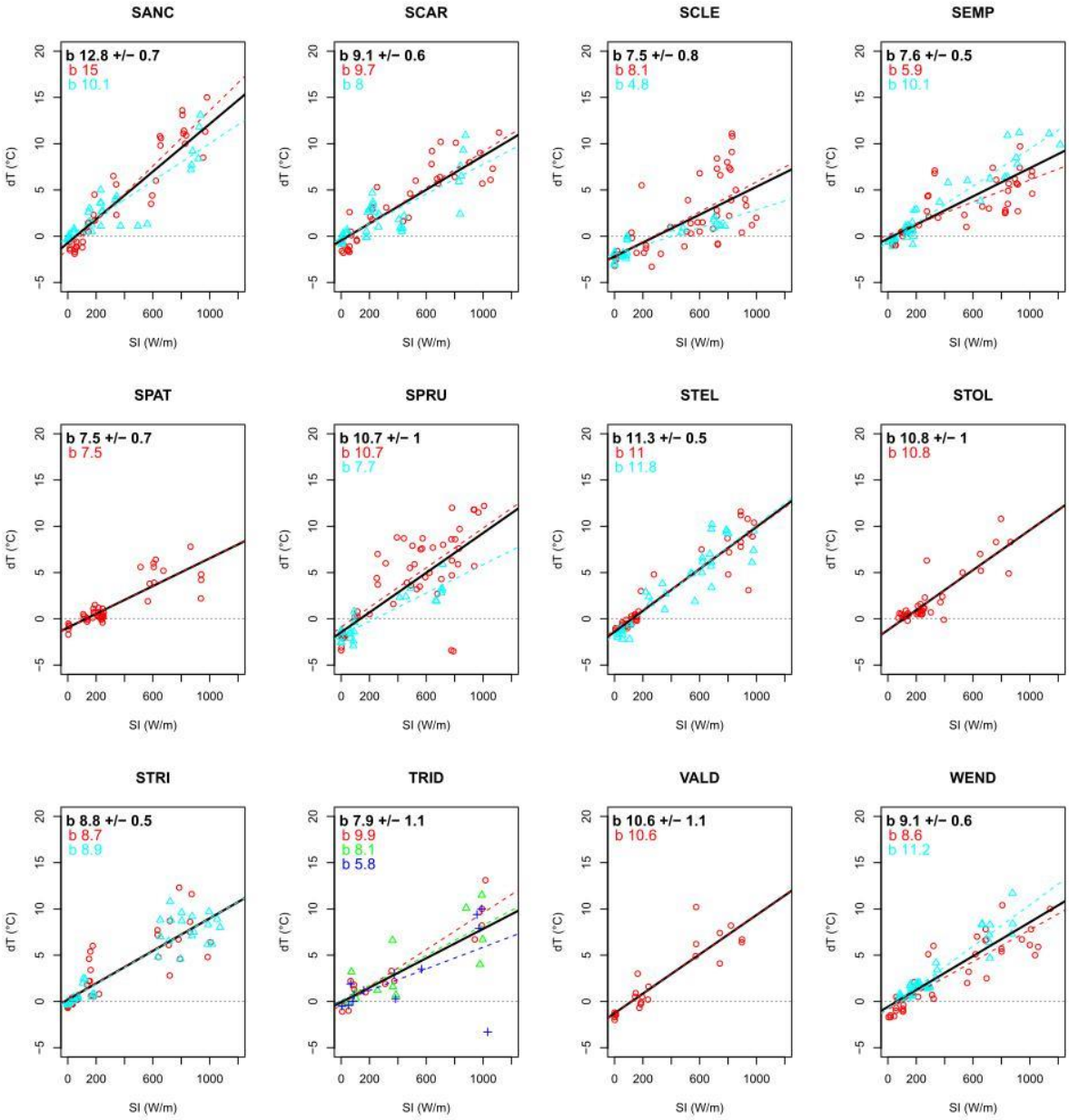

Appendix 4.2: Slope of ΔT (°C) measured by SI (W m^{-2}). Black point and line colours depict entire dataset for a taxon, while other colours depict individual plants. Inset numbers show slope values (b). Includes species removed due to being marked as unfit due to leaf deterioration.

APPENDIX 4.3

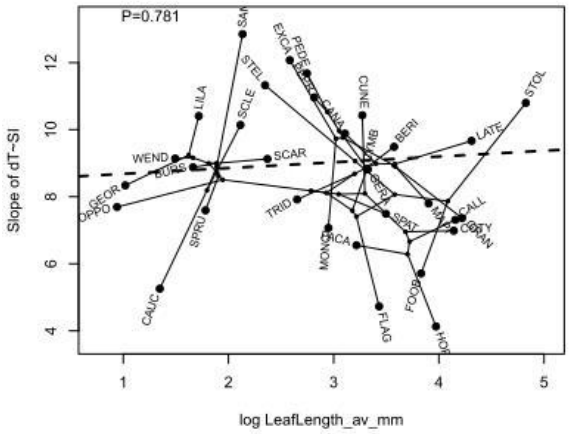
P=0.781
Slope of dT~SI
log LeafLength_av_mm

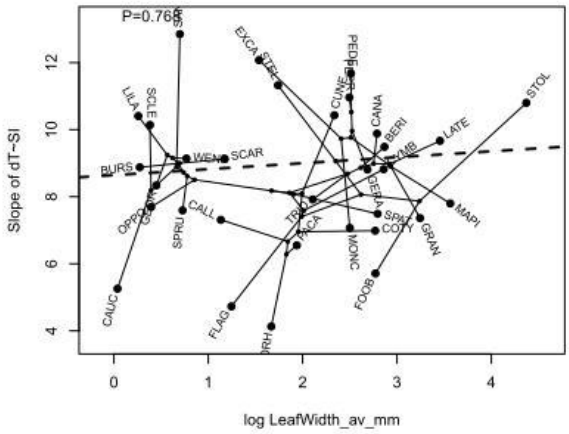
P=0.768
Slope of dT~SI
log LeafWidth_av_mm

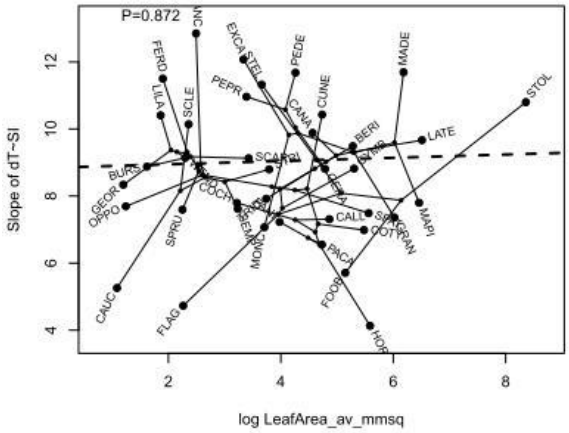
P=0.872
Slope of dT~SI
log LeafArea_av_mmsq

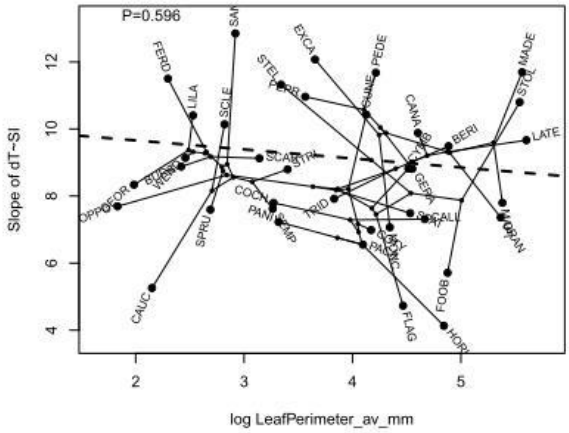
P=0.596
Slope of dT~SI
log LeafPerimeter_av_mm

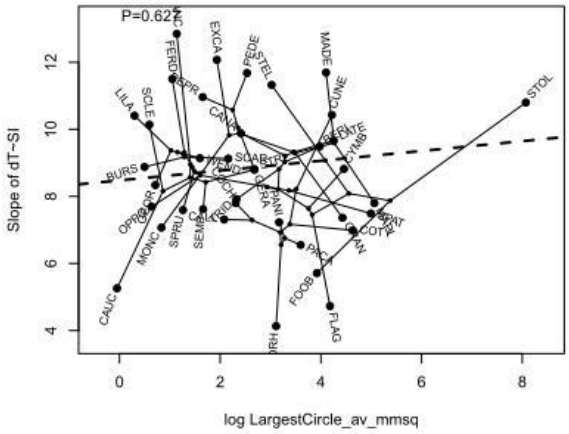
P=0.627
Slope of dT~SI
log LargestCircle_av_mmsq

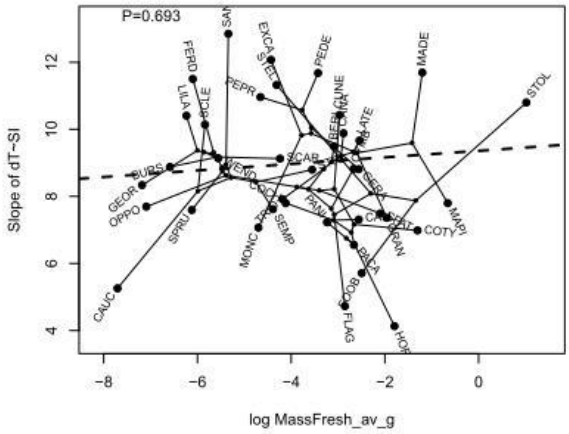
P=0.693
Slope of dT~SI
log MassFresh_av_g

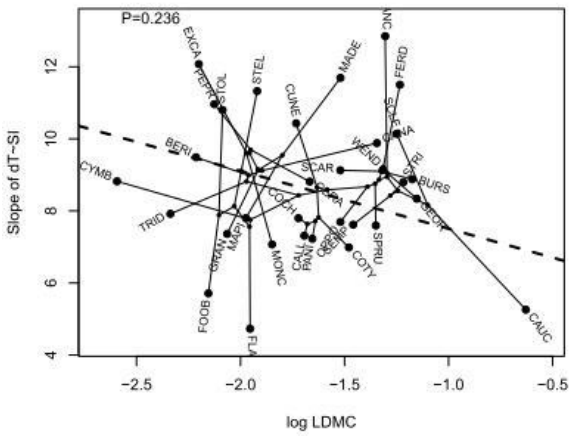
P=0.236
Slope of dT~SI
log LDMC

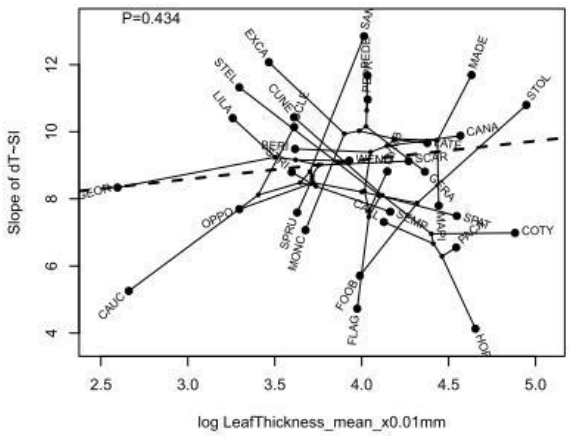
P=0.434
Slope of dT~SI
log LeafThickness_mean_x0.01mm

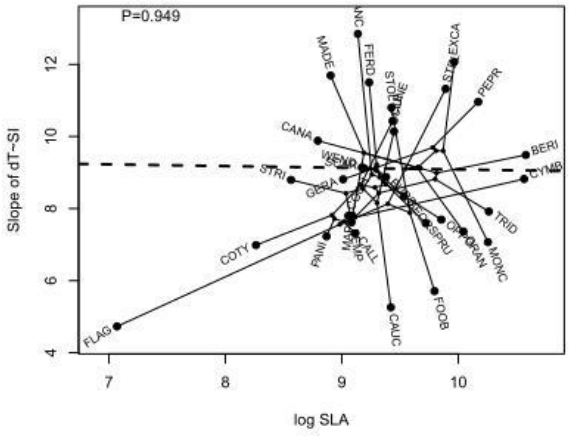
P=0.949
Slope of dT~SI
log SLA

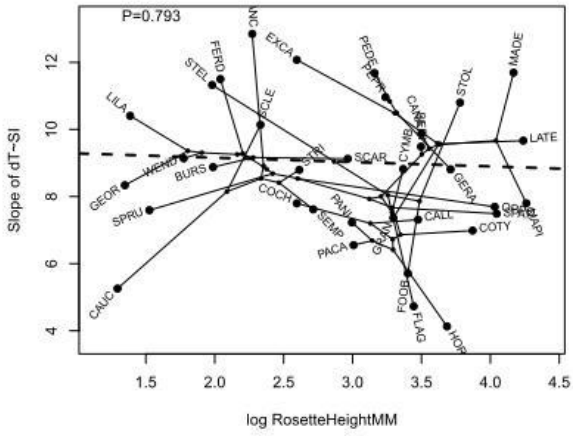
P=0.793
Slope of dT~SI
log RosetteHeightMM

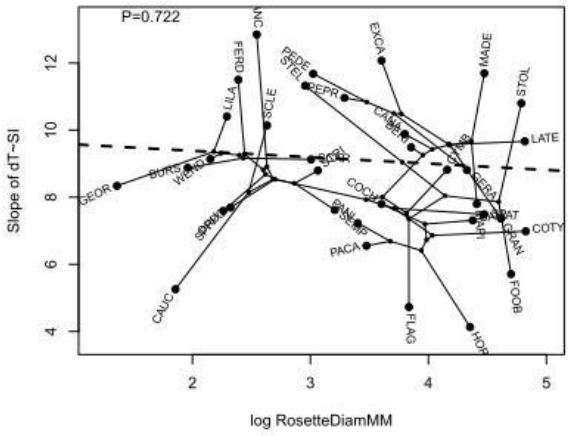
P=0.722
Slope of dT~SI
log RosetteDiamMM

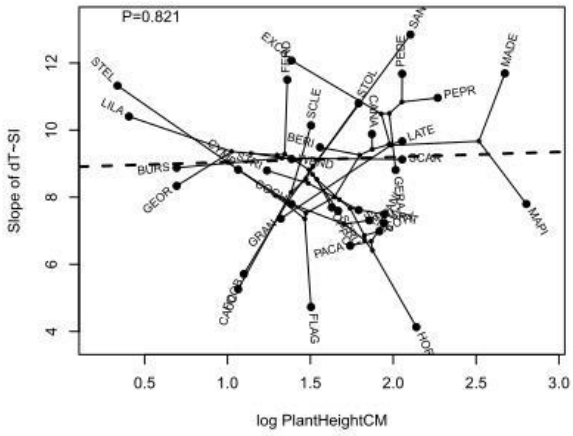
P=0.821
Slope of dT~SI
log PlantHeightCM

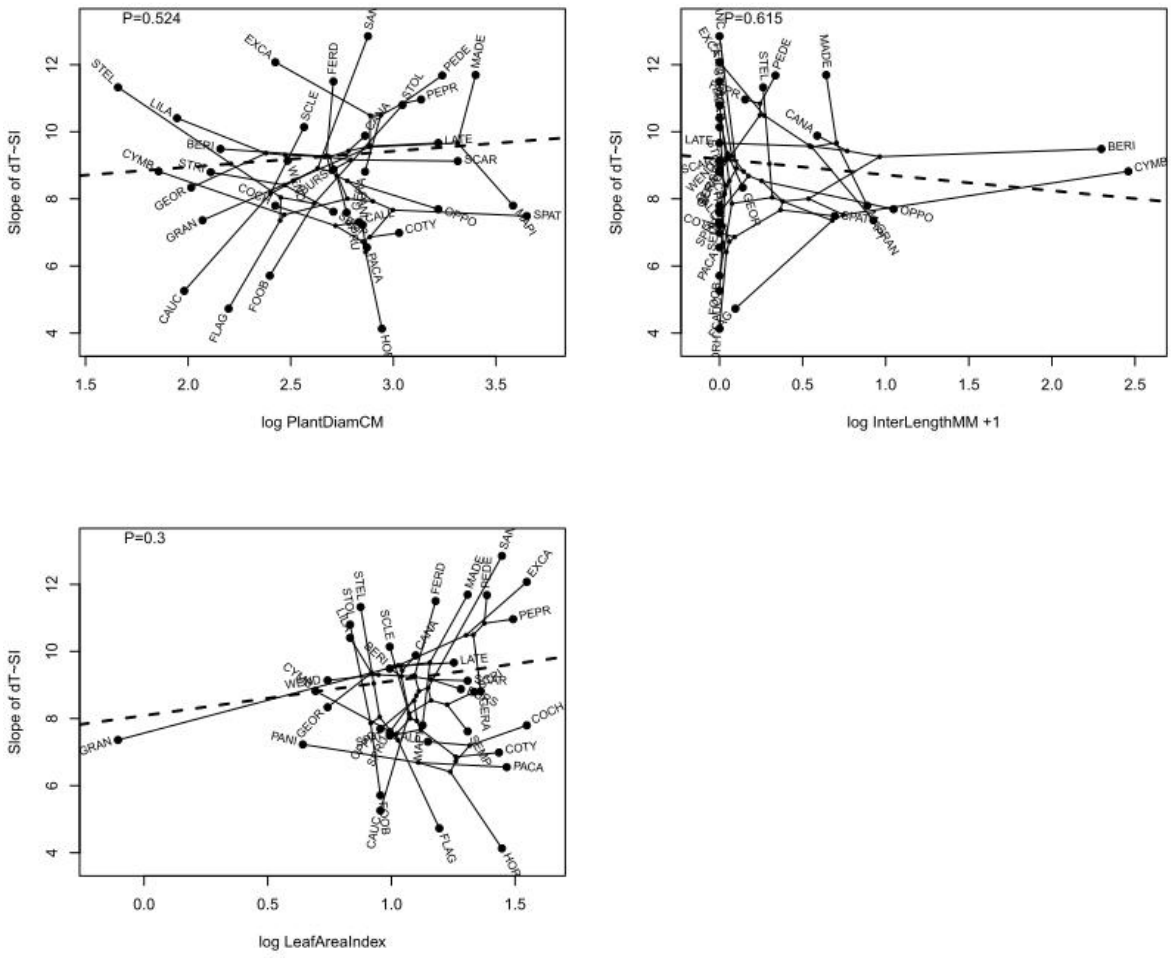

Appendix 4.3: Phylomorphospace plots of the slope of the temperature offset (ΔT ~ SI) as a function of plant morphological variables. The species identities are indicated by four letter abbreviations (large dots), and the ancestral states are reconstructed for each internal node (small dots). None of the slopes are significant.

APPENDIX 4.4: PCoA eigenvalues for all traits used to find the main axes through the matrix in figure 4.X. Many eigenvectors are notably negative, which could have various reasons, among which is missing data.

Trait	PCA1	PCA2
Fresh Mass	-0.90002	-0.28226
Dry Mass	-0.9133	-0.25236
Leaf Thickness	-0.69119	0.264359
Leaf Length	-0.93862	-0.03788
Leaf Width	-0.96349	-0.15844
Leaf Area	-0.90412	-0.32615
Leaf Perimeter	-0.8831	0.041495
Largest Circle Area	-0.83442	-0.40206
Specific Leaf Area	0.168872	-0.55891
Plant Height	-0.43564	0.733375
Plant Diameter	-0.56175	0.583379
Rosette Height	-0.68891	0.408014
Rosette Diameter	-0.80003	0.175664
Leaf Area Index	-0.80003	0.538912
Internode Length	-0.80003	-0.4521

APPENDIX 4.5: Values of phylogenetic signal analysis under lambda model (λ). Lambda values show phylogenetic signal for all traits except plant height and leaf area density. Lower signal values present in fresh mass, specific leaf area and rosette diameter. Computed values for Akaike's information criterion (AIC) for a lambda model and the difference with second-order AICc are given.

	Trait	lambda	AICc_free	AICc_0	AICc_1	dAICc_0	dAICc_1
Leaf traits	Fresh Mass	8.69E-01	164.3007	190.5469	166.753	-26.24618	-2.45E+00
	Dry Mass	1.00E+00	-212.5858	-135.458	-212.5858	-77.127801	8.53E-13
	Leaf Thickness	1.00E+00	479.8401	490.9246	479.8401	-11.0845	5.12E-13
	Leaf Length	1.00E+00	735.4207	801.8849	735.4207	-66.464133	1.14E-13
	Leaf Width	1.00E+00	607.1953	679.5791	607.1953	-72.383836	2.27E-13
	Leaf Area	1.00E+00	1415.7151	1527.0469	1415.7151	-111.3318	1.14E-12
	Leaf Perimeter	1.00E+00	1090.254	1187.4811	1090.254	-97.227147	0.00E+00
	Largest Circle Area	1.00E+00	1260.6791	1333.3892	1260.6791	-72.710135	2.27E-13
	Specific Leaf Area	9.68E-01	1584.8779	1609.2648	1585.4953	-24.386874	-6.17E-01
Whole plant traits	Plant Height	1.28E-51	218.9583	218.9583	222.8296	0	-3.87E+00
	Plant Diameter	1.00E+00	338.0308	357.0707	338.0308	-19.039913	6.25E-13
	Rosette Height	1.00E+00	373.5224	377.5548	373.5224	-4.032418	1.14E-13
	Rosette Diameter	8.48E-01	428.2159	434.3136	429.0324	-6.097617	-8.16E-01
	Leaf Area Index	1.39E-214	123.4642	123.4642	138.0164	0	-1.46E+01
	Internode Length	1.00E+00	173.1695	187.9452	173.1695	-14.775725	5.40E-13

APPENDIX 4.6

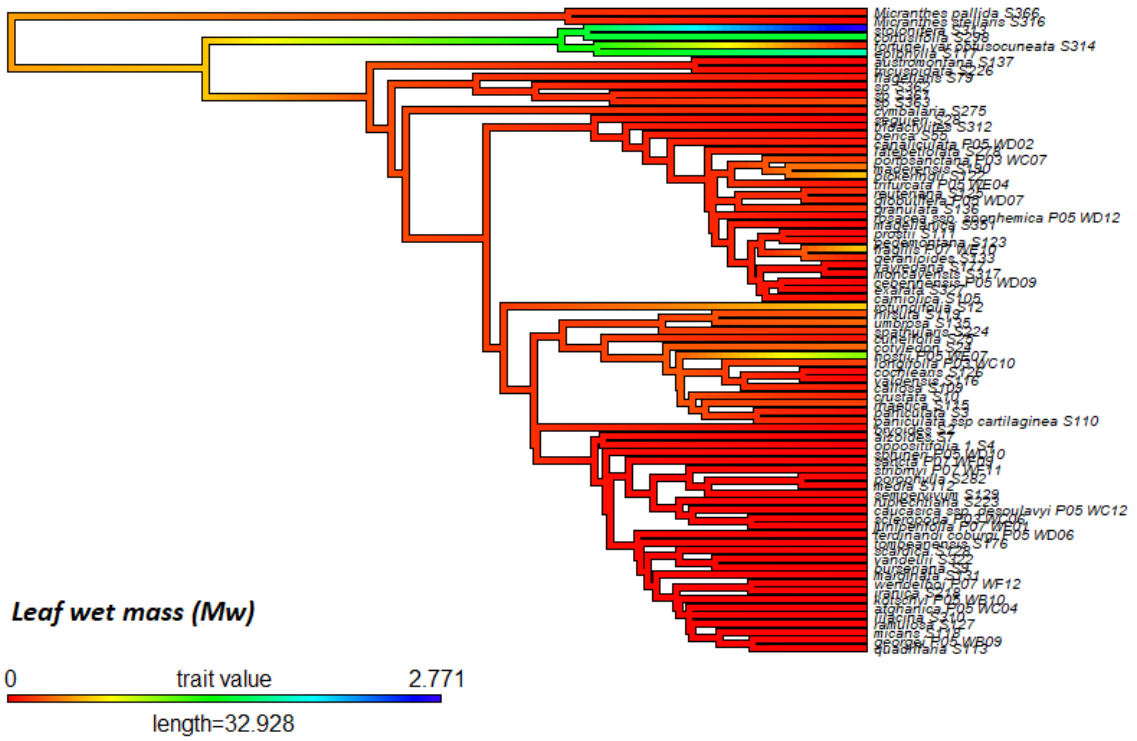
Micranthes pallida S366
Micranthes stellaris S316
stolonifera S358
fortunei var obtusocuneata S314
epiphylla S112
glaucophylla S137
hirculoides S326
flagellaris S79
sp S361
sp S363
cymbalaria S275
granulifera S184
sequieri S28
tridactylites S312
bergii S55
canaliculata P05 WD02
composaniana P03 WC07
madeirensis S150
pickeringii S22
triflorata P05 WE04
rauteriana S105
globulifera P05 WD07
granulata S136
rossea ssp. arachemica P05 WD12
magellanica S351
prostii S113
fragilis P07 WE10
geranioides S133
hayesiana S117
moncayensis S317
cebennensis P05 WD09
exarata S327
camtschatica S105
rotundifolia S12
hirsuta S13
umbrosa S135
curtisiella S26
conjugata S24
hostii P05 WE07
lonchitis P03 WC10
cochlearis S126
valdensis S16
calycosa S109
crustata S10
paniculata S3
bryoides S2
alpestris S7
oppositifolia 1 S4
sphenera P05 WD10
sancta P07 WE09
smithii P07 WE11
pomphylla S282
media S112
sempervivum S129
caucasica ssp. diasoulavyi P05 WC12
sclerophylla P07 WC06
juniperifolia P07 WE01
ferdinandi coburgi P05 WD06
tomineanensis S176
scardica S128
burseriana S8
marginata S101
werdermannii P07 WF12
kotschyi P05 WB10
afghanica P05 WC04
ramulosa S127
micans S18
george P05 WB09
quadrifaria S113
Leaf wet mass (Mw)
0
trait value
2.771
length=32.928

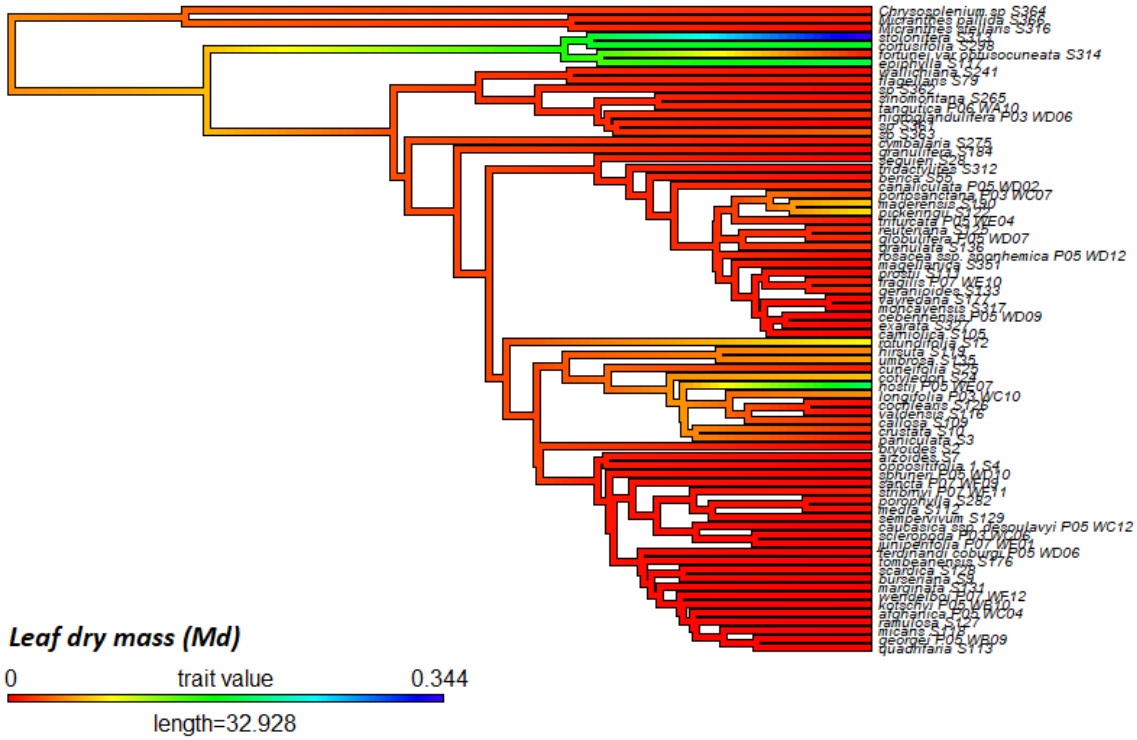
Chrysosplenium sp S364
Micranthes pallida S366
Micranthes stellaris S316
stolonifera S358
fortunei var obtusocuneata S314
epiphylla S112
glaucophylla S137
flagellaris S79
sp S361
sp S363
cymbalaria S275
granulifera S184
sequieri S28
tridactylites S312
bergii S55
canaliculata P05 WD02
composaniana P03 WC07
madeirensis S150
pickeringii S22
triflorata P05 WE04
rauteriana S105
globulifera P05 WD07
granulata S136
rossea ssp. arachemica P05 WD12
magellanica S351
prostii S113
fragilis P07 WE10
geranioides S133
hayesiana S117
moncayensis S317
cebennensis P05 WD09
exarata S327
camtschatica S105
rotundifolia S12
hirsuta S13
umbrosa S135
curtisiella S26
conjugata S24
hostii P05 WE07
lonchitis P03 WC10
cochlearis S126
valdensis S16
calycosa S109
crustata S10
paniculata S3
bryoides S2
alpestris S7
oppositifolia 1 S4
sphenera P05 WD10
sancta P07 WE09
smithii P07 WE11
pomphylla S282
media S112
sempervivum S129
caucasica ssp. diasoulavyi P05 WC12
sclerophylla P07 WC06
juniperifolia P07 WE01
ferdinandi coburgi P05 WD06
tomineanensis S176
scardica S128
burseriana S8
marginata S101
werdermannii P07 WF12
kotschyi P05 WB10
afghanica P05 WC04
ramulosa S127
micans S18
george P05 WB09
quadrifaria S113
Leaf dry mass (Md)
0
trait value
0.344
length=32.928

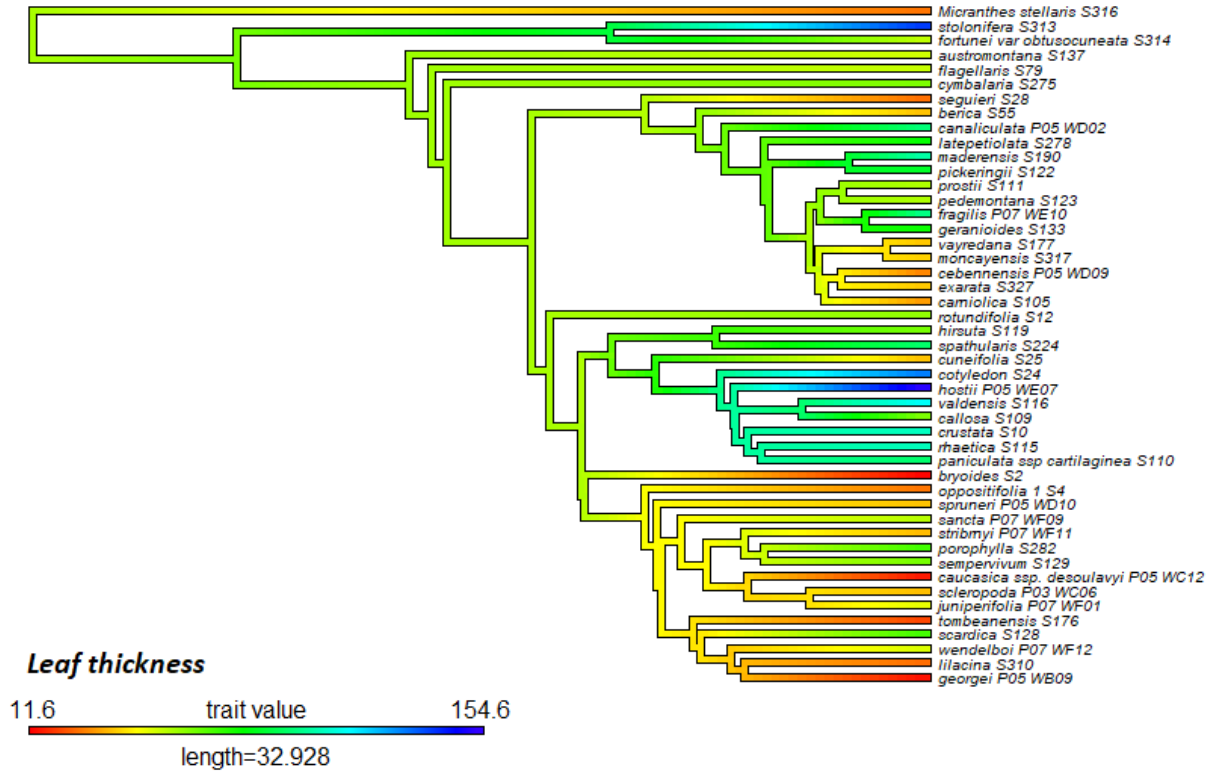
Micranthes stellaris S316
stolonifera S313
fortunei var obtusocuneata S314
austromontana S137
flagellaris S79
cymbalaria S275
seguieri S28
berica S55
canaliculata P05 WD02
latepetiolata S278
maderensis S190
pickeringii S122
prostii S111
pedemontana S123
fragilis P07 WE10
geranioides S133
vayredana S177
moncayensis S317
cebennensis P05 WD09
exarata S327
carniolica S105
rotundifolia S12
hirsuta S119
spathularis S224
cuneifolia S25
cotyledon S24
hostii P05 WE07
valdensis S116
callosa S109
crustata S10
rhaetica S115
paniculata ssp cartilaginea S110
bryoides S2
oppositifolia 1 S4
spruneri P05 WD10
sancta P07 WF09
stribmyi P07 WF11
porophylla S282
sempervivum S129
caucasica ssp. desoulavyi P05 WC12
scleropoda P03 WC06
juniperifolia P07 WF01
tombeanensis S176
scardica S128
wendelboi P07 WF12
lilacina S310
georgei P05 WB09
Leaf thickness
11.6
trait value
154.6
length=32.928

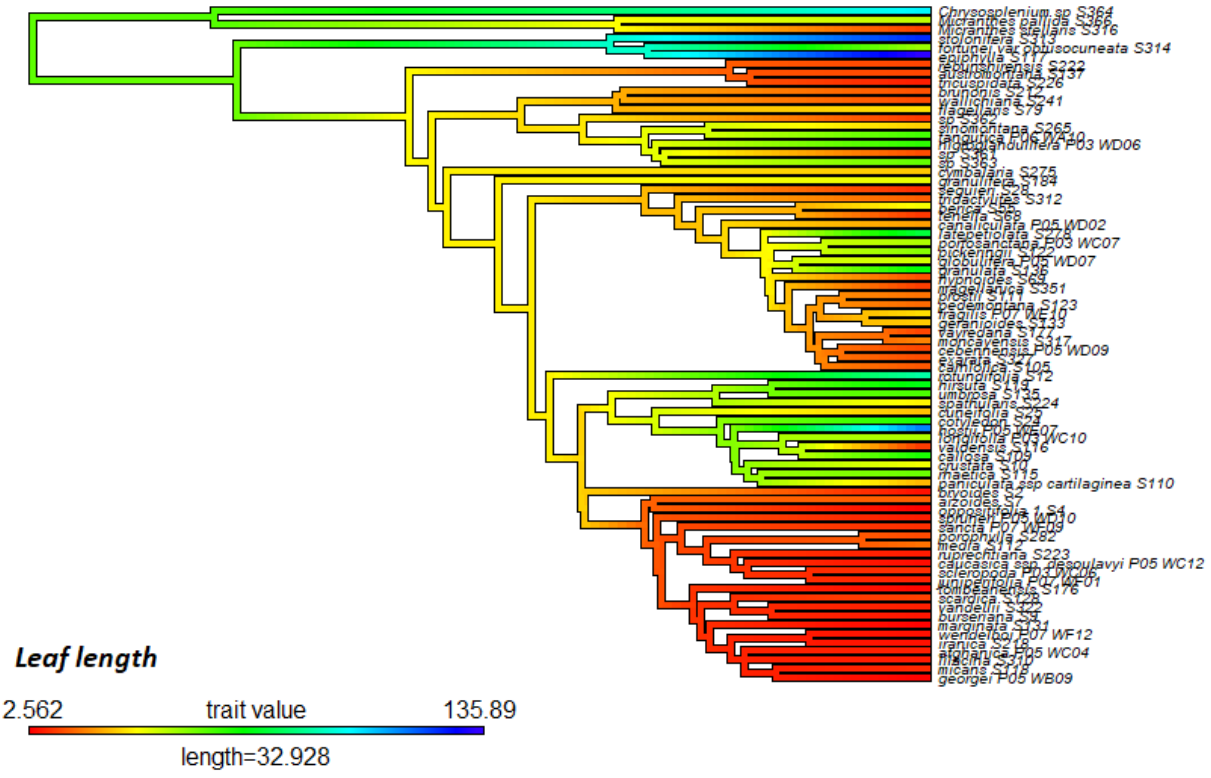
Chrysosplenium sp S364
Micranthes pallida S86
Micranthes stellaris S316
stolonifera S313
fortunei var obtusocuneata S314
austromontana S137
flagellaris S79
cymbalaria S275
granulifera S184
seguieri S28
berica S55
canaliculata P05 WD02
latepetiolata S278
pickeringii S122
prostii S111
pedemontana S123
fragilis P07 WE10
geranioides S133
vayredana S177
moncayensis S317
cebennensis P05 WD09
carniolica S105
rotundifolia S12
hirsuta S119
spathularis S224
cuneifolia S25
cotyledon S24
hostii P05 WE07
valdensis S116
callosa S109
crustata S10
rhaetica S115
paniculata ssp cartilaginea S110
bryoides S2
oppositifolia 1 S4
sancta P07 WF09
porophylla S282
media S112
rupicnitiana S223
caucasica ssp. desoulavyi P05 WC12
scleropoda P03 WC06
juniperifolia P07 WF01
tombeanensis S176
scardica S128
spruneri P05 WD10
wendelboi P07 WF12
georgei P05 WB09
Leaf length
2.562
trait value
135.89
length=32.928

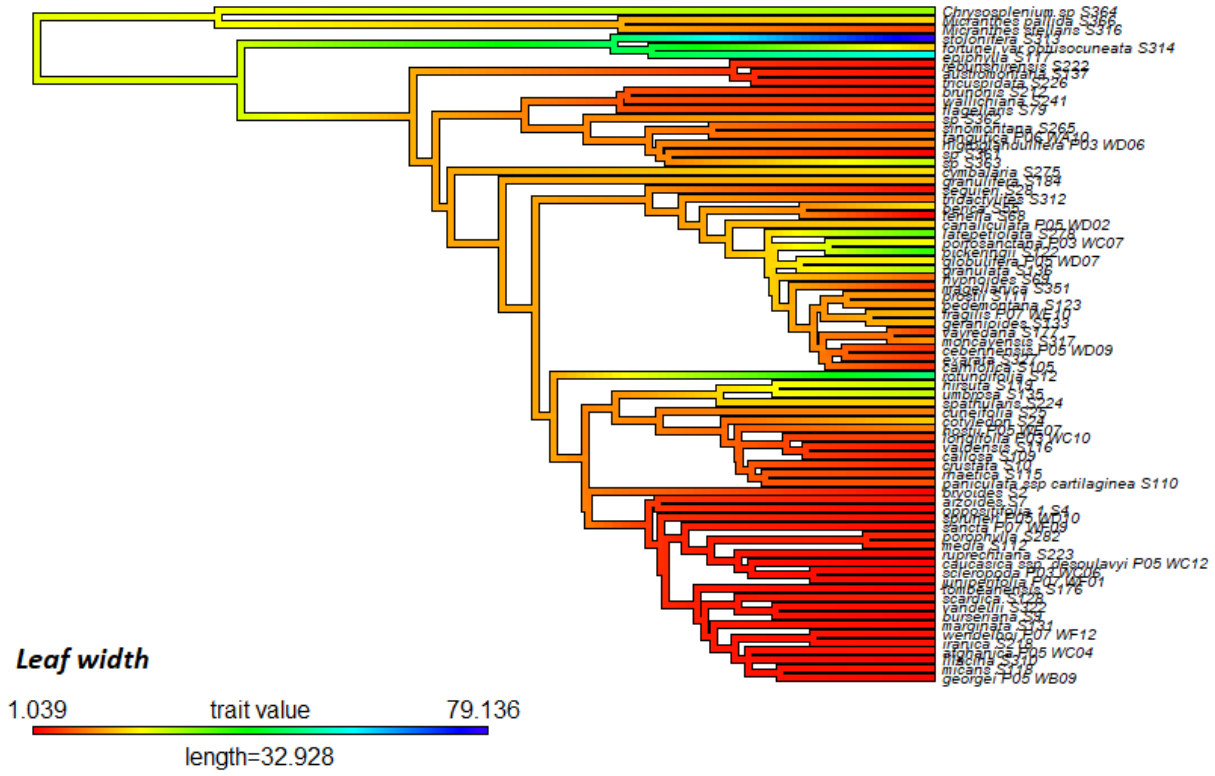

Leaf width

1.039 trait value 79.136

length=32.928

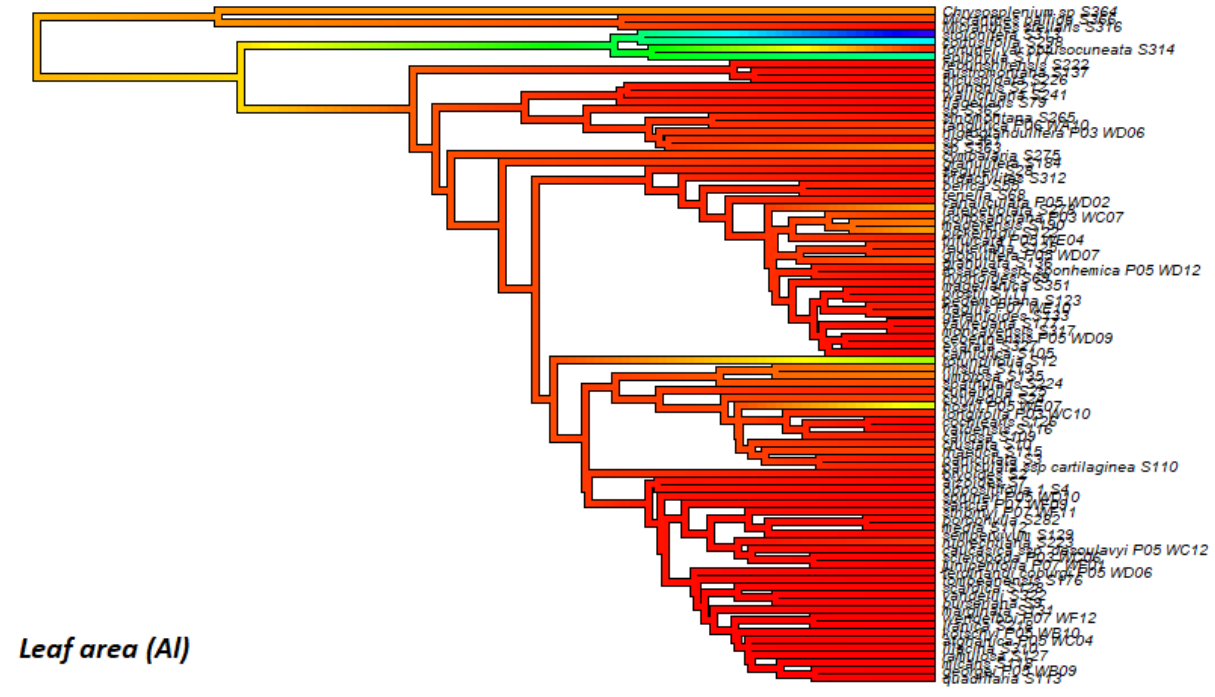

Leaf area (Al)

2.964 trait value 4266.202

length=32.928

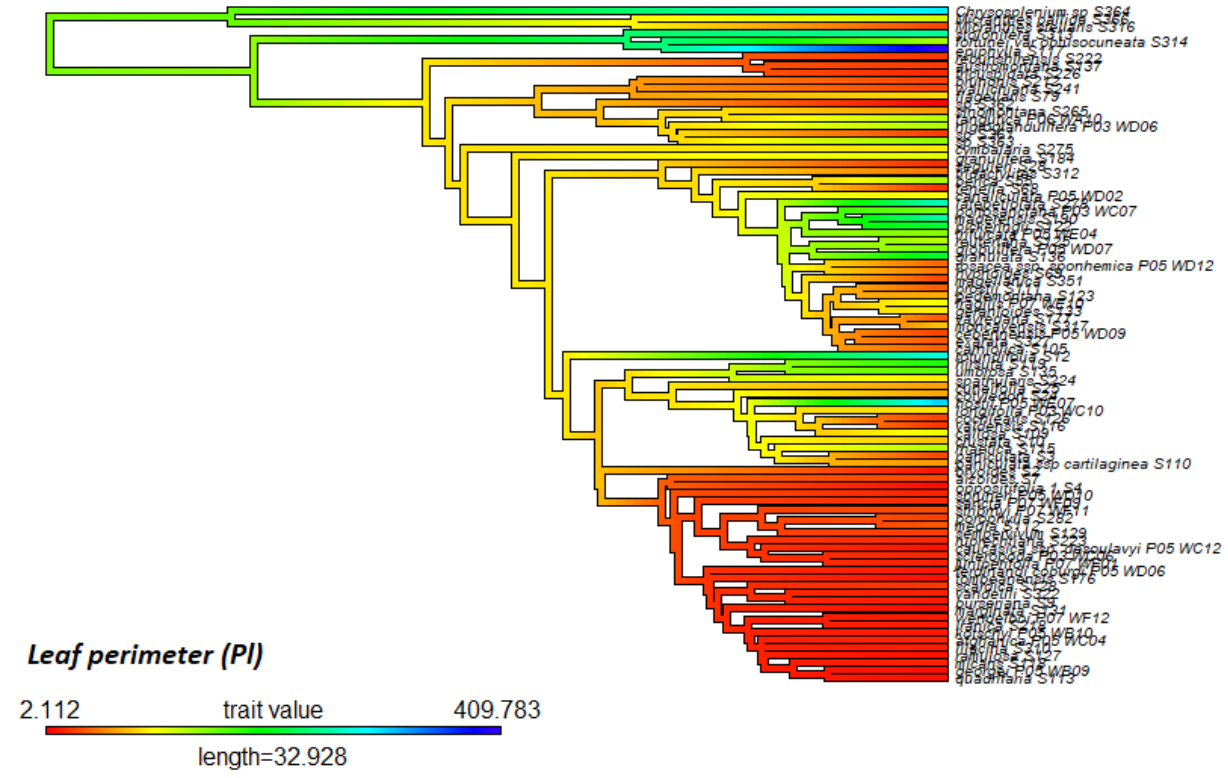
Leaf perimeter (PI)
2.112
trait value
409.783
length=32.928

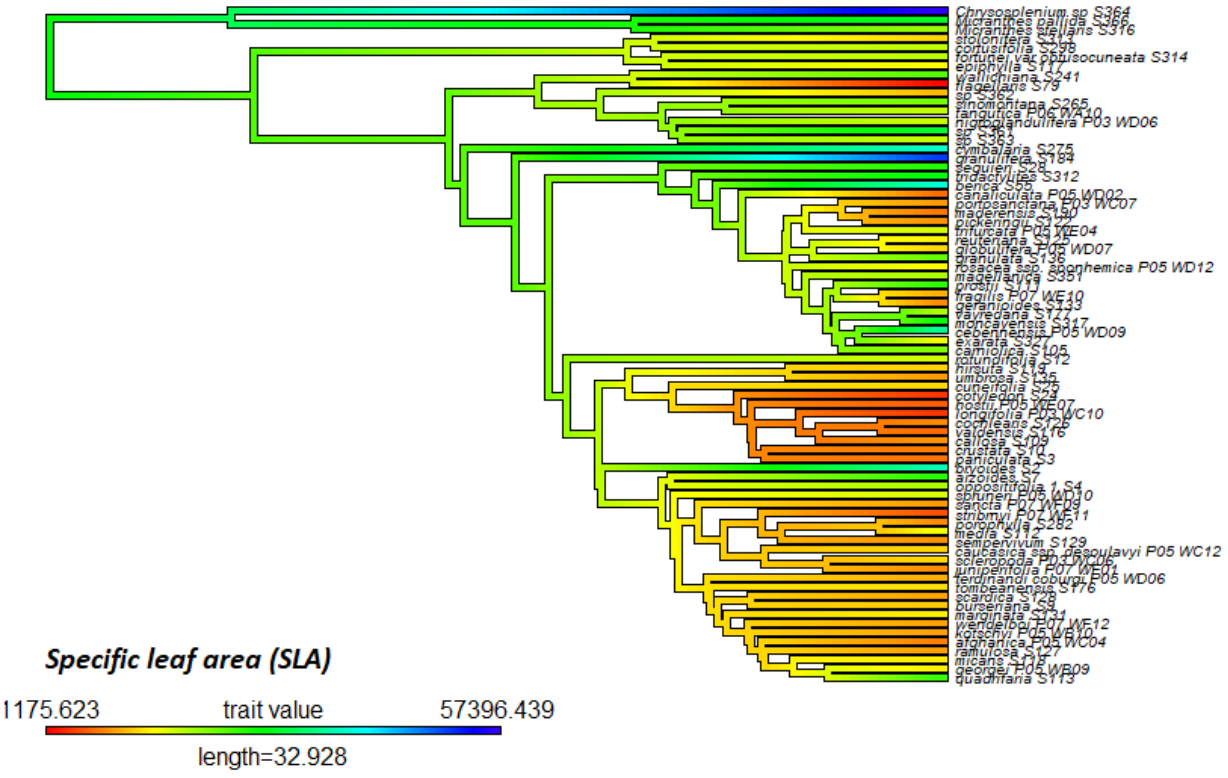
Specific leaf area (SLA)
1175.623
trait value
57396.439
length=32.928

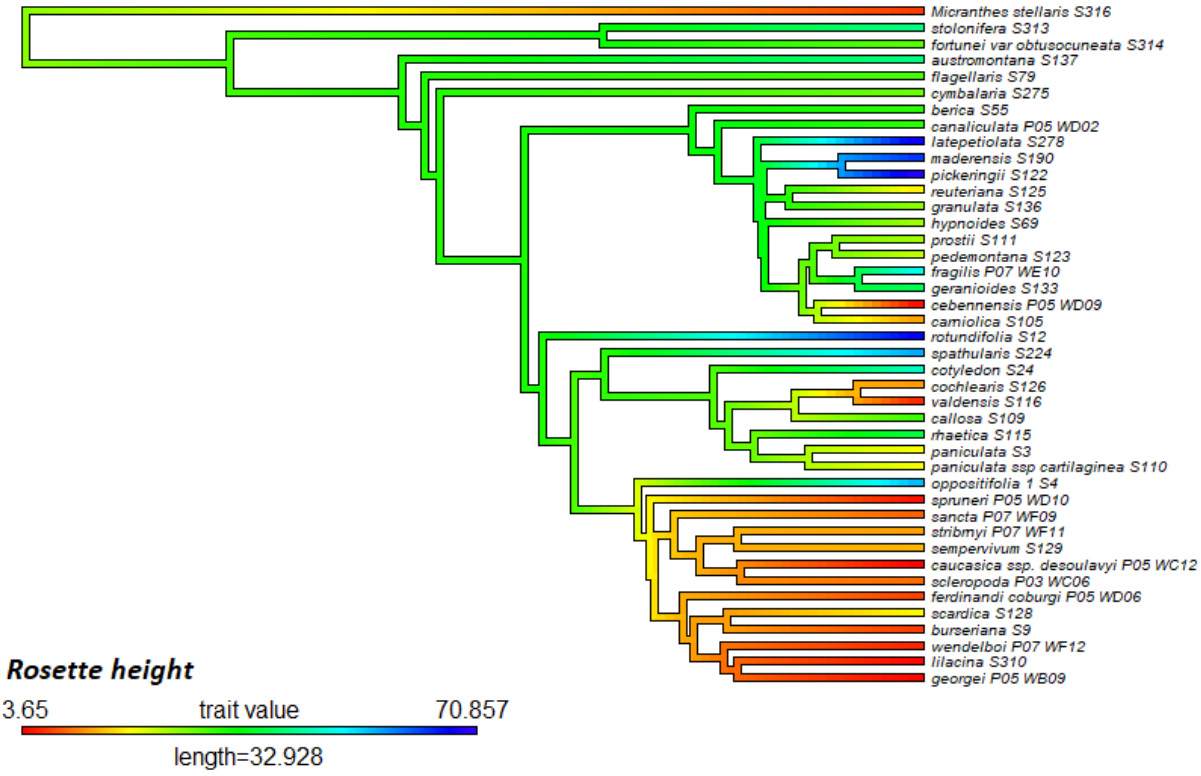
Micranthes stellaris S316
stolonifera S313
fortunei var obtusocuneata S314
austromontana S137
flagellaris S79
cymbalaria S275
berica S55
canaliculata P05 WD02
latepetiolata S278
maderensis S190
pickeringii S122
reuteriana S125
granulata S136
hypnoides S69
prostii S111
pedemontana S123
fragilis P07 WE10
geranioides S133
cebennensis P05 WD09
camiolica S105
rotundifolia S12
spathularis S224
cotyledon S24
cochlearis S126
valdensis S116
callosa S109
rhaetica S115
paniculata S3
paniculata ssp cartilaginea S110
oppositifolia 1 S4
spruneri P05 WD10
sancta P07 WF09
stribmyi P07 WF11
sempervivum S129
caucasica ssp. desoulavyi P05 WC12
scleropoda P03 WC06
ferdinandi coburgi P05 WD06
scardica S128
burseriana S9
wendelboi P07 WF12
lilacina S310
georgei P05 WB09
Rosette height
3.65
trait value
70.857
length=32.928

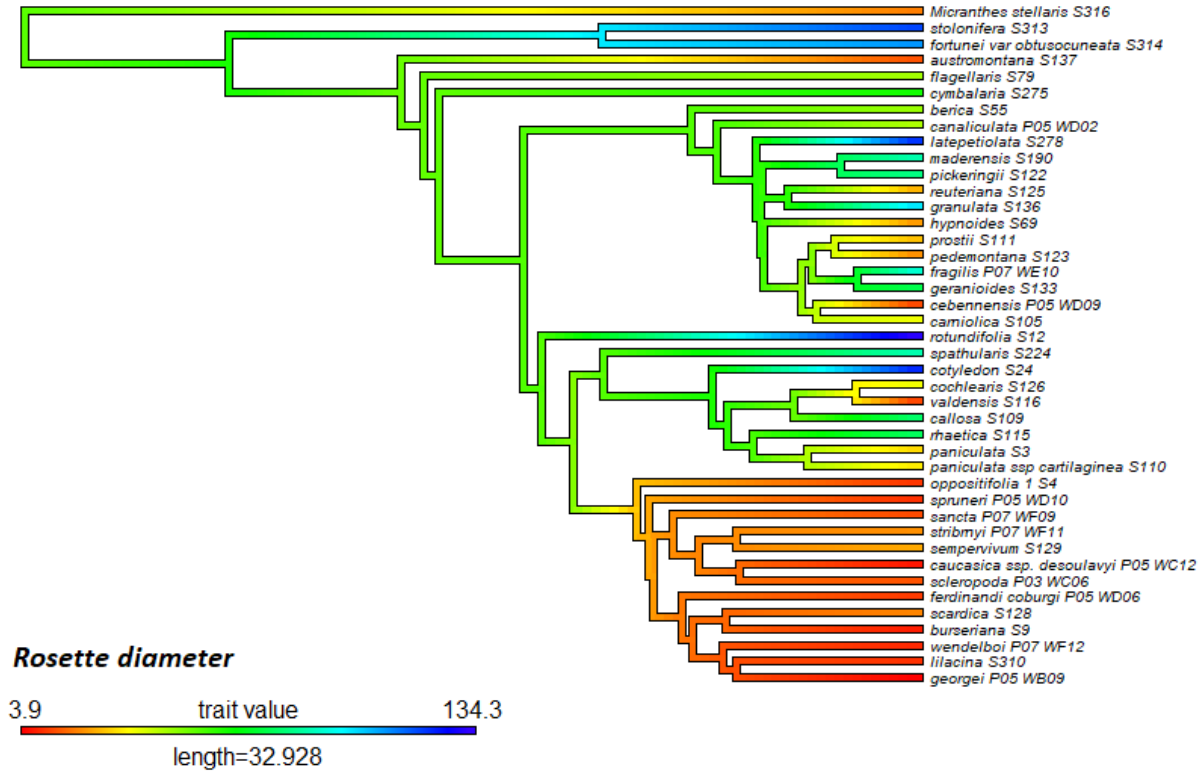
Micranthes stellaris S316
stolonifera S313
fortunei var obtusocuneata S314
austromontana S137
flagellaris S79
cymbalaria S275
berica S55
canaliculata P05 WD02
latepetiolata S278
maderensis S190
pickeringii S122
reuteriana S125
granulata S136
hypnoides S69
prostii S111
pedemontana S123
fragilis P07 WE10
geranioides S133
cebennensis P05 WD09
camiolica S105
rotundifolia S12
spathularis S224
cotyledon S24
cochlearis S126
valdensis S116
callosa S109
rhaetica S115
paniculata S3
paniculata ssp cartilaginea S110
oppositifolia 1 S4
spruneri P05 WD10
sancta P07 WF09
stribmyi P07 WF11
sempervivum S129
caucasica ssp. desoulavyi P05 WC12
scleropoda P03 WC06
ferdinandi coburgi P05 WD06
scardica S128
burseriana S9
wendelboi P07 WF12
lilacina S310
georgei P05 WB09
Rosette diameter
3.9
trait value
134.3
length=32.928

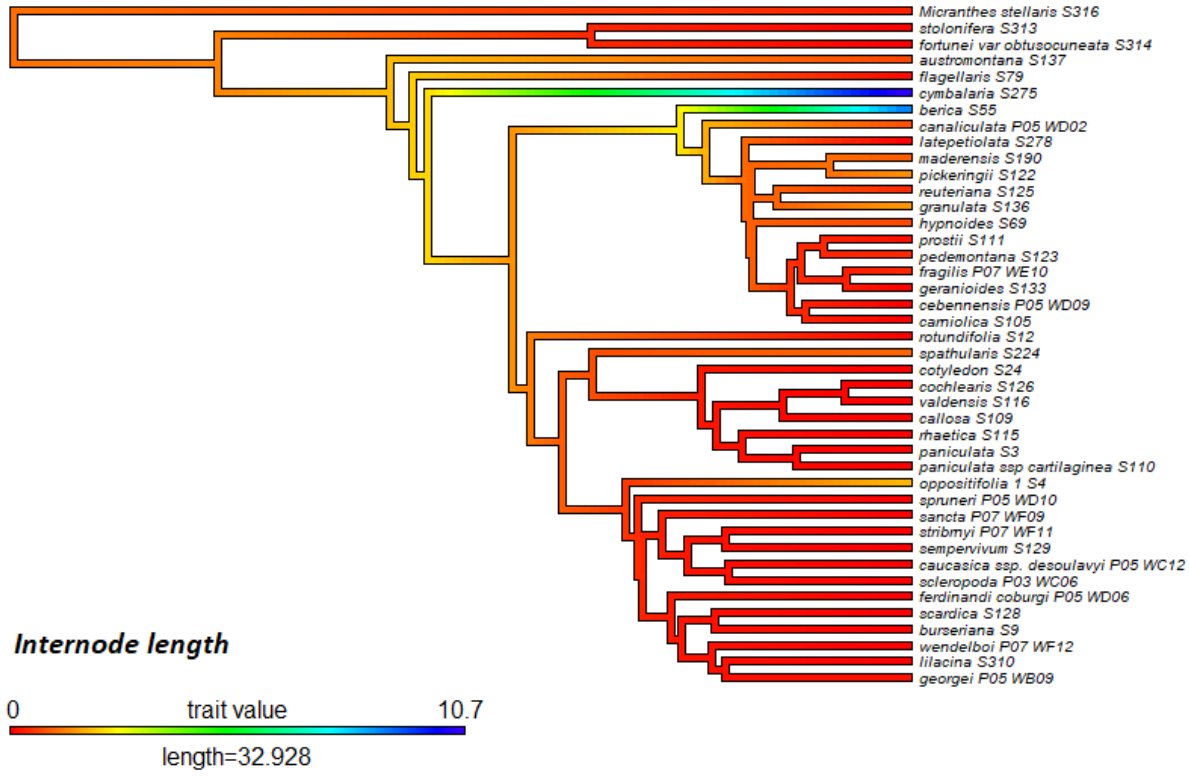

***Appendix 4.6: Phylogenetic trees with continuous traits mapped to branches. For the traits included in the figure the* related species have more similar values under a lambda (ʎ) model of evolution (see Appendix 4.5 for ʎ values).**